DEVELOPMENT OF STATISTICAL AND GEOSPATIAL-BASED FRAMEWORK FOR DROUGHT-RISK ASSESSMENT

A Thesis submitted by

Kavina Shaanu Dayal

BSc (Meteorology)

MSc (Meteorology)

For the award of

Doctor of Philosophy

2018

ABSTRACT

Drought is an insidious, complex and one of the least understood natural phenomena resulting from a deficiency of water resources. While droughts cannot be prevented, its impacts, however, can be mitigated through proper design of water storage infrastructure and management strategies. A comprehensive drought management plan necessitates the development of a framework that can help reduce the drought-related risk. In Australia, there are limited drought vulnerability and risk assessment models that must (1) include the drought monitoring index that measures the supply-demand balance of water resources, (2) incorporate large-scale climate drivers influencing amplitude of drought events in the statistical prediction models, and (3) objectively quantify the drought-risk on both temporal and spatial scales. The goal of this study is to apply statistical and geospatial tools in developing a framework for assessing drought-related risks in light of improving the drought mitigation strategies.

A new, temporal and spatial-explicit analytical framework for drought-risk assessment is developed based on three objectives focussed in the drought-prone southeast Queensland (SEQ) region. (1) Evaluating and affirming the suitability of the Standardised Precipitation-Evapotranspiration Index (SPEI) for the characterisation of drought events. (2) Developing a copula-based statistical, probabilistic model for predicting the SPEI and the jointly distributed drought properties (*i.e.*, durations, severities and intensities) conditional on the large-scale climate mode indices. (3) Developing a spatially descriptive drought-risk index by combining the drought hazard, exposure and vulnerability factors using a fuzzy logic algorithm.

The first objective of this study demonstrates the scientific relevance of the SPEI as a robust drought assessment metric that incorporates the influence of water supply-demand balance on drought events. Subsequently, the severity (S; accumulated negative SPEI in a drought-identified period), intensity (I; minimum SPEI) and the duration (D; number of months with continuously negative SPEI representing the below average water resources) based on run-sum approach are enumerated to identify historical water deficit periods. Significant disparities in the identified *D-S-I* affirms the significance of SPEI for regional drought impact assessments. Accordingly, this study advocates the SPEI as a convenient metric for detecting drought onsets and terminations, including its ability for drought ranking and drought recurrence evaluations that are considered vital for water resource management.

The second objective models the joint behaviour of SPEI and *D-S-I* properties using copula model, conditional upon the pertinent climate mode indices (*i.e.,* El-Niño Southern Oscillation indicators). The vine copula algorithm is employed to derive the bivariate and trivariate joint-distributions of drought variables for conditional probability-based predictions. The results yield marginal differences between the observed and the predicted drought properties, elucidating the effectiveness of copula functions in drought-risk modelling. The results have implications for drought and aridity management in agricultural regions where complex relationships between climate drivers and drought properties are likely to exacerbate the risk of a future event.

The third objective develops a methodology using vulnerability, exposure and hazard indicators to provide a spatio-temporal framework for drought-risk assessment. The conditional joint probability of each drought indicator is estimated using the Bayes theorem. Various fuzzy membership functions are then applied to standardise and aggregate the indicators to derive drought vulnerability, exposure and hazard indices. The resulting indices are integrated with fuzzy GAMMA overlay operation to generate optimal drought-risk maps. The maps reveal varying levels of drought risk in different austral seasons and annually that is well represented by the drought hazard index, *i.e.,* rainfall departure. The validation of the method with respect to the upper and lower layer soil moisture reveal significant correlations with the spatial drought-risk index. It is therefore prudent to state that the fuzzy logic-based analytical technique applied for spatio-temporal drought-risk mapping can be considered as a practical tool that can enable better drought management, drought mitigation and relief-planning decisions.

The statistically and spatially relevant drought-risk assessments frameworks formulated in this study provides promising outcomes that are valuable for the mitigation of drought impacts, and therefore, sets a pathway to construct strategic planning procedures and management of water resources in drought-prone, arid or semi-arid regions.

CERTIFICATION OF THESIS

This thesis is entirely the work of Kavina Shaanu Dayal except where otherwise acknowledged. The work is original and has not previously been submitted for any other award, except where acknowledged.

Principal Supervisor: Dr Ravinesh C. Deo

Associate Supervisor: Professor Armando A. Apan

Student and supervisors signatures of endorsement are held at the University.

PUBLICATIONS

Refereed Journal Articles

1. **Dayal Kavina S.**, R. C. Deo and A. A. Apan, (2018) "Investigating drought duration-severity-intensity characteristics using Standardised Precipitation-Evapotranspiration Index: a case study in drought-prone, southeast Queensland", ASCE *Journal of Hydrologic Engineering*, 23(1), 1-16. (Impact Factor = 1.600, Quartile 1 in Civil & Structural Engineering).

2. **Dayal Kavina S.**, R. C. Deo and A. A. Apan, (2018) "Spatio-temporal drought-risk mapping approach for southeast Queensland, Australia", *Natural Hazards*, (Accepted). (Impact Factor = 1.776, Quartile 1 in Water Science and Technology).

3. **Dayal Kavina S.**, R. C. Deo and A. A. Apan, (2018) "Development of a copula-statistical drought prediction model using the Standardised Precipitation-Evapotranspiration Index", *Water Resources Planning and Management*, (In preparation). (Impact Factor = 3.05, Quartile 1 in Civil & Structural Engineering).

4. **Dayal Kavina S.**, R. C. Deo and A. A. Apan, (2018) "Trend analysis of drought events based on SPEI: a case study", *Atmospheric Research*, (In Preparation). (Impact Factor = 3.778, Quartile 1 in Atmospheric Science).

Refereed Conference Proceedings/Book Chapters

1. **Dayal, Kavina S**, Deo Ravinesh C, Apan Armando A, (2017) Drought Modelling Based on Artificial Intelligence and Neural Network Algorithms: A Case Study in Queensland, Australia. In Leal Filho, W. (Ed) *Climate Change Adaptation in Pacific Countries: Fostering Resilience and Improving the Quality of Life*. Springer, Berlin. ISBN 978-3-319-50093-5. DOI: 10.1007/978-3-319-50094-2_11. Page 177-198. (https://link.springer.com/chapter/10.1007%2F978-3-319-50094-2_11).

2. **Dayal, Kavina S**. and Deo, Ravinesh C. and Apan, Armando A, (2016) Application of hybrid artificial neural network algorithm for the prediction of Standardised Precipitation Index. In: 2016 IEEE Region 10 International Conference: Technologies for Smart Nation (TENCON 2016), 22-25 Nov 2016, Singapore. (http://ieeexplore.ieee.org/document/7848588/?reload=true).

ACKNOWLEDGMENTS

TABLE OF CONTENTS

LIST OF FIGURES

LIST OF TABLES

ACRONYMS AND ABBREVIATIONS

General Acronyms

ANFIS	Adaptive Neuro-Fuzzy Inference System
ANN	Artificial Neural Networks
AWAP	Australian Water Availability Project
BoM	Bureau of Meteorology
CUSUM	Cumulative Sum
CSIRO	Commonwealth Scientific and Industrial Research Organisation
CWT	Continuous Wavelet Transform
DEM	Digital Elevation Model
DI	Drought Index
DVI	Drought Vulnerability Indicator
GDP	Gross Domestic Product
GIS	Geographic Information System
GWP	Global Water Partnership
IOD	Indian Ocean Dipole
IPO	Interdecadal Pacific Oscillation
MDB	Murray Darling Basin
NAO	North Atlantic Oscillation
NSW	New South Wales
NT	Northern Territory
PAWC	Plant Available Water Capacity
PDO	Pacific Decadal Oscillation
POAMA	Predictive Climate Ocean Atmosphere Model for Australia
QLD	Queensland
SA	South Australia
SAM	Southern Annular Mode
SEQ	Southeast Queensland
SOI	Southern Oscillation Index
SWAT	Soil and Water Assessment Tool
VIC	Victoria
WA	Western Australia
WMO	World Meteorological Organization
XWT	Cross Wavelet Transform

Acronyms for Drought Indices

ADI	Aggregated Drought Index
API	Antecedent Precipitation Index
CMI	Crop Moisture Index
CSA	Cumulative Streamflow Anomaly
CSM	Computed Soil Moisture
CZI	China-Z Index
DAI	Drought Area Index
DCPA	Discrete and Cumulative Precipitation Anomalies
DM	Drought Monitor
EDI	Effective Drought Index
K-BDI	Keetch-Byram Drought Index

MAI	Moisture Adequacy Index
MCZI	Modified China-Z Index
PDSI	Palmer Drought Severity Index
PHDSI	Palmer Hydrological Drought Severity Index
PMAI	Palmer Moisture Anomaly Index
PN	Percent Normal
RAI	Rainfall Anomaly Index
RD	Rainfall Departure
RDDI	Rainfall Decile-based Drought Index
RDI	Reclamation Drought Index
sc-PDSI	Self-Calibrated Palmer Drought Severity Index
SMAI	Soil Moisture Anomaly Index
SMDI	Soil Moisture Deficit Index
SMDDI	Soil-Moisture Decile-based Drought Index
SPEI	Standardised Precipitation-Evapotranspiration Index
SPI	Standardised Precipitation Index
SWSI	Surface Water Supply Index
TWD	Total Water Deficit
VCI	Vegetation Condition Index

Variable Symbols

P	Precipitation	$WRel1$	Upper layer soil moisture
ETo	Reference Evapotranspiration	$WRel1End$	Upper layer end of month aggregate soil moisture
T	Temperature	D	Duration
T_{max}	Maximum Temperature	S	Severity
T_{min}	Minimum Temperature	I	Intensity

Chapter 1

INTRODUCTION

1.1 Background

A drought is a global, natural, and recurring climatic feature that results from a prolonged period of abnormally low rainfall. According to Hewitt (2014), drought ranks first among other natural disasters with numbers of individuals directly affected. It is the least understood climatic feature due to its complex nature, yet it results in on average 6-8 billion USD of annual damage globally (Keyantash and Dracup 2002). The slow development of drought poses difficulty in its detection while the drought preparedness and mitigation solely depends on timely information of the onset, progress and areal extent (Mishra and Singh 2011). Therefore, there is a pressing need to explore new mechanisms for investigating drought characteristics by examining historical events and developing robust predictive and risk evaluative frameworks for the spatial and temporal features. Scientific studies that develop new methods for drought-risk assessments can add new and valuable dimensional information for better preparedness, mitigation, adaptation and regional vulnerability assessment.

Given the highly variable climate, severe droughts in Australia can produce significant reductions in agricultural productivity and farming income. The Millennium Drought that occurred from 1996-2010 serves as a recent reminder of the wide-reaching impacts that drought can have on people and environment (Commonwealth of Australia 2017). In fact, Australia is the driest inhabited continent and is known for its harsh and extreme climate with highly variable rainfall and stream-flow conditions (Davidson 1969; Ummenhofer et al. 2009). While droughts are common periodic events that may be considered as a 'normal' feature (Jones 2001), over the past, however, Australia has been deeply affected by numerous and prolonged

extreme droughts (CSIRO 2008a; CSIRO 2008b). Table 1.1 lists the major droughts that occurred in Australia. Increasing population leading to increasing in demand per capita, and a projected increase in the temperature and decrease in rainfall, is likely to make droughts become an issue that is even more relevant. According to the Australian Bureau of Statistics, the national population in Australia is projected to double by 2075 (Statistics 2013). The increase in population size and warming climate can have vast implications on water supply, and therefore, drought studies are very important for identifying ways to lessen the magnitude of impacts that drought may trigger.

Table 1.1: List of major droughts in Australia. After Deo et al. (2015).

Drought Year	Descriptions
1895 – 1903 (Federation Drought)	Felt nationwide but was mostly persistent in QLD, inland NSW, SA and central Australia. Sheep numbers reduced to half and cattle numbers declined by more than 40%. The wheat yield dropped from 8 bushels/acre to 2.4 bushels/acre in 1902.
1911 – 1916	Affected nationwide with varying severity.
1918 – 1920	Affected nationwide.
1922 – 1923 and 1926 – 1929	Nationwide with varying severity.
1933 – 1938	Nationwide with varying severity
1939 – 1945 (World War II Drought)	Affected nationwide.
1946 – 1949	Nationwide with varying severity.
1951 – 1952	Pastoral areas were particularly affected in QLD, NT, WA.
1958 – 1968	Most widespread, consistently prominent for long period. Affected nationwide with varying intensity.
1970 – 1973	Affected WA caused by a successive decline in average rainfall.
1976	Affected western NSW and most of VIC and SA due to lack of autumn-winter rains.
1982 – 1983	Short-lived yet very intense. Affected mostly eastern Australia and particularly severe in southeastern Australia. A total loss of $3 billion in agricultural production alone.

	The Wimmera Southern Mallee region of Victoria experienced 80% and 40% reduction in grain and livestock production, respectively.
1991 – 1995	Affected northeastern NSW and much of QLD as a result of lowest levels of rainfall on record. The reservoirs water levels went critically low, the average rural population declined by over 10% while unemployment went up. The estimated loss of the economy was around $A5 billion.
1996 – 2010 (Millennium Drought or "Big Dry")	A prolonged period of dryness affected much of southern Australia. The drought condition was severe in the densely populated southeast and southwest and affected the Murray-Darling Basin (MDB) severely. Southeast Australia experienced its lowest 13-year rainfall record since 1865. Agricultural production fell from 2.9% to 2.4% of GDP between 2002 and 2009. It was estimated that drought reduced national GDP by roughly 0.75% between 2006 and 2009 while regional GDP in MDB fell by 5.7% below forecast that accompanied the temporary loss of 6000 jobs between 2007 and 2008.

Other Sources: Wittwer et al. (2002), Year Book Australia, 1988, Australian Government and Council (2015). *Acronyms* – QLD: Queensland, NSW: New South Wales, SA: South Australia, VIC: Victoria, NT: Northern Territory, WA: Western Australia. Bold years are major drought events.

1.2 Statement of the Problem

Indisputably, the impact of droughts is devastating to health, economy, ecosystems and urban water supply. Droughts can contribute to decline in human health and increase in mental health problems such as post-traumatic stress and suicidal behaviour (Haines et al. 2006). In fact, the World Meteorological Organization (WMO) has linked drought to 680,000 deaths globally from 1970-2012 (Golnaraghi et al. 2014). In rural affected populations in Australia, droughts can exacerbate mental health issues and increase suicide rates (Alston 2012). Droughts also have severe economic repercussions on agriculture, tourism, employment and livelihood in Australia. For example, between 2002 and 2003, decreases in agricultural production due to drought resulted in 1% reduction in Gross Domestic Product (GDP) (ABS 2004). Carroll et al. (2009) predicted that an increase in drought frequency in the future is likely to have an estimated cost of $5.4 billion annually, reducing GDP by 1% per annum.

Similarly, drought has economic repercussions on Australia's tourism industry. The reduced visitor days in 2008 in the Murray River region had caused an estimated loss of $70 million (TRA 2010). Drought also significantly impacts on Australia's ecosystem. During the Millennium Drought, there was a marked decline in water bird, fish and aquatic plant populations in the Murray Darling Basin (MDB) (Leblanc et al. 2012) and loss of 57,000 ha of planted forests (van Dijk et al. 2013). Additionally, droughts can reduce inflows into vital urban water catchments. During the Millennium Drought in southeast QLD, severe water restrictions were implemented where in some areas the average water use declined to 129 litres per person per day, in comparison to a regional consumption of 375 litres under normal (non-drought) operating conditions (Council 2015).

Challenges in drought assessment measures are restraining the translation of scientific insights into water resources management, strategic disaster resilience policy development including the design of hydrologic, and water resource systems (Trenberth et al. 2014; Van Loon 2015; Vogel et al. 2015). The fact that droughts are a major problem of interest in Australia, yet the understanding of this phenomenon is far from complete. Decision makers undergo multifaceted challenge in characterising drought properties for water resource management. Therefore, having identified

4

significant issues mentioned above, this study aimed to address the following research gaps to make significant contributions to this study area:

1. Given highly variable climate and prone to climate change effects, a drought monitoring index based solely on precipitation (such as Rainfall Decile-based Drought Index; RDDI) may not reveal the detailed information for drought-risk assessment in Australia. This study, therefore, employed the SPEI to take into account both precipitation and reference evapotranspiration to capture impacts of increased temperatures on water demand, to identify onset and termination points of historical drought, and to estimate their corresponding severity, intensity and duration properties. Additionally, drought is a multi-scalar phenomenon where the timescale over which water deficits accumulate is extremely important and functionally separates meteorological, hydrological and agricultural droughts. There has been a paucity of such analysis for Australian droughts, and therefore, this study characterises droughts on multiple scales. This can enable monitoring and management of different usable water resources.

2. Several large-scale climate drivers, such as the El-Niño Southern Oscillation (ENSO), influence droughts in Australia. Therefore, the drought-risk assessment must include models for the prediction of droughts conditional on climate drivers, particularly for economically sensitive agricultural regions. The literature search shows that the prediction of drought based on interacting elements is beneficial for understanding the simulated drought-risk, *e.g.,* Wong et al. (2009), yet this practice, conditional on climatic conditions, needs further investigation and application to any drought-prone regions in Australia.

3. As it is known, the nature of droughts is temporal and spatial. From a practical viewpoint, the need for a spatial representation of drought-risk in Australia is far from complete, especially in terms of identifying its demographic impacts and for the planning of water resources, agricultural expansion, water-management or water demand allocations requirements. The premise to develop a spatially representative drought-risk index using physiographic and climatic factors to demonstrate drought-risk analysis is yet to be applied to the

drought-prone regions in Australia. Studies performed elsewhere integrated various physiographic and climatic factors based on certain assumptions that incline towards subjective assessments of droughts. This study has integrated the fuzzy logic theory to provide a mere objective assessment of drought and generate the descriptive drought-risk maps using vulnerability, exposure and hazard indices. As such the subjectivity in the assessment of drought can potentially be minimised.

This study attempts to fill the critical information and knowledge gaps and provides new scientific insights to the field of drought-risk monitoring and preparedness. There are three essential components of drought-risk identified in this study. First, the ability to monitor the episodic or gradual progression of droughts on various time-scales, performed using drought indices. Second, being able to provide a framework for the predictions of drought-risk using predictive models via joint distributions of predictors (*e.g.,* climate mode indices) and predictands (*e.g.,* drought indices) where the estimated level of future risk can be assessed. Finally, being able to represent drought-risk on a spatial map in terms of drought vulnerability, exposure and hazard indices on seasonal and annual scales. This is intended to help in identifying regions that are most prone to drought-associated risks.

1.3 Research Aims and Objectives

The aim of this study is to develop a statistical and geospatial-based framework and verify its suitability for drought-risk research with three main objectives. The application on drought-risk management framework is expected to improve the modelling precision for accurate assessment and prediction of drought events using the available hydro-meteorological, climatic and physiographic parameters. Specifically, this study addresses the following three objectives:

(1) **To apply the Standardised Precipitation-Evapotranspiration Index (SPEI) for drought assessment by considering jointly the impact of precipitation and reference evapotranspiration on the water deficit**. This objective assesses the relationship between SPEI and other drought-related variables where such comparison is expected to aid in addressing impacts of droughts on agriculture. The SPEI is also applied to estimate the drought return periods for a given severity and intensity amounts, as well as to analyse the multi-scalar properties for drought monitoring. This objective is addressed in Chapters 4 and 5.

(2) **To model joint distributions of SPEI and severity-intensity-duration with climate mode indices using multivariate copula functions to examine the risk and return periods and to emulate conditional probabilistic predictions**. This objective evaluates the potential utility of vine copula for studying multivariate associations of SPEI and drought properties with the synoptic scale climate mode indices that act to influence the severity of droughts. The vine copula is also used to develop the probabilistic drought prediction model using the information from climate mode indices. The conditional joint probabilities and joint return periods elucidates the importance of multivariate copula modelling for drought-risk assessment. This objective is addressed in Chapter 6.

(3) **To devise an appropriate drought-risk index by integrating hydro-meteorological and physiographic factors using fuzzy logic algorithms to assess drought-risk temporally and spatially**. This objective assesses drought-risk in both temporal and spatial context using multiple hazards, vulnerability and exposure factors. The subjectivity in the drought assessment is minimised by the incorporation of the fuzzy logic algorithm. This objective is addressed in Chapter 7.

7

The three objectives of this study are illustrated in Figure 1.1 below.
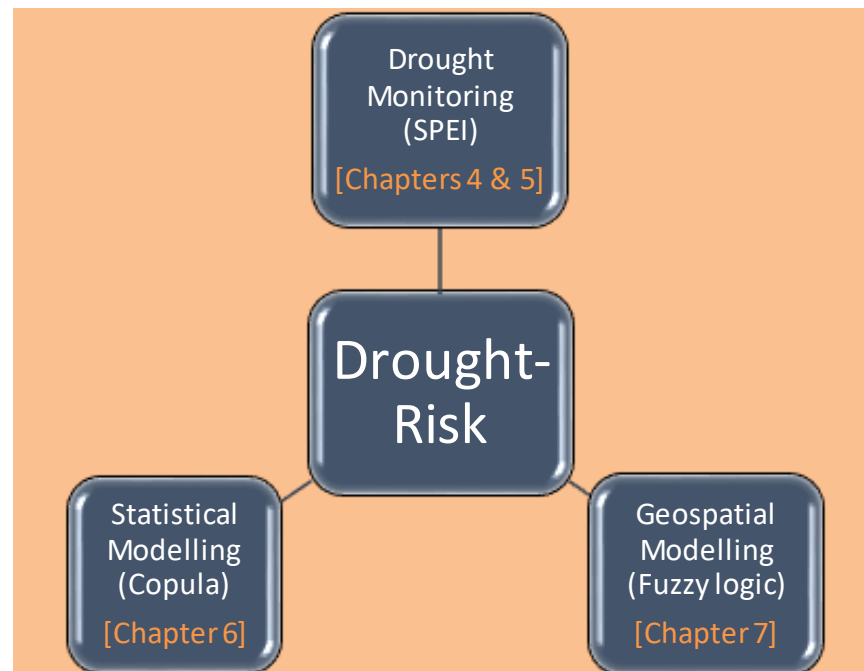
Figure 1.1: Three main objectives of this study.

In achieving these objectives, this study hypothesises that: "*statistically and spatially explicit drought-risk models can provide sets of information that are useful in planning and developing strategies from the potential effects of extreme drought events to agriculture and availability of water resources*".

1.4 Significance of the Study

To develop robust drought management strategies, including adaptive and mitigation measures for drought, a framework that can combine multiple intelligent techniques for assessing the drought risk is extremely crucial.

The new knowledge gained from this study can contribute to improving our understanding of the drought characteristics: onset, termination, duration, severity and intensity in the study regions. A framework for drought-risk comprising spatial maps of drought-risk, and joint distribution for drought characteristics with conditional return periods and drought predictions, can strongly disseminate drought-risk information and serve as the strong basis for policy and management strategies for drought mitigation and adaptation. The study also presents a novel application of the GIS-based fuzzy logic tool to include various physiographic and hydro-meteorological parameters that are expected to lessen the amount of subjectivity in drought vulnerability and risk assessments. The techniques evolved from this study can be made applicable to other drought-prone regions globally.

It is especially noted that drought-risk studies through multivariate modelling and elucidation of its properties in respect to universal precursors (*i.e.,* climate mode indices) are centrally important for agricultural water management, and decision-making by farmers and the populations in south-east Queensland where drought is considered a perpetuating risky phenomenon. Therefore, this study offers new insights to the body of knowledge in drought-risk management.

1.5 Organisation of the Thesis

This thesis is organised into eight chapters:

Chapter 1 presents the introductory background to the research, identifies the research problems and significance of the study, and sets out the objectives.

Chapter 2 reviews the subjects of knowledge that are relevant to this study: drought monitoring, drought modelling, and spatial representation of drought-risk. Discussion on existing drought monitoring indices, suitability of the SPEI, copula for probabilistic drought predictions as well as drought vulnerability and risk assessment is done.

Chapter 3 describes the study area, data and discusses scope and limitation of the study. This chapter serves as the gateway to Chapters 4-7.

Chapter 4 presents the methodology and first set of results in response to the first objective of the study. Here, the SPEI is compared with other precipitation-based drought indices and its selection for this study is justified.

Chapter 5 presents the methodology and second set of results in response to the first objective of the study. Here, the SPEI is evaluated and affirmed its suitability for drought monitoring and characterising purposes.

Chapter 6 presents the methodology and third set of results in response to the second objective of the study. Here, the copula models are used to derive joint distributions of SPEI and drought properties (duration, severity and intensity) coupled with climate mode indices. Subsequently, the development of probabilistic prediction models is made using the joint distribution of multiple variables.

Chapter 7 presents the methodology and fourth set of results in response to the third objective of the study. Here, geospatial representation of drought-risk is made using the fuzzy logic algorithm.

Finally, *Chapter 8* covers the conclusion and recommendations for future work.

Chapter 2

LITERATURE REVIEW

Chapter 1 has presented the overview of the research problem and objectives in regards to the development of the drought-risk assessment framework. This second chapter presents a general review of the literature and then discusses research problems on drought monitoring, modelling and risk-assessment studies in detail. This chapter also establishes the niche for drought-risk management, as well as the relevant sciences and technologies (statistical and geospatial) tools. In brief, Chapter 2 provides the journey towards exploring the relationship of the three major components of this study: (1) characterisation of drought events using the SPEI time series; (2) statistical drought modelling using joint distribution of the SPEI and its properties with climate drivers (climate mode indices); and (3) assessment of drought-risk on temporal and geospatial scales.

2.1 Bureau of Meteorology definitions of drought

The Australian Bureau of Meteorology (BoM) defines meteorological drought as 'acute water shortage', which is indicated by the rainfall deficiency for over three months (BoM 2015). The monthly-standardised metric used by BoM to identify drought conditions is the RDDI, which is a measure of rainfall deficiency in terms of *serious* or *severe* that have occurred for three months or more. The *serious* rainfall deficiency is met when the rainfall lies above the lowest five percent of recorded rainfall but below the lowest tenth percentile (decile range 1) for the period in question. A *severe* rainfall deficiency occurs when the rainfall is among the lowest five percent for the period in question. This definition of drought is solely dependent on rainfall due to the availability of long-term record of rainfall data across most of Australia,

hence does not take into account other variables such as temperature and evaporation that are essential for establishing climatic surface water balance. Figure 2.1 shows the spatial distribution of rainfall in terms of the deciles for part of the Millennium Drought (1/11/2001 to 31/10/2009) in southeast Australia with significant rainfall deficiency.
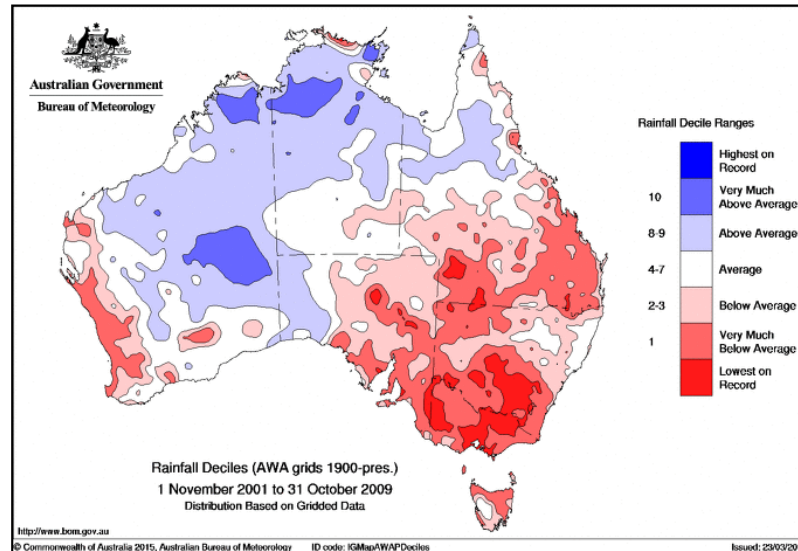
Figure 2.1: Rainfall deciles for the period 1 November 2001 to 31 October 2009 [Source: Australian Bureau of Meteorology].

The Australian BoM currently provides seasonal climate outlook for one to three months ahead that are updated monthly. The outlooks are generated by the Predictive Climate Ocean Atmosphere Model for Australia (POAMA), which is a dynamical (physics based) climate model developed by the BoM and Commonwealth Scientific and Industrial Research Organization (CSIRO) Marine and Atmospheric research division. In 2014, the Australian government announced a significant investment in the capabilities of BoM through the purchase of a new supercomputer that would deliver high-quality forecasts and warning services across Australia through an initiative called White Paper Actions (Commonwealth of Australia 2017). In the Agricultural Competitiveness White Paper, the government allocated $3.3 million to BoM to implement better seasonal forecasts for farmers by providing forecasts that are: (1) more localised – by increasing the modelling spatial resolution from current 250 km to 60km, (2) more frequent – weekly updates rather than monthly, and (3) more accurate. While these initiatives are useful, there remains a dire need for improvement and advancement on the computational aspect of dissecting drought

characteristics (*e.g.,* duration, severity, intensity) in order to understand the phenomenon even better and develop more strategic mitigation plans.

2.2 Drought Monitoring

Why is it important to monitor droughts? Droughts are a normal part of the climate system and occur in virtually all climate regimes globally, including deserts that are naturally arid. According to Wilhite (2000), drought is the most costly natural disaster on a year-to-year basis, with impacts being extremely significant and widespread, affecting many people and economic sectors at any one time. The areas affected by droughts are typically larger than any other hazards. The slow onset of droughts allows time to observe changes in precipitation and status of surface and groundwater supply in a region over time. To help track of the drought condition, drought indicators or indices are often used, and these tools vary depending on region and season.

Like other hazards, droughts can be categorised in terms of location, onset, duration, severity, intensity, areal extent and cessation. A range of hydro-meteorological processes that suppress the precipitation and/or limit the surface or groundwater availability resulting in soil moisture deficiency can cause droughts. Therefore, monitoring of droughts is crucial for preparedness and proactive actions in mitigating the impacts. As such, the indicators and indices help identify and evaluate the characteristics of droughts. To monitor different aspects of the hydrologic cycle, a variety of indicators and indices are required. As droughts evolve, the impacts can vary by region and by season, therefore, for drought early warning system, it is important that indicators and indices accurately reflect and represent the impacts.

Droughts are regional in nature and their characteristics are often region-specific, there is thus no universal definition of drought. To circumvent this, Wilhite and Glantz (1985) classified droughts into four categories: meteorological, hydrological, agricultural and socio-economic. Each category uses different indicators for drought monitoring metric calculation. For instance, (1) the meteorological drought is measured in terms of rainfall deficit in relation to the regions average amount. (2) The hydrological drought is measured in terms of streamflow and surface runoffs. (3) The agricultural drought is monitored in terms of soil moisture deficit and evapotranspiration, and (4) the socio-economic drought is assessed in terms of supply

and demand of economic goods during drought conditions. The latter three drought categories lag behind meteorological drought that are all linked to it. A better understanding of the meteorological category of drought can help understand the impacts of other category of events. There is a general consensus that the slow development of drought, often called "creeping nature of the event" poses difficulty in its detection. From the same standpoint, drought preparedness and mitigation plans solely rely on the timely information about their onset, progression and areal extent or coverage (Mishra and Singh 2011; Morid et al. 2006). This very important information is obtained from drought monitoring that is usually performed using Drought Indices, hereafter called DIs. This investigation tests the suitability of standardised precipitation-evapotranspiration index (SPEI) for the first time as the novel application for monitoring and assessing characteristics of drought events in south-east Queensland, Australia.

2.2.1 Existing indices for drought monitoring

Several drought indicators and indices have evolved over the years. Scientists, stakeholders and decision-makers may use indicators and/or indices for drought monitoring purposes. It is important to understand what is meant by the terms 'indicators' and 'indices'. According to WMO and GWP (2016), the *indicators* are "variables or parameters used to describe drought conditions. Examples include precipitation, temperature, streamflow, groundwater and reservoir levels, soil moisture and snowpack", whereas *indices* are "typically computed numerical representations of drought severity, assessed using climatic or hydro-meteorological inputs including the indicators listed above". As opposed to the indicators, DIs are generally standardised metrics that simplify the complex relationships and provide useful communication tools for diverse audiences and users. Indices are used to quantify the drought characteristics that enable drought early warning (Kogan 2000) and drought risk (Hayes et al. 2004) analysis, which in turn allows improved preparedness and contingency planning.

The nature of DIs reflects different drought conditions, *i.e.,* some reflect the climate dryness anomalies (precipitation-based), some correspond to delayed agricultural and hydrological impacts such as soil moisture deficit or reduced reservoir

levels, while some indices represent aggregate nature of meteorological, hydrological and agricultural droughts. There is also a considerable number of indices that use remote-sensing imagery, for *e.g.,* to detect vegetation health as an indicator of droughts. DIs have a wide range of applications, including drought monitoring, prediction, quantitative assessment, and developing management strategies under current climate (Karl 1983) as well as under climate change associated with global warming (Le Houérou 1996).

In the early days, scientists and decision makers would use one indicator or index that was available to them. However, in recent decades, there has been strong global interest for the development of new indices comprising more than one indicator that are suitable for different applications (meteorological, hydrological, or agricultural) and scales (temporal and spatial). Despite many choices, the confusion can arise when trying to determine which indicator or index to use as their suitability depends on the location, area, basin or region. In order for a DI to be useful for operational drought monitoring, Heim Jr (2002) made four recommendations on the data. They are: (1) data need to be available on near-real-time basis; (2) data need to be monitored on national scale; (3) complete and reliable historical data over a common reference period to allow conversion of the observations to meaningful forms that could be merged objectively with other indicators; and (4) data need to be debiased to remove non-climatic influences (Heim Jr 2002). Based on the literature search, some of the commonly used DIs, their applications, strengths and weaknesses are listed in Table 2.1 below. The suitability of an index to one region does not guarantee its suitability to another region as most of these DIs are either region specific or need specific. A comprehensive list of DIs and their properties are available in WMO and GWP (2016) and discussion on popular indices in Zargar et al. (2011), Mishra and Singh (2010) and Heim Jr (2002).

Table 2.1: Commonly used drought indices. After WMO and GWP (2016).

Index Name	Variables Needed	Applications	Strengths	Weaknesses
Percent of Normal (PN) Werick et al. (1994)	P	Can be used for identifying and monitoring meteorological, agricultural, and hydrological droughts.	A popular method that is quick and easy to calculate with basic mathematics.	What is normal for an area is a calculation that some will confuse with mean or average precipitation. It is hard to compare different climate regimes with each other, especially those with defined wet and dry seasons.
Standardised Precipitation Index (SPI) McKee et al. (1993)	P	Can be calculated at various timescales that allows for applications across meteorological, agricultural, and hydrological drought events. Meteorological drought events may focus on SPI values of 3 months or less; agricultural drought events, values of 6 months or less; and hydrological droughts, values of 12 months or longer, give or take. The SPI can also be calculated on gridded precipitation data sets, which allows for	Using only precipitation data is the greatest strength of the SPI, as it makes it very easy to use and calculate the index. It is applicable in all climate regimes. It can be computed for short periods of record, which contain missing data, is also valuable for those regions that may be data poor or lacking long-term, cohesive data sets. The program used to calculate the SPI is easy to use and readily available. The ability to be calculated over multiple timescales	With precipitation as the only input, the SPI falls short when accounting for the temperature component, which is important to the overall water balance and water use of a region. This drawback can make it more difficult to compare events of similar SPI values but different temperature scenarios. The flexibility of the SPI to be calculated on short periods of record, or on data that contains many missing values, can also lead to misuse of the output, as the program will provide output for whatever input is provided. SPI requires a long span of data, at least 50years.

16

		a wider scope of users than those just working with station-based data.		
Standardised Precipitation-Evapotranspiration Index (SPEI) Vicente-Serrano et al. (2010)	P, T	With the same versatility observed with the SPI, the SPEI can be used to identify and monitor conditions associated with meteorological, agricultural, and hydrologic drought conditions.	The inclusion of temperature data along with precipitation allows the SPEI to account for the impact of temperatures on a drought situation. The output of the SPEI is applicable for all climate regimes, with the results being comparable side by side as the results are standardised. With the use of temperature data, the SPEI is an ideal index when looking at the impact of climate change on model output under various future scenarios.	The requirement of needing a serially complete data set for both temperature and precipitation may limit the use of the SPEI because the available data may not allow it to be used. Being a monthly index, rapidly developing drought situations may not be identified quickly.
Rainfall Anomaly Index (RAI) Van Rooy (1965)	P	Addresses meteorological, agricultural, and hydrological drought, as the RAI is flexible in that it can be analysed at various timescales.	Ease in calculations with a single input (precipitation) that can be analysed on monthly, seasonal, and annual scales.	The index requires no missing data, and a serially complete data set with estimates of missing values is needed. Variations within the year need to be small compared to the temporal variations. Missing data need to be accounted for to create a serially complete data set.
Rainfall Decile based Drought Index (RDDI) Gibbs and Maher (1967)	P	With the ability to look at different timescales and time steps, deciles can be used in meteorological, agricultural, and hydrological drought situations.	With a single variable being considered, the methodology is simple and flexible for many situations. With clearly defined thresholds, the current data is put into a historical context and drought status can be recognized. Useful in both wet and dry situations.	As with other indicators that only use precipitation, the impact of temperatures and other variables are not considered in the development of drought. A long period of record will provide the best results because

				many wet and dry periods will be included in the distribution.
Palmer Drought Severity Index (PDSI) Palmer (1965)	*P, T, AWC*	Developed mainly as a way to identify agricultural droughts, the PDSI has been used in identifying and monitoring meteorological and hydrological droughts as well. With the longevity of the PDSI, there are numerous examples of how the index has been utilized over the years.	The PDSI is used around the world and the code and output are widely available. With the legacy of the index, the scientific literature is full of papers related to the PSDI. The use of soils data and a total water balance methodology makes the PSDI quite robust in identifying drought.	The need for serially complete data will make using the PDSI problematic for some. The PDSI has a timescale of approximately 9 months, which leads to a lag in identifying drought conditions based upon the simplification of the soil moisture component within the calculations. This lag may be up to several months, which is a drawback when trying to identify a rapidly emerging drought situation. Seasonal issues also exist, as the PDSI does not handle frozen precipitation or frozen soils well.
Self-Calibrated Palmer Drought Severity Index (sc-PDSI) Wells et al. (2004)	*P, T, AWC*	Can be applied to meteorological, hydrological and agricultural drought.	Is specific to the station location allowing for more accurate comparisons between regions. Can be calculated on different timescales.	The methodology is not significantly different from PDSI. It has same issues as PDSI in terms of time lag and frozen precipitation and frozen soils.

China Z Index (CZI) Kendall and Stuart (1977)	*P*	Similar to the SPI, in which both wet and dry events can be monitored over multiple timescales. Drought applications would apply to meteorological, agricultural, and hydrological droughts.	Simple calculations, which can be computed for several time steps. Can be used for both wet and dry events. Allows for missing data, similar to the SPI.	The Z-Score data does not require adjusting the data by fitting them to the Gamma or Person Type II distributions, and it is speculated that because of this, shorter timescales may not be represented as well compared to the SPI.
Crop Moisture Index Palmer (1968)	*P, T*	Used to monitor droughts where agricultural impacts are the primary concern.	The output is weighted, making it possible to compare different climate regimes. Responds quickly to rapidly changing conditions.	It was developed specifically for the grain-producing region in the United States, therefore CMI may show a false sense of recovery from long-term drought events, as improvements in the short term may be insufficient to offset long-term issues.
Soil Moisture Deficit Index (SMDI) Narasimhan and Srinivasan (2005)	*Mod*	Useful for identifying and monitoring short-term drought affecting agriculture.	Takes into account full profile as well as different depths, making it adaptable to different crop types.	Calculations are based upon the output from SWAT model and there are auto-correlation concerns when all depths are being used.
Reclamation Drought Index (RDI)	*P, T, S, RD, SF*	Used mainly to monitor water supply for river basins.	Specific to each basin. Accounts for temperature effects on climate.	Calculations are made for the individual basin, so comparisons are hard to make.

19

Weghorst (1996)			Standardised scale allows for monitoring of wet and dry conditions.	Putting together all inputs in operational setting may cause a delay in data production.
Surface Water Supply Index (SWSI) Shafer and Dezman (1982)	P, RD, SF, S	Used to identify droughts associated with hydrological fluctuations.	Taking account of full water resources of a basin provides a good indication of the overall hydrological health of particular basin or region.	The index has to undergo recalculation when data source changes or inclusion of additional data, making it difficult to construct a homogeneous time series. Calculations vary between basins, making it difficult to compare.
Effective Drought Index (EDI) Byun and Wilhite (1999)	P	The EDI is a good index for operational monitoring of both meteorological and agricultural drought situations because its calculations are updated daily.	With only a single input needed for calculations, it is possible to calculate the EDI at any location where precipitation is recorded. Support documentation explaining the processes are available for the program. The EDI also is standardised so that outputs from all climate regimes can be compared. The EDI is effective in identifying the beginning, ending, and duration of drought events.	With only precipitation accounted for, the impact of temperatures on drought situations is not directly acknowledged. With using daily data, it may be difficult to use the EDI in an operational situation as daily updates to input data may not be possible.

Acronyms: *P*: Precipitation, *ETo*: Evapotranspiration, *T*: Temperature, *AWC*: Available Water Capacity, *RD*: Reservoir, *S*: snowpack, *SF*: streamflow, *mod*: modelled.

2.2.2 Selection of indicators and indices

Just as there is no single definition of drought, there is no single indicator or index that is suitable for all drought types, climate regimes and sectors affected by droughts. Also, the simplest indicator/index may not necessarily be the best or most applicable for the region. The drought analyst must feed in many factors before determining which indicator, index (or both) to use for the particular need or application. Some of the questions that the drought analyst may need to consider include: (1) is the indicator/index sensitive to climate, space and time in order to determine the accurate onset and cessation of drought? (2) does the indicator/index allow for timely detection of drought in order to trigger appropriate communication and coordination of drought mitigation or response actions? (3) are data and resultant indicator/indices reliable? *i.e.,* are the data available for a long period of record in order to understand historical droughts? and (4) is the indicator/index easy to implement? (WMO and GWP 2016). For the evaluation of meteorological DIs, Keyantash and Dracup (2002) suggested considering six criteria: robustness, tractability, transparency, sophistication, extendability and dimensionality.

2.2.3 Comparison of existing drought indices for quantifying drought events

Several meteorological DIs and their inter-comparisons are available in published literature. A thorough review of meteorological-based DIs can also be found in Mishra and Singh (2010) and Zargar et al. (2011). In previous studies, one can notice that there are some limitations with all of these indices, which originate from various factors that make it difficult to apply them universally. Common concerns to consider are: (1) definition of the period of water deficit; (2) definition of the time unit of assessment where many DIs utilise monthly or longer periods that may not measure the short-term or medium-term precipitation return to normal; (3) lack of a rationale for the storing term for water resources to account for changes in soil moisture or factors such as evaporation; and (4) the type of data used in the DI calculation where most DIs only uses current rainfall data with no rationale on how the antecedent rainfall will change with time compared to the current rainfall. Table 2.2 below provides a summary of the

studies that have compared popular indices for drought monitoring and modelling for future climate change scenarios.

Table 2.2: Studies comparing various drought indices.

Study	Indices Compared	Notes and Outcomes	Recommendations
Mpelasoka et al. (2008) Australia	RDDI and SMDDI	Indices were used to assess future drought events over Australia under global warming attributed to low and high greenhouse gas emission scenarios for 30-year periods, centred on 2030 and 2070. Both indices showed a general increase in drought frequency associated with global warming. *ETo* and *T* were important in determining the severity of droughts and be even more as climate changes in warmer conditions.	SMDDI appeared to be more relevant to resource management as it accounts for 'memory' of water status. Considering soil-moisture delays tend to indicate realistic severity and persistence for drought events, meteorological drought indices (*i.e.,* RDDI) were inadequate for reliable assessment of drought.
Morid et al. (2006) Tehran, Iran	Decile Index, PN, SPI, CZI, MCZI, Z-Score and EDI	The study compared the performance of seven drought indices for 32-years of data. SPI, CZI and Z-Score performed similarly with regards to drought identification and respond slowly to drought onset. Decile Index appeared to be very responsive to rainfall events of a particular year but had inconsistent spatial and temporal variation. MCSI and PN were not recommended for drought monitoring as they were found to declare 'extreme drought' conditions unreasonably frequently.	SPI and EDI were able to detect drought onset, spatial and temporal variation consistently, thus may be recommended for operational drought monitoring. EDI was found to be more responsive to the emerging drought and overall performed better.

Dogan et al. (2012) Konya, Turkey	PN, RDDI, Z-Score, CZI, SPI and EDI	The study compared drought indices under different climatic conditions and on 18 different timescales. Results showed median timescales were essential for future studies while 1-month timescale was irrelevant in arid/semi-arid regions where rainfall deficiency was common. Drought indices for 6-, 9-, and 12-month timescales were found essential for long-term drought studies, while 1-month drought indices not to be used for comparison studies for the recommendation of an index.	EDI was best correlated with other indices on all timescales and was preferable for monitoring long-term droughts in arid/semi-arid regions.
Barua et al. (2010) Yarra River Catchment in Victoria, Australia.	ADI, SPI, SWSI	The study attempted to show the significance of Aggregated Drought Index (ADI) by considering significant components of the water cycle. The principal component analysis was used to consider hydro-meteorological variables that describe fluctuations in hydrologic cycles. The ADI was compared with SPI and SWSI. ADI incorporated precipitation, evapotranspiration, streamflow, surface reservoir storage, soil moisture content. The main advantage of ADI included its assessment of droughts from aggregate perspective of meteorological, hydrological and agricultural water shortages.	ADI was found to be more robust than SPI and SWSI where ADI was able to detect historical droughts more clearly.
Lloyd-Hughes and	SPI and PDSI	The study compared drought indices on timescales 3, 6, 9, 12, 18 and 24 months for the period 1901-1999.	Near-equivalent performance between SPI and PDSI was demonstrated on timescales 9 to 12 months.

Saunders (2002) Europe		Trends in SPI and PDSI values indicated the proportion of Europe experiencing extreme and/or moderate drought conditions changed insignificantly during the 20th century.	Overall, SPI provided better spatial standardization than PDSI. SPI was recommended for it is a simple and effective tool for the study of European droughts.
Dubrovsky et al. (2009) 45 stations in the Czech Republic	SPI and PDSI	The study applied relative SPI and PDSI to assess climate-change impacts on drought conditions over 1961-2000 and 2060-2099 periods. PDSI exhibited the widest spectrum of drought conditions across Czech, in part because it depended not just on precipitation (as does SPI) but also on temperature. In future climate analysis, SPI-based drought risk closely followed modelled changes in precipitation while PDSI indicated an increase in drought-risk.	The study concluded on PDSI being more appropriate for use over SPI in assessing the potential impact of climate change on future droughts.
Pandey et al. (2008) Orissa, India	SPI and EDI, Decile Index, Departure from long-term mean and median	This study has used SPATSIM for drought analysis on monthly (SPI, Decile Index, Departure from long-term mean and median) and DWRAM software for daily (EDI) bases. All SPI, EDI and annual deviation from mean showed a similar trend of drought severity.	EDI better-represented droughts in any area over other DIs. Decile index was found to be not suitable.
Heim Jr (2002)	Munger's, Kincer's, Marcovitch's,	This study showed how the insights into the understanding of droughts have changed over past hundred years.	Author complemented on newer indices where incorporation of evapotranspiration as a measure of water demand had led to a

USA	Blumenstock's indices, API, MAI, PDSI, PHDI, CMI, K-BDI, SWSI, SPI, VCI, DM		landmark development, and that indices must address the total environmental moisture status. The Drought Monitor (DM) index has shown a considerable progress with comprehensive, objective national drought index.
Keyantash and Dracup (2002) Oregon, USA	*Meteorological*: DCPA, RD, PDSI, DAI, RAI, SPI *Hydrological*: TWD, CSA, PHDSI, SWSI *Agricultural*: CMI, PMAI, CSM, SMAI	This study carried out a comprehensive evaluation of most prominent drought indices in meteorological, hydrological and agricultural categories using the weighted set of six criteria: robustness, tractability, transparency, sophistication, extendability, and dimensionality. Drought indices were ranked in terms of usefulness for the assessment of drought severity, for two test regions.	The evaluation scores showed overall superior drought indices were rainfall deciles (RD), total water deficit (TWD) and computed soil moisture (CSM) for meteorological, hydrological and agricultural drought, respectively.
Jain et al. (2015) Ken River Basin, India	SPI, EDI, Z-Score, CZI, RD, RDDI	DIs on five timescales (1, 3, 6, 9 and 12-months) were compared with each other (monthly) and with EDI (daily). 1-month timescale may produce erroneous estimates of drought duration and 9-month timescale was best correlated.	RD and RDDI were not recommended due to their disagreement on estimates of drought duration and frequencies with other indices. EDI was found to be more suitable for the study region for its better correlation with other indices at all timescales, with highest at 9-month timescale.

2.2.4 Standardised Precipitation-Evapotranspiration Index (SPEI) for drought monitoring

In the current era, it is a common knowledge that drought events, as prolonged climatological deficits in precipitation, continue to foster serious hydrological imbalances (Wilhite and Glantz 1985), and trigger agricultural, health and environmental repercussions (Wilhite et al. 2014). Objective characterisation of drought in terms of duration, severity, intensity (*D-S-I*) properties and the spatial extent and inter-arrival times is naturally difficult since drought exhibits a creeping nature with a slow emergence profile. Therefore, DIs that provide normalised comparisons of drought in climatologically diverse regions, are normally applied to monitor a drought event. As a supply-side assumption, droughts are primarily driven by precipitation variability, however, many DIs neglect the importance of the variables other than precipitation that can act to exacerbate the drought impacts. This study explores, for the first time in the drought-prone zone of southeast Queensland (SEQ), the utility of the SPEI for drought assessments. The SPEI (Vicente-Serrano et al. 2010) has been adopted as a multi-scalar and a relatively new metric, utilising precipitation and estimated reference evapotranspiration for statistical quantification of drought characteristics.

Among various exemplary drought characterisation metrics, some of the widely used DIs (*i.e.,* RDDI, RAI, SPI and EDI) in many studies incorporated precipitation data as the only variable. The SPI is the World Meteorological Organisation (WMO) (Jarraud 2008) recommended drought index for monitoring meteorological drought. However, the requirement of precipitation data only can either be an advantage or a disadvantage, depending on the application region and the purpose. The drawback of the SPI is that it does not have the ability to take increased evapotranspiration into account if the temperature is likely to change due to climate change. In arid or semi-arid regions such as eastern Australia (Deo et al. 2009; McAlpine et al. 2009; Nicholls 2004), drought appears to not only exacerbated by but also be driven by temperature. Similar to SPI, the RDDI currently used by BoM lack the ability to incorporate water supply-demand balance as it also based on the precipitation data only.

The PDSI has been widely adopted for it utilises precipitation, temperature, soil water recharge, runoff, water loss from soil and soil water capacity (Lloyd-Hughes and Saunders 2002) to examine water balance whilst assessing the moisture status in a comprehensive (and hydrologically-relevant) manner. However, it carries some challenges and limitations. While the PDSI is an ideal metric for an assessment of hydrological drought, its high demand for input data and fundamental assumptions make it too complex to account for the physical and biological factors associated with a drought event (Felch 1978). Also, the PDSI appears to be unsuitable for many climatic regions (including Australia) due to its normalisations based on limited comparisons and unsolidified justification by physical and statistical basis (Alley 1984; Gibbs and Maher 1967; Guttman et al. 1992; Keyantash and Dracup 2002). General applicability of the scaling process with a limited number of empirical factors becomes a constraint of PDSI to be applied outside the USA, as questioned by some studies (*e.g.,* (Dai 2011)). A similar sentiment was shared by Redmond (2002), indicating that the creator of PDSI did not intend to apply PDSI beyond the Great Plains in the central USA. Moreover, studies showed that PDSI underperforms for climatic regions with extreme variability of rainfall and run-off, and this is especially true for Australia (Burke et al. 2006). To avoid abovementioned empirical relationships, Wells et al. (2004) developed the self-calibrated PDSI (sc-PDSI). Nevertheless, the necessary data requirement in the sc-PDSI was not reduced.

This study has employed the SPEI, formulated as an improved version of the SPI. Unlike in the case of the SPI, the SPEI has an ability to encapsulate the contributory influence of temperatures on the demand for water, and therefore, it appears to be more suitable for the monitoring of hydrological and agricultural impacts. Also, unlike the case of PDSI, the SPEI is able to operate on multiple timescales (1-48 months), acting as an essential tool for assessment of hydrologic cycles and for accounting for different category of droughts (meteorological, hydrological and agricultural). The SPEI can replicate the sensitivity embedded in the PDSI for the monitoring of hydrological status in terms of the estimated evaporation and transpiration driven by warm temperatures, whilst assessing the multi-temporal nature of drought afforded by SPI. An idealistic characteristic of the SPEI is its ability to capture the evaporative demand of the hydrosphere (*i.e.,* via reference evapotranspiration; *ETo*) and the indicative aberrations in overall water resource

conditions. Other advantages include less data requirement, flexibility, and simple computation. These accord to the viewpoint of Keyantash and Dracup (2002) that a drought metric must be simple, clear, comprehensible and statistically robust, and also be independent of the climatic characteristics (*i.e.,* standardised) to be comparable in the wider temporal and spatial domains across geographically diverse regions. However, the unavailability of *ETo* data for computing the SPEI can be a potential drawback since its estimation requires multiple input variables (*e.g.,* humidity, solar radiation, and wind speed information) for the recommended FAO-56 Penman-Monteith technique (Allen et al. 1998).

Despite its infancy in the hydrologic research community, many case studies performed outside of Australia have applied the SPEI for drought assessment and demonstrated its statistical correlation with hydro-meteorological variables that has drought impacts in such diverse climatic regions. For example, the SPEI was used for drought variability studies (Das et al. 2016; Li et al. 2012; Paulo et al. 2012; Potop 2011), hydrological impact assessments, agricultural drought studies, impact of drought on ecological systems (Barbeta et al. 2013; Cavin et al. 2013; Martin-Benito et al. 2013; Toromani et al. 2011; Vicente-Serrano et al. 2013) as well as in the monitoring of drought events (Fuchs et al. 2012). However, to date, only three studies have applied this index for drought studies in Australia (Dayal et al. 2018; Dayal et al. 2017; Deo and Şahin 2015). Therefore, the successful application of SPEI elsewhere and its features relevant to Australia's climate, *i.e.,* incorporation of evapotranspiration as a measure of water demand, would add to new insights on understanding Australian droughts better and be made recommended for drought monitoring purposes.

2.3 Drought Modelling

The water demand has increased manyfold due to the growth in population and expansion of agricultural, energy and industrial sectors, and partly due to climate change and contamination of water supplies. Droughts can affect both surface and groundwater resources, causing further reduction in the water supply leading to crop failure (Riebsame et al. 1991). As such, modelling drought and its components have drawn the attention of meteorologists, hydrologists, ecologists, and agricultural scientists.

2.3.1 Drought forecasts and predictions

Drought forecasting is a critical component of drought hydrology that plays a major role in the risk management, drought preparedness and mitigation. There has been a significant amount of work done on modelling various aspects of drought, such as estimation and prediction of its severity and duration. However, the major challenge has been to develop techniques to forecast drought onset and termination points for months or years in advance (Mishra and Singh 2011). Several studies have predicted drought or its properties using regression, probability, machine learning and hybrid models. For instance, Kumar and Panu (1997) developed a **regression model** to predict grain yield that would in turn aid in the assessment of agricultural drought severity as a function of time. In another study, Leilah and Al-Khateeb (2005) employed statistical procedures to study the relationship between wheat grain and its components under drought conditions of Saudi Arabia. Liu and Juárez (2001) used multiple linear regression techniques to predict drought onset using El-Niño Southern Oscillation (ENSO) indices (independent variables) and satellite-recorded Normalised Difference Vegetation Index (dependent variables). The multiple regression predicts one variable from two or more independent variables, *i.e.,* $Y = a + bX_1 + cX_2 + dX_3$ where Y is the dependent variable (predictand such as drought index) and X_1, X_2 and X_3 are independent variables (predictors such as rainfall, streamflow, and soil moisture) and a, b, c and d are constants. There are several limitations albeit regression models been a commonly used method. One major limitation is the assumption of linearity between predictor (*e.g.,* climate mode indices) and the predictand (*e.g.,* drought index) that makes it less capable for long-term forecasting. This is due to the highly stochastic nature of the environmental factors where the linear relationship may not hold true between variables. The other limitation is the difficulty in understanding causal mechanisms and multicollinearity, *i.e.,* the conceptual framework of the regression models (Mishra and Singh 2011).

The **probabilistic models** are useful for predicting droughts due to their complex nature and the ability to quantify uncertainties associated with hydro-meteorological variables. The Markov chain models have been commonly used for drought predictions. A Markov chain is a stochastic process with a property that at the

value of the process at any time t, the X_t would only depend on its value at a time $t-1, X_{t-1}$, and not in the sequence of values $X_{t-2}, X_{t-3},...,X_0$, which can be written as (Haan 2002):

$$Prob\left(X_t = a_j \mid X_{t-1} = a_i, X_{t-2} = a_k, X_{t-3} = a_1,...,X_0 = a_q\right)$$
$$= Prob\left(X_t = a_j \mid X_{t-1} = a_i\right) \qquad (2.1)$$

The $Prob\left(X_t = a_j \mid X_{t-1} = a_i\right)$ is the conditional probability that gives the probability that the process at a time t will be in "state j", given that at a time $t-1$, the process was in "state i" (Mishra and Singh 2011). The $Prob\left(X_t = a_j \mid X_{t-1} = a_i\right)$ is commonly termed as one-step transition probability that is basic to the structure of Markov chains.

The study of Gabriel and Neumann (1962) was among the first to apply Markov chain models for dry spell analysis. Lohani and Loganathan (1997) used a non-homogenous Markov chain model based on PDSI to characterise the stochastic behaviour of droughts for an early warning system. This characterisation was in the form of a decision tree enumerating all possible sequences of drought progression, which was useful for drought management. Bogardi et al. (1994) described that the statistical properties of droughts can be obtained by conditioning monthly drought indices on large-scale atmospheric circulation patterns, which can predict droughts under the changing climate scenarios. Based on the current drought class described by Palmer index, Lohani et al. (1998) forecasted drought conditions for future months using first-order Markov chains. In a different study, Sen (1990) had used the second-order Markov chain to predict possible critical drought durations that may result from any hydrologic conditions during any future periods.

In the recent two decades, studies have shown further usability of Markov chain probabilistic models. For instance, Banik et al. (2002) evaluated probabilities of getting a sequence of wet and dry weeks during monsoon periods in India that would be useful for agricultural planners and irrigation engineers. Ochola and Kerkides (2003) predicted the critical dry spells using the first-order Markov chain by incorporating the concept of conditional probability, Poisson probability distribution function and chi-square. Steinemann (2003) used homogenous Markov model to propose drought trigger preparedness plan at the basin scale based on multiple scales

of SPI, PDSI and PHDI. Paulo et al. (2005) used Markov chain on SPI to estimate the probability, recurrence time of drought classes and expected time for SPI to change from one class to another. In another study, Cancelliere et al. (2007) did a seasonal forecast of the SPI by computing transition probabilities from a current drought condition to one in the future based on the statistics of underlying monthly precipitation. While probabilistic models are appropriate for hydro-meteorological variables, as portrayed in aforementioned studies, developing prediction models that can use joint-distribution of the predictor and predictand can produce outcomes with even higher accuracy. Such models can be developed using copula statistical algorithms.

In the pioneering research on drought modelling, the focus shifted to using **machine-learning** techniques for forecasting and predicting drought events until recently. Artificial Neural Networks (ANN), a non-linear model, has the ability to learn from experience and estimate any complex functional relationship with high accuracy. Application of ANNs for modelling droughts has been shown in many studies. For instance, Morid et al. (2007) predicted quantitative values of drought indices using different combinations of past rainfall, EDI and SPI in preceding months, as well as climate mode indices such as SOI and North Atlantic Oscillation (NAO) as inputs for the model. Mishra et al. (2007) compared linear stochastic models with the recursive multistep neural network (RMSNN) and direct multistep neural network (DMSNN) for drought forecasting. Their study found that RMSNN was useful for short-term drought forecasting while DMSNN for long-term. Deo and Şahin (2015) predicted SPEI for eight candidate stations in eastern Australia using ANN with hydro-meteorological parameters and climate mode indices as the inputs. In a different study, Dayal et al. (2017) used ANN to predict SPEI for assessing drought conditions in the southeast QLD region in Australia. Despite its widespread use, the ANN model has disadvantages of having a black box nature, has a slow response to gradient-based learning algorithm utilised by hidden neurons and is prone to over-fitting.

Extreme Learning Machines (ELM) has become popular in hydrological variable forecasting. Deo and Şahin (2016) used ELM to forecast monthly mean streamflow that has practical implications on the hydrological cycle. In another study, Deo and Şahin (2015) applied ELM algorithms to predict the Effective Drought Index (EDI) in eastern Australia. In a different study, Deo et al. (2017) evaluated the

performance of three standalone models (Multivariate Adaptive Regression Spline (MARS), Least Square Support Vector Machine, and M5 Tree) to forecast droughts in eastern Australia and noted that the MARS and M5 Tree superseded the performance of their counterpart for different stations.

Until recently, the scholars started embracing the **hybrid models** for predicting droughts for improved accuracy and for a higher lead time in comparison to standalone models. For instance, incorporating wavelet transformation to capture useful information at various resolution levels and then using the decomposed sub-signals into the ANN model as several inputs to forecast the desired variable. Kim and Valdés (2003) used hybrid ANN model to forecast droughts using PDSI and recorded improved ability of neural networks to forecast regional droughts. Mishra et al. (2007) combined linear stochastic model and a nonlinear ANN to forecast droughts using SPI where the hybrid model performed with higher accuracy compared to standalone ANN model. Dayal et al. (2016) developed a hybrid model by integrating discrete wavelet with ANN to predict droughts using SPI and noted its outperformance against standalone ANN. Özger et al. (2012) developed a wavelet and fuzzy logic combination model for long lead time drought forecasting and obtained significant improvement over the standalone fuzzy logic model. In another study, the hybrid Adaptive Neuro-Fuzzy Inference System (ANFIS) outperformed ANN in forecasting drought based on SPI (Bacanli et al. 2009). In a recent study, Prasad et al. (2017) developed a hybrid model by integrating wavelet and iterative input selection with ANN (IIS-W-ANN) and M5 Tree (IIS-W-M5) models and found the former model to be a more robust compared to the latter and their standalone counterparts where IIS integration improved the model performance remarkably.

While data-driven models are viable for drought forecasting, they, however, may not be able to capture the dependence between variables. For instance, the drought phenomenon is paradigmatic whereby the characterisation of droughts requires joint analysis of duration, severity, intensity; and so on. As we already know, the hydrological phenomena are often multi-dimensional and hence require joint modelling of several random variables. Therefore, it is often of fundamental importance to be able to link the marginal distributions of different variables in order to obtain a joint relationship describing the main features of the drought events.

2.3.2 Univariate drought modelling

Earlier studies on DIs focused on meteorological, hydrological and agricultural applications that solely depend on measurements of physical characteristics, such as precipitation. While DIs are essential tools for drought monitoring, Dracup et al. (1980) recognised that most research was basin-specific or of particular historical drought events, and consequently have ignored the study of drought in terms of *D-S-I*. However, there was an exception of Yevjevich (1967) study that described hydrologic droughts by their duration, severity, areal extent, the probability of recurrence, onset and termination. That study was applied to annual streamflow with which Yevjevich (1967) developed the theory of run-sum by categorising each hydrologic drought event with its attributes: *D-S-I*.

In terms of risk-based studies, the understanding of the characteristics of drought is paramount for the development of drought management plans. The univariate frequency analysis has been investigated separately for drought properties in many studies, (Cancelliere and Salas 2004; Fernández and Salas 1999; Serinaldi et al. 2009; Tallaksen et al. 1997). However, drought is a complex phenomenon and one variable cannot provide a comprehensive evaluation of drought (Shiau et al. 2007). Likewise, separate analysis of *D-S-I* cannot reveal the significant correlation between them. Hence, drought-risk assessment based on univariate analysis has been overcome by the approach of joint distribution (bivariate) of drought variables - intensity/severity and/or duration/severity (Bonaccorso et al. 2003; Cancelliere and Salas 2010; González and Valdés 2006; Kim et al. 2003; Salas et al. 2005; Shiau and Shen 2001). The limitation of the bivariate analysis was its complex mathematical derivations needed for fitting parameters from observed data (Shiau 2006). This limitation was overcome by the approach of multivariate distributions using copula models.

2.3.3 Use of copula in hydrology

Before copula was introduced in hydrological studies, the most common models then were described by bivariate distributions, such as bivariate normal, log-normal, Gamma, and extreme-value distributions (Genest and Favre 2007). However, these

models had limitations. The variables fit different marginal distributions but the same parametric family of univariate distributions characterised the individual behaviour of the two variables. Also, the dependence between parameters was measured via canonical Pearson's coefficient of linear correlation, which may not hold true or exist for variables attaining non-linear relationships (De Michele et al. 2005). Copula avoids such restrictions and advanced into hydrological studies in the early 2000s (De Michele and Salvadori 2003; De Michele et al. 2005; Favre et al. 2004; Salvadori and De Michele 2004). Copula models have existed in the various field of study, however, its first use in drought-risk studies was in Shiau (2006). The multivariate copula has been used in modelling joint probability distribution, such as in Song and Singh (2010) and Serinaldi et al. (2009). Despite its complex computation, previous studies have indicated that copulae perform well for bivariate problems.

The theory of copula dates back to Sklar (1959) who introduced the notion and the name, *copula* and proved the theorem that now bears his name. This theorem states that if $F_{X_1,X_2,...,X_m}(x_1,x_2,...,x_m)$ is a multivariate distribution function of m correlated random variables, $X_1, X_2,..., X_m$ with corresponding marginal distributions $F_{X_1}(x_1), F_{X_2}(x_2),..., F_{Xm}(x_m)$, then there exists a copula C such that:

$$F_{X_1,X_2,...,X_m}(x_1,x_2,...,x_m) = C\Big[F_{X_1}(x_1), F_{X_2}(x_2),..., F_{Xm}(x_m)\Big] \quad (2.2)$$

Copulae offer greater flexibility to construct a multivariate joint distribution from univariate marginal distributions that are well fitted to the observed data (Nelsen 1999; Sklar 1959).

Shiau (2006) investigated the bivariate joint distribution of drought severity and duration derived from the SPI in the southern Taiwan, using the theory of copula. Since then a number of studies applied copula to assess drought-risk in terms of joint return periods and the conditional probability of occurrence (of *e.g.,* severity) given a certain threshold of another parameter (*e.g.,* duration). For instance, Song and Singh (2010) derived and modelled the joint probability distribution function of drought duration, severity and inter-arrival time using the Plackett copula, for a case study in China. In fact, there are different types of copula family where each family is known to have different characteristics. Janga Reddy and Ganguli (2012) tested classes of four

different copulae – Archimedean, extreme value, Plackett, and elliptical families for modelling the bivariate joint distribution of drought characteristics and their analysis found Gumbel-Hougaard copula (from extreme value family) performed better compared to other classes of copulae. Using Gumbel-Hougaard copula, they then derived drought severity-duration-frequency (*S-D-F*) curves, where *S-D-F* were extracted from SPI, for the western Rajasthan region in India. In separate studies, Shiau et al. (2007), Shiau and Modarres (2009) and Shiau (2006) modelled bivariate joint distribution of drought duration and severity using two-dimensional copulae to evaluate drought frequency.

Droughts are regional in nature and the most appropriate copula for deriving joint distributions of drought properties may not be the same for every region. For instance, Lee et al. (2013) studied the influence of tail shapes of four copulae: Gumbel-Hougaard, Frank, Clayton and Gaussian copula for bivariate frequency analysis of drought properties in Iran and Canada. Their findings showed that Clayton copula was not an appropriate choice for drought modelling because the dependence between two variables in the upper tail of Clayton copula was very weak and resembled that of the independence case, while Frank and Gumbel-Hougaard copula were recommended for application based on their better performance. Sadri and Burn (2012) studied copula-based pooled frequency analysis of droughts in Canadian prairies using severity and duration properties extracted from the monthly streamflow data. They used Gumbel, Clayton and Frank copulae for bivariate frequency analysis and their results suggested that longest droughts do not necessarily correspond to the most severe one and that droughts occur in almost all regions, humid or arid. They also showed that copula-based model provided shorter return periods compared to bivariate Gamma distribution for the same value of duration and severity. Reddy and Ganguli (2013) presented a spatio-temporal analysis of droughts using the 6-month SPI that showed an increase in the frequency of droughts in the central part of their study region, western Rajasthan India. The Gumbel-Hougaard copula among Frank and Plackett copulae best represented the joint dependence between drought variables and assessed conditional return periods and intensity-area-frequency (*I-A-F*) curves that helped in evaluating the drought-risk in a given region.

Similarly, several other studies have used copula for multivariate distributions in order to overcome the difficulties of representing drought frequency analysis using

single variables that cannot reveal the significant correlations between other drought properties. For example, copulae have been used for rainfall frequency analysis (De Michele and Salvadori 2003; Grimaldi and Serinaldi 2006; Kao and Govindaraju 2007; Kuhn et al. 2007; Zhang and Singh 2007), flood frequency analysis (Favre et al. 2004; Renard and Lang 2007; Shiau et al. 2006; Wang et al. 2010; Zhang and Singh 2006), and drought frequency analysis (Kao and Govindaraju 2010; Shiau and Modarres 2009; Song and Singh 2010; Song and Singh 2010). The aforementioned studies described the ability of copula statistical models for assessing the risk associated with drought hazard, yet its application for Australian droughts has been limited to only three studies, Wong et al. (2008), Wong et al. (2009) and Wong (2013).

2.3.4 Role of climate mode indices on droughts

Many climate drivers influence Australia's weather. The large-scale global atmospheric circulation such as ENSO has a major effect on Australia's rainfall. The ENSO phenomenon is described as large-scale interactions between the ocean and atmospheric circulations in the equatorial Pacific Ocean. An El-Niño occurs when the sea-surface temperature (SST) in the central and eastern tropical Pacific become substantially warmer than average, causing a shift in the atmospheric circulation. During El-Niño, Australian rainfall is usually reduced through winter-spring, particularly across eastern and northern parts of the continent. It is important to note that the strength of El-Niño is not directly proportional to the reduction in Australian rainfall amounts. Even though most major Australian droughts have been associated with El-Niño, however, not all widespread droughts have occurred with every El-Niño events. In Australia, it is usual to take persistently negative Southern Oscillation Index (SOI) as an indicator of an El-Niño event where such events are associated with droughts. The SOI is defined to be the sea-level pressure difference between Tahiti and Darwin. The intensity of El-Niño can also be classified based on the SST anomalies exceeding a pre-selected threshold in a certain region of the equatorial Pacific, *i.e.,* Niño 3, Niño 3.4, Niño 4 and Niño1+2 regions. The positive SST departure from the normal greater than or equal to +0.5°C indicates El-Niño condition.

There is no single climate driver of drought in southeast Australia. Besides ENSO, previous works have shown several other climate drivers affect Australian

climate on inter-annual to multi-decadal timescales *e.g.,* (Hendon et al. 2007; Kiem and Verdon-Kidd 2010; Kiem and Franks 2004; Meneghini et al. 2007; Verdon et al. 2004). For instance, the Federation Drought was mostly driven by ENSO, the WWII Drought was at large driven by Indian Ocean Dipole (IOD) but ENSO and Southern Annual Mode (SAM) also had some influence, and the Millennium Drought was mostly driven by ENSO and SAM (Verdon-Kidd and Kiem 2009). However, authors also acknowledge several challenges, where anticipating the future droughts to be systematically different from the past ones is one of them. Therefore, climate forecasting (both short and long-term) needs to account for all climate mode and their interactions in order to be successful.

2.3.5 Copula-based drought analysis using climate mode indices

The southeast Australian rainfall is influenced by many climate drivers where ENSO, SAM, IOD, as well as Inter-decadal Pacific Oscillation (IPO) are described as most influential (Verdon-Kidd and Kiem 2010). A handful of studies have incorporated climate mode indices in the copula models to assess risks associated with droughts, *e.g.,* Wong et al. (2009) and Ganguli and Reddy (2013). These studies provided useful information on incorporating climate mode indices, they however only considered ENSO, and also carried out analysis for three ENSO states separately. It would be very useful for management of water resources if other climate mode indices were also conditioned upon drought properties (such as duration, severity and intensity) as well as on the drought-monitoring index (such as SPEI) to make probabilistic predictions using the information of climate mode indices alone. The two studies discussed next address this need, but for the precipitation forecast by applying vine copula algorithms.

Khedun et al. (2014) used ENSO and Pacific Decadal Oscillation (PDO) and assessed their seasonal correlation with precipitation for the state of Texas, USA. They developed the bivariate and trivariate copula-based models to examine the dependence structure between large-scale climate mode indices and average monthly seasonal precipitation. The most suitable copulae for different climatic (semi-arid, wet, and subtropical humid) regions were used to simulate the precipitation anomalies. Their analysis showed the inclusion of PDO improved simulation results and also the trivariate models performed better in predicting droughts due to La-Niña and negative

PDO conditions. A recent study by Nguyen-Huy et al. (2017) employed vine copula to examine the influence of ENSO and IPO Tripole Index (TPI) on Spring season precipitation forecasting in the agro-ecological zones in Australia's wheat belt. They developed bivariate and trivariate copula models that could capture the single (ENSO) and dual (ENSO & TPI) predictor(s) influence on the seasonal rainfall from a total of ten *one-* and *two-*parameter bivariate copulae from Elliptical and Archimedean families. Their results ascertained the success of copula models for investigating the joint behaviour of seasonal precipitation with climate mode indices. As such, copula-based probabilistic forecasting has significant implication for water resource and crop health management.

To date, copula applications have shown significant importance in hydrology. The need for research in order to understand and be able to provide forecasts of potential magnitudes of drought characteristics ahead of time is a never-ending endeavour. The application of vine copula for multivariate drought-risk assessment is yet to be tested for Australian droughts, therefore such investigation would add new insights on an understanding of drought characteristics and their return periods to a greater depth.

2.4 Geospatial Representation of Drought-risk

The impact of droughts can be mitigated through effective drought management and mitigation. While numerous studies have focussed on temporal modelling of drought-risk in Australia *e.g.,* (Dayal et al. 2016; Dayal et al. 2017; Deo et al. 2017), the spatial assessment in terms of mapping drought-risk has been limited. Drought-risk is a function of vulnerability, exposure and hazard, where vulnerability refers to the degree of the susceptibility of a society to the natural hazard either as the result of varying exposure to the extreme event or because of the variations in the ability to cope with the impacts (Downing and Bakker 2000; Pandey et al. 2010; Tánago et al. 2016). The term *hazard* is often confused with *disaster*. Hazard signifies the potential while the disaster is the actual event. The risk is the probability or chance that hazard poses (Pradhan 2011), and consequently can be reduced by developing a suitable risk management plan, which is important in ensuring the safety of the community and environment.

Care must be taken when using the term *vulnerability* as it has a different meaning in a different context. For instance, vulnerability and adaptation come in many terms viz., vulnerability, resilience, sensitivity, resilience, adaptation, adaptive capacity, hazard, risk, coping range, adaptation baseline, and so on (Adger et al. 2002; Burton et al. 2002; Parry et al. 2007). The drought vulnerability of a region basically depends on the degree of exposure to drought and the regions' ability to cope with the impacts. The level of drought-risk of a region is subject to change over time because the vulnerability component is dynamic in nature, *i.e.,* the vulnerability has temporal and spatial dimensions that change constantly due to changes in technology, land use, population density, practices and policies (Downing and Bakker 2000; Wilhite 2000). Hence, vulnerability manifests time and space specificity that relates to the context and to the perspective of the analyst who is assessing it (Adger 2006). Therefore, the context-specific nature of vulnerability means that there can be no single, unified, or general approach to conceptualising it (Thomas et al. 2016). Adger (2006) demonstrated that the challenges for vulnerability research are to develop robust and credible measures, to incorporate diverse methods that include perceptions of risk and vulnerability, to incorporate governance research on the mechanisms that mediate vulnerability and eventually promote the adaptive action and resilience.

2.4.1 Vulnerability assessment

The growing interest in the development of methodologies for policy making in the context of climate change is making the drought vulnerability and risk assessment an active area of research. The assessment of drought vulnerability and risk is a new paradigm for drought management, which is expected to benefit decision-makers to prepare for droughts, manage resources and mitigate the impacts. The climatic events or other static or semi-static factors such as technology, population behaviour, practices and policies vary albeit over longer-term scales, making the vulnerability assessment a challenging task. Drought vulnerability is different for different individuals, seasons, regions and nations. Due to the complex nature of droughts, the vulnerability assessments become mainly subjective and vary between regions and hazard potential. Therefore, the continuous assessment of drought vulnerability and risk on spatial scale is as important as temporal and has been addressed in the literature,

e.g., (Downing and Bakker 2000; Ekrami et al. 2016; Hewitt 2014; Jain et al. 2015; Pandey et al. 2010; Tánago et al. 2016; Thomas et al. 2016; Wilhelmi and Wilhite 2002).

The drought vulnerability assessment is a relative measure due to its region-specific nature, therefore the analyst must define the critical levels (Downing and Bakker 2000). There are numerous factors that influence drought vulnerability in a region (Price et al. 2011) and their inclusion for assessment may depend on the data availability. The available information on drought vulnerability of the region can help the decision makers and water management committees to identify appropriate mitigation actions to lessen the impacts of future droughts. Undeniably, the drought vulnerability has a close correlation with man-made infrastructure and socio-economic conditions (Wilhelmi and Wilhite 2002). As mentioned earlier, drought vulnerability varies between nations whereby in developing countries the livelihood and ability to maintain production systems are threatened, whereas in developed countries the economies, public enterprises, commercial infrastructures and governments are impacted by droughts. Therefore, the region-specific integrated physiographic, climatic and social factors are critical for assessment of drought vulnerability, and this approach is yet to be tested on Australian droughts.

Several studies on vulnerability assessment have been carried out in various disciplines, such as geography, water resources, agricultural science, climate research and social science sectors, *e.g.,* (Baethgen 1997; Eakin and Conley 2002; Wilhelmi and Wilhite 2002). In fact, there have been studies that conceptualised the nature of vulnerability from a theoretical perspective, *e.g.,* (Cutter 1996; Turner et al. 2003; Villa and McLEOD 2002) while others attempted to develop quantitative measures of vulnerability, *e.g.,* (Cutter et al. 2003; Gogu and Dassargues 2000). As previous studies have shown the complexity of the hazard under analysis and the fact that vulnerability is not a direct measurable (or observable) phenomenon, developing measures for quantifying vulnerability has been proven a difficult task (Downing et al. 2001; Luers et al. 2003).

2.4.2 Drought vulnerability assessment

Specific to droughts, there exists a number of studies for vulnerability assessments. The Wilhelmi et al. (2002) study was one of the earlier works that came up with the

idea of integrating various environmental factors using which they developed a numerical weighting scheme to evaluate the agricultural drought potential. Their analysis showed that the most vulnerable areas to agricultural drought were non-irrigated cropland and rangeland on sandy soils in the state of Nebraska, USA. Later, Acosta-Michlik et al. (2006) measured the vulnerability to drought under climatic stress in India using a security diagram concept. They derived environmental stress using indicators of water stress generated from the *WaterGap* model. Dougill et al. (2010) employed dynamic system tools in their study to investigate food system vulnerability to climate change as well as land degradation with the focus on drought sensitivity in the Kalahari region of Botswana. Fraser et al. (2011) provided an overview of the vulnerability to climate change in coupled social-ecological systems.

In another study, Zarafshani et al. (2012) assessed drought vulnerability for three drought intensity levels, *i.e.,* very high, extremely high, and critical areas for the wheat farmers in Western Iran and concluded that farmers' vulnerability is influenced mainly by economic, technical, sociocultural, infrastructural, as well as by psychological factors. Using Me-Bar and Valdes formula, Khoshnodifar et al. (2012) measured drought vulnerability for wheat farmers in Mashhad County, Iran by incorporating economic, social and technical indicators. Babaei et al. (2013) used multi-attribute decision-making methods based on a set of preferences, criteria and multiple indicators to develop a new, highly effective method for spatial assessment of drought vulnerability for Zayandeh-Rood river basin in Iran. Using an indicator-based analysis for assessing drought vulnerability in Africa, Naumann et al. (2014) integrated various renewable natural capital, economic capacity, human and civic resources, infrastructure and technological factors to develop a drought vulnerability indicator (DVI) that reflected different aspects of drought vulnerability level for early warning systems in Africa.

While above studies have indicated various ways to assess drought vulnerability, there are a few that align closely with this investigation. The summary of these studies is given in Table 2.3. In these studies, the authors integrated various physiographic and climatic factors to derive spatial drought vulnerability maps.

Table 2.3: Summary of studies that integrated various physiographic and climatic factors to assess drought vulnerability.

Study	Indicators Used	Method	Index formula
Wilhelmi et al. (2002) **Aim**: derive a framework for the derivation of an agricultural drought vulnerability map through the use of numerical weighting scheme based on GIS tools. **Study region**: Nebraska, USA	Biophysical factors: climate (monthly precipitation) and soils. Social factors: land use and irrigation.	Using GIS to produce composite maps by integrating weighted factors.	Not applicable
Stone and Potgieter (2008) **Aim**: review issues associated with drought risks and vulnerability. Identify factors that define agricultural drought risk and vulnerability in rainfed cropping and agricultural systems. **Study region**: Australia	Plant Available Water Capacity (PAWC), probability of seasonal crop moisture deficiency	Use of inputs from specialist agronomists to produce maps of PAWC. The incorporation of regional shire scale analysis to show regional differences, with the emphasis on the summer crop – sorghum. Use of tactical-scale with the integration of PAWC, soil moisture recharge level, crop simulation model and climate	Not applicable

		forecasting for drought-risk assessment.	
Pandey et al. (2010) **Aim**: devise a suitable method for assessment of vulnerability to drought on the temporal and spatial scale. **Study region**: Ken River system in Madhya Pradesh, India	Topography, land-use types, soil types, the relative availability of surface water and groundwater, water demand and utilization, rainfall departures from the mean.	100 x 100 m grid scale Using GIS to produce composite maps by integrating weighted factors.	$$DVI = \frac{\sum w_i}{kN},$$ **DVI:** drought vulnerability index **N**: number of indicators; **W_i**: weights of drought vulnerability indicators (i=1,2,…N); **k**: upper limit of vulnerability weights (i.e. highest value of W_i)
Safavi et al. (2014) **Aim**: to present an integrated index for assessment of vulnerability to agricultural drought using multiple factors. **Study region**: Zayandehrood River basin, Iran	Land-use, slope, soil type, precipitation, evapotranspiration, temperature, surface water storage, groundwater levels, and environmental needs.	Using GIS for integrated assessment of vulnerability to drought in time and space. Different layers of factors are integrated using numerical weighting scheme.	Not applicable
Yuan et al. (2015) **Aim**: to assess the spatial vulnerability to agricultural using the geographic information system (GIS) technique in order to identify the areas which are the most vulnerable and to	*Sensitivity index*: water resources amount per unit area; irrigation water use rate; sown area rate of farm crops; population density. *Adaptation capacity index*: GDP per capita; net income of residents	Using the VCI formula, the SI and ACI indices were integrated and marginal values for various levels of vulnerability were determined and classified	$VCI = SI + ACI$ $$= \sum_{i=1}^{n} DI_i \times \omega_i$$ VCI: vulnerability composite index; SI:

develop the appropriate mitigation measure **Study region**: Yellow River Basin	in a rural area; the rate of irrigation area to cultivation area; the rate of groundwater resources; effective utilisation coefficient of irrigated water use; land reclamation rate; the rate of the regular secondary school.	according to the equidistant classification method. Use of fuzzy comprehensive evaluation method, multi-layer and multi-index fuzzy clustering iterative model to obtain optimal index weight factor of given accuracy.	sensitivity index; ACI: adaptation capacity index; DI_i: the value of assessment index, i; ω_i: weight of assignment index i.
Jain et al. (2015) **Aim**: propose a method for assessment of drought vulnerability at spatial and temporal scales by integrating relative influence of physiographic, hydrologic and climatic factors at the hydrologic response units (HRU) scale. **Study region**: Ken River system in Madhya Pradesh, India	*Physiographic*: land-use, irrigation support, slope, elevation zone, distance from river reach, soil type, soil depth, population density *Climatic/hydrologic*: rainfall departure, soil moisture deficit index	Using GIS to produce composite maps by integrating weighted factors.	$$IDVI = \frac{\sum_{i=1}^{n} w_i}{\sum_{i=1}^{n} w_{i\,\max}}$$ **IDVI**: integrated drought vulnerability index; W_i: weight scored by HRU
Ekrami et al. (2016)	Slope, aspect, precipitation, geological formation, Qanat	Using GIS and Analytical Hierarchical Process (AHP) technique to	Not applicable

Aim: generate first agricultural drought vulnerability map of Iran. **Study region**: Taft town, Iran	discharge (underground channel), evaporation and soil texture.	produce composite maps by integrating weighted factors.	
Thomas et al. (2016) **Aim**: to develop an approach to measuring the vulnerability to drought using temporary varying factors responsible for drought vulnerability. **Study region**: Bundelkhand, India	Spatial: water demand, topography features such as river basin reach and watershed slope, land use, soil-type. Temporal: rainfall departure from normal, groundwater drought index, soil moisture availability, surface water availability.	50 x 50 m grid scale Using GIS for integrated assessment of vulnerability to drought in time and space. Different layers of factors are integrated using numerical weighting scheme.	Not applicable
Wu et al. (2017) **Aim**: to develop a model for assessing drought vulnerability using the overlay and index method, integrated with normalization, analytic hierarchy process. **Study region**: Guanzhong Plain, China	Precipitation, evapotranspiration, surface water availability, depth to groundwater, well yield capacity, slope, potential water storage of soil, GDP from agriculture	Normalization for assigning rating values, AHP for assigning weights	$DVI = M_w M_R + SA_w SA_R + GA_w GA_R + S_w S_R + P_w P_R + G_w G_R$ M: meteorology, SA: surface water availability, GA: groundwater availability, S: slope, P: potential water storage of soil, G: GDP from agriculture

Few studies have reported uniform weighting scheme to compute the drought vulnerability index using multiple factors by assigning equal importance to these factors. However, it is a well-known fact that various physical, climatic, hydrologic and social factors influence the water demand and availability differently; therefore, different causative factors that could potentially influence the vulnerability of an area to drought hazard should be viewed in accordance with their relative importance. Integration of such information could be of immense help for systematic planning to minimise adverse impacts of drought in appropriately demarcated vulnerable areas. For effective implementation of mitigation measures, hydrologically similar areas could be identified. To address the issue of equal weighting, this study adopts the Bayes theorem to estimate the conditional probability of each factor to the drought hazard in consideration. The Bayes theorem is discussed in Section 7.3.4.

2.4.3 GIS-based integrated fuzzy logic

Fuzzy logic, introduced in Zadeh (1965), is an intelligent technique widely used to map an input space to an output space. The fuzzy set operates over a well-defined range of real numbers (0, 1), reflecting the degree of membership (Pradhan 2011) instead of using crisp sets that only allow values of 0 or 1 (Jun et al. 2013). Therefore, it allows identification of different degrees of impacts instead of overly crude, binary understandings, such as 'vulnerable' or 'non-vulnerable'. It provides a procedure for systematically calculating uncertain, imprecise, or incomplete information used in processing knowledge (Bui et al. 2012). Fuzzy logic enables the exposure and sensitivity levels between municipalities over time by offering a flexible and straightforward standardisation of spatial objects of different values favouring comparison (Espada Jr et al. 2013).

Although fuzzy logic is a traditional concept, its application in Geographic Information System (GIS), however, made a breakthrough in the early 21st century. Pradhan (2011) stated that the use of fuzzy logic in GIS: (1) allows researchers to evaluate complex systems in a practical way, (2) is easy to understand and implement, (3) allows flexibility in the combination of maps, and (4) is easily implemented in the GIS language. Studies that have applied fuzzy logic affirmed that its preference stems from its simple application, *e.g.,* (Gorsevski and Jankowski 2010) as well as that it

47

affords different fuzzy operators (*i.e.,* AND, OR, SUM, PRODUCT, and GAMMA) for solving complex decision-making problems (Lee 2007).

Studies that applied GIS-based fuzzy logic tool have shown its suitability for geospatial mapping. For instance, the fuzzy logic tool was applied to assess groundwater vulnerability and risk to pollution *e.g.,* (Mohammadi et al. 2009; Neshat et al. 2014; Pathak and Hiratsuka 2011; Rezaei et al. 2013). Other areas that embraced the application of fuzzy logic concept in GIS were in the environmental impact assessment (Bojórquez-Tapia et al. 2002), urban vulnerability to earthquake hazards (Rashed and Weeks 2003), land-use suitability analysis (Malczewski 2006), landslide susceptibility maps in Malaysia (Pradhan 2011), modelling of dynamic processes (Dragicevic and Marceau 2000), siting municipal solid waste landfills (Gemitzi et al. 2007), eco-environmental vulnerability assessment for Danjiangkou reservoir in China (Li et al. 2009), vulnerability assessment of buildings from earthquakes (Giovinazzi and Lagomarsino 2004), landslide vulnerability zonation (Sharma et al. 2013), flood vulnerability to climate change (Kang and Lee 2012), urban multi-hazard impact assessment in Chile (Araya-Muñoz et al. 2017), and assessing water-harvesting zones in Iraq (Al-Abadi et al. 2017).

It is apparent that there has been no study to date that investigated the suitability of GIS-based fuzzy logic tools for drought-risk assessment. In particular, the spatial assessment of drought vulnerability and risk assessment using multiple factor integration technique is limited to only one study (Stone and Potgieter 2008) for Australian droughts. Owing to the dire need for an easy to understand and implement a technique for Australian droughts, the incorporation of fuzzy logic tool would be a novel contribution to the scientific community as well as for water resource managers.

2.5 Summary of Chapter

Drought monitoring, modelling, and vulnerability and risk assessment techniques have been reviewed in this chapter. It has been argued that for monitoring droughts in Australia, a DI should not be based on a single variable (*i.e.,* precipitation) only. To address the issue of a sole parameter-based DI, this chapter argued the use of SPEI to be more effective for monitoring and characterising Australian droughts where temperature impact on water resources is critical. This led to the formulation of the

first objective of the study. Also discussed in this chapter is the importance modelling drought-risk using copula models that are useful statistical models for deriving joint return periods and predicting droughts based on derived joint distributions between input and output variables. This led to the formulation of the second objective of the study. Finally, presented also in the chapter is the composition of a drought-risk assessment framework that must include descriptive geospatial representation with minimum subjectivity using the fuzzy logic algorithms. This led to the formulation of the third objective of the study.

Chapter 3

DATA AND STUDY AREA

3.1 Introduction

The previous chapter has reviewed the literature on continuous drought monitoring using the SPEI, modelling the joint behaviour of multiple variables using copula model, spatial representation of drought-risk and the formulation of research objectives for this study. In order to address those objectives, the current chapter outlines the general research design, including a description of the study area, data acquisition and pre-processing. The specific methods are detailed in the respective Chapters 4-7. The methods and frameworks for drought-risk assessment are developed for the southeast Queensland (SEQ) region. However, the developed framework can be applied to any study area of interest where drought is a challenging phenomenon.

3.2 Data

3.2.1 Unprocessed data

Several gridded and point-based data has been used in the study. Gridded at $0.05^{o} \times 0.05^{o}$ (equivalent to 5km$\times$5km) latitude and longitude, the monthly meteorological variables have been obtained from the Australian Water Availability Project (AWAP) historical runs (Raupach et al. 2009; Raupach et al. 2012). The AWAP data availability ranges from 1900 to present, but for this study, only the data from 1915 to 2016 have been considered. AWAP data are *WaterDyn* 26M model output from daily gridded meteorological fields provided by the Australian BoM. The *WaterDyn* model developed by the CSIRO uses raw daily data to model the state and trend of the terrestrial water balance across Australia, using model-data fusion methods

to combine the measurements and model prediction (Raupach et al. 2009). Basically, the AWAP output is composed of a reprocessed meteorological data without any missing values. The raw rainfall and temperature data from BoM are the measurements from a network of rain gauges and weather stations. The gridded rainfall datasets have been produced for up to 7278 rainfall stations across the continent (Gallant et al. 2013).

The AWAP historical runs utilises the BoM Version 3 recalibrated rainfall products that are generated by rescaling daily rainfall at the end of each month so that the daily rainfall amount matched the subsequent monthly reanalysis. Rainfall data from each station are divided into monthly climatological averages and their anomalies interpolated onto a $0.05^{\circ} \times 0.05^{\circ}$ grid using three-dimensional smoothing splines and the Barnes successive-correction method, respectively (Jones et al. 2009). Any discrepancies between the original daily rainfall amounts and the end-of-month reanalysis caused by the differences in interpolation methods for their different spatial structures have been removed in the recalibrated rainfall and replaced for the missing data. This problem mainly existed for the desert regions, not including the state of Queensland. The missing temperature values (observed for the period 1900-1910) have been replaced with a 30-year (1911-1940) monthly temperature climatology. The modelled output accuracy has been mainly subject to the limitations imposed by the assumptions and parameterisations in the model and limitations of parameters due to the sparseness of sampling networks.

The AWAP data have been used in this study for the following reasons. First, they are a high-quality set of historical and ongoing real-time climate analysis for Australia (Jones et al. 2009). Second, the data are a gridded field with high resolution (5km × 5km), making it both spatial and temporal. Third, the original source of meteorological fields is BoM that remains a standard, however, AWAP modelled recalibrated rainfall output is discrepancy corrected between summed-daily and monthly values, and improved homogeneity of temperature interpolation between climate and epochs. Fourth, the multi-day rainfall and temperature accumulation errors have been corrected in the AWAP products. Finally, AWAP data has preserved the background climatology (Jones et al. 2009). Studies that utilised AWAP data had acknowledged this data for being spatially complete high-quality gridded set, such as Gallant et al. (2013).

Some of the variables have been obtained from the Scientific Information for Land Owners (SILO). SILO is an enhanced climate database hosted by the Science Delivery Division of the Department of Science, Information Technology and Innovation (SILO 2017). It provides daily datasets for a range of climate variables from 1889 (to present) on national coverage with no missing values and ready to use. Similar to the AWAP data, the SILO data have also been constructed from the observational records provided by the BoM. It processed the raw data to derive datasets that are both temporally and spatially complete. The SILO and AWAP data have been used in Chapters 4-6 of this study.

In addition to the meteorological variables, thirteen climate mode indices have also been used in Chapter 6 of this study. These indices are: the Niño3 Sea-Surface Temperature, Niño3.4 Sea-Surface Temperature, Niño4 Sea-Surface Temperature, Southern Oscillation Index, Pacific Decadal Oscillation, Dipole Mode Index, El- Niño Modoki Index, El- Niño Modoki Index, Southern Annular Mode, Trans-Polar Index, Quasi-Biennial Oscillation, Western Pacific Index, Oceanic Niño Index and Multivariate ENSO Index.

The data from AWAP, SILO and climate mode indices sources used in this study are listed in Table 3.1.

Table 3.1: List of data used in Chapters 4-6 of this study.

Data	Symbol; Units	Temporal Resolution	Source
Meteorological			
Precipitation	*P*; m/d	Monthly: 1960 - 2016	Australian Water Availability Project (AWAP) (Raupach et al. 2012)
Maximum Temperature	*Tmax*; °C		
Minimum Temperature	*Tmin*; °C		
Upper Layer Soil Moisture (0 – 0.2m depth)	*WRel1*; fractional on [0, 1]		
Upper Layer end of month aggregate Soil Moisture (0.2m – 1.5m depth)	*WRel1End*; fractional on [0, 1]		
Precipitation	*P*; mm	Daily converted to Monthly: 1960 - 2016	Scientific Information for Land Owners (SILO) (SILO 2017)
Reference Evapotranspiration	*ETo*; mm		
Climate mode indices			

Niño3 Sea-Surface Temperature	Niño3 SST; °C		National Climate Prediction Centre
Niño3.4 Sea-Surface Temperature	Niño3.4 SST; °C		CPC (2014)
Niño4 Sea-Surface Temperature	Niño4 SST; °C		
Southern Oscillation Index	SOI		Bureau of Meteorology
Pacific Decadal Oscillation	PDO		Joint Institute of the Study of the Atmosphere and Ocean (JISAO)
Dipole Mode Index	DMI	Monthly: 1960 - 2016	KNMI Climate Explorer

El- Niño Modoki Index	EMI		Japan Agency for Marine-Earth Science and Technology
Southern Annular Mode	SAM		British Antarctic Survey
Trans Polar Index	TPI		National Climate Prediction Centre
Quasi-Biennial Oscillation	QBO		National Climate Prediction Centre

Western Pacific Index	WPI		National Climate Prediction Centre
Oceanic Niño Index	ONI		National Climate Prediction Centre
Multivariate ENSO Index	MEI		National Climate Prediction Centre

Table 3.2: List of geospatial data used in Chapter 7 of this study.

Data	Year Recorded	Resolution / Units	GCS Projection/Datum	Source
Precipitation (mm)	Monthly data from 1900 to present	R: 5km×5km U: mm/day	Unprojected: - Referenced to GDA94/MGA Zone 56 in geographic decimal degrees (equivalent to WGS84 for practical purposes)	AWAP (Raupach et al. 2012)

Digital Elevation Model (DEM; m)		90m×90m		Queensland Spatial Catalogue (Q-Spatial)
Plant Available Water Capacity (PAWC; mm)	2014	250m×250m Units: mm	GDA94	ASRIS-CSIRO National Soil Grids
Population (per sq. km)	2011	Cell size: (1000,1000) Angular Unit: Degree (0.0174532925199433) Linear Unit: Meter (1.0)	GDA_1994_Albers D_GDA_1994	Australian Bureau of Statistics (ABS)
Soil type - Sand Soil Depth (m)	2014	Cell size: (0.00083333333, 0.00083333333) Angular Unit: Degree (0.0174532925199433) Units: %	GCS_WGS_1984 D_WGS_1984	Terrestrial Ecosystem Research Network (TERN) (Soil and Landscape grid of Australia)

| Landscape (derived from DEM-S from SRTM):
- Slope (%) | 2000 | Cell size: 3 arc second (90m)
: (0.00083333333, 0.00083333333)

Angular Unit: Degree (0.0174532925199433) | GCS_WGS_1984
D_WGS_1984 | |
| Land Use | 2016 | Cell size: (1000,1000)
Angular Unit: Degree (0.0174532925199433)
Linear Unit: Meter (1.0)

(0.00083333333, 0.00083333333) | PCS:
GDA_1994_Australia_Albers | Queensland Land use Mapping Program (QLUMP) available at Q-Spatial |

3.2.2 Data pre-processing

Some variables were pre-processed for the analysis. For SPEI computation, the units of precipitation and reference evapotranspiration needs to be in the same units. As such, the monthly precipitation from AWAP (initially in meters/day (m/d)) have been multiplied by the number of days (N) in the respective month followed by a multiplication factor of 1000 to convert into millimetres (mm), using the formula:

$$P_{(mm,month)} = P_{m/d;month} \times N_{days} \times 1000 \tag{3.1}$$

The daily-based precipitation data from SILO have been converted to monthly by summing the daily values. Note that there were no missing data values from either AWAP or SILO sources for any of the point based study locations as the missing data had been recovered with standard statistical tests.

The physiographic factors used in Chapter 7 comprised different spatial projections and resolutions. Part of the processing component has been the definition of the map datum, coordinate system, UTM zone and equivalent grid cell size. The maps used in this study have been defined based on the Geocentric Datum of Australia 1994 (GDA94) with Map Grid of Australia (MGA) as the coordinate system and 56 as the UTM zone. The cell size for mapping is chosen to be 100m× 100m.

3.2.3 Data limitations

In Chapter 7, the percent rainfall departure was used as a drought hazard indicator instead of the SPEI due to the unavailability of the gridded reference potential evapotranspiration (ET_o) data required for the computation of SPEI. While AWAP does provide temperature data that could be used to calculate the potential evapotranspiration (PET) via Thornthwaite (1948) or Hargreaves (1994) methods, the methods, however, are strongly discouraged. Over the past ten years or so there have been many articles demonstrating that PET should not be forced by temperature (T) alone, particularly in drought analyses (*e.g.,* Hobbins et al. (2008); (Roderick et al. 2007; Sheffield et al. 2012)). Roderick et al. (2007) showed that long-term changes in pan evaporation in Australia were driven by wind speed, not T. Hobbins et al. (2008)

also demonstrated that a drought index driven by *T*-based *PET* yielded soil moisture trends that bore no relation to those driven by a *PET* derived from pan evaporation observations. Similarly, Hobbins et al. (2012) and Hobbins (2016) showed that temperature was not the most significant driver of *PET* variability (*i.e.,* the demand side of drought) over much of the continental USA. Also, Sheffield et al. (2012) showed that increasing global long-term trends in drought were vastly overstated using a *T*-based *PET* compared to a physically based one.

The *PET* could also be calculated via Priestley-Taylor (Priestley and Taylor 1972) method that uses humidity and net solar radiation where the latter measure can be combined with temperature to permit the derivation of a more physically-based estimate of *PET*. However, this study has disregarded the use of *T*-based *PET* that could have been possible otherwise (net solar radiation data available in AWAP) to compute the gridded SPEI over the study region in Chapter 7. To circumvent this limitation, this study has used percent rainfall departure that has also been successfully used in previous studies to generate integrated drought vulnerability index, *e.g.,* Jain et al. (2015) and Thomas et al. (2016).

There are numerous physiographic and climatic factors associated with drought events that could have been integrated together with ones used in this study to produce a more defined drought-risk index map in Chapter 7. However, due to the unavailability of such data for the entire study region, only those factors that were readily available has been utilised. While the data unavailability has been a limitation, the generated output maps in Chapter 7 are nevertheless, strongly representative of drought-risk.

3.3 Location of the Study Area

The general study area is located in the southeast Queensland (SEQ), Australia. It covers an area of 123,897.53 square kilometres. Rural areas make up about 85% of SEQ, much of which is managed by farmers. Grazing takes up major portion of the land use by about 51% of the land area. Other intensive agricultural activities include horticulture and animal production. For sustainable agriculture, some of the key challenges in the SEQ region include climate change, water supply, population growth

and economic pressures. The projected impact of climate change directly affecting agriculture includes more frequent and severe droughts (Pearce et al. 2007). As such, the agricultural production will require more water-efficient practices due to increasing demand for water when supply becomes less reliable under drought conditions in the study region.

The study area covers six catchments: Condamine – Balonne, Moonie, Border Rivers, Logan, Gold Coast, and Moreton. The topography of the study area varies between 14.74 m below sea-level to 1360.24 m high. The higher elevations prevail on the Great Dividing Range (or the Eastern Highlands) that is Australia's most substantial mountain range and the third longest land-based range in the world. The high elevated terrains have high slopes as well.

Figure 3.1 shows the map of the study area. For Chapters 4-6, point based locations within the major study region have been used. These points have been labelled as R1 (153.05°E, 27.45°S), R2 (148.60°E, 28.05°S), R3 (152.25°E, 28.25°S) and R4 (143.25°E, 26.75°S) that has distinct climatological characteristics where R1 is simply the location for the populous Brisbane city. Locations R2 and R3 are located in the Murray Darling basin that is an area of national significance for social, cultural, economic and environmental reasons and it contains nationally significant environmental assets that are reliant on water to maintain ecosystem health (ABS 2012). Australia is one of the world's major agricultural producers and exporters of grain, beef, dairy, cotton, wool, wine and other horticulture, where the Murray Darling basin alone contributes about 39% of Australian production. Agriculture occupies 84% of the Murray Darling Basin land area with products to a value of approximately $AUS 15 billion per annum (2005–2006) (ABS 2012). The R4 is located in the predominantly arid region in Queensland that mostly consist grazing/pasture activity on a broad scale. The study area is often declared drought-prone, hence it is important to prepare an appropriate drought monitoring, modelling and risk assessment study.
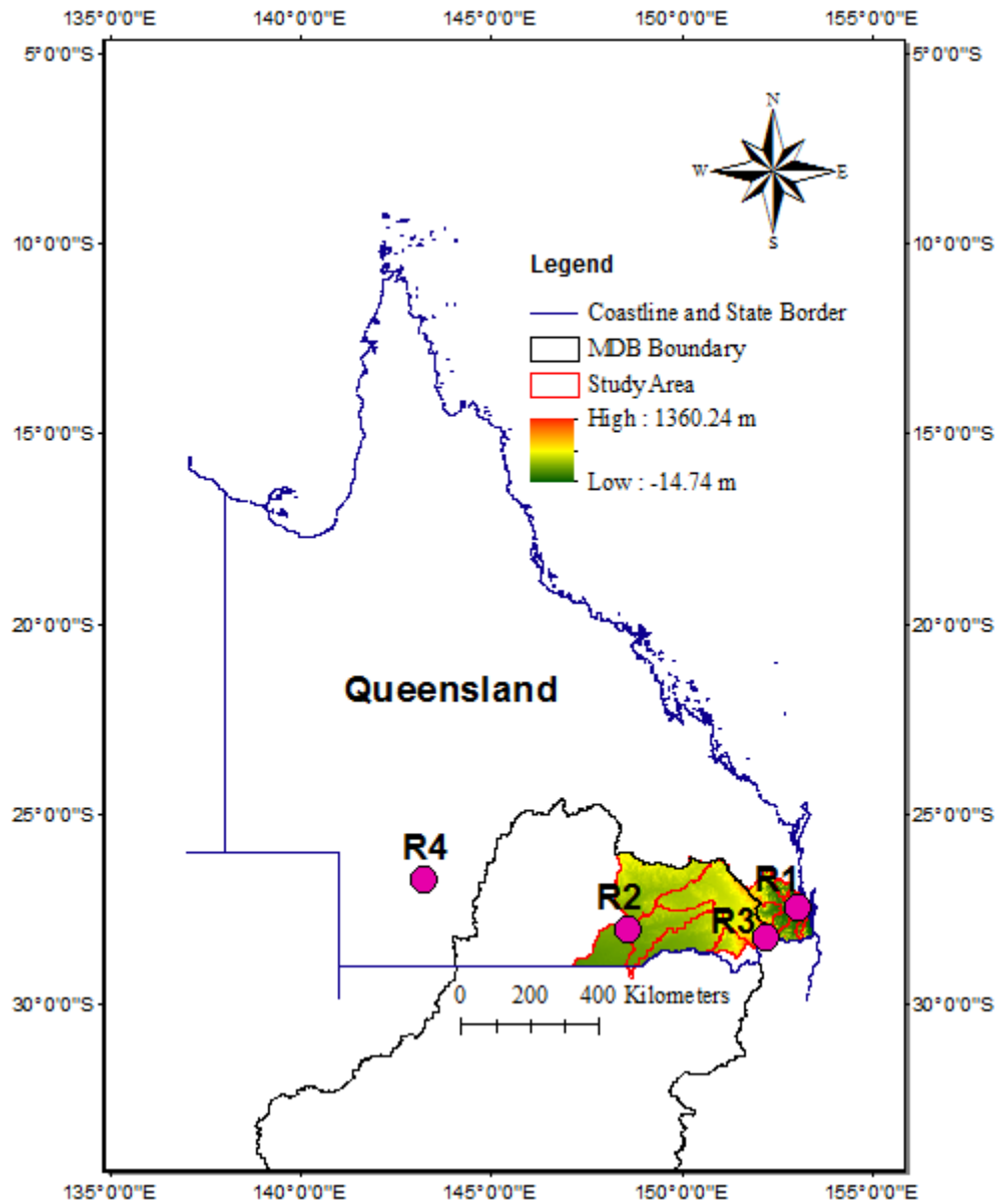
Figure 3.1: Map of the study region. Colour shading depicts digital elevation model (DEM) (meters). MDB refers to the Murray Darling Basin.

3.4 Scope and Limitation of the Study

The study has been scoped based on several considerations such as the availability of temporal and spatial datasets, strategic locations significantly and frequently affected by droughts (*i.e.,* populous and the agriculture intensive areas), and the availability of essential tools and software for timely analyses (*e.g.,* Matlab, *R*, ArcGIS). The rationale and key considerations in the way how this study has been scoped are based on the current challenges faced by the physical models in assessing drought-risk and the need for forecasting models to assess the consequences of water resource depletion from severe drought events, for instance, the 1996-2010 Millennium Drought. As a very topical and significant issue, this study aims to develop a technical framework using statistical and geospatial tools that can help improve the study regions' resiliency from drought events.

A variety of limitations that can be explored in follow up studies have been identified. The most obvious one is the extent of the study area. Its selection has been approached on the basis of providing detailed solution wherein Chapters 4-6 are mainly case studies. Ideally, drought vulnerability and risk assessment should be integrative and comprehensive as well as integrate various aspects such as social, economic, physical and environmental factors where obtaining such data has been beyond the scope of this study. This accords to many scholars who argue that vulnerability has a multifaceted and multi-dimensional nature (Birkmann 2006; Birkmann and Wisner 2006; Hufschmidt 2011; Turner et al. 2003; Vogel and O'Brien 2004) where no single measure can fully capture its complexity (Gbetibouo and Ringler 2009; Luers et al. 2003).The second limitation has been the unavailability of other geospatial factors that covered the entire study region for Chapter 7, as discussed in Section 3.2.3.

Furthermore, due to the complexity and difficulty to "predict" the future conditions of the study area and its critical interdependent land use in the future, the climate change factors for assessing future drought-risk in the study area have also been excluded from the analysis. Also, the assumptions associated with the factors in setting the Bayes equation have been mainly based on the existing literature; hence,

no actual experimentation, which could have involved actual field study, has been performed.

3.5 General Methodology
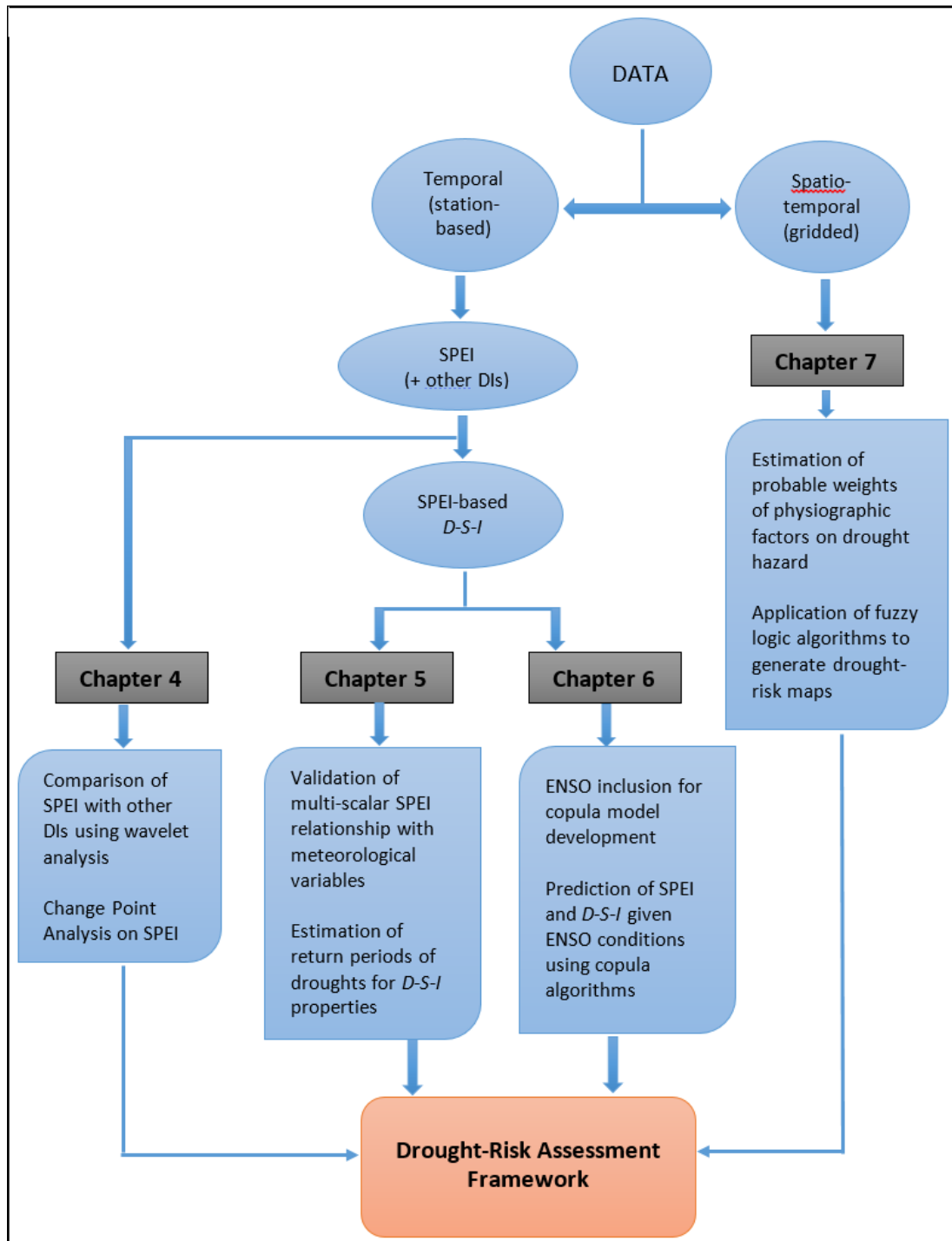
Figure 3.2: Flowchart describing general methodology of the study.

The Chapters 4-7 have self-contained and detailed methodology. Figure 3.2 gives an overview of the research methodology workflow for developing a framework for drought-risk assessment.

3.6 Summary of Chapter

In this chapter, the types of data used and the description of the study have been provided. The data pre-processing methods are described and limitations encountered are acknowledged. The study area selection has also been discussed in this chapter.

Chapter 4

DROUGHT INDICES COMPARISON AND TREND ANALYSIS

Note:

The results from this chapter are used in an article preparation. The following is the tentative reference to the article:

Dayal KS., Deo RC, and Apan A., (2018) "Trend analysis of drought events based on SPEI: a case study", *Atmospheric Research*, (In preparation).

4.1 Introduction

The previous chapter has listed the data types and discussed the data pre-processing required for the analysis presented in Chapters 4-7. The current chapter aims to generate and discuss the first set of results, in response to the first objective of the study (listed in Section 1.3). Here, the application of the SPEI for comparison with the popular precipitation-based DIs and assessment of changes in time series trend is presented. This chapter illustrates why SPEI is more relevant for the monitoring and characterising of drought events in the present study region.

This investigation has employed the SPEI, formulated as an improved version of the WMO-approved SPI. Unlike in the case of the SPI, the SPEI has an ability to encapsulate the contributory influence of temperatures on the demand for water, and therefore, it appears to be more suitable for the monitoring of hydrological and agricultural impacts. Also, unlike the case of the PDSI, the SPEI is able to operate on multiple timescales (1-48 months), acting as an essential tool for assessment of the

hydrologic cycles and for accounting for different category of drought (meteorological, hydrological and agricultural). The SPEI can replicate the sensitivity embedded in the PDSI for monitoring of hydrological status in terms of the estimated evaporation and transpiration driven by warm temperatures, whilst assessing the multi-temporal nature of drought afforded by SPI. An idealistic characteristic of the SPEI is its ability to capture the evaporative demand of the hydrosphere (*i.e.,* via reference evapotranspiration; *ETo*) and the indicative aberrations in overall water resource conditions. SPEI holds the advantages of less data requirement, flexibility, and simple computation. These accord to the viewpoint of Keyantash and Dracup (2002) that a drought metric must be simple, clear, comprehensible and statistically robust, and also be independent of the climatic characteristics (*i.e.,* standardised) to be comparable in the wider temporal and spatial domains across geographically diverse regions.

Despite its infancy in the hydrologic research community, many case studies performed outside of Australia have applied SPEI for drought assessment and demonstrated its strong statistical correlation with hydro-meteorological variables that affect drought impacts in such diverse climatic regions. For example, the SPEI has been used for drought variability studies (Das et al. 2016; Li et al. 2012; Paulo et al. 2012; Potop 2011), hydrological impact assessments, agricultural drought studies, impact of drought on ecological systems (Barbeta et al. 2013; Cavin et al. 2013; Martin-Benito et al. 2013; Toromani et al. 2011; Vicente-Serrano et al. 2013) as well as for the monitoring of drought events (Fuchs et al. 2012). To contribute to the growth of knowledge in the subject area, this study has performed several analysis using SPEI as the primary drought monitoring index.

The breakdown of the first major objective outlined in Section 1.3 is done in two separate chapters (4 & 5), where each chapter has its own specific objectives. The main objectives of this chapter are to (1) compare SPEI with precipitation-based SPI, RDDI and RAI drought indices using statistical metrics and Wavelet Analysis and (2) assess any change in the trend of the SPEI time series over the period 1915-2016 using the Change-Point Analysis. Chapters 4 & 5 thus present the reasons for choosing SPEI for characterising drought events in Australia.

4.2 Materials and Method

4.2.1 Hydrological data and study area

Four case study locations in the southeast Queensland (SEQ), referred to as R1, R2, R3 and R4, with distinct climatological characteristics are selected for the analysis. Figure 4.1 plots their locations and Table 4.1 lists their geographic coordinates with the average annual precipitation for the base period (1971-2000). The monthly precipitation data (P; in millimetres), maximum temperature ($Tmax$; in degree Celsius) and FAO-56 Penman-Monteith based Reference Evapotranspiration (ETo; in millimetres) for any grid point, interpolated from gridded datasets on 5km × 5km resolution, are acquired from SILO database for the period 1915–2016. The upper layer soil moisture ($WRel1$; fractional [0 1]) is acquired from AWAP.

The sensitivity of potential evapotranspiration in any calculations involving the SPEI requires caution since previous studies have demonstrated that the potential evapotranspiration should not be forced by temperature data alone (*e.g.,* (Hobbins et al. 2012; Roderick et al. 2007; Sheffield et al. 2012). Therefore, this study utilises the FAO-56 Penman-Monteith based ETo data to compute the SPEI. Note that instead of using the generic term 'potential evapotranspiration', hereafter this study refers to 'reference evapotranspiration' specifically (denoted as ETo). The ETo data available in the SILO database has been estimated via the FAO-56 Penman-Monteith formula (Allen et al. 1998). The ET_O values correspond to the short crop cases whereby a hypothetical reference with the assumed grass top height of 0.12m, a fixed surface resistance of 70sm^{-1}, an albedo of 0.23, wind speed value at 2m height, radiation derived from cloud oktas, and the hours of sunshine using the procedure documented in Zajaczkowski et al. (2013) has been used. The monthly upper layer soil moisture ($WRel1$; fractional [0, 1]) and end of the month aggregated soil moisture ($WRel1End$; fractional [0, 1]) are obtained from the AWAP historical runs constructed from the *WaterDyn* hydrological model for the period 1915 to 2016 (Raupach et al. 2009; Raupach et al. 2012). The AWAP and SILO data are all obtained for the matching geographical locations for this case study (*i.e.,* R1, R2, R3 and R4).
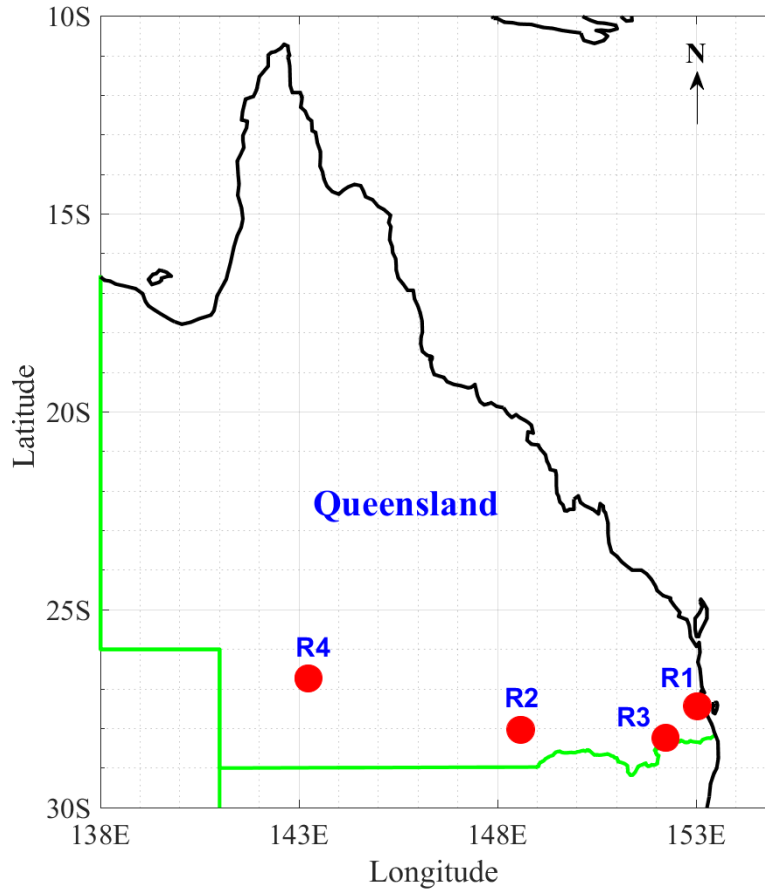
Figure 4.1: Map of point-based study locations: R1 – Subtropical, R2 – Grassland, R3 – Temperate, and R4 – Desert.

Table 4.1 Study locations and their descriptive statistics.

Location Label	Climatic Regions	Geographical Location	Elevation above sea-level (m)	Annual Mean Precipitation (P; mm)
R1	Subtropical	153.05°E, 27.45°S	61	1154.61
R2	Grassland	148.60°E, 28.05°S	250	551.93
R3	Temperate	152.25°E, 28.25°S	561	739.70
R4	Desert	143.25°E, 26.75°S	211	307.82

4.2.2 Theoretical overview

4.2.2.1 Standardised Precipitation-Evapotranspiration Index (SPEI)

The point-based monthly time series, comprised of the standardised precipitation-evapotranspiration index over 1915–2016 period based on the cumulative effects of *P* and *ETo,* are generated where *ETo* is used to depict the evaporative demand of the atmosphere. *i.e.,* the evapotranspiration that would occur if sufficient water was available. This representation of drought aimed to incorporate the role of *ETo* that could act to moderate or exacerbate the underlying hydrological cycles in a drought situation (Hanson 1988). To examine drought periods within the historical data, the *ETo* is subtracted from the total *P* (where $SDB_i = P_i - ETo_i$ and i = the month) to deduce the surplus or the deficit of water resources (*i.e.,* the computation of Supply-Demand Balance; *SDB*).

As precipitation data generally exhibit seasonality within the case study regions and the distribution of these data are especially pronounced in different regimes, it is necessary to transform the *SDB* time series via an equal probability framework to a normal distribution with a mean of zero ($\mu = 0$) and standard deviation of one ($\alpha = 1$). This allows the water deficits and surpluses to be comparable in space and time, and the SPEI to be standardised so that it is free from seasonality and the data distribution effects when assessing the different drought event. To achieve this, the *SDB* time series are fitted to the three-parameter log-logistic, Gamma and Pearson III distributions based on the goodness-of-fit tests, *i.e.,* Kolmogorov-Smirnov (K-S) statistic. With the null hypothesis that the *SDB* time series follows a specified distribution at significance level (α=0.05), the best (smallest) K-S statistic is obtained for log-logistic distribution, concurring with Vicente-Serrano et al. (2010). Thus the transformation of the *SDB* time series employed a probability density function of a three-parameter (α, β and γ) log-logistic distribution, *F(x)* according to Vicente-Serrano et al. (2010):

$$F(x) = \left[1 + \left(\frac{\beta}{x - \gamma} \right)^{\alpha} \right]^{-1} \tag{4.1}$$

The SPEI is then computed as (Vicente-Serrano et al. 2010):

$$SPEI = W - \frac{C_o + C_1 W + C_2 W^2}{1 + d_1 W + d_2 W^2 + d_3 W^3} \tag{4.2}$$

In Equation (4.2), the term $W = \sqrt{-2\ln(P)}$ for $P \leq 0.5$, and P is the exceedance probability of a determined SDB value, $P = 1 - F(x)$ while $C_0 = 2.515517$, $C_1 = 0.802853$, $C_2 = 0.010328$, $d_1 = 1.432788$, $d_2 = 0.189269$ and $d_3 = 0.001308$ are the empirical constants. The SPEI values corresponding to deficits or surpluses of water resources at six timescales (T = 1, 3, 6, 9, 12 and 24 months) are computed; where for instance, the SPEI$_9$ is constructed by a sum of SDB values from eight months before to the current month. In all SPEI calculations, the base period is set to be 30 years (*i.e.,* 1971–2000), which is a common practice for drought studies in Australia (Deo et al. 2015; Deo et al. 2009).

In this chapter, only the SPEI at a 1-month timescale has been used. The multi-scalar SPEI has been tested in the ensuing Chapter 5.

4.2.2.2 Rainfall Decile-based Drought Index (RDDI)

The RDDI is a measure of rainfall deficiency (Gibbs and Maher 1967). It is calculated from monthly rainfall values. While maintaining the traditional ten classes (deciles) and instead of sorting rainfall data into slices of 10%, this study has sorted rainfall data into slices of 5%, (20-quantiles) to obtain a better accuracy in detecting the drought signatures. First, the rainfall values of each Julian calendar month, for the base period, are sorted in ascending order and ranked from lowest to highest to construct a cumulative frequency distribution. The distribution is then split into 20 quantiles (slices of 5%). Using the monthly rainfall amount for each quantile obtained for the base period, the monthly rainfall amounts for the study period are then assigned the corresponding quantile. The first quantile that has the lowest rainfall values indicate driest months in the series while the 20th quantile indicates the wettest months. The other quantiles show the range from driest to wettest months. The ten classes (deciles) are assigned to each rainfall value as integers from 0.5 to 10 at intervals of 0.5.

4.2.2.3 Standardised Precipitation Index (SPI)

Developed by McKee et al. (1993), the SPI primarily defines and monitors drought events. To compute SPI for the desired station, a frequency distribution is constructed for a long-term precipitation record. It is then fitted to a theoretical probability

distribution, *i.e.,* Gamma distribution, and then transformed into a normal distribution so that the mean SPI is zero with a unit variance. The transformed distribution helped determine the extent of rainfall deficit, thus facilitated comparison and monitoring of spatial drought conditions at various temporal scales. The following equations are useful for calculating SPI. A Gamma distribution defined by its probability density function is given by:

$$g(x) = \frac{1}{\beta^{\alpha}\Gamma(a)} x^{\alpha-1} e^{-\frac{x}{\beta}}, \text{ for } x > 0 \tag{4.3}$$

The α (shape) and β (scale) parameters are calculated as:

$$\alpha = \frac{1}{4A}\left(1 + \sqrt{\frac{4A}{3}}\right) \text{ and } \beta = \frac{\bar{x}}{\alpha} \tag{4.4}$$

where $\bar{x}$ represent the rainfall average over the base period and n is the number of observations, *i.e.,* 1224 months, for each study location, and;

$$A = \ln(\bar{x}) - \frac{\sum \ln(x)}{n} \tag{4.5}$$

The above parameters are then used to derive the cumulative probability distribution, given as:

$$G(x) = \int_{0}^{x} g(x)dx = \frac{1}{\beta^{\alpha}\Gamma(\alpha)} \int_{0}^{x} x^{\alpha-1} e^{-\frac{x}{\beta}} dx \tag{4.6}$$

Since the Gamma distribution is undefined for zero rainfall amount, the cumulative probability, *H(x)*, of zero and non-zero rainfall is calculated as:

$$H(x) = q + (1-q)G(x) \tag{4.7}$$

where q is the probability of zero rainfall. For instance, if there are m number of months with zero rainfall, then q is estimated as m/n and the cumulative probability is transformed into a standardised normal distribution that gives mean SPI and variance to be 0 and 1, respectively.

4.2.2.4 Rainfall Anomaly Index (RAI)

The monthly RAI is computed according to Van Rooy (1965):

$$RAI = x_i - \bar{x} \tag{4.8}$$

where x_i is the monthly precipitation and $\bar{x}$ is the mean precipitation for the base period, 1971–2000.

4.2.2.5 Wavelet Analysis (WA)

A wavelet is a function localised in both frequency ($\Delta\omega$ or bandwidth) and time (Δt) with zero mean (Torrence and Compo 1998). The Morlet wavelet is selected in this study because it comprises both real and imaginary parts in the function that enables it to investigate a signal's coherence and phase angle, after Chang et al. (2017) and Grinsted et al. (2004). It is expressed as:

$$\psi_0\left(\eta\right) = \pi^{\frac{-1}{4}} e^{i\omega_0\eta} e^{\frac{-1}{2}\eta^2} \tag{4.9}$$

where ω_0 and η are dimensionless frequency and time, respectively. For feature extraction purposes, Morlet wavelet with $\omega_0 = 6$ is a recommended choice since it provides a good balance between time and frequency localisation (Grinsted et al. 2004).

4.2.2.5a The Continuous Wavelet Transform (CWT)

The CWT has been used to apply a bandpass filter to the time series. Unlike Fourier transformation, the CWT has the ability to construct time-frequency localisation of a signal. By varying its scale (s), the wavelet is stretched in time so that, $\eta = s \cdot t$ and subsequently normalising it to have a unit energy. The CWT of a time series ($x_n, n = 1,...,N$) with a uniform time steps δt, is defined as the convolution of x_n with scaled and normalised wavelet (Grinsted et al. 2004) as:

$$W_n^X\left(s\right) = \sqrt{\frac{\delta t}{s}} \sum_{n'=1}^{N} x_n \psi_0\left[\left(n'-n\right)\frac{\delta t}{s}\right] \tag{4.10}$$

4.2.2.5b Cross Wavelet Transform (XWT)

While CWT divides a continuous-time function into wavelets, the similarity between two series in the same period is generally hard to identify. To overcome this, the XWT

has been used. The XWT of two-time series x_n and y_n is defined as $W^{XY} = W^X W^{Y*}$ (Grinsted et al. 2004) where * refers to complex conjugation and the absolute value of W^{XY} is the cross-wavelet power. Detailed theoretical distribution of the XWT is given in Torrence and Compo (1998).

The CWT and XWT are powerful methods for testing proposed linkages between the two data time series.

4.2.2.6 Change-Point Analysis (CPA)

A CPA is a powerful tool that determines whether a change has taken place in a series. There are numerous ways to perform a CPA on a times series. This study has used the approach implemented in Taylor (2000). It is capable of detecting subtle changes and better characterises the detected changes by providing confidence levels and confidence intervals. The confidence levels indicate the likelihood that a change has occurred while the confidence interval indicates when the change has occurred.

The change-point analysis iteratively uses a combination of cumulative sum charts (CUSUM) and bootstrapping to detect the changes. In this study, the CUSUM charts are constructed by calculating and plotting a cumulative sum based on the data, viz. Taylor (2000). Suppose $X_1, X_2,..., X_N$ are N number of data points. The cumulative sums (CUSUM) $S_0, S_1,..., S_N$ are then calculated in three steps:

1. Calculate the average of the data series: $\overline{X} = \dfrac{X_1 + X_2 + ... + X_N}{N}$;

2. Set the initial condition, $S_0 = 0$;

3. Compute S recursively, $S_i = S_{i-1} + (X_i - \overline{X}), \quad i = 1,2,...,N$

The interpretation of a CUSUM chart requires close attention to the pattern of S_i. For the case of SPEI time series, consider a period of time where SPEI is above the average value. Most values adding up to the cumulative sum can produce positive values so the trend line is expected to rise steadily. In this case, a segment with increasing S_i indicates a period where SPEI values are above average. Likewise, a

segment with a decreasing S_i indicates a period where values are below average. A sudden change in the direction of the time series, detected by the change in the sign of the gradient of S_i at a stationary point, x, is likely to indicate a sudden, abrupt shift in the average value of the time series. However, S_i following a relatively straight path indicate a period where the average does not change. Based on this, we can detect any abrupt changes over the given study period.

To be certain that a change has occurred, a confidence interval can be used for the obvious change by performing a bootstrap analysis. For bootstrap analysis, an estimator of the magnitude of change is required and in this case, it is the difference between the maximum and minimum cumulative sums, S_i, *i.e.,* $S_{diff} = S_{i\max} - S_{i\min}$. A single bootstrap analysis is then performed in four steps:

1. Generate a bootstrap sample of N values, denoted as $X_1^{\,0}, X_2^{\,0}, ..., X_N^{\,0}$, by randomly reordering the original N values in the series. This is called sampling without replacement;

2. Calculate CUSUM based on the bootstrap sample, denoted as $S_1^{\,0}, S_2^{\,0}, ..., S_N^{\,0}$;

3. Calculate $S_{\min}^{\,0}$, $S_{\max}^{\,0}$ and $S_{diff}^{\,0}$;

4. Determine whether the bootstrap $S_{diff}^{\,0}$ is less than the original S_{diff}.

Bootstrapped samples represent a random reordering of the data that "mimic" the behaviour of the CUSUM if no change has occurred. With a large number of bootstrap samples, we can estimate by how much S_{diff} would vary if no change has taken place, *i.e.,* the Confidence Interval. To determine the Confidence Level, let M be the number of bootstrap samples performed and Y be the number of bootstraps for which $S_{diff}^{\,0} < S_{diff}$, then:

$$Confidence\ Level = \frac{Y}{M} \tag{4.11}$$

The corresponding exceedance probability of bootstrapped samples $p - value$ is computed viz:

$$p - value = 1 - Confidence\ Level \qquad (4.12)$$

The $p - value$ is then compared against $\alpha = 0.001$, 0.05 and 0.1.

The other estimator of when the change occurred is the mean square error (MSE). If the point m estimated the last point before the change occurred, then the MSE(m) is defined as (Taylor 2000):

$$MSE(m) = \sum_{i=1}^{m} \left(X_i - \bar{X}_1 \right)^2 + \sum_{i=,m+1}^{N} \left(X_i - \bar{X}_2 \right)^2 \qquad (4.13)$$

where,

$$\bar{X}_1 = \frac{\sum_{i=1}^{m} X_i}{m} \quad and \quad \bar{X}_2 = \frac{\sum_{i=m+1}^{N} X_i}{N - m} \qquad (4.14)$$

4.3 Results and Discussion

4.3.1 Comparison between DIs

The comparison between SPEI and only precipitation-based DIs, *i.e.,* SPI, RDDI and RAI, are carried out. Figure 4.2 and Figure 4.3 shows the area plot of monthly SPEI and SPI, respectively. The negative range of values refers to the water deficit periods. Since SPEI and SPI are the standardised indices with mean equal to zero and standard deviation equal to 1, the two are comparable. It is apparent that the SPEI extremes are more compared to SPI extremes, especially distinguishable for location R4 for the Millennium Drought period (1996-2010). Such difference could be explained by the location of R4, which is in an arid to the semi-arid region where water deficit through evapotranspiration is consequential. This difference can also be assessed numerically viz. Pearson correlation values listed in Table 4.2. The correlation of SPEI with SPI, RDDI and RAI are slightly less in R4, as compared to the other study regions. Additionally, while SPEI has a high correlation with SPI for their similar computational procedure, the former also has a reasonably high correlation with RDDI that is predominantly used by BoM in Australia. This preliminary comparison suggests that SPEI is a high-calibre drought index for characterising drought events.
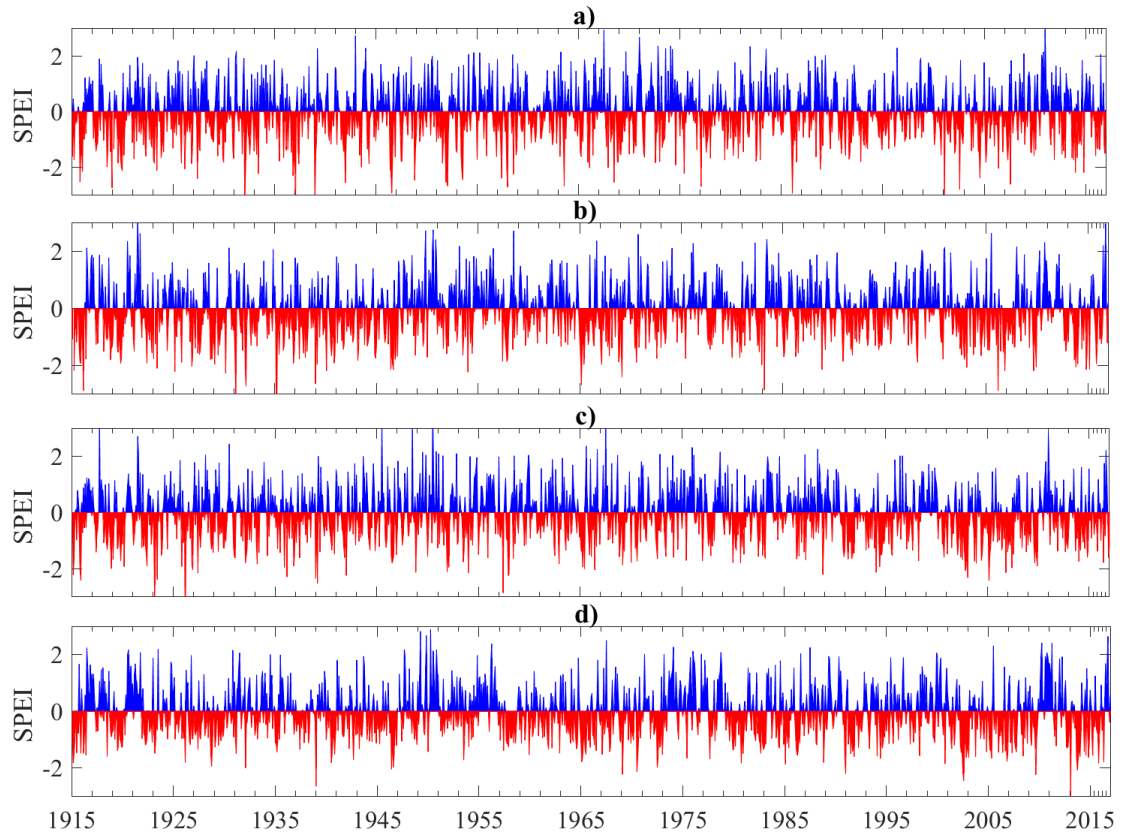
Figure 4.2: Area plot of the monthly SPEI from 1915 to 2016 for (a) R1, (b) R2, (c) R3 and (d) R4.
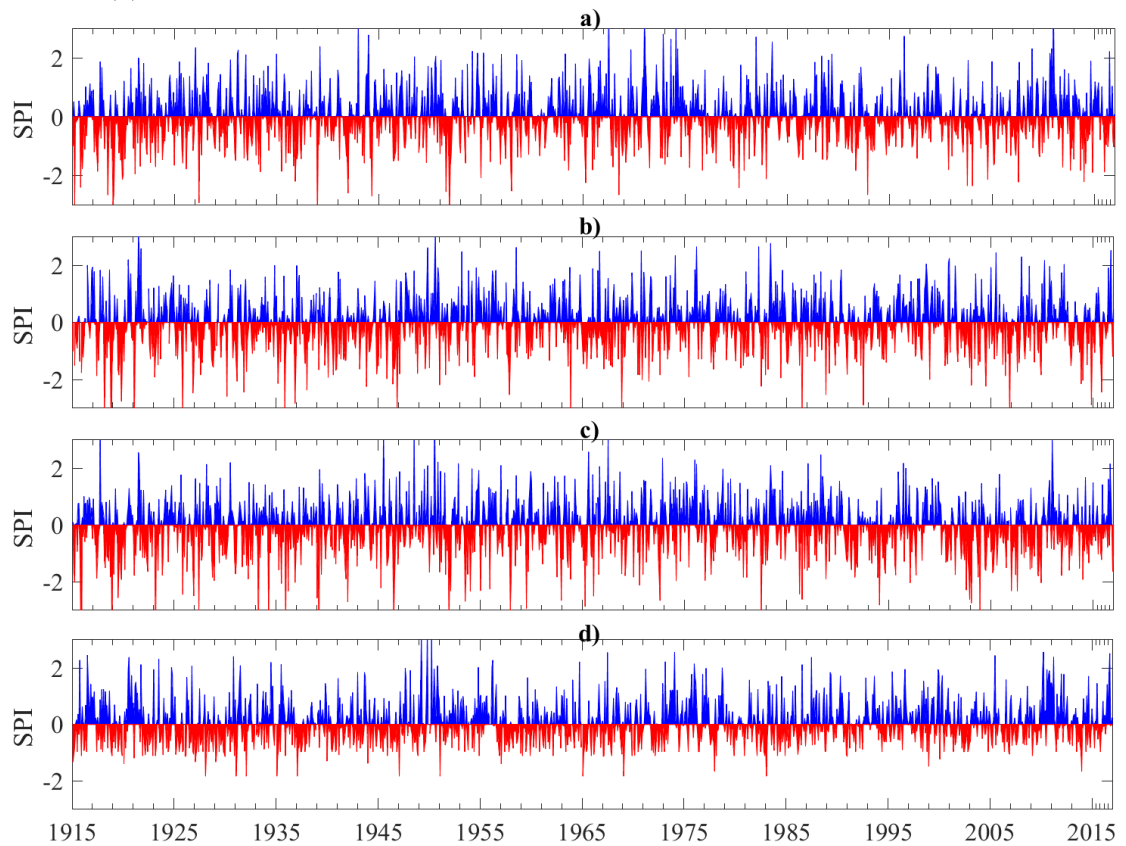
Figure 4.3: Area plot of the monthly SPI from 1915 to 2016 for (a) R1, (b) R2, (c) R3 and (d) R4.

Table 4.2: Pearson correlation between drought indices.

Drought Indices	Pearson Correlation			
	R1	**R2**	**R3**	**R4**
SPEI vs. SPI	0.9604	0.9148	0.9367	0.8950
SPEI vs. RDDI	0.9569	0.9375	0.9492	0.8778
SPEI vs. RAI	0.8290	0.8450	0.9109	0.7608
SPI vs. RDDI	0.9402	0.9400	0.9285	0.9402
SPI vs. RAI	0.8561	0.8366	0.8914	0.8238
RDDI vs. RAI	0.8104	0.8488	0.8941	0.7323

A comparative study using wavelet analysis on DIs is the first study of its kind for assessment of droughts in Australia. Figure 4.4 shows the wavelet power spectrum for *WRel1*, SPEI, SPI, RDDI and RAI time series for the location R1. Similar results for locations R2, R3 and R4 are provided in the Appendix. The bold contour lines indicate 95% confidence level. The period is measured in months. Clearly, there are common features in the wavelet power of all time series between 128-256 months band for the Millennium Drought during mid-1990s to 2010. However, the significance level varies where RAI appears to have the smallest region during this drought period. While there are various smaller bands with significant wavelet spectrum for all time series, the SPEI, however, clearly captures the significant power spectra for the World War II drought between ~ 32-80 months band. Nonetheless, the CWT reveals the common feature between the DIs, however, it is hard to tell if there is merely any confidence. As such, the XWT is used to identify the common features.
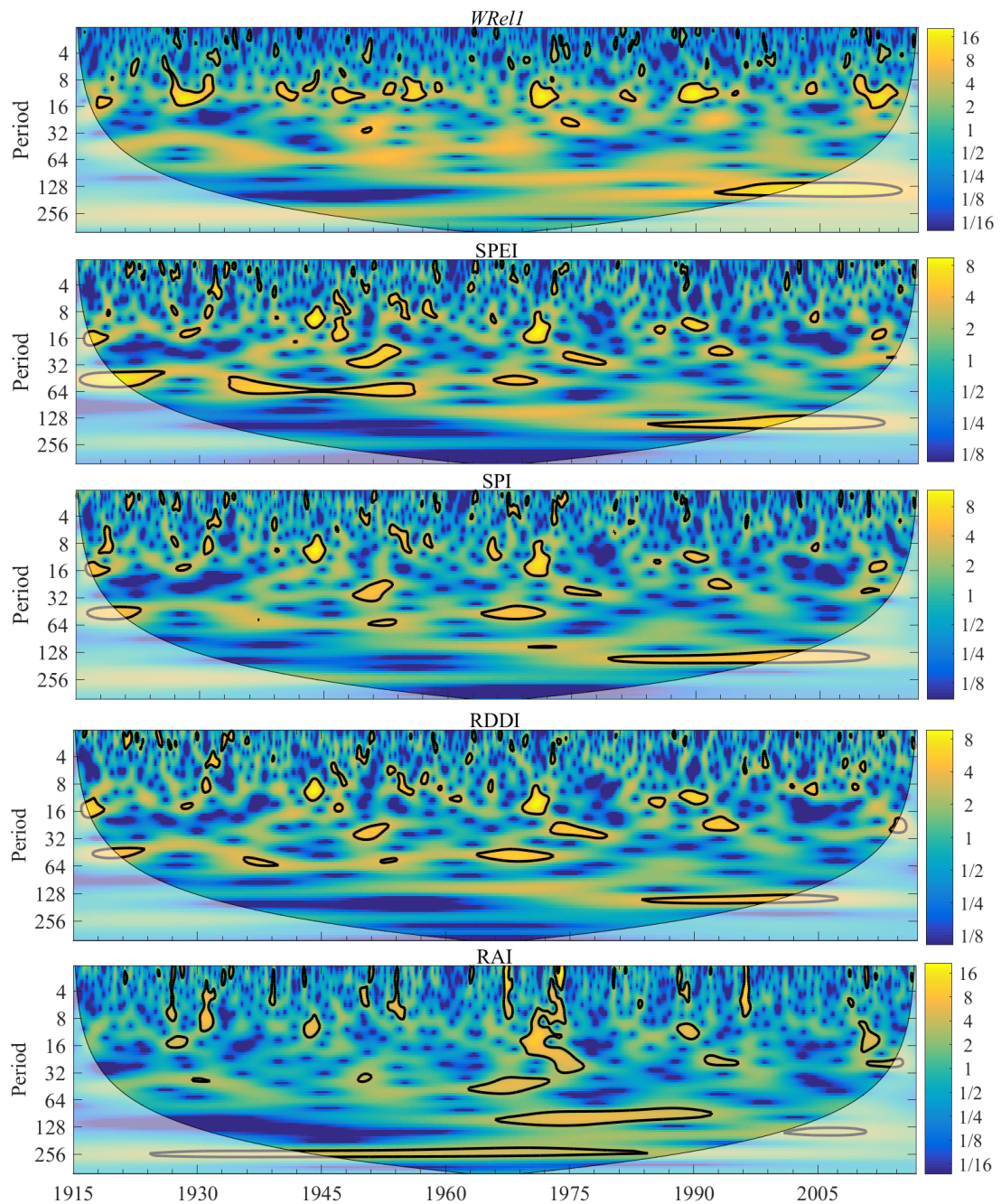
Figure 4.4: Continuous wavelet transform (CWT) power spectrum for the time series of upper layer soil moisture (*WRel1*), SPEI, SPI, RDDI and RAI drought indices.

Figure 4.5 shows the XWT computed between *WRel1* and DIs. Note that *WRel1* is used for comparison as it is an important indicator of the agricultural drought and is expected to have a high correlation with DIs. It is clearly evident that the DIs have a significant correlation with *WRel1* for all major droughts occurred at the location R1. However, the significant correlation of *WRel1* with SPEI is more

conspicuous for the World War II drought in the band range ~32-80 from the period 1930-1960, compared to that with SPI, RDDI and RAI. The arrows pointing to the east implies both time series are in phase. From the significant power spectrum and phase relationship, particularly for the major drought events, we can speculate that there is a strong link between soil moisture content and DIs, where SPEI stands out to be more prominent. The cross-power spectrum for locations R2, R3 and R4 can be found in the Appendix. The correlation assessment of SPEI with other DIs has demonstrated that SPEI is in fact very effective at identifying the historical drought events and thus can be advocated for monitoring of drought events in real-time.
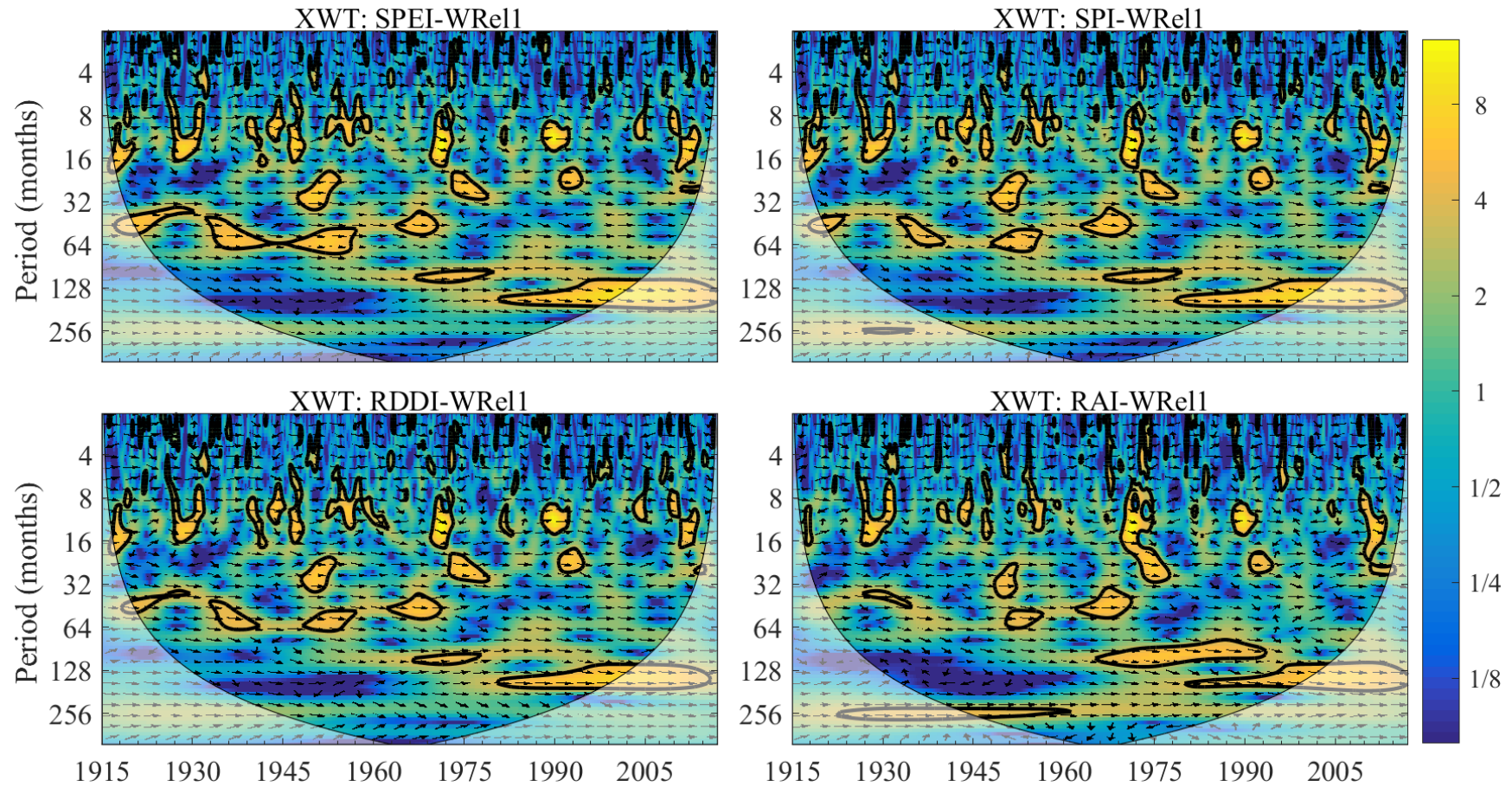
Figure 4.5: Cross-wavelet spectrum (XWT) between the upper layer soil moisture *(WRel1)* and drought indices.

4.3.2 Trend changes in the SPEI

In studying drought climatology, it is important to investigate whether there has been any change in the trend of the SPEI, which reveals the periods of water deficiency in its standardised form. A change-point analysis has been carried out on the monthly SPEI time series for the 1915-2016 period for each study location. Tables 4.3, 4.4 and 4.5 shows the results for locations R2, R3 and R4. No significant change has been observed in the location R1. For the discussion purpose, only those change points are considered that has a confidence level of 100%. At the location R2, of the nine changes, there are two periods when a change has occurred with 100% confidence. Those are 387th and 1172nd month in the time series, corresponding to March 1947 and August 2012. At 95% confidence interval, the first change with 100% level of confidence occurred between June 1939 and August 1951, while the second change occurred between February 2012 and November 2013. The fact that the confidence interval for the first change is wider indicates that the time for this change cannot be as accurately pinpointed compared to the second change. In the table, we can also see the average SPEI values prior to and after the change has occurred, *i.e.,* prior to the March 1947 change the average SPEI value was -0.27877 while after the change the SPEI was 0.19399. Similarly, the average SPEI values for the August 2012 change are 0.62607 and -0.39774. The table also gives a level associated with each change that gives an indication of the importance of the change. For instance, the level 1 change denotes first change detected while level 2 changes are detected on a second pass through the data, and so on.

Table 4.3: Table of significant changes in the time series of SPEI for location R2.

Confidence Level for Candidate Changes = 50%, Confidence Level for Inclusion in Table = 90%, Confidence Interval = 95%, Bootstraps = 1000, Without Replacement, MSE Estimates					
Row	Confidence Interval	Conf. Level	From	To	Level
16	(11, 185)	96%	-1.2308	-0.27877	7
387	(294, 440)	100%	-0.27877	0.19399	1
476	(391, 494)	94%	0.19399	0.66059	5
506	(494, 553)	98%	0.66059	-0.019886	6
1041	(958, 1072)	95%	-0.019886	-0.5149	11
1116	(1084, 1129)	93%	-0.5149	0.24262	8
1136	(1129, 1137)	98%	0.24262	-1.4479	6
1141	(1141, 1143)	93%	-1.4479	0.62607	4
1172	(1166, 1187)	100%	0.62607	-0.39774	3

The question as to whether all nine changes are significant or not is cross-checked using 1000 bootstraps without replacement and MSE. To graphically illustrate the results, Figure 4.6 shows the CUSUM chart with significant changes shown in the background for the location R2. The number of significant changes is indicated by the number of times the background colour has changed. It appears that the significant changes in the SPEI have occurred nine times at location R2, concurring with Table 4.3.
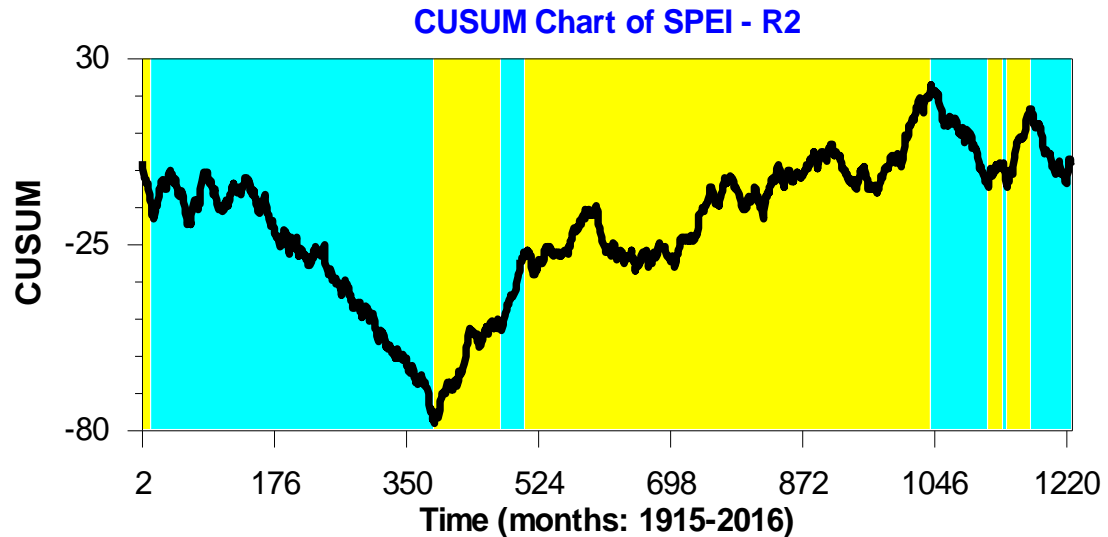
Figure 4.6: CUSUM chart of the SPEI data for location R2 with significant changes shown in the background.

Similarly, the change with 100% level of confidence occurred at the 1023rd month (*i.e.,* March 2000) as given in Table 4.4 for the location R3. There are six periods in total where significant change has occurred. The graphical representation of the change in terms of CUSUM is shown in Figure 4.7. As opposed to the locations R1, R2 and R3, the location R4 has twenty-six periods where a significant change in the SPEI trend has occurred, see Table 4.5 and corresponding CUSUM in Figure 4.8. Of the twenty-six, nine changes have occurred with 100% confidence. These points are (numerically in month/year format) 07/1916, 07/1920, 12/1921, 01/1949, 03/1973, 04/1979, 03/2001, 02/2010 and 07/2016. Most of these changes occurred when the phase of ENSO changed as well. The significant difference at R4, compared to the locations R1, R2 and R3, could be due to its location in the arid/semi-arid region where meteorological parameters are highly variable.

Table 4.4: Table of significant changes in the time series of the SPEI for location R3.

	Confidence Level for Candidate Changes = 50%, Confidence Level for Inclusion in Table = 90%, Confidence Interval = 95%, Bootstraps = 1000, Without Replacement, MSE Estimates					
Row	Confidence Interval	Conf. Level	From	To	Level	
916	(829, 917)	96%	-0.023271	-1.2465	2	
925	(923, 956)	98%	-1.2465	-0.46026	3	
970	(940, 1001)	98%	-0.46026	0.033142	2	
1003	(983, 1010)	96%	0.033142	0.75432	4	
1023	(1021, 1032)	100%	0.75432	-0.48461	3	
1141	(1082, 1209)	96%	-0.48461	-0.059474	5	
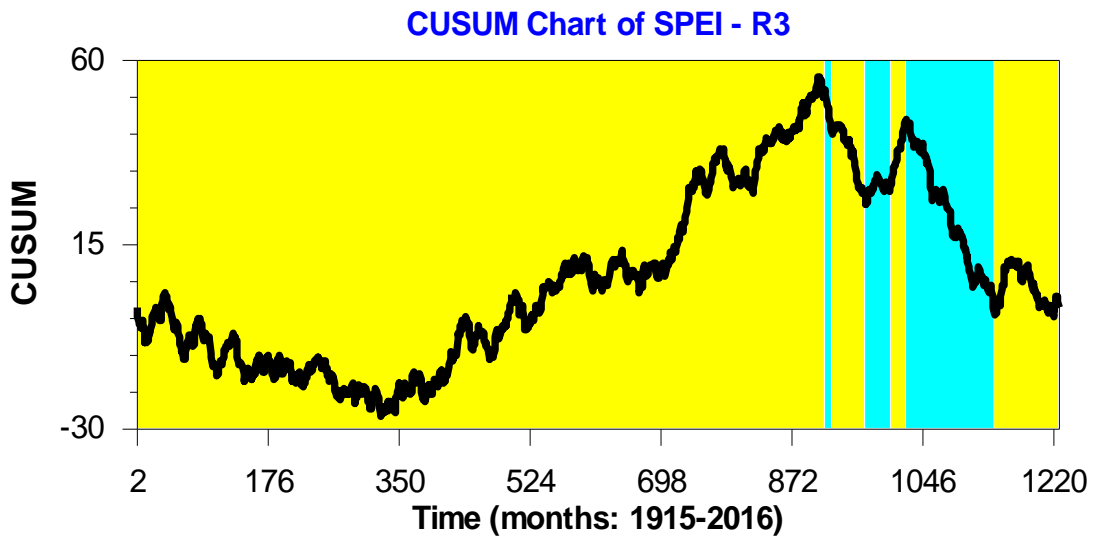
Figure 4.7: CUSUM chart of the SPEI data for location R3 with significant changes shown in the background.

Table 4.5: Table of significant changes in the time series of the SPEI for location R4.

Confidence Level for Candidate Changes = 50%, Confidence Level for Inclusion in Table = 90%, Confidence Interval = 95%, Bootstraps = 1000, Without Replacement, MSE Estimates					
Row	Confidence Interval	Conf. Level	From	To	Level
19	(15, 20)	100%	-0.63934	1.2351	9
28	(26, 40)	93%	1.2351	0.24884	10
47	(37, 52)	98%	0.24884	-0.58503	8
67	(65, 68)	100%	-0.58503	1.1087	11
84	(82, 90)	100%	1.1087	-0.23955	6
164	(85, 172)	94%	-0.23955	-0.74341	14
182	(178, 200)	90%	-0.74341	0.17805	7
263	(210, 322)	98%	0.17805	-0.22256	10
409	(396, 421)	100%	-0.22256	0.79671	9
434	(415, 443)	96%	0.79671	-0.017313	10
479	(465, 487)	99%	-0.017313	0.77868	11
503	(499, 514)	98%	0.77868	-0.28625	8
699	(682, 713)	100%	-0.28625	0.5016	9
772	(762, 774)	100%	0.5016	-0.6594	12
794	(787, 805)	94%	-0.6594	0.058864	15
809	(799, 811)	94%	0.058864	-0.96257	14
820	(818, 867)	91%	-0.96257	-0.067982	13
893	(865, 893)	91%	-0.067982	1.5758	15
896	(896, 896)	96%	1.5758	-0.024475	19
904	(903, 904)	99%	-0.024475	1.1383	18
909	(909, 912)	95%	1.1383	-0.63758	15
934	(925, 962)	96%	-0.63758	0.14244	18
1035	(1008, 1058)	100%	0.14244	-0.4749	4
1142	(1139, 1144)	100%	-0.4749	1.4303	5
1157	(1155, 1162)	99%	1.4303	-0.37256	7
1219	(1205, 1223)	100%	-0.37256	1.0161	2
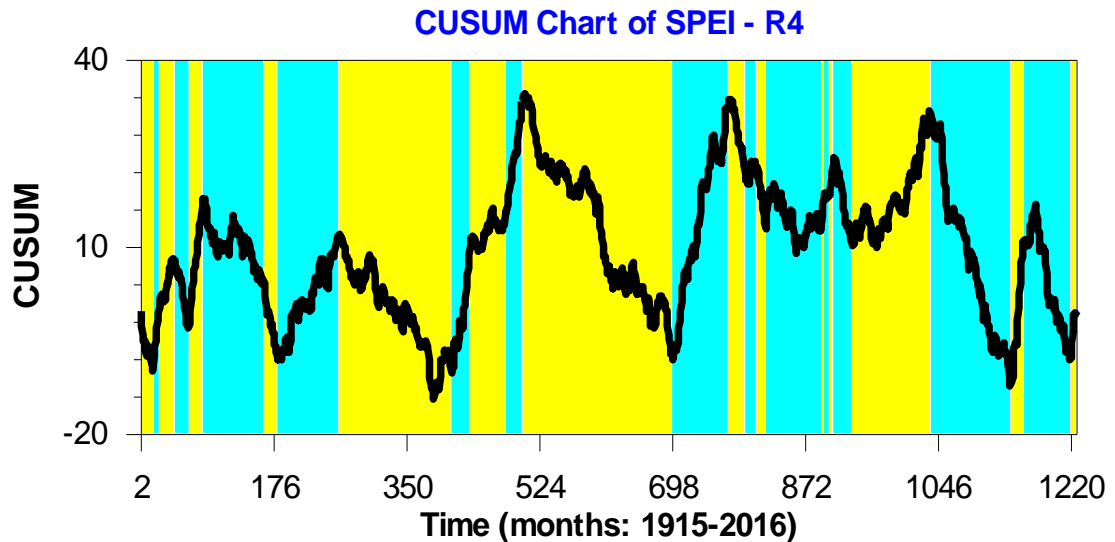
Figure 4.8: CUSUM chart of SPEI data for location R4 with significant changes shown in the background.

4.4 Conclusion

The main conclusions that can be drawn from this chapter are:

1. SPEI is able to identify extreme droughts better than the SPI;

2. SPEI highly correlates with precipitation-based DIs, especially with SPI and RDDI but can additionally provide complementary information about hydrological effects of drought;

3. Illustrated by the wavelet analysis, the SPEI concurs with all major drought events to a greater extent, significant at 95% confidence interval, compared to SPI, RDDI and RAI;

4. DI cross-wavelet analysis with the upper layer soil moisture (*i.e., WRel1*) indicated SPEI to be in phase more significantly at 95% confidence interval compared to the SPI, RDDI and RAI.

5. The change-point analysis represents a powerful tool that is able to detect changes in the SPEI trend with associated confidence levels and confidence intervals. The study found the location R4 (in the arid/semi-arid region) to have undergone 26 changes in the SPEI trend compared to locations R1, R2 and R3 with 0, 9 and 6, respectively. The location of the study matter where inland from the coastline experiences more variability in the environmental parameters that define the SPEI.

86

Chapter 5

INVESTIGATING DROUGHT DURATION-SEVERITY-INTENSITY CHARACTERISTICS USING THE STANDARDISED PRECIPITATION-EVAPOTRANSPIRATION INDEX

Note:

The results from this chapter have been published in *ASCE Journal of Hydrologic Engineering*. The following is the reference to the article:

Dayal KS., Deo RC, and Apan A., (2018) "Investigating drought duration-severity-intensity characteristics using Standardised Precipitation-Evapotranspiration Index: a case study in drought-prone, southeast Queensland", ASCE *Journal of Hydrologic Engineering*, 23(1): https://doi.org/10.1061/(ASCE)HE.1943-5584.0001593.

5.1 Introduction

Chapter 4 has provided the first set of results following the first objective of the study (listed in Section 1.3). There, the comparison of DIs showed SPEI surpassing SPI, RDDI and RAI in the detection of major droughts. Continuing with addressing the first objective of the study, the current chapter provides a further innovative contribution of the SPEI for assessment of drought properties.

The aim of this chapter is to uncover potential merit of the SPEI for drought assessment in southeast Queensland and to deepen our understanding of drought

characteristics, whilst searching for a robust drought tool. The novelty is to apply SPEI for drought analyses in the SEQ region that has been subjected to several severe and prolonged drought events (Deo et al. 2009; Hertzler et al. 2006; McAlpine et al. 2007; McAlpine et al. 2009; van Dijk et al. 2013). The purpose of the study in this chapter is fivefold: (1) to apply the SPEI for drought assessment by considering jointly the impacts of rainfall and *ETo* on water deficit periods, (2) to analyse the time series of SPEI using a run-sum theory in order to deduce the drought properties in terms of accumulated drought severity (S), duration (D) and intensity (I) based on the identified onsets and terminations of drought to accord with thresholds of SPEI in water deficit periods, (3) to identify the relationships between SPEI and other drought variables (*i.e.,* precipitation, soil moisture, and maximum temperature data) where such comparisons are expected to aid in addressing the impacts of an agricultural drought event, (4) to apply SPEI for estimating drought return periods for a given severity, S or intensity, I, and (5) to analyse the multi-scalar properties of drought using timescales (T) = 1, 3, 6, 9, 12 and 24-monthly drought monitoring data.

5.2 Materials and Method

5.2.1 Hydrological data and study area

The same point-based study locations R1, R2, R3 and R4 used in Chapter 4 are also used in this chapter. Figure 5.1 shows the mean monthly climatological pattern for precipitation, maximum temperature, supply-demand balance (*i.e.,* $P - ETo$; hereafter called *SDB*) and upper layer soil moisture (*WRel1*) for the base period (1971-2000) for each study location. The precipitation and temperature data shows warmer and wetter summer and cooler and drier winter seasons for all locations, while the *SDB* and soil moisture reveal distinct seasonality. The precipitation and soil moisture appear to be in statistical congruence with each other, where a particular region receiving relatively high precipitation appears to exhibit a generally high soil moisture value and vice versa. Notably, the location denoted as R4 exhibited the lowest amount of precipitation and this region has also been generally the warmest, with the smallest *SDB* value and lowest soil moisture content compared to the other study regions, coinciding well with its location in the semi-arid zone.
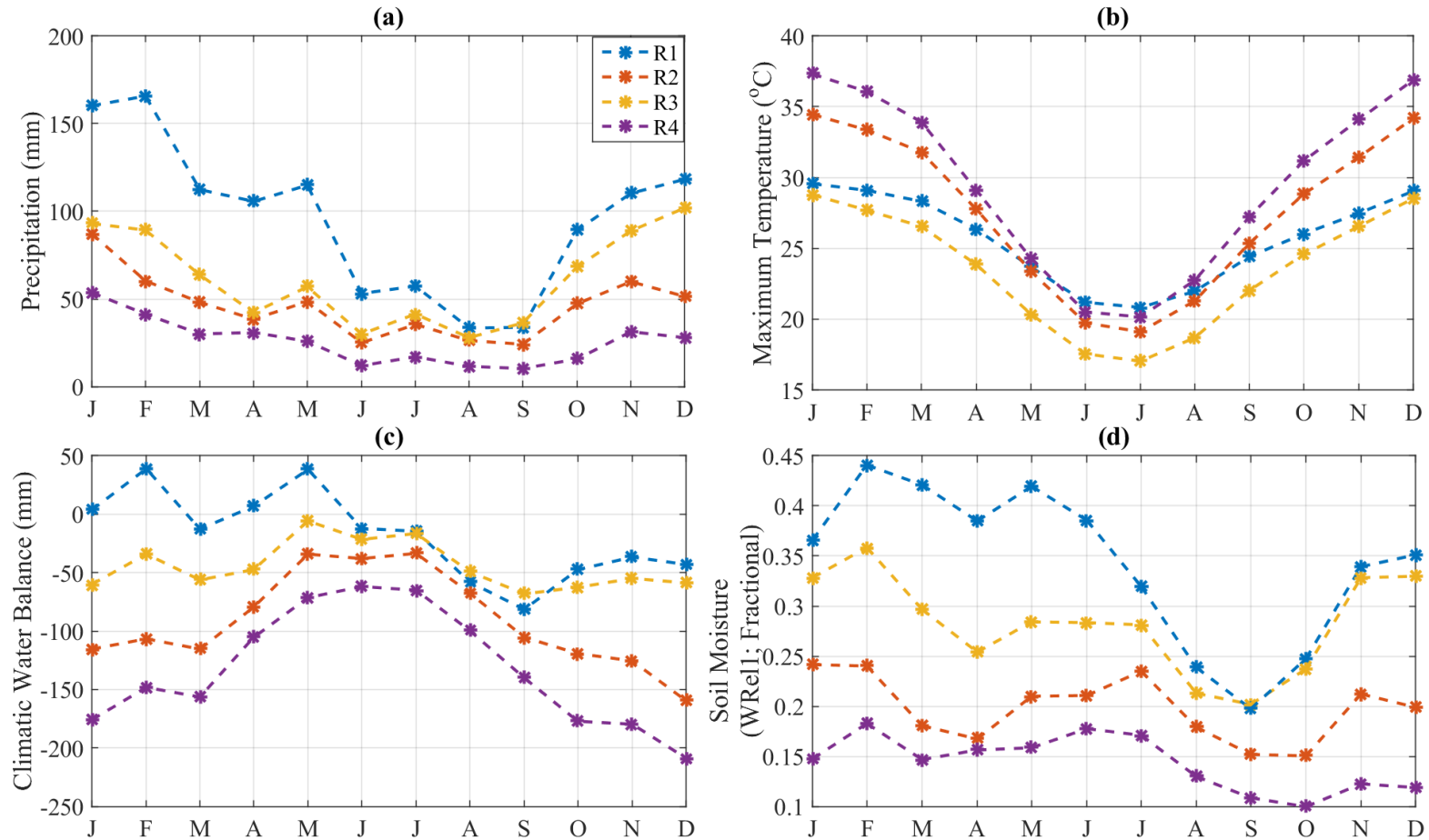
Figure 5.1: Monthly climatology of (a) precipitation (*P*; mm), (b) maximum temperature (*Tmax*; ˚C), (c) climatic water balance (mm), and (d) upper layer soil moisture (*WRel1*; fractional). Legend applies to all panels.

To generate climate statistics and check the overall distribution of climate data, a violin plot (which aimed to integrate a boxplot with a kernel density plot) has been prepared (see Figure 5.2). This figure shows the median, quartiles and the 95% confidence interval for the *P*, *Tmax* and *WRel1* data for the period T=3 and T=12-months (running sum for *P* and running mean for *Tmax* and *WRel1*). Evidently, the *P* and *WRel1* data appear to mimic a unimodal pattern in their distribution with a relatively large number of months exhibiting high probability. In terms of the *Tmax* data, a bimodal behaviour can be noted at all case study locations on a T=3-month scale where the range of *Tmax* data appears to be relatively large for location R4, followed by that for locations R2, R3 and R1. However, the climatic patterns become more distinct on the T=12-month scale. Overall, the climatic conditions in the case study regions (Figure 5.1 and 4.2) highlight significant variability in their climates, and possibly, indicating the complexity of any observed drought events explored using the present SPEI data.
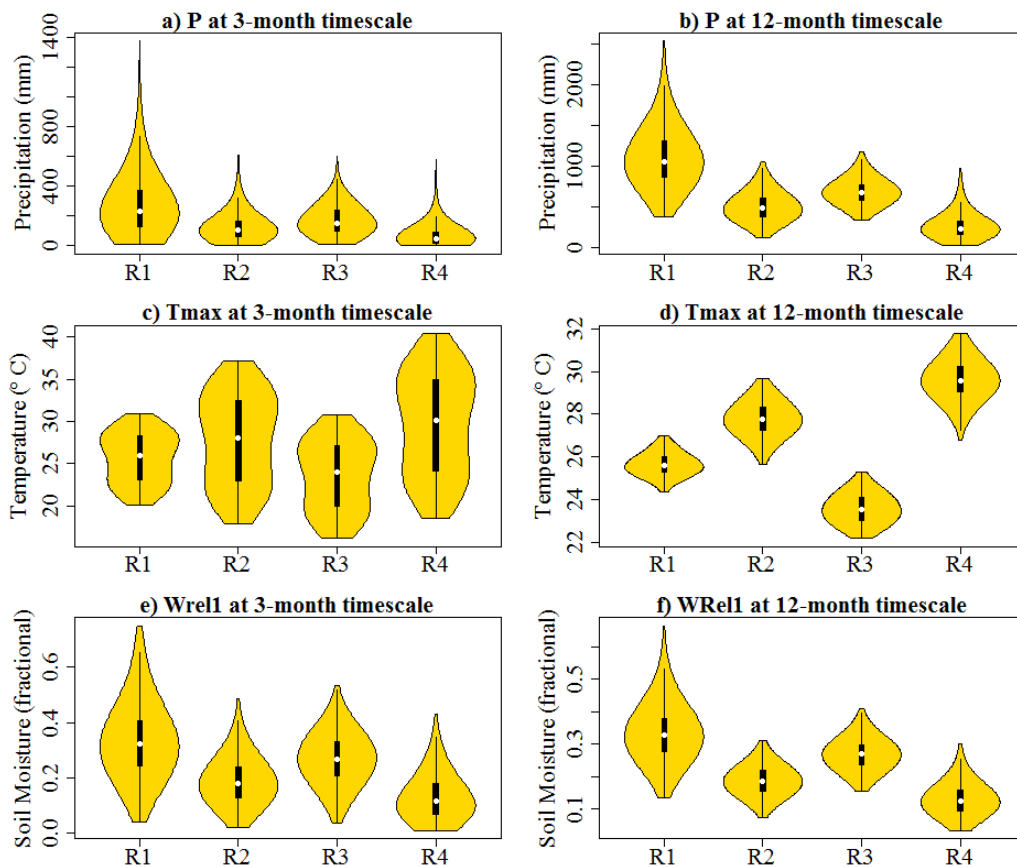
Figure 5.2: Violin plots with a combination of boxplot and kernel density distribution for (a, b) precipitation (*P*), (c, d) maximum temperature (*Tmax*), and (e, f) upper layer soil moisture *(WRel1)* on 3-month and 12-month timescales.

5.2.2 Characterisation of drought properties

In accordance with SPEI representing the normalised deficits or surpluses of water resources relative to a climatological base period, the drought onsets and terminations are then identified in a period when the SPEI declined to a value below zero (*i.e.,* the standardised water deficit was below the normal value). The drought duration (*D*), severity (*S*), and intensity (*I*) characteristics are thus estimated via the commonly adopted run-sum approach described in Yevjevich (1967):

$$S = \sum_{i=1}^{D} -\left(SPEI_i\right) \tag{5.1}$$

$$I = \min\left(SPEI_i\right) \tag{5.2}$$

$$D \equiv \sum_{i=1}^{i=n} n \tag{5.3}$$

In Equations (5.1–5.3), $i = 1$ is the start of a drought event when the SPEI drops below zero and its continuation as a negative value for at least three months, $D =$ total duration from the onset to the termination period, n is the number of months with consecutive negative values, while the intensity, $I =$ the drought peak (*i.e.,* minimum SPEI) for a given drought event. It is imperative to note that a drought event that lasted for less than 3-month duration, which is generally regarded as insufficient to impact the available water resources, has been ignored in this case study following the Australian BoM's definition (*i.e.,* a drought condition is declared when precipitation is below normal for consecutive three or more months) (Mpelasoka et al. 2008).

Figure 5.3 illustrates the *D*, *S* and *I* properties of identified drought events in the designated region (R1) from 1991 to 1996 on a $SPEI_3$ time series. Since the SPEI is a standardised metric, a value of 0 refers to the normal supply-demand balance (*i.e.,* the current supply-demand balance matching the mean climatological conditions), whereas SPEI = -1 indicates a deficit equivalent to about 1 standard deviation below the normal and SPEI = 1 indicates a surplus equivalent to 1 standard deviation above the normal supply-demand balance. In this case study, all consecutively negative values of SPEI that corresponded to the significantly dry period(s) are investigated. In congruence with the shading shown in Figure 5.3, a drought event that commenced in

91

July 1992, for example, are seen to attain $S = -12.99$, $D = 14$ months and $I = -1.52$ values, and can thus be classified as severe drought event.
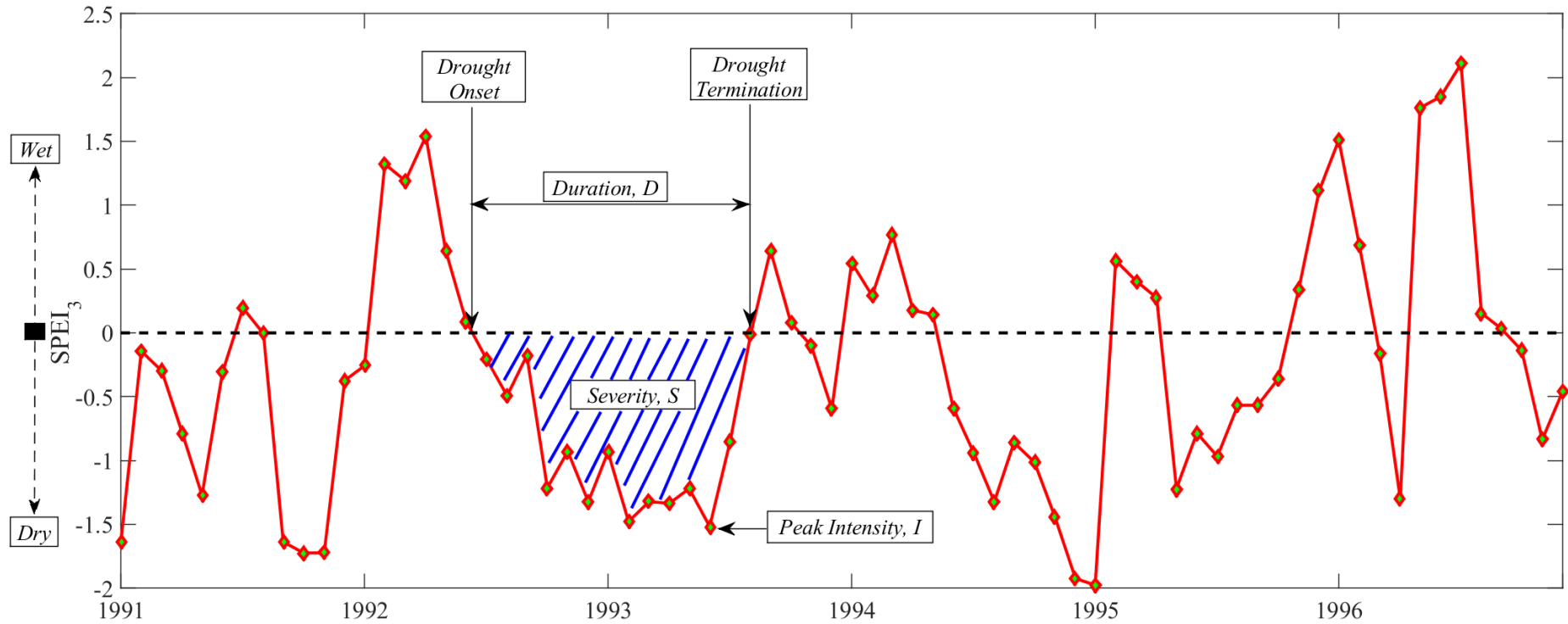
Figure 5.3: Graphical definition of drought onset and termination, drought severity *(S)*, drought duration *(D)*, and peak intensity *(I)*. The time series is taken for R1 from 1991 to 1996 on the 3-month timescale.

All drought cases that are evaluated for any dry event with a value of $D \geq 3$ months are also categorised into various classes, *i.e.*, normal conditions (-0.99$\leq$ SPEI $\leq$0.99), moderate drought (-1.49$\leq$ SPEI $\leq$-1.00), severe drought (-1.99$\leq$ SPEI $\leq$-1.50) and an extreme drought (SPEI $\leq$-2.00) case as in Yu et al. (2014) and Nam et al. (2015). Drought events deduced from the SPEI data are therefore validated against the monthly precipitation, soil moisture (*WRel1* and *WRel1End*) and RAI.

In terms of understanding the practical benefit of SPEI, one could consider its potential utility in the context of designing hydrologic structures (*e.g.,* dams or irrigations) that may require a prior knowledge of the analysis of risk in terms of whether a design may be appropriate for a drought event with a certain return period. Hence, drought events assessed with respect to their frequency of occurrence using the concept of a return period of an event in any observation can be designated as the inverse of exceedance probability, $p = P(X > X_T)$ (Kim et al. 2003):

$$T = \frac{1}{P(X > x_T)} = \frac{1}{1 - P(X \leq x_T)} \tag{5.4}$$

In Equation (5.4), X_T = magnitude (*i.e.,* drought severity) with a return period (T) and X (random variable) is the drought severity of a given magnitude. If a marginal cumulative distribution of the severity parameter, S for a threshold level is denoted by $F_S(S)$, the univariate return period for a drought severity, T_s, is then (Kim et al. 2003):

$$T_s(years) = \frac{N}{n[1 - F_S(s)]} = \frac{1}{\theta[1 - F_S(s)]} \tag{5.5}$$

where $\theta = n/N$; N = total length of observed SPEI data (102 years in this case study) and n = total number of events, during N. Similarly, the return periods based on I and D are determined using Eq. 5.5.

5.3 Results and Discussion

In this section, the results generated for drought studies in the four case study regions (R1, R2, R3, R4) with distinct climatic conditions (Figures 5.1, 5.2) are presented and argued in light of the usefulness of the SPEI for an objective characterisation of drought. Identifying the number of drought events using a run-sum approach is a key

towards understanding drought duration (D) and its potential recurrence intervals. Using the criteria of $D \geq 3$ months and the epochs with $SPEI \leq -1$ (*i.e.,* supply-demand balance lower than normal by at least 1 standard deviation), the number of drought events have been identified at each case study region on different timescales (see Table A5.1 in the Appendix).

The World War II (WWII) drought event, reigning over the period 1935–1947, was an iconic dry event in Australia that affected quite significantly a number of socio-economic activities in the SEQ region (Verdon-Kidd and Kiem 2009). In this case study, the response of SPEI for the characterisation of this episode based on precipitation and soil moisture data has been tested in order to better understand the agricultural consequences of a persisting drought. The soil moisture data is thus adopted for its comparison with SPEI, as this parameter is an important component of the regional hydrological cycle, *e.g.,* (Yamaguchi and Shinoda 2002). Figure 5.4 illustrates a segment of this drought event at location R2. It is apparent that for a low precipitation and soil moisture epoch, the SPEI is able to capture quite well the temporal variation in a drought situation, in accord with the notable WWII drought.

In fact, the upper layer (*WRel1*) mean value and the upper layer end of month (*WRel1End*) fractional soil moisture, bounded by [0, 1] is in phase with the SPEI and precipitation data. This showed several periods with relatively low values of the SPEI that corresponded with values of low soil moisture (*i.e.,* demonstrating the agricultural effect of the underlying dryness). Such an assessment of a drought event from an agricultural perspective, which utilises the role of a supply-demand balance measure for drought impact assessment, is impossible with solely rainfall-based *DIs* and is therefore of potential scientific value to socio-economic activities like sustainable agriculture, irrigation and water resource management (Vicente-Serrano et al. 2012).
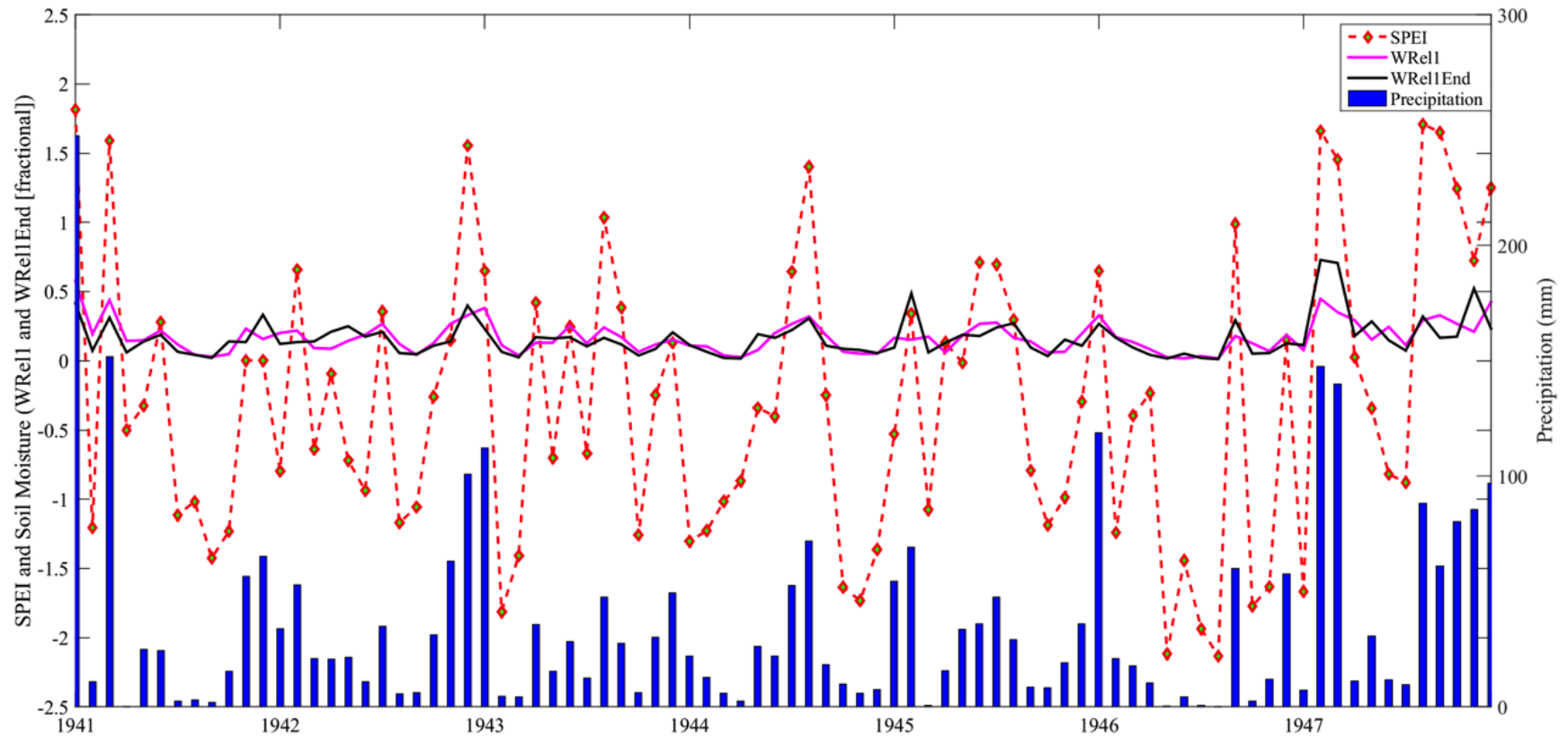
Figure 5.4: Upper layer (*WRel1*) and upper layer end of the month (*WRel1End*) soil moisture plotted with SPEI and precipitation (mm) for the WWII drought period: 1941-1947 for study location R2.

In Figure 5.5, the annual SPEI *vs.* the annual rainfall anomaly index (RAI); a metric that is commonly utilised for meteorological drought assessment is displayed. Note that, a time series of the RAI has been adopted to cross-check the epochs of annual precipitation below (above) normal for dry (wet) events within the historical period. A synchronicity between the objective drought metric (*i.e.,* SPEI) and the traditional meteorological metric (*i.e.,* RAI) is clearly evident, where the dry years (with significantly negative values of the RAI) are temporally in-phase with the annual SPEI data. In all case study regions considered, the coefficient of determination (R^2) for the SPEI *vs.* RAI is more than 0.90, revealing that the objective drought index possesses statistically equivalent skills of the estimated deviation in rainfall from a normal period for the depiction of anomalously dry and wet periods. It should be mentioned, however, that the SPEI is a superior index due to its fundamental ability to incorporate the influence of *ETo*, a notion that is consistent with previous research perspectives (*e.g.,* (Lorenzo-Lacruz et al. 2010; Vicente-Serrano et al. 2010; Vicente-Serrano et al. 2012; Vicente-Serrano et al. 2013; Vicente-Serrano et al. 2011)). In several of these works, the ability of SPEI to measure the level of exacerbation has been stipulated, outlining its robust skill for the assessment of hydrological and agricultural impacts of a persisting meteorological drought condition. A similar comparison of multi-scalar SPEI with multi-scalar RAI and soil moisture (*WRel1*) has been carried out in terms of Kendall's tau (τ) values, which ranged from 0.60 to 0.92 with RAI and from 0.50 to 0.85 with *WRel1,* where τ values were small on smaller timescales, and vice versa (see Table A5.2 in the Appendix).
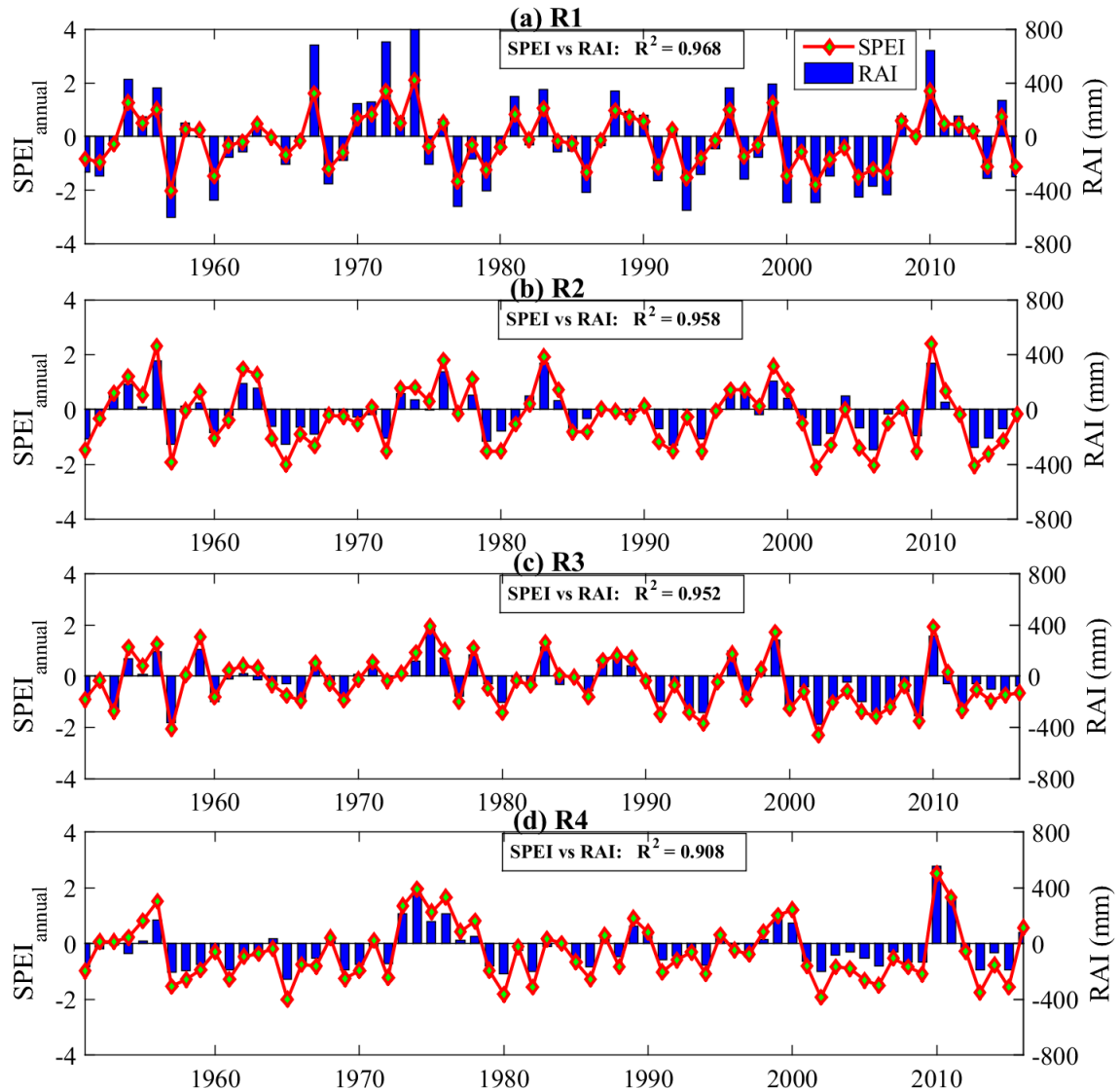
Figure 5.5: Annual SPEI plotted against annual RAI for (a) R1, (b) R2, (c) R3 and (d) R4 with a coefficient of determination (R^2) values. Legend applies to all panels.

Drought phenomena display a high degree of serial correlation (or persistence) arising from precipitation as a source of the surface run-off, but its intrinsic relationship with the underlying soil moisture and the groundwater recharge can act to moderate the rainfall–runoff and hydrological processes; consequently, impacting the seriousness of the dry episode. The drought has a memory of several months arising from antecedent rainfall so it does affect the local or regional catchment hydrology. Concurrent or lagged correlation between SPEI and its inter-related variables (*e.g.*, precipitation, temperature, soil moisture and reference evapotranspiration) can be thus utilised to assess a drought impact via a purely statistical sense (Chiew et al. 1998; McBride and Nicholls 1983). Figure 5.6 shows the monthly value of SPEI, cross-

correlated with monthly precipitation (Column 1), upper layer soil moisture (Column 2), upper layer end of month aggregated soil moisture (Column 3), maximum temperature (Column 4) and reference evapotranspiration (Column 5). Here, the row plots refer to the case study regions, and the lags represent the antecedent month while the blue line marks the threshold of 95% confidence interval. At a lag of zero, a statistically significant cross-correlation coefficient (at $\alpha = 0.05$) exists for the SPEI *vs. P*, *WRel1*, *WRel1End*, *Tmax* and *ETo* data. The cross-correlation coefficient is also significant at several other lags for these five variables, indicating their overall importance in moderating the hydrological cycle that could impact the way an agricultural drought manifests itself in a given region. The cross-correlation coefficient of SPEI with precipitation data is significant only at lag zero and/or lag 1 since SPEI is estimated using precipitation data. However, with soil moisture data (*WRel1* and *WRelEnd*) at all study regions, SPEI exhibited a statistically significant correlation at lags up to 3 months that reflects the seasonality of drought events via the memory of rainfall and soil moisture.
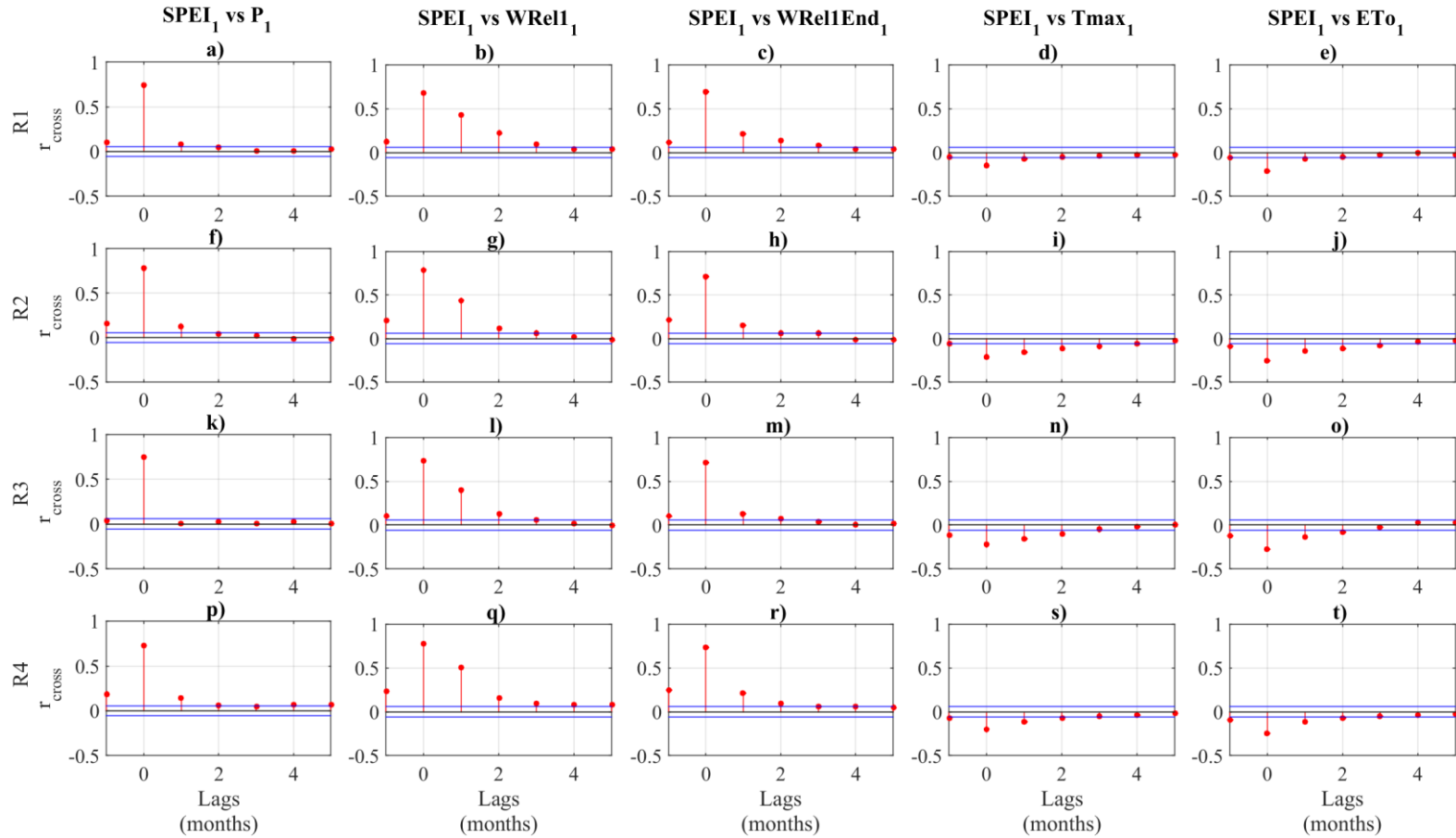
Figure 5.6: Cross-correlation of SPEI with precipitation *(P)* (a, f, k, and p), upper layer soil moisture *(WRel1)* (b, g, l, and q), upper layer end of month soil moisture *(WRel1End)* (c, h, m, and r), maximum temperature *(Tmax)* (d, i, n, and s), and reference evapotranspiration *(ETo)* (e, j, o, and t). Solid lines indicate 95% confidence interval.

Owing to their practical benefit in risk evaluation, duration-severity-intensity (*D-S-I*) properties are key defining characteristics for droughts. As such, the statistical correlation between *D-S-I* properties can help explain their interdependence, allowing hydrologists to objectively assess the overall damage caused by a given drought event. Table 5.2 enumerates Kendall's tau values between *S* and *I*, *S* and *D*, and *D* and *I* properties of identified drought events at different timescales. The effect of seasonality on smaller timescales is noticeable with smaller correlation values whereas the association between properties becomes stronger across larger timescales. While Table 5.2 provides vital information on the bivariate relationships of *D-S-I*, an understanding of the trivariate relationships of *D-S-I* concurrently is a more relevant measure of the combined impact of drought in the sustainable management of water resources. Figure 5.7 plots the annual drought severity, annual peak drought intensity and annual drought duration for T=3, 6, 9 and 12 months at R1, R2, R3 and R4, respectively.

Table 5.1 Kendall's tau between drought duration and severity (*D* and *S*), duration and intensity (*D* and *I*) and severity and intensity (*S* and *I*) for different timescales.

Regions	Timescale 1	Timescale 3	Timescale 6	Timescale 9	Timescale 12	Timescale 24
			D and *S*			
R1	-0.52	-0.65	-0.79	-0.83	-0.83	-0.88
R2	-0.67	-0.75	-0.82	-0.85	-0.89	-0.92
R3	-0.55	-0.76	-0.81	-0.85	-0.88	-0.87
R4	-0.65	-0.72	-0.82	-0.85	-0.88	-0.86
			D and *I*			
R1	-0.20	-0.32	-0.52	-0.62	-0.65	-0.71
R2	-0.38	-0.46	-0.56	-0.60	-0.70	-0.72
R3	-0.32	-0.49	-0.62	-0.65	-0.65	-0.69
R4	-0.31	-0.47	-0.57	-0.60	-0.75	-0.74
			S and *I*			
R1	0.56	0.63	0.68	0.75	0.80	0.79
R2	0.64	0.65	0.70	0.72	0.80	0.77
R3	0.64	0.69	0.77	0.76	0.75	0.80
R4	0.58	0.71	0.72	0.71	0.83	0.84

For a generally lengthy drought event, the severity and intensity parameters appear to register relatively high values. For instance, consider at location R4 (Fig. 5.7d), the case of the 1958 drought (one of the major droughts recorded by Australian

BoM) at T=12 months had an estimated severity metric of about -23.67 and an intensity metric of -2.65, and a duration period of about 12 months in accordance with droughts identified by the SPEI. The opposite trend is noted for a drought event with a shorter duration; for example, at location R4 the drought duration estimated to be about 3 months within the year 1979 had a severity metric of about -2.10 and an intensity metric of about -0.96. This relationship, however, is not likely to be perfectly proportional in terms of the magnitude of properties for some drought events that may be short-lived but very severe and intense. Therefore, a multivariate analysis of drought events (*e.g.,* the use of copula-statistical models) could be a further step in developing a better understanding of the associations between the various drought properties.
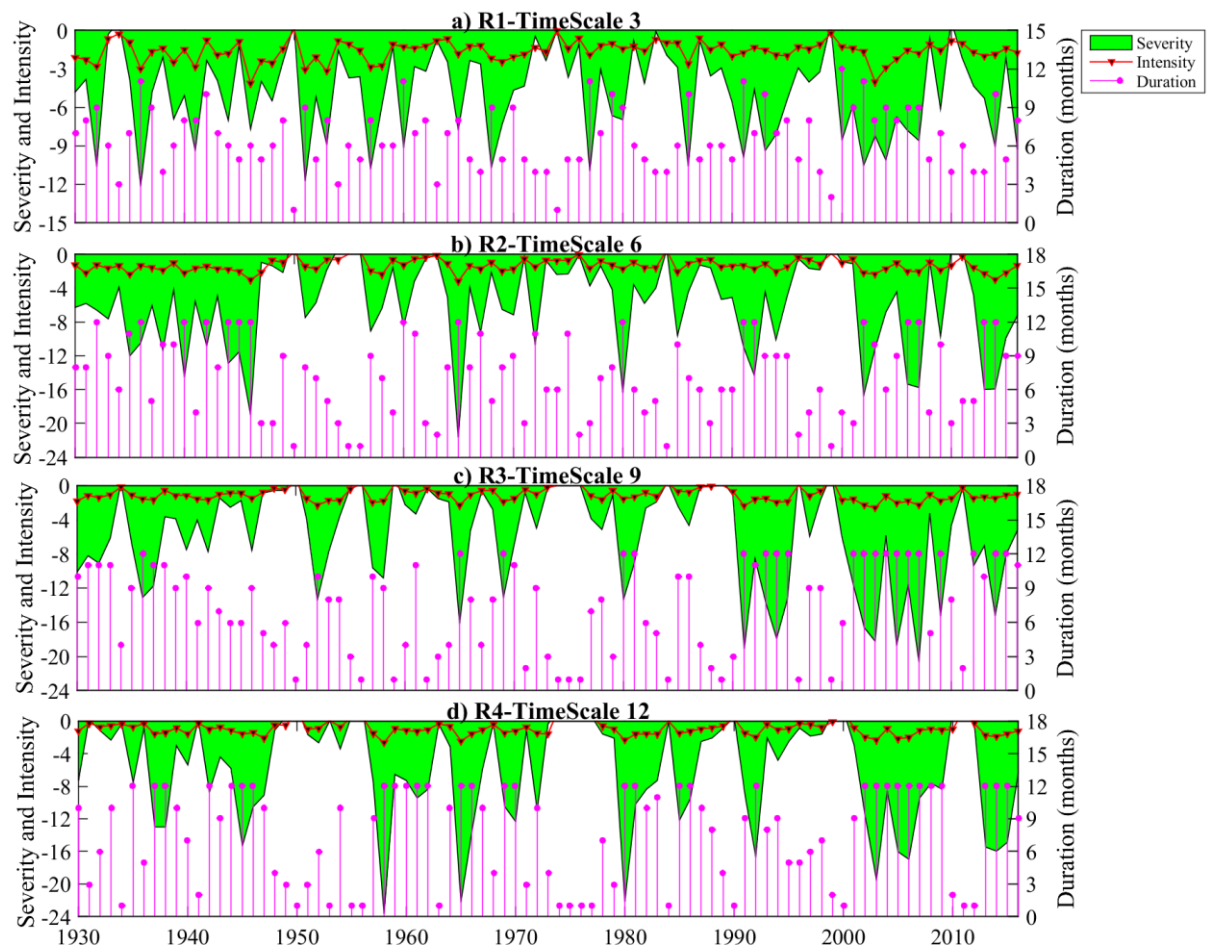
Figure 5.7: Annually accumulated drought duration (D), severity (S) and intensity (I) for: (a) R1, (b) R2, (c) R3 and (d) R4 at 3-, 6-, 9-, and 12-month timescales, respectively. Legend applies to all panels.

In the sustainable management of water resources and for designing hydrologic systems (*e.g.,* irrigation and water storage dams), an estimation of the drought return

period based on some certain threshold criteria can be very useful in practical applications. Using *D-S-I* properties of drought deduced from SPEI time series, the estimated return period of drought for given thresholds can be determined, as stipulated in Figure 5.8 for T=3 (first row) and T=12 (second row) months. It is evident in Fig 5.8a, for example, that for a given short-term drought severity of magnitude -15.00, the estimated return period is expected to be about 70 years at R1, 10 years at R2 and R4 and 15 years at R3. This shows that a drought event with a severity of about -15.00 is likely to occur more frequently in location R2, R3 and R4 compared to the location R1. At T=12 months, droughts with a return period of 20 years have variable severity ranging from -45 to -35 in magnitudes between study regions.

It is also revealed in Fig 5.8a and 5.8d that short- or long-term droughts at location R1 are much less severe compared to other regions that could be associated with its location-specific climatic conditions. On the other hand, a return period based on the peak drought intensity as a criterion (Fig. 5.8b and 5.8e) demonstrates that for an intensity of about -2.50 (*i.e.,* extreme drought), the recurrence interval of the short-term drought events can attain values between 5 and 25 years, while those of long-term droughts vary from 18 to 105 years. The comparison also shows that the short-term and long-term extreme droughts occur more often (*i.e.,* lower recurrence interval) at locations R1 and R2, respectively than at R3 and R4. Taken together, it can be averred that the water resource availability is expected to be lower than the normal amount by at least 2.50 standard deviations of the climatological base period, so a design of hydrologic structures to withstand this event must consider the different recurrence intervals for the different case study sites.

In the foregoing discussion, it is imperative to note that since drought duration is estimated in terms of integers (*i.e.,* months), there can be many different return periods for the same duration, as shown in Fig. 5.8c and 5.8f for T=3 and T=12 months, respectively. For instance, at location R1, the drought event with an estimated duration of about 10 months had return periods ranging from 8-13 years. Therefore, the structural design for water storage media based on a certain drought duration must withstand the drought impacts by allowing the structures to last throughout the range of estimated years. Additionally, it can be noted that the less severe, less intense and short-lasting droughts are seen to occur more frequently as indicated by their small

return periods, *i.e.,* less than 5-years in all case study regions. In general, the return period concept can illustrate the importance of each drought property, especially from the perspective of water resource management and in various decision-making tasks related to hydrological systems.
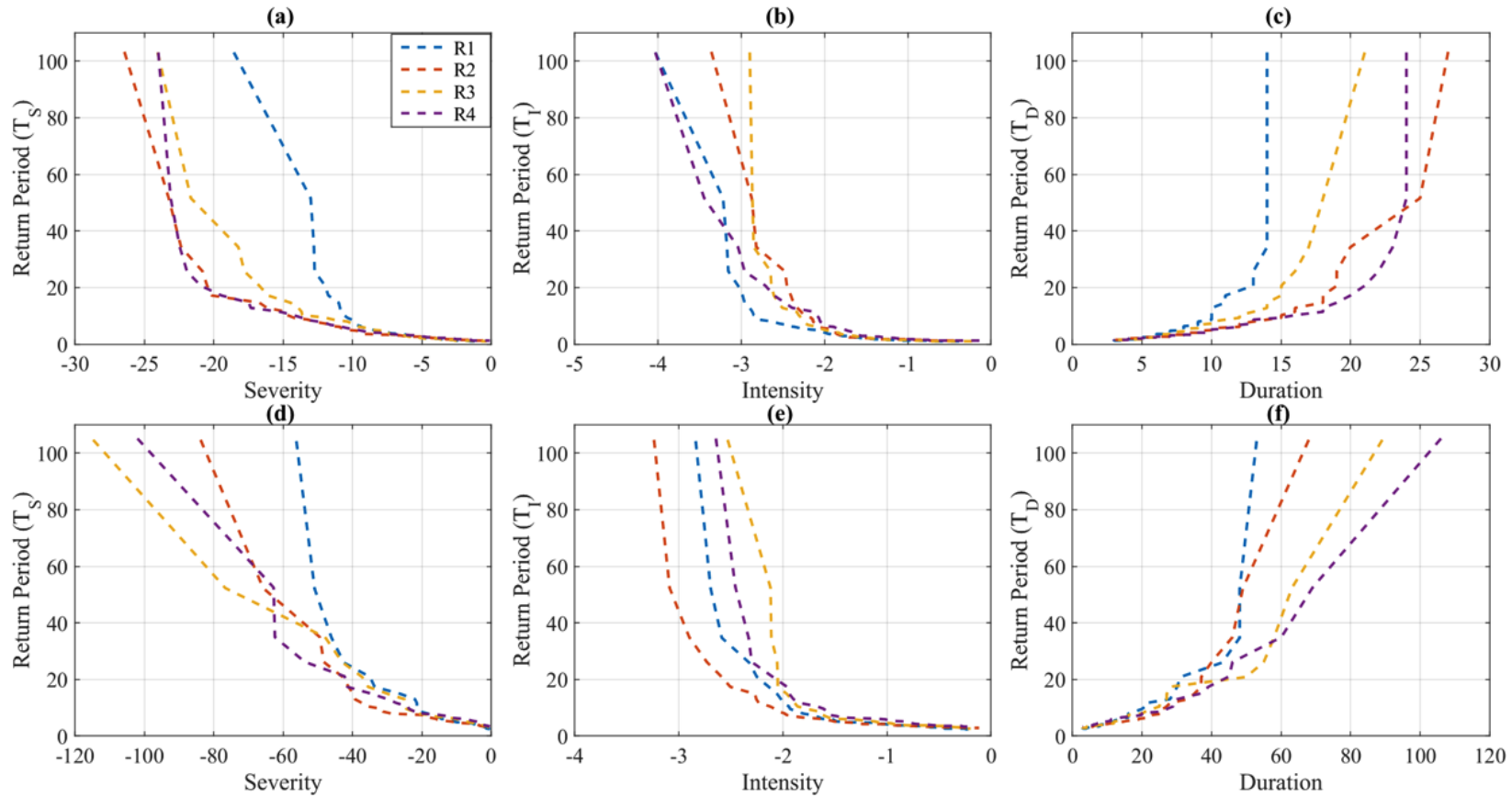
Figure 5.8: The drought return period based on severity (a, d), intensity (b, e) and duration (c, f) for 3-month (row 1) and 12-month (row 2) timescales. Legend applies to all panels.

Table 5.3 lists return periods based on the severity and intensity (for T=3 and T=12 months) properties of top 5 droughts (with largest magnitudes) return periods. Only at locations R3 and R4 the Millennium drought and the 1964-drought were most severe and most intense based on the short- and long-term drought assessment. The years of drought onset and the duration agree quite well with the worst drought observed in southeast Australia, including the WWII and Millennium drought events. Since drought characteristics vary from one climatic region to another, the most appropriate and suitable drought index is crucial to identify the differences, as demonstrated by the SPEI in this case study.

Table 5.2 Ranked drought events based on the severity and intensity of 3- and 12-month timescales. The top 5 events are listed here. The worst droughts are shown in boldface for each region.

Drought Year	Onset Month	Severity (S)	Intensity (I)	Duration (D; Months)	Return Period (Years)	Drought Year	Onset Month	Severity (S)	Intensity (I)	Duration (D; Months)	Return Period (Years)
Based on Severity of T3						**Based on Severity of T12**					
R1						**R1**					
1968	**4**	**-18.55**	**-2.44**	**13**	**103.06**	**2004**	**2**	**-56.09**	**-1.94**	**53**	**104.27**
1992	7	-13	-1.52	14	51.53	1917	4	-50.93	-2.84	48	52.13
2013	9	-12.8	-2	11	34.35	2000	6	-46.09	-2.13	43	34.76
1977	2	-12.72	-1.91	13	25.77	1977	2	-42.56	-1.93	48	26.07
1985	12	-11.99	-2.61	10	20.61	1935	12	-34.94	-2.33	29	20.85
R2						**R2**					
2005	**9**	**-26.45**	**-2.14**	**27**	**103.23**	**1942**	**1**	**-83.76**	**-3.09**	**68**	**104.76**
1921	12	-23.26	-2.4	25	51.61	2012	12	-65.85	-2.26	49	52.38
1918	10	-22.37	-2.26	20	34.41	1964	3	-49.34	-2.59	46	34.92
1964	12	-20.8	-3.36	12	25.81	2005	1	-48.36	-2.27	37	26.19
1945	10	-20.48	-2.45	16	20.65	1928	8	-42.85	-2.51	40	20.95
R3						**R3**					
2006	**1**	**-24.02**	**-2.01**	**21**	**103.06**	**2000**	**9**	**-114.85**	**-2.53**	**89**	**104.62**
2002	1	-21.63	-2.85	15	51.53	1991	2	-76.65	-1.92	63	52.31
2004	5	-18.25	-2.64	17	34.35	2012	3	-48	-1.65	55	34.87
1994	5	-17.82	-2	18	25.77	1935	4	-42.96	-1.77	58	26.15
1925	10	-16.73	-2.51	15	20.61	1918	9	-37.25	-2.11	27	20.92
R4						**R4**					

1964	12	-24	-4.03	20	103.17		2001	4	-102	-2.33	106	105.19
1979	5	-23.1	-2.06	24	51.59		1957	4	-62.76	-2.65	69	52.59
1928	2	-22.47	-2.02	24	34.39		1925	10	-62.46	-1.94	60	35.06
1956	11	-21.94	-2.05	23	25.79		2012	12	-53.71	-1.9	45	26.3
2012	9	-20.95	-2.39	18	20.63		1964	3	-42.32	-2.45	39	21.04

Based on intensity for T3							Based on Intensity for T12					
R1							**R1**					
2002	9	-7.95	-4.03	7	4.29		1917	4	-50.93	-2.84	48	52.13
1919	6	-10.99	-3.22	7	14.72		1968	6	-26.07	-2.69	21	14.9
1953	5	-6	-3.17	5	3.22		1951	10	-22.07	-2.59	16	13.03
1919	2	-4.95	-3.15	3	2.34		1935	12	-34.94	-2.33	29	20.85
1951	4	-11.72	-3.04	9	17.18		1922	6	-33.63	-2.25	31	17.38
R2							**R2**					
1964	12	-20.8	-3.36	12	25.81		2001	11	-37.24	-3.24	26	11.64
1930	11	-7.26	-2.88	5	3.13		1942	1	-83.76	-3.09	68	104.76
1984	12	-10.54	-2.82	8	5.16		1922	6	-35.7	-2.9	26	10.48
1928	7	-14.24	-2.47	9	9.38		1918	10	-39.21	-2.73	27	13.09
1945	10	-20.48	-2.45	16	20.65		1964	3	-49.34	-2.59	46	34.92
R3							**R3**					
1957	10	-8.86	-2.9	5	5.73		2000	9	-114.85	-2.53	89	104.62
1951	9	-11.97	-2.87	7	9.37		1915	2	-24.75	-2.12	21	10.46
2002	1	-21.63	-2.85	15	51.53		1918	9	-37.25	-2.11	27	20.92
1932	1	-5.34	-2.64	4	2.4		1951	10	-17.33	-2.06	15	7.47
2004	5	-18.25	-2.64	17	34.35		1925	10	-24.96	-2.05	25	11.62

R4						**R4**					
1964	**12**	**-24**	**-4.03**	**20**	**103.17**	**1957**	**4**	**-62.76**	**-2.65**	**69**	**52.59**
1986	2	-10.06	-3.45	5	5.43	1964	3	-42.32	-2.45	39	21.04
2004	8	-11.83	-3.04	10	7.37	2001	4	-102	-2.33	106	105.19
2002	3	-19.44	-2.96	13	17.2	1979	10	-34.93	-2.3	29	15.03
1934	11	-8.06	-2.71	7	3.97	1943	12	-41.6	-2.11	46	17.53

To identify agricultural consequences (with multi-scalar effects of a drought) that can emanate from a meteorological drought event both on short and long periods, a multi-scalar index is considered more appropriate to assess the time-lagged associations between the meteorological (*e.g.,* rainfall) and agricultural (*i.e.,* soil moisture) parameters. Previous studies have shown how the different usable water sources respond to various timescales of a drought metric (*e.g.,* (Szalai et al. 2000; Vicente-Serrano 2007; Vicente-Serrano et al. 2010; Vicente-Serrano and López-Moreno 2005)). In this study, the SPEI on six different timescales with a view to validating the importance of this index for long-term assessment of drought have been analysed.

Figure 5.9 shows the SPEI time series with precipitation data for T = 3, 6, 9 and 12 months, each taken for a different study region (over the period 2004 to 2010 spanning the partial Millennium drought). Evidently, the SPEI has been able to capture temporal variation in precipitation at various timescales, revealing its statistical ability for drought analyses at any timescale in consideration. Similar results are obtained for other timescales of each study region (not shown here). The multi-scalar SPEI has the advantage of showing that some months may not be in a drought condition on short timescales, whereas all years are under drought on longer timescales, as according to $SPEI_{12}$ (Fig. 5.9d).
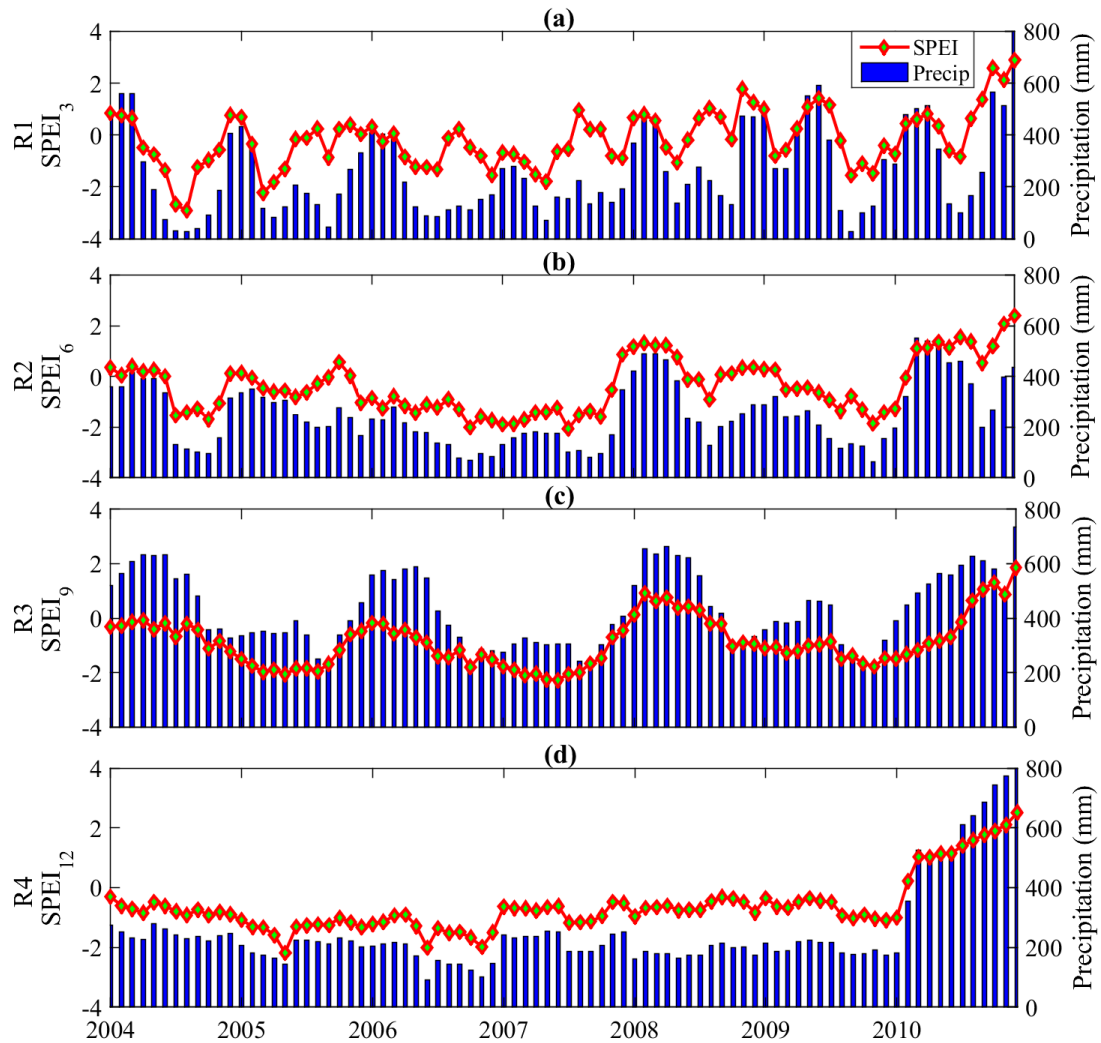
Figure 5.9: SPEI and precipitation (*P*) for different timescales taken for part of the Millennium Drought (2004-2010), for (a) 3, (b) 6, (c) 9, and (d) 12-month timescales, for locations R1, R2, R3 and R4, respectively. Legend applies to all panels.

Evaluating the estimated frequency of drought in terms of its multi-scalar properties, via different drought classes can reveal important merits and practicality of a drought index. Estimation of how frequently a drought can occur in a given class is extremely useful for the assessment of the cumulative impact over various timescales. The relative frequency in different drought classes, *i.e.,* moderate, severe and extreme, for different SPEI timescales are shown in Figure 5.10. Notably, the percentage of moderate drought events is relatively higher compared to the severe and extreme drought for all case study regions, although a distinct spread in the percentage of drought classes exist among the different timescales. For instance, in case study

location R1, the $SPEI_6$ recorded the lowest percentage of extreme cases ($\approx 2.12\%$) whereas $SPEI_1$ recorded the highest number ($\approx 3.35\%$).

In contrast, at the location R4, the highest percentage of extreme drought has been recorded by $SPEI_{24}$ ($\approx 3.51\%$) and the lowest percentage by $SPEI_1$ ($\approx 0.82\%$), suggesting that the impact of drought on long-term water resources (including seasonal or annual cropping/agriculture) can be more serious than the other case study regions. The differences show the importance of drought assessment based on various timescales, which can be facilitated by the SPEI. It is thus conceived that SPEI can be considered as a powerful statistical metric for studying the different types of drought, their impacts, and in estimating their relative frequencies.
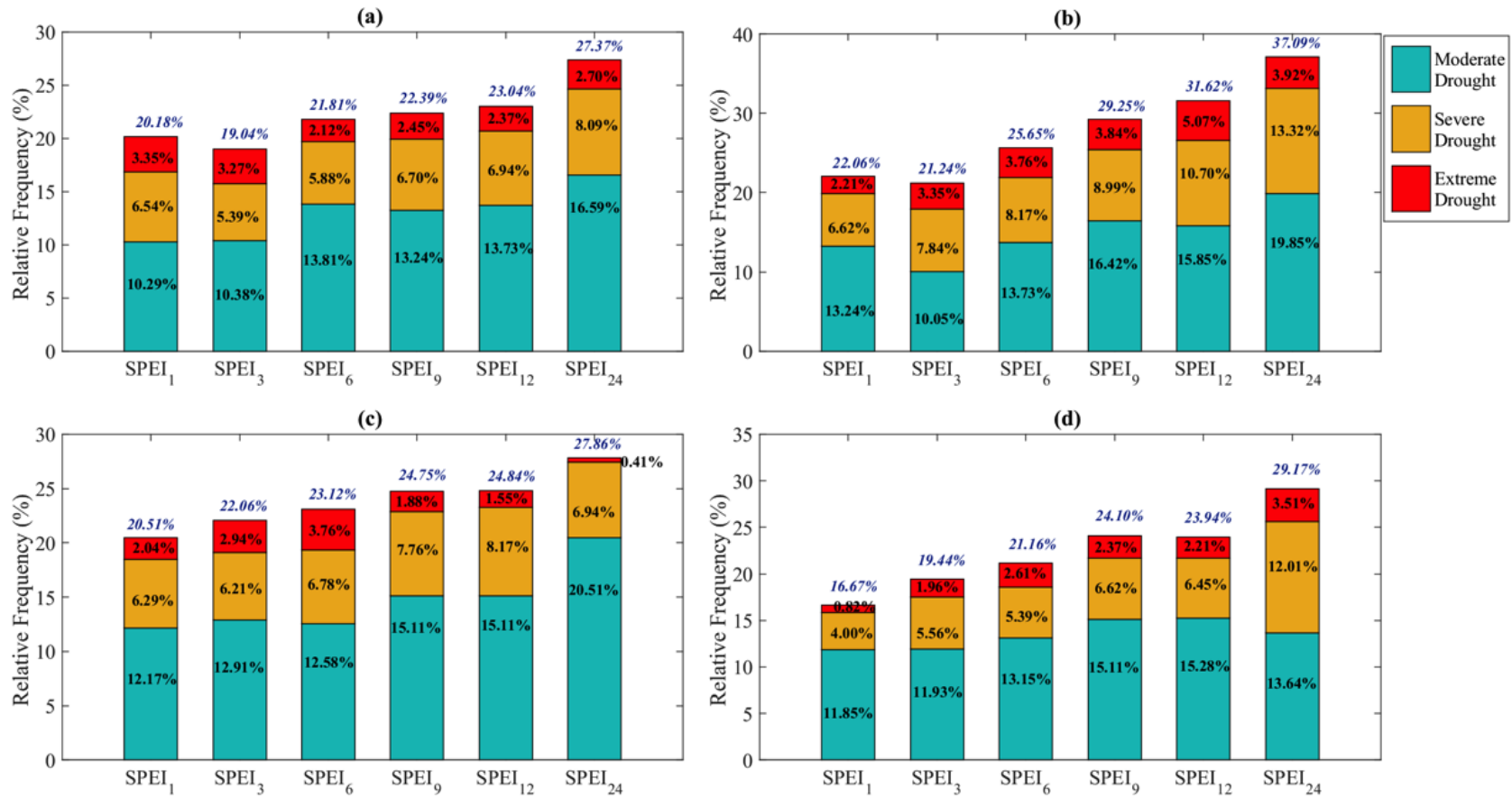
Figure 5.10: Drought class relative frequency for SPEI timescales (1, 3, 6, 9, 12, and 24 months) for (a) R1, (b) R2, (c) R3 and (d) R4. Legend applies to all panels.

Table 5.4 shows the highest ranked severity for each considered timescale. Consequently, the ranked drought events have been validated based on their corresponding soil moisture, precipitation, temperature and supply-demand balance. The drought properties according to their severity, intensity and duration are also shown. For the location R1, the $SPEI_1$ captures the year 1951 drought event as a most severe case, with an estimated duration of 8 months and an intensity of -2.67. The $SPEI_3$, however, captures the 1968 drought event, lasting for about 13 months with a severity of -18.55 and an intensity of -2.44 where both the $SPEI_1$ and $SPEI_3$ has soil moisture in their lower 20th percentile. Notably, the $SPEI_9$, $SPEI_{12}$ and $SPEI_{24}$ data (*i.e.,* long-term droughts) captured the Millennium Drought event as a severe case at locations R1, R3 and R4, where the soil moisture has been distributed within its lower (30th) percentile and supply-demand balance in deficit, which concurs well with an iconic drought event in Australia (Kiem 2013; Ummenhofer et al. 2009; Verdon-Kidd and Kiem 2009).

On a separate note, Table 5.4 also shows that the drought intensity for most severe events differs from the timescales into consideration. For instance, the most intense drought event with an estimated magnitude of -4.26 has been identified by the $SPEI_6$ data within the 1918 period at location R1, whereas at location R2, the $SPEI_{12}$ data reveals the WWII drought (the year 1942) as the most intense drought period (magnitude -3.09). At location R3, however, the Millennium Drought event is evident as the most intense case, revealed by the $SPEI_9$ data with an intensity = -2.57. Interestingly, of all the other case study regions, the location R4 has been exposed to very intense short-term drought event. In accordance with this, the 1964 drought exhibited an intensity of -4.03, as identified by $SPEI_3$ data. As also measured emphatically by the SPEI at many timescales in this case study, undoubtedly the Millennium drought is regarded as the exceptionally extreme event in Australia (Timbal and Fawcett 2013; van Dijk et al. 2013). In fact, Zhang et al. (2011) stated that the more extreme a drought event is, the more likely it is to cause societal or environmental damage. In accordance with the multi-scalar property of SPEI, the assessment of drought over short- and long-term periods is found to be particularly useful to yield information on various water policies. The table also reveals that the most severe drought does not necessarily need to be the most intense.

Table 5.3 Top ranked most severe drought events estimated for each timescale.

Timescales (months)	Drought Year	Onset Month	Severity (S)	Intensity (I)	Duration (D; months)	Precipitation (P; mm)	Maximum Temperature (Tmax; °C)	WRel1 (fractional on [0 1])	WRelEnd (fractional on [0 1])	Climatic Water Balance (P-ETo; mm)
Region: R1
1	1951	7	-12.00	-2.67	8	27.51	26.06	0.12	0.14	-109.55
3	1968	4	-18.55	-2.44	13	39.45	26.25	0.20	0.17	-85.48
6	1918	5	-40.36	-4.26	28	48.84	25.37	0.24	0.21	-66.00
9	2004	4	-47.38	-1.79	45	60.71	26.17	0.25	0.26	-58.14
12	2004	2	-56.09	-1.94	53	68.98	26.32	0.27	0.27	-49.22
24	2001	1	-138.00	-2.12	99	74.74	26.37	0.29	0.28	-45.57
Region: R2
1	1964	11	-15.10	-2.67	13	15.11	28.90	0.08	0.10	-143.30
3	2005	9	-26.45	-2.14	27	27.60	28.96	0.13	0.12	-124.11
6	1943	5	-50.80	-3.02	46	28.14	27.91	0.14	0.14	-117.82
9	2012	11	-61.25	-2.55	46	30.53	28.74	0.13	0.14	-116.33
12	1942	1	-83.76	-3.09	68	31.55	27.77	0.16	0.16	-110.46
24	1926	8	-322.90	-2.32	262	34.80	28.03	0.17	0.16	-109.06
Region: R3
1	1991	3	-11.22	-1.65	9	15.87	23.70	0.10	0.11	-90.27
3	2006	1	-24.02	-2.01	21	33.84	24.03	0.19	0.17	-73.51
6	1992	10	-41.44	-2.05	38	46.52	24.37	0.22	0.21	-67.52
9	2000	7	-109.29	-2.57	90	44.32	24.39	0.21	0.21	-68.39
12	2000	9	-114.85	-2.53	89	46.20	24.54	0.22	0.21	-67.48

24	2001	3	-158.51	-2.11	117	46.42	24.07	0.23	0.23	-62.59
				Region: R4						
1	2002	3	-16.44	-2.44	11	1.65	31.24	0.03	0.02	-174.85
3	1964	12	-24.00	-4.03	20	6.30	29.71	0.05	0.04	-160.70
6	2012	9	-47.17	-3.97	47	15.61	31.42	0.09	0.08	-155.20
9	2002	3	-90.45	-2.97	95	15.81	30.70	0.10	0.10	-152.38
12	2001	4	-102.00	-2.33	106	16.10	30.58	0.10	0.10	-151.10
24	2002	4	-131.39	-2.35	95	17.63	30.66	0.10	0.10	-149.84

In spite of the promising utility of the multi-scalar SPEI for a comprehensive drought assessment in SEQ region, this study has analysed the overall extent of drought events. However, the study of drought impacts certainly requires more extensive analyses of various impact assessment data, *e.g.,* economic outlook, environmental impacts, etc. Also, the comparison of the SPEI with other existing drought indices could not be accommodated in this investigation, instead the precision of the SPEI has been validated against the major drought events recorded by Australian BoM. Moreover, every drought event tends to vary remarkably from another for the reasons of its influence by teleconnection through the large-scale climatic phenomena (*e.g.,* ENSO, Indian Ocean Dipole, Southern Annular Mode, etc.). This study did not perform this investigation, hence creating space for a separate study to be undertaken in the future.

As an added comparison, Taylor diagrams (Taylor 2001) providing a concise summary of how well patterns match each other in terms of their correlation, root mean squared error (RMS) difference and the ratio of their variances, is presented in Figure 5.11 for R1. On the diagram, the red asterisk located on the abscissa is the correlation of the SPEI with itself, thus having a perfect coefficient of 1.00. This diagram concisely summarises the increasing degree of the correspondence between SPEI and other drought variables (*P*, *WRel1*, *WRel1End*, *Tmax*, and *ETo*) at increasing SPEI timescales. Undoubtedly, the precipitation is seen to have the largest association with SPEI, as depicted by its location closer to the SPEI with a higher correlation coefficient value and smaller centred RMS difference (marked dashed curves) compared to other drought variables. Needless to say, the soil moisture (*WRel1* and *WRel1End*) is seen to be the second most important variable to the precipitation in terms of higher correlation coefficient values. Therefore, as described earlier, the consideration of soil moisture in the assessment is pivotal in investigating the drought manifestation on the agricultural drought perspective.
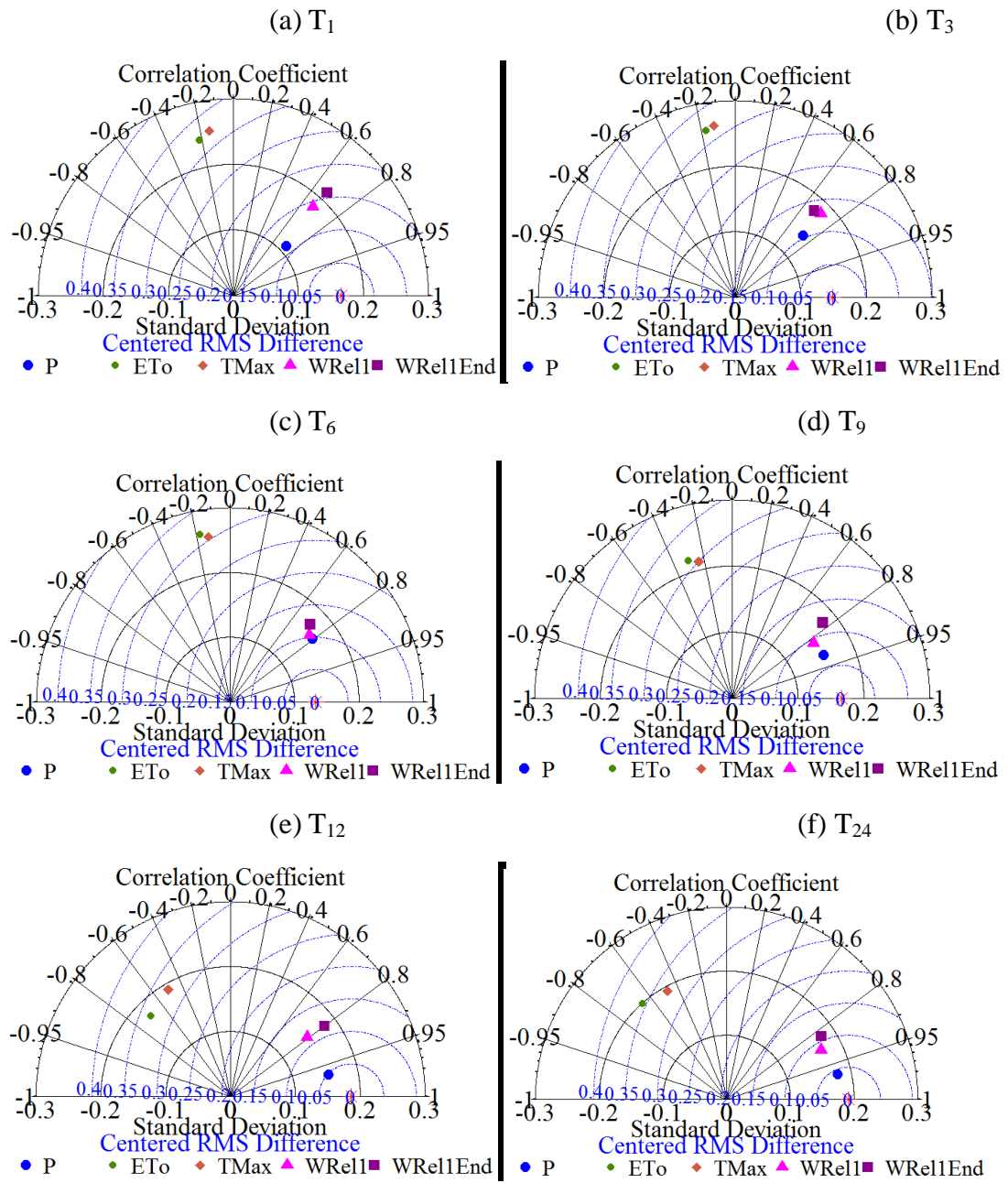
Figure 5.11: Taylor diagram displaying comparison with monthly observation (SPEI – red) with precipitation (*P*), reference evapotranspiration (*ETo*), soil moisture (*WRel1* and *WRel1End*), and maximum temperature (*Tmax*) for different timescales taken at location R1.

5.4 Conclusions

Improved, robust and comprehensive drought monitoring metric (with the multi-scalar ability for hydrological assessments) is essential for developing adaptation, mitigation and coping strategies for potentially changing drought patterns in the current climate-change era. For the first time, the utility of the SPEI has been explored to quantify drought events in the southeast Queensland, Australia. The objective index (SPEI) has been adopted to consider the effects of reference evapotranspiration on the drought severity as an essential tool that could allow the monitoring and management of key water resources over short- and long-term periods. Below are the primary findings of this case study:

1. For all case study regions, the SPEI has successfully identified major, well-documented, drought events in the drought-prone southeast Queensland region, concurring well with significant rainfall deficit periods as verified by rainfall anomalies and notable reductions in overall fraction of soil moisture;

2. Based on SPEI≤0, this study has successfully detected the onset and termination periods of major and minor drought events. Evidently, the results have shown a significant difference in the number of drought events over the historical study period, with 96, 83, 96, and 87 at T=3 months, while 45, 37, 39 and 32 at T=12 months in case study locations R1, R2, R3, and R4, respectively;

3. Owing to the wide disparities of drought properties (*D-S-I*) between the four case study regions, the results have confirmed the practical benefit of the SPEI for the detailed quantification of its complex nature for different sites within the southeast Queensland region;

4. The drought *D-S-I* properties in the present case study regions have exhibited a strong association between each other where the majority of drought cases with longer duration have also attained a higher severity and peak intensity. However, the drought events with a high peak intensity did not necessarily have high severity or long duration, because such events can be short-lived, yet, very acute in terms of the paucity of water resources relative to a climatological base period, demonstrating drought's complex nature;

119

5. The water resource availability has been found to decrease from normal by at least 2.5 standard deviations (extreme droughts) more frequently at locations R1 and R2 on both short- and long-term drought assessments, indicating possible threats to agriculture and another water usage;

6. In terms of agricultural drought implications, the SPEI has been found to correspond relatively well with soil moisture data; validating its utility for agricultural drought impact assessments. It is particularly noteworthy that the soil moisture status can take months to update and respond in terms of a drought status, according to the accumulated precipitation. Therefore, it is clear that the multi-scalar property of the SPEI can allow decision-makers to assess drought impacts over multiple timescales;

7. The SPEI, analysed on longer timescales (*i.e.,* 9, 12 and 24 months) on distinct climatic conditions, has been able to consistently detect, estimate and rank the severity of various drought classes that lasted for generally long periods based on the *D-S-I* properties, as exemplified by the case of the Millennium and WWII droughts.

In summary, the investigation in this chapter has shown the efficacy of the SPEI as a robust drought metric possessing the multi-scalar ability for drought assessment that is useful for generating crucial information on droughts' regional impact. The implications of this study meet the precise need for a robust methodology allowing hydrologists to assess both short- and long-term drought impacts, including an estimation of recurrence intervals based on severity, duration and intensity properties. Such information is of value to the design of hydrologic systems (*e.g.,* dam and irrigation systems), and to foster the sustainable management of water resources and more resilient agricultural practices. As this has been a pioneering work in case study regions, it has provided a sound basis for future research where multivariate joint relationships of drought properties (*D-S-I*) can be evaluated using statistical copula models on modelling the jointly correlated *D-S-I* properties. In addition, the comparison of SPEI with other drought indices (meteorological, hydrological and agricultural) on shorter timescales (1-month) could be another independent and a more in-depth study.

Chapter 6

DEVELOPMENT OF COPULA-STATISTICAL DROUGHT PREDICTION MODEL USING THE STANDARDISED PRECIPITATION-EVAPOTRANSPIRATION INDEX

Note:

The results from this chapter has been submitted to and is *Under Review* in the *ASCE Journal of Hydrologic Engineering* journal. The following is the tentative reference to the article:

Dayal Kavina S., R. C. Deo and A. A. Apan, (2017) "Development of a copula-statistical drought prediction model using the Standardised Precipitation-Evapotranspiration Index", *ASCE Journal of Hydrologic Engineering*, (Under Review).

6.1 Introduction

Chapter 5 has comprehensively discussed the suitability of SPEI for the characterisation of drought events. The drought properties derived in Chapter 5 are used in the current chapter to statistically assess the drought-risk in terms of joint return periods using copula models. The main contribution of this chapter is the development of probabilistic conditional prediction model to predict SPEI and drought properties (duration, severity and intensity). The conditional variables used are the climatic

indices (Niño4 SST, SOI and EMI). Using the bivariate and trivariate joint distribution function derived from copula, this chapter investigates the potential drought-risk in terms of joint and conditional return periods for two or three variables.

Copula applications for modelling drought properties in Australia have been limited (Rauf and Zeephongsekul 2014; Wong 2013; Wong et al. 2009; Wong et al. 2008). Copulae have been successfully applied for risk evaluation for several problems in hydrology and drought frequency analysis (*e.g.*, (Ganguli and Reddy 2012; Reddy and Ganguli 2012; Shiau and Modarres 2009; Shiau 2006). With copula, we can derive joint distribution functions of climate mode indices and drought index (and properties *D*, *S* and *I*) and develop a probabilistic prediction model. The motivation for exploring and developing copula models for an adequate estimate of drought-risk is an interesting research endeavour in view of the plethora of hydrological applications. In a very recent study, Nguyen-Huy et al. (2017) used vine copula model for the first time in Australia's agro-ecological zones for probability-based seasonal rainfall predictions conditioned on SOI and IPO Tripole Mode Polar Index (TPI). That study had utilised vine copula for trivariate forecasting to yield a better accuracy than the bivariate model for the east and southeast agro-ecological zones. Importantly, the trivariate forecasting model was found to improve the forecasting of rainfall during the La Niña and negative TPI.

Following the earlier study on drought risk monitoring (Dayal et al. 2018) *i.e.,* Chapter 5 of this study, the temporal behaviour of SPEI has been investigated as an original contribution for identifying and modelling the drought properties by the means of developing bivariate and trivariate copula-based joint relationships. The specific objectives of the study in the current chapter, after the breakdown of the second major objective outlined in Section 1.3, are the following: (1) to compute SPEI, including the duration *(D)*, severity *(S)* and intensity *(I)* properties of identified drought events, and to statistically fit the marginal distributions based on goodness-of-fit tests; (2) to evaluate the non-parametric correlations between SPEI (and *D-S-I*) in terms of an thirteen climatic mode indices and to screen the relevant indices for copula-statistical modelling; (3) to evaluate the potential utility of vine copulae and to deduce the optimum copula-statistical models for studying the bivariate and trivariate associations of SPEI and climate mode indices, *D-S-I* and climate model indices, and between *D-S-I* properties; (4) to evaluate the utility of copula-based conditional models for

probabilistic prediction of SPEI and *D-S-I* parameters using the information of climate mode indices; and (5) to deduce conditional probabilities and joint return periods elucidating the importance of bivariate and trivariate copula models in drought-risk studies. It is especially noted that drought-risk studies through multivariate modelling and elucidation of its properties in respect to universal precursors (*i.e.,* climate mode indices) are centrally important for agricultural water management, and decision-making by farmers in south-east Queensland where drought is a considered a perpetuating risky phenomenon.

6.2 Materials and Methods

6.2.1 Theoretical background

6.2.1.1 Copula Theory

This study has adopted copulae to model the bivariate and trivariate joint behaviour of SPEI data and the identified drought properties with climate mode indices. The marginal distribution functions, $F_X(x)$ and $F_Y(y)$ of any two correlated variables, X and Y, is expressed by copula function, C using Sklar (1959) theorem as:

$$F_{X,Y}(x,y) = C[F_X(x), F_Y(y)] = C(u,v) \tag{6.1}$$

where $F_{X,Y}(x,y)$ is the joint cumulative distribution function (CDF) of X and Y. Copulae are scale-invariant under strictly increasing transformations of X and Y, hence the X and Y are transformed to [0 1]. This yields two uniformly distributed variables u and v, where $u = F_X(x)$ and $v = F_Y(y)$. In order to jointly model drought properties, a primal task is to construct a function $C(\bullet)$ as a bivariate distribution function with a mapping such that $C:[0,1]^2 \rightarrow [0,1]$. Similarly, three or more variables are formulated as:

$$F(x_1,...,x_n) = C[F_1(x_1),...,F_n(x_n)] = C(u_1,...,u_n) \tag{6.2}$$

The u and v in any copula function, $C(u,v)$ must be monotonically increasing and therefore, satisfy (Sklar 1959): $C(u,0) = 0, C(0,v) = 0$ and $C(u,1) = u, C(1,v) = v$.

A copula consists of a joint CDF by its definition, and their graphs are generally hard to interpret given that they are deduced as monotonically increasing functions. Because of this, plots of copula densities are typically used to illustrate distributions. Thus, if $C(\bullet)$ is a continuous function, the bivariate copula density is defined as the double derivative of C with respect to its marginal distributions, expressed as:

$$c(u,v) = \frac{\partial^2 C(u,v)}{\partial u \partial v} \tag{6.3}$$

where $c(\bullet)$ is the respective bivariate copula density constructed using the variables X and Y.

This study uses Archimedean copula family, namely Clayton, Gumbel, and Frank copulae. Table 5.1 lists the mathematical expressions of bivariate Clayton, Gumbel and Frank copulae, where u and v are the uniform variables, and θ is the copula parameter. The Archimedean family of copulae is popular in hydrological and agricultural applications because it includes multivariate extreme distributions that exhibit tail dependence and reasonable empirical fit to the hydrological data, *e.g.*, (Serinaldi et al. 2009). The Archimedean symmetric one-parameter copula has the form:

$$C(u_1,...,u_n) = \varphi^{-1}[\varphi(u_1) + ... + \varphi(u_n)] \tag{6.4}$$

where φ is the unique generator of the copula and $u_1,...,u_n$ is the uniform random variable. The symmetric copula is restrictive to two variables only because the correlations between any pair of variables are identical. However, this assumption is unrealistic for many hydrological variables. To overcome this, an asymmetric copula is constructed by nesting symmetric copulae (Joe 1997), expressed:

$$C(u_1,...,u_n) = C_1\{u_n, C_2[u_{n-1},...,C_{n-1}(u_2,u_1)...]\} \tag{6.5}$$

$$= \varphi_1^{-1}\Big[\varphi_1(u_n) + \varphi_1\Big(\varphi_2^{-1}\Big(\varphi_2\big\{u_{n-1} + ... + \varphi_{n-1}^{-1}[\varphi_{n-1}(u_2) + \varphi_{n-1}(u_1)]...\big\}\Big)\Big)\Big]$$

In the case of three variables, the asymmetric Archimedean copula is given by:

$$C(u_1,u_2,u_3) = C_1[C_2(u_1,u_2),u_3] = \varphi_1^{-1}\Big(\varphi_1\big\{\varphi_2^{-1}[\varphi_2(u_1) + \varphi_2(u_2)] + \varphi_1(u_3)\big\}\Big) \tag{6.6}$$

where C_2 describes the dependence between variables u_1 and u_2 and the outer copula C_1 is a function of C_2 and variable u_3. This model assumes identical correlations between inner variables and outer variables, *i.e.,* marginal copulae $C_1(u_1,u_3)$ and $C_2(u_2,u_3)$ are identical. Given the non-stationary nature of hydrological variables, any two pairs of variables will have different marginal copulae; therefore, a vine copula would be more suitable for constructing joint distributions of three or more variables.

Table 6.1: Mathematical expressions for bivariate copula functions.

Copula	Generator	Parameter	Bivariate Copula	Kendall's tau (τ)	Tail Dependence (lower, upper)
Clayton	$t^{-\theta}-1$	$\theta > 0$	$\left(u^{-\theta}+v^{-\theta}-1\right)^{-\frac{1}{\theta}}$	$\dfrac{\theta}{\theta+2}$	$\left(2^{-\frac{1}{\theta}},0\right)$
Gumbel	$(-\ln t)^{\theta}$	$\theta \geq 1$	$\exp\left\{-\left[(-\ln u)^{\theta}+(-\ln\right.\right.$	$1-\dfrac{1}{\theta}$	$\left(0,2-2^{\frac{1}{\theta}}\right)$
Frank	$-\ln\dfrac{e^{-\theta t}-1}{e^{-\theta}-1}$	$-\infty < \theta < \infty,$ $\theta \neq 0$	$-\dfrac{1}{\theta}\log\left[1+\dfrac{\left(e^{-\theta u}-1\right)}{e^{-\theta}}\right.$	$1-\dfrac{4}{\theta}+4\dfrac{D_1(\theta)}{\theta}$	$(0,0)$

Where: $D_1(\theta)=\int_0^{\theta}\dfrac{x/\theta}{\exp(x)-1}dx$ and $\Phi=\int_0^1 x\log(x)(1-x)^{\frac{2(1-\theta)}{\theta}}dx$

6.2.1.3 Vine Copula

The vine copula, introduced in Joe (1996), is a graphical tool for describing multivariate, high-dimensional probability distributions through a cascade of bivariate copulae, so-called *pair-copulae* (Brechmann and Schepsmeier 2013). It uses the Markov trees to construct bivariate, pair-copulae. A vine copula decomposes a multivariate probability density into bivariate copulae where each pair-copula can be selected in an independent manner while allowing for an enormous flexibility in dependence modelling. The pair-copulae considers the asymmetries and tail dependence, as well as conditional independence to build models that are more parsimonious. The "statistical breakthrough" of vines was due to Aas et al. (2009) who

described statistical inference of vine into special classes of Canonical (C-) and D-vine functions. In the C-vine, the pair-copula for n variables can be constructed as (Bedford and Cooke 2002):

$$
\begin{aligned}
(Tree\,1) \qquad & (u_1, u_2), (u_1, u_3), (u_1, u_4), ..., (u_1, u_n) \\
(Tree\,1) \qquad & (u_2, u_3 \mid u_1), (u_2, u_4 \mid u_1), ..., (u_2, u_n \mid u_1) \\
& ,..., \\
(Tree\,n-2) \qquad & (u_{n-1}, u_n \mid u_1, ..., u_{n-2})
\end{aligned}
\tag{6.7}
$$

The vines arrange the $\dfrac{n(n-1)}{2}$ pair-copulae of an n-dimensional pair-copula construction in $n-1$ linked trees. In C-vine $Tree\,1$, the dependence with respect to one particular variable (first root node, *i.e.,* conditional variable) is modelled using bivariate copulae for each pair. Conditioned on this variable, the pairwise dependency with respect to a second variable is modelled to obtain a C-vine $Tree\,2$ (second root node). For n-dimensional copula, the decomposition of multivariate density with root nodes is written as:

$$
f(x_1, ..., x_n) = \prod_{k=1}^{n} f_k(x_k) \times \prod_{i=1}^{n-1} \prod_{j=1}^{n-i} c_{i,j+1|1:(i-1)} \left[F(x_i \mid x_1, ..., x_{i-1}), F(x_{i+j} \mid x_1, ..., x_{i-1}) \right]
\tag{6.8}
$$

For three-dimensional copula model, this study adopts the recursive conditioning method, given as:

$$
\begin{aligned}
f(x_1, x_2 \mid x_3) = {}& f_1(x_1) \cdot f_2(x_2) \cdot f_3(x_3) \cdot c_{1,3}\left[F_1(x_1), F_2(x_2) \right] \\
& \cdot c_{2,3}\left[F_2(x_2), F_3(x_3) \right] \cdot c_{1,2|3}\left[F_{1,3}(x_1 \mid x_3), F_{2,3}(x_2 \mid x_3) \right]
\end{aligned}
\tag{6.9}
$$

where the three-dimensional joint density is represented in terms of bivariate copulae $C_{1,3}$, $C_{2,3}$ and $C_{1,2|3}$ with densities $c_{1,3}$, $c_{2,3}$ and $c_{1,2|3}$ of pair-copulae, which can be independent of each other to achieve a wide range of dependence structures.

The pair-copula requires construction of conditional distribution function, $F(x \mid v)$ for an n-dimensional vector v. For a pair-copula term in tree $n+1$, the conditional distribution function can be established using pair-copula of previous trees $1, ..., n$ and by sequentially applying the relationship given as (Brechmann and Schepsmeier 2013):

$$h(x \mid v, \theta) := F(x \mid v) = \frac{\partial C_{xv_j \mid v \_ j}\left[F(x \mid v \_ j), F(v_j \mid v \_ j) \mid \theta\right]}{\partial F(v_j \mid v \_ j)} \qquad (6.10)$$

where v_j is an arbitrary component of v and $v \_ j$ denotes $(n-1)$-dimensional vector v, excluding $v \_ j$ (Joe 1996).

6.2.1.4 Conditional Prediction Model

The construction of prediction model uses the inverse form of the conditional distribution functions (Chen et al. 2009; Liu et al. 2015). Given two random variables (x_1, x_2) for a case of the bivariate copula, the conditional distribution function, $h(u_1, u_2)$, can be used to obtain u_1 based on the information of u_2. For known probabilities, P on (0, 1), u_1 can be derived from the formula $u_1 = C_{1|2}^{-1}(P \mid u_2) = h^{-1}(P \mid u_2)$, where $C_{1|2}^{-1}$ is the inverse of copula $C_{1|2}$. The variable x_1 is then obtained by:

$$x_1 = F^{-1}(u_1) = F^{-1}\left[C_{u_1 \mid u_2}^{-1}(P, u_2)\right] = F^{-1}\left[h^{-1}(P \mid u_2)\right] \qquad (6.11)$$

where $F^{-1}(u_1)$ is the inverse marginal of u_1. Similarly, for a three-dimensional case, the random variable x_3 can be obtained based on the information of u_1 and u_2. Following Eq. (6.11), x_3 is computed as:

$$x_3 = F^{-1}(u_3) = F^{-1}\left\{h^{-1}\left[h^{-1}(P \mid h(u_2, u_1))\right]u_1\right\} \qquad (6.12)$$

6.2.1.5 Joint Return Periods

A common approach undertaken for the proper design of hydrologic systems (*e.g.*, water storage dams and agricultural irrigation systems) is the frequency analysis of drought, including the estimated recurrence interval or the return period of hydrologic drought events (Shiau and Shen 2001). This is important to empower farmers and agricultural engineers in understanding the perpetuating risk of drought. The drought return periods, in particular, can provide useful information on the controlled use of water under drought conditions (Serinaldi et al. 2009). The return period of a drought event can be defined in terms of the mean elapsed time (E_L) between the onsets of any two drought events (Shiau and Shen 2001).

The univariate return period for *D, S* and *I*, according to Shiau and Shen (2001), for a severity, $S \geq s$; duration, $D \geq d$; or intensity $I \geq i$ using the mean elapsed time (E_L) can be calculated as:

$$T_D = \frac{E_L}{1 - F_D(d)}; \qquad T_S = \frac{E_L}{1 - F_S(s)}; \qquad T_I = \frac{E_L}{1 - F_I(i)}; \tag{6.13}$$

The joint bivariate return period, according to Shiau (2006), can be calculated as either T_{AND} or T_{OR}, given as:

$$T_{AND} = \frac{E_L}{1 - P(X_i \geq x_i, X_j \geq x_j)} = \frac{E_L}{1 - F(x_i) - F(x_j) + C[F(x_i), F(x_j)]} \tag{6.14}$$

$$T_{OR} = \frac{E_L}{1 - P(X_i \geq x_i \text{ or } X_j \geq x_j)} = \frac{E_L}{1 - C[F(x_i), F(x_j)]} \tag{6.15}$$

where X_i and X_j are two random variables.

Similarly, the joint trivariate return period can be defined as:

$$T_{AND} = \frac{E_L}{1 - P(X_i \geq x_i, X_j \geq x_j, X_k \geq x_k)} \tag{6.16}$$

$$= \frac{E_L}{1 - F(x_i) - F(x_j) - F(x_k) + C[F(x_i), F(x_j)] + C[F(x_i), F(x_k)] + C[F(x_j), F(x_j)] - C[F(x_i), F(x_j), F(x_k)]}$$

$$T_{OR} = \frac{E_L}{1 - P(X_i \geq x_i \text{ or } X_j \geq x_j \text{ or } X_k \geq x_k)} \tag{6.17}$$

$$= \frac{E_L}{1 - C[F(x_i), F(x_j), F(x_k)]}$$

In addition, drought return periods conditioned on the certain variable threshold is also useful for management of water resources. Shiau (2006) defined bivariate conditional drought return period as:

$$T_{x_i|x_j} = \frac{E_L}{(1 - F_{x_j}(x_j))(1 - F_{x_i}(x_i) - F_{x_j}(x_j) + C(x_i, x_j))} \tag{6.18}$$

where $T_{x_i|x_j}$ is the conditional return period for X_i given $X_j \geq x_j$. The bivariate conditional return period of drought *D, S,* and *I* are calculated in this study where climate mode indices act as the conditioned variables.

6.2.2 Study area and data

The case study area is a point-based location, R3, in the southeast Queensland (SEQ) region (Figure 6.1), Australia with the geographical coordinate (152.25°E, 28.25°S). This location has an elevation of 521m above sea-level and falls within the Murray-Darling Basin, the hub for major agricultural activities. The Millennium Drought (1996-2010), the longest and most severe in the region, unveiled the vulnerability of SEQ's water supplies. With 2.6% population growth per annum (1985-2015), SEQ is expected to experience a significant increase in the demand for water and the need for water management strategies in terms of the more efficient design of hydrologic systems (Seqwater 2015). The annual evaporation rate is expected to increase by almost 16% in the next 60 years due to the increasing concentration of greenhouse gases (Helfer et al. 2012). Considering the increase in evaporation rate and SEQ region is prone to frequent droughts, hydrologists and policy-makers must adopt statistical models that can provide probabilistic predictions of drought monitoring index and properties.
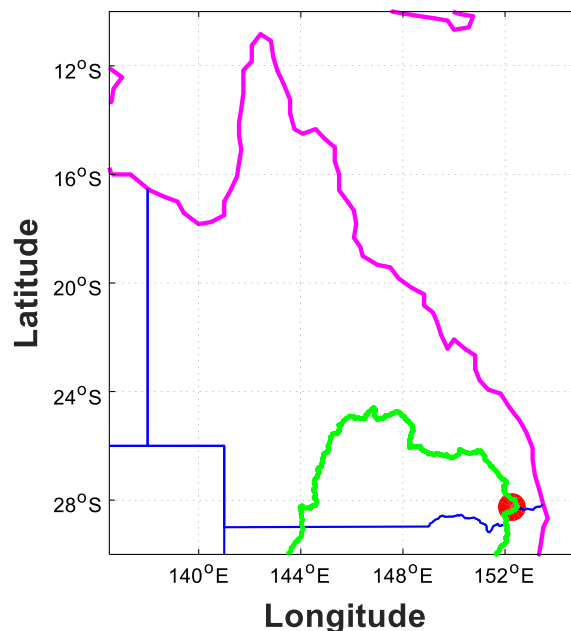
Figure 6.1: Map of the study location R3.

The monthly rainfall and reference evapotranspiration data are obtained from the SILO database for the period 1960 to 2016. The 13 different climate mode indices, *i.e.,* Niño 3 SST, Niño 3.4 SST, Niño 4 SST, Southern Oscillation Index (SOI), Pacific Decadal Oscillation (PDO), Dipole Mode Index (DMI), El-Niño Modoki Index (EMI),

Southern Annular Mode (SAM), Trans Polar Index (TPI), Quasi-Biennial Oscillation (QBO), Western Pacific Index (WPI), Oceanic Niño Index (ONI), and Multivariate ENSO Index (MEI), were obtained from various sources, such as National Climate Prediction Center, British Antarctic Survey, JAMSTEC, and Bureau of Meteorology.

6.2.2.1 Characterisation of Drought Properties

In this chapter, the SPEI for drought analysis is employed that has been embraced recently for detecting drought onsets and terminations, drought ranking and recurrence evaluation (Dayal et al. 2018). Using total rainfall and the reference evapotranspiration data, the SPEI on a 3-month timescale is calculated for the present case study location. Since the SPEI is a standardised index, the value SPEI = 0 correspond to the mean (normal) with respect to the base period 1971-2000 (Deo et al. 2009), and the SPEI = ±1 correspond to the standard deviation where the negative (positive) SPEI indicate dry (wet) condition.

In accordance with the SPEI time series representing the deficits and surpluses of water resources relative to a well-defined base period, the drought onsets and terminations are then identified in periods when the SPEI declined to a value below zero (*i.e.,* the standardised water deficit below the normal value). The drought duration D, S and I properties are thus identified from the SPEI time series via the widely adopted run-sum approach and enumerated using Equations (6.1-6.3).

The study follows the rationale that a drought event that lasted for less than 3-month duration, which is generally regarded as insufficient to impact the available water resources, has been ignored in this case study following the Australian BoM's definition (*i.e.,* a drought condition is declared when precipitation is below normal for consecutive three or more months) (Mpelasoka et al. 2008). Therefore, only the drought events with $D \geq 3$ months are used in the analysis, following earlier studies (*e.g.,* (Deo et al. 2009)).

6.2.2.2 Copula-Statistical Model Development

Before constructing the copula-statistical models, the significance of the correlation between SPEI and climate mode indices (*CIs*), and the *D-S-I* and climate mode indices (averaged for the corresponding duration of drought events) is evaluated. The non-parametric Kendall's τ and corresponding p-values at 95% confidence interval for SPEI, and 90% confidence interval for D, S and I drought properties are obtained in

130

order to test the hypothesis of no correlation against the alternative. That is, the *p*-values < 0.05 *(or 0.10)* indicate a significant correlation between SPEI *(or D, S and I)* and *CIs* as shown in Table 6.2.

Evidently, all *CIs* except the PDO, QBO, and WPI exhibited significant correlation with the SPEI time series data. Those *CIs* having smaller correlations with SPEI have been disregarded and consequently, the Niño 4 SST and SOI are selected for the drought analysis and prediction. The Niño 4 SST and SOI, with larger correlation values (*i.e.,* -0.22 and 0.20, respectively), are used to assess ENSO independently whereby the Niño 4 SST is solely based on sea-surface temperature while SOI on pressure (difference between pressure at Tahiti (149.6˚W, 17.5˚S) and Darwin (130.9˚E, 12.4˚S)). The warm phase of ENSO, *i.e.,* El-Niño, is known to influence (enhance) drought conditions in Australia *e.g.,* (van Dijk et al. 2013; Wong 2013; Wong et al. 2008), therefore probability-based statistical prediction of drought properties based on ENSO indicators are expected to provide useful information for water resource management.

In the case of drought properties, the Niño 4 SST for Duration, and EMI for Severity and Intensity have been selected based on the indicating *p*-values for significant correlations. The Niño 4 SST has a significant correlation with the drought duration (0.22), while the EMI has a significant correlation with the severity (-0.20) and intensity (-0.20) of drought events. The joint behaviour of drought properties based on Niño 4 SST and EMI, which can aid in better management of agricultural systems, (including irrigations and dams) is likely to be beneficial for the prediction of drought properties, given their reasonably acceptable statistical dependencies.

Table 6.2: Kendall's tau (τ) and an associated *p*-value of the SPEI, and drought severity, duration and intensity with 13 climate mode indices. Statistically significant correlations are in bold italics and selected for the study are in bold red italics.

Climate mode indices	SPEI		Severity		Duration		Intensity	
	τ	*p-value*	τ	*p-value*	τ	*p-value*	τ	*p-value*
Niño3	*-0.0760*	*0.0029*	0.0889	0.4565	-0.0795	0.5181	0.0000	1.0000
Niño3.4	*-0.1501*	*4.37E-09*	0.0476	0.6949	-0.0331	0.7939	0.0349	0.7764

Niño4	*-0.2247*	*1.57E-18*	-0.1714	0.1459	*0.2221*	*0.0675*	-0.1206	0.3094
SOI	*0.2050*	*1.07E-15*	0.0636	0.5952	-0.1046	0.3939	0.0541	0.6530
PDO	-0.0355	0.1648	-0.0095	0.9461	0.0630	0.6110	-0.0349	0.7764
DMI	*-0.0986*	*0.0002*	0.0317	0.7973	0.0331	0.7939	0.1841	0.1177
EMI	-0.2145	4.70E-17	-0.1968	0.0940	0.1723	0.1567	-0.2032	0.0836
SAM	*0.0991*	*0.0001*	0.0635	0.5978	-0.0166	0.9015	0.1905	0.1054
TPI	*0.0881*	*0.0007*	0.0487	0.6930	0.0070	0.9657	0.0017	1.0000
QBO	-0.0177	0.4897	0.0984	0.4088	-0.1061	0.3864	0.0032	0.9892
WPI	-0.0050	0.8451	0.0317	0.7973	-0.0762	0.5361	-0.0571	0.6359
ONI	*-0.1845*	*5.54E-13*	-0.0381	0.7558	0.0696	0.5730	-0.1079	0.3641
MEI	*-0.1818*	*1.15E-12*	-0.0857	0.4731	0.1094	0.3715	-0.0921	0.4403

Note: Significance test of SPEI at 95% confidence interval while Severity, Duration and Intensity at 90% confidence interval.

6.2.2.3 Selection of Marginal Distributions

Since copula functions are able to join the marginal distributions of multivariate data to construct a joint distribution function, the foremost task is to fit an appropriate marginal distribution to each drought-related variable. The suitable marginal distribution of SPEI, Niño 4 SST and SOI for the monthly data from 1960 to 2016, as well as for the D, S, I, Niño 4 SST and EMI for all drought cases are determined. For an accurate estimation, several distributions defined by the extreme value, Gamma, generalized extreme value (GEV), Logistic, Log-logistic, Log-normal, Nakagami, normal, Rician, exponential, and Weibull equations are evaluated based on the maximum likelihood method. The statistical significance is determined by p-values based on the Anderson-Darling (AD) and Kolmogorov-Smirnov (KS) test statistics. This considered the null hypothesis that variables are not from the assumed distribution against the alternative hypothesis that they are. That is, the larger the p-value, the more suitable fit the distribution is to the variable. Table 6.3 lists the selected marginal distributions, parameters and corresponding p-values for the variables used in the analysis.

Table 6.3: Marginal distribution parameters and *p*-values of observed variables.

Variable	Distribution	Parameters	KS *p*-value	AD *p*-value
For Monthly Data from 1960 to 2016				
SPEI	GEV	k= -0.2312, σ= 0.9697, μ= -0.5228	0.8288	0.8987
Niño4 SST	Weibull	a= 52.1350, b= 28.7875	0.5337	0.4622
SOI	Logistic	μ= -0.4517, σ= 5.2521	0.9528	0.8160
For Drought Case Only				
Duration	Log Logistic	μ= 0.3145, σ= 1.7105	0.2338	0.2750
Severity	GEV	k= 0.3909, σ= 2.5901, μ= 3.1580	0.9695	0.9940
Intensity	GEV	k= -0.1927, σ= 0.5662, μ= 1.1355	0.9897	0.9989
EMI	GEV	k= -0.3997, σ= 0.4466, μ= -0.0798	0.3697	0.7620
Niño4 SST	Weibull	a= 55.9410, b= 28.8905	0.8495	0.9046

Mathematical equations of marginal distribution, KS and AD test:

GEV: $f(x\,|\,k,\mu,\sigma) = \left(\dfrac{1}{\sigma}\right)\exp\left(-\left(1+k\,\dfrac{(x-\mu)}{\sigma}\right)^{\frac{-1}{k}}\right)\left(1+k\,\dfrac{(x-\mu)}{\sigma}\right)^{-1-\frac{1}{k}}$,

Weibull: $f(x\,|\,a,b) = \dfrac{b}{a}\left(\dfrac{x}{a}\right)^{b-1} e^{-\left(\frac{x}{a}\right)^{b}}$,

Logistic: $f(x\,|\,\mu,\sigma) = \dfrac{\exp\left\{\dfrac{x-\mu}{\sigma}\right\}}{\sigma\left(1+\exp\left\{\dfrac{x-\mu}{\sigma}\right\}\right)^{2}}$,

Log Logistic: $f(x \mid \mu, \sigma) = \dfrac{1}{\sigma} \dfrac{1}{x} \dfrac{e^{\frac{\log(x) - \mu}{\sigma}}}{\left(1 + e^{\frac{\log(x) - \mu}{\sigma}}\right)^2}; \quad x \geq 0$,

$$AD^2 = -n - \frac{1}{n} \sum_{i=1}^{n} (2i - 1) \left[\ln F(X_i) + \ln\left(1 - F(X_{n-i+1})\right) \right],$$

$$KS = \max_{1 \leq i \leq n} \left(F(x_i) - \frac{i-1}{n}, \frac{1}{n} - F(x_i) \right)$$

6.2.2.4 Selection of Copulae

For any random variable with continuous marginal, the copula requires the variable to be uniformly distributed. The pseudo-observation values are then produced for each variable, transformed on [0,1] interval. Subsequently, the *BiCopSelect* function from 'VineCopula' library in the statistical *"R"* software is applied to the transformed variables to construct the appropriate bivariate copula functions in order to model the joint relationships of SPEI with *CIs* and drought properties with *CIs*. The *BiCopSelect* function investigates a rich variety of copulae and returns the most appropriate copula function based on the selection criteria.

During the selection of the copulae, statistical validation is undertaken using AIC, BIC and log-likelihood, where the copula that yielded the minimum *(largest)* value of AIC and BIC *(log-likelihood)* at significance level $\alpha = 0.05$ is selected. Table 6.4 (a-c) lists the selected bivariate and trivariate copula statistics where C-vine is used for trivariate conditional copula selection. Note that transforming the variables on [0, 1] interval does not affect the correlation between variables, *i.e.,* the observed and copula generated Kendall's τ values are similar.

$$AIC := -2 \sum_{i=1}^{N} \ln\left[C(u_i, v_i) \mid \theta \right] + 2k \tag{6.19}$$

$$BIC := -2 \sum_{i=1}^{N} \ln\left[C(u_i, v_i) \mid \theta \right] + \ln(N)k \tag{6.20}$$

$$\begin{aligned} LogLik &= \ln L(x, y; params, \theta) \\ &= \ln L_C\left(F_X(x), F_Y(y); \theta\right) + \ln L_X(x; params) + \ln L_Y(y; params) \end{aligned} \tag{6.21}$$

The *params* are the parameters of the marginal distribution of *X* and *Y* variables.

The three different sets of copula-drought analysis are carried out: (1) bi- and the trivariate copula of SPEI with *CIs*, (2) bivariate copula of drought properties with *CIs*, and (3) bi- and trivariate copula of drought properties. Table 6.4 lists the copula parameters and corresponding goodness of fit measures for each set of analysis. Since SPEI, SOI and EMI are all standardised indices that represent drought and synoptic-scale climate patterns where the values of these can range from being positive to negative, the Frank copula is found to be the most appropriate fit mainly because of its properties related to radial symmetry (Nelsen 1999).

Table 6.4: Copula parameters and goodness-of-fit measures of the fitted copula models.

(a)   *For SPEI with CIs*

	Copula	Par	*Kendall's tau	Kendall's tau	Upper TD	Lower TD	LogLik	AIC	BIC
				Bivariate Model					
$C(u_{spei}, u_{nino4})$	Frank	-2.34	-0.25	-0.25	N/A	N/A	47.36	-92.72	-88.19
$C(u_{spei}, u_{soi})$	Gumbel	1.29	0.24	0.23	0.29	N/A	51	-99.99	-95.46
$C(u_{nino4}, u_{soi})$	Frank	-7.85	-0.6	-0.6	N/A	N/A	331.07	-660.14	-655.61
				Trivariate Model					
$C(u_{nino4}, u_{soi}|u_{spei})$	Frank	-6.79	-	-0.55	N/A	N/A	372.49	-738.98	-725.39

*Kendall's tau of observed data

(b)   *For drought properties with CIs*

	Copula	Par	*Kendall's tau	Kendall's tau	Upper TD	Lower TD	LogLik	AIC	BIC
				Bivariate Model					
$C(u_1, u_2)$	Clayton	0.65	0.1723	0.25	N/A	0.35	2.53	-3.06	-1.48
$C(u_3, u_5)$	Frank	1.89	0.1968	0.2	N/A	N/A	1.56	-1.13	0.45
$C(u_4, u_5)$	Frank	2.02	0.2032	0.22	N/A	N/A	1.81	-1.62	-0.04

Note – u_1: uniform Duration; u_2: uniform Niño4 SST; u_3: uniform Severity; u_4: uniform Intensity; u_5: uniform EMI
*Kendall's tau of observed data

(c)   *For drought properties*

	Copula	Par	*Kendall's tau	Kendall's tau	Upper TD	Lower TD	LogLik	AIC	BIC
				Bivariate					

$C(u_d, u_s)$	Gumbel	4.36	0.81	0.77	0.83	N/A	35.81	-69.63	-68.04
$C(u_d, u_i)$	Frank	4.87	0.47	0.45	N/A	N/A	8.45	-14.89	-13.31
$C(u_s, u_i)$	Clayton	2.74	0.61	0.58	N/A	0.78	18.86	-35.72	-34.13
				Trivariate					
$C(u_s, u_d\|u_i)$	Frank	8.90	-	0.63	N/A	N/A	47.99	-89.99	-85.24

*Kendall's tau of observed data.

Note - TD: tail-dependence; LogLik: Log-likelihood; AIC: Akaike Information Criterion; BIC: Bayesian Information Criteria.

137

6.2.2.5 Dependence Modelling

A potential avenue to validate the dependence structure of bivariate copula models is a Chi-plot proposed by Fisher and Switzer (1985). Chi-plot is based on two types of statistics: Chi-statistic, χ_i and Lambda-statistic, λ_i viz (Genest and Favre 2007):

$$\chi_i = \frac{\hat{F}_{X,Y}(u_i, v_i) - \hat{F}_X(u_i)\hat{F}_Y(v_i)}{\sqrt{\hat{F}_X(u_i)\left(1 - \hat{F}_X(u_i)\right)\hat{F}_Y(v_i)\left(1 - \hat{F}_Y(v_i)\right)}} \qquad (6.22)$$

$$\lambda_i = 4 \operatorname{sgn}\left(\overline{F}_X(u_i), \overline{F}_Y(v_i)\right) * \max\left(\overline{F}_X(u_i)^2, \overline{F}_Y(v_i)^2\right) \qquad (6.23)$$

where $i = 1, ..., N$ is the set of observations for (u_i, v_i), and $\hat{F}_X, \hat{F}_Y$, and $\hat{F}_{X,Y}$ are the empirical distribution functions of the uniform random variables u and v, and $\widetilde{F}_X = \hat{F}_X - 0.5$ and $\widetilde{F}_Y = \hat{F}_Y - 0.5$.

In accordance with Eqs. (6.22 & 6.23), λ_i is adapted to estimate the distance between bivariate data points (u_i, v_i) and the median of the dataset while the χ_i corresponds to a correlation coefficient between dichotomised values of X and Y. Thus, a positive λ_i means that both u_i and v_i are large relative to their respective medians, or both small whereas, a negative corresponds to u_i and v_i being on opposite sides of their respective medians. Asymptotically, $\chi_i \sim \mathrm{I}\left(0, \frac{1}{N}\right)$ and $\lambda_i \sim \mathrm{Y}[-1, 1]$ under the condition of independence where a value of χ_i close to zero can indicate that the properties X and Y are independent of each other, *i.e.*, $F_{X,Y} = F_X F_Y$. When there is a positive dependence margin between the properties, the pairs of (λ_i, χ_i) tend to be located above the confidence band and vice versa for negative dependent margins while the points enclosed within the confidence band can indicate independence of the bivariate pair of the drought properties.

To further establish the statistical fitness of the bivariate joint dependence structure, the K-plot (also known as Lambda plot), which is a rank-based graphics tool for visualising the dependence structure between two associated variables (Genest and Boies 2003), is prepared. For any observation pair (u_i, v_i), where $i = 1, ..., N$, the K-plot

is able to consider the two bivariate quantities that comprise of: firstly the ordered values of the empirical bivariate distribution function $H_i := \hat{F}_{uv}(u_i, v_i)$ and secondly, the quantity $W_{i:N}$ that shows the expected values of the order statistics from a random sample of size N of random variable, $W = C(X, Y)$. Under the null hypothesis of independence between the bivariate pairs X and Y, this is written as (Genest and Favre 2007):

$$W_{i:n} = N \binom{N-1}{i-1} \int_0^1 \omega k_0(\omega)(K_0(\omega))^{i-1}(1 - K_0(\omega))^{N-i} d\omega \qquad (6.24)$$

where $K_0(\omega) = \omega - \omega \log(\omega)$ and $k_0(\bullet)$ is the corresponding copula density.

A plausible physical interpretation of the K-plot is that, if the datum points in the distribution lie on the diagonal, then the X and Y are independent of each other, whereas any deviation from this line is expected to indicate significant dependence. Importantly, when there is a positive dependence between bivariate properties, datum points are expected to lie above the diagonal, and vice versa for the negative dependence. Also, the degree of positive dependency between the drought-risk properties is likely to be strongest when the datum points $(W_{i:N}, H_i)$ are situated on the curve $K_0(\omega)$, above the diagonal $y = x$ line and the perfect negative dependence between X and Y exist when the points $(W_{i:N}, H_i)$ lie on the x-axis (Schirmacher and Schirmacher 2008).

The joint variables X and Y can be related in terms of their extremes (*i.e.,* minimum and maximum) values, whereby the tail-dependence notion is expected to relate to their amount of dependence in the upper-right or lower-left quadrant tail of the bivariate joint distribution. The interpretation of upper *(lower)* tail-dependence parameter is that the probability of one margin exceeds a high *(low)* threshold under the condition where the other margin exceeds a high *(low)* (Poulin et al. 2007). The formulae for the upper and lower tail dependence parameters are (Joe 1997):

$$\lambda_U = \lim_{u \to 1^-} \frac{1 - 2u + (u, u)}{1 - u}; \quad \lambda_L = \lim_{u \to 0^+} \frac{C(u, u)}{u} \qquad (6.25)$$

6.3 Results and Discussion

6.3.1 Applications on SPEI and climate mode indices

A random sample of 250 datum points is simulated to yield the Chi-plot of the SPEI versus the Niño 4 SST (Fig. 6.2a) and the SPEI versus the SOI data (Fig. 6.2c). There exists a strong positive dependence since most of the simulated datum points are situated outside the confidence band of 0.1. Notwithstanding this, it is important that for the bivariate case of Niño 4 SST and SPEI joint behaviours, almost all of the simulated datum points are situated outside this confidence band, and that the magnitude of χ_i is significantly large, indicating very strong joint dependence. In fact, the Chi-plot shows a bent course with the Chi-values concentrated around the zero mark of λ_i, confirming that the dependency is strong around the median of the distribution than around the tails. In contrast, the bivariate combinations of the SPEI and SOI data (Fig. 6.2c) shows strong dependence around the median while a weak dependence around the tail ends of the plot.

Figure 6.2 (b, d) shows the K-plot for bivariate joint distributions of Niño 4 SST and SPEI, and SOI and SPEI using the simulated sample of 250 random points. It is evident that the lower tailed bivariate pair of data points appear to be independent, as the points lie closer to the diagonal line $y = x$, while the higher values indicate stronger negative (positive) dependence between the Niño 4 SST and SPEI (SPEI and SOI).
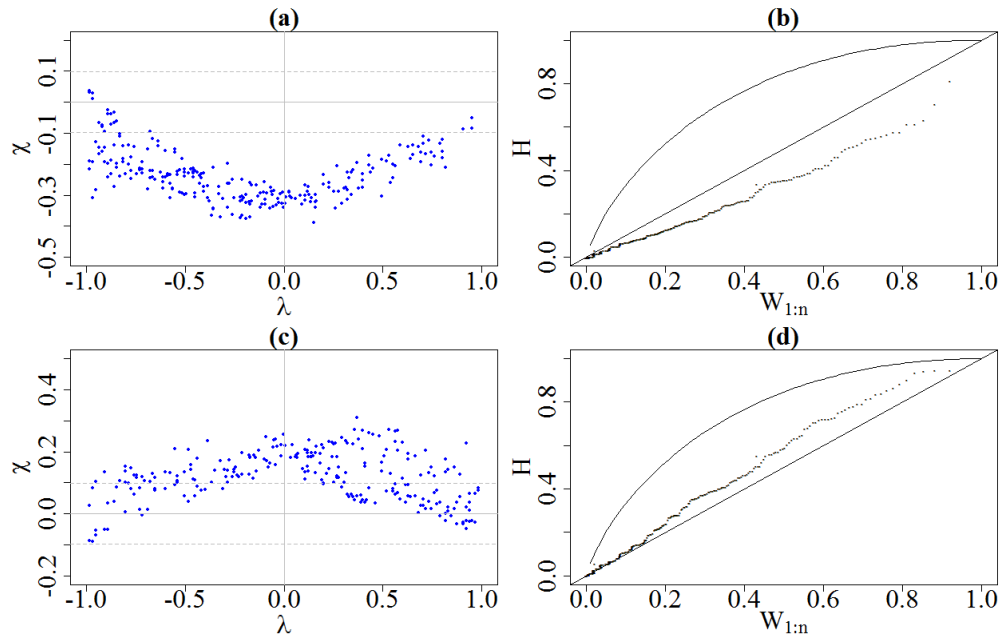
Figure 6.2: Chi-plots with "confidence band at $\alpha = 0.1$ (dashed lines) for SPEI with (a) Niño 4 SST and (c) SOI. K-plots with the straight line $(y = x)$ and a smooth curve $K_0(\omega)$ for (b) Niño 4 SST and (d) SOI joint distribution.

To address the limitations posed by the different marginal distributions, copula parameters from the selected bivariate and trivariate copula functions are applied to simulate margins of 2,000 random pairs of (u_{nino4}, u_{spei}) and (u_{soi}, u_{spei}) that are then back-transformed to their original units using their respective inverse marginal distributions. Figures 6.3a and 6.3b show the observed versus simulated SPEI and Niño 4 SST, and the SPEI and SOI, respectively. The black solid lines separate the El-Niño (SOI < -7.0) and La-Niña phases (SOI > 7.0) while everything in between correspond to neutral ENSO conditions. The observed values in the scatter plot clearly overlap the simulated samples.

Figure 6.3c and 6.3d shows the joint probabilistic predictions, expressed via the conditional bivariate and the conditional trivariate copula, respectively. In order to address the stochastic nature of drought and uncertainty in its predictions, the copula-statistical model is applied to generate an ensemble of 1,000 predictions that are then averaged to obtain a single set of predictions with the same length (or a number of datum points) as observed time series particularly for comparison purposes. The blue (*red*) scatters are the predicted SPEI for the random probabilities using features

available from the SOI (*Niño 4 SST*) as shown in Figure 6.3c based on their respective bivariate copula functions.

Using the trivariate Frank copula, the SPEI data is also predicted conditioned on the Niño 4 SST and SOI data shown in Figure 6.3d. Notice that observed and the predicted values do not form a linear relationship (which are not expected to) since the predictions are made for any random probability of the event. Note that in context of the present investigation, the simulations and predictions differ from each other. That is, in the simulation process, all variables are randomly generated at the same time using the optimal copula parameters. Conversely, the predictions are conditional where one variable is then evaluated at a certain probability based on the information available from the other variable(s), which in fact, may assist decision-makers in predicting the overall risk of the drought event. It is important to note that the copula-statistical models are able to predict the SPEI data directly based on the information derived from the Niño 4 SST and the SOI data, which act as synoptic-scale precursors of drought events.
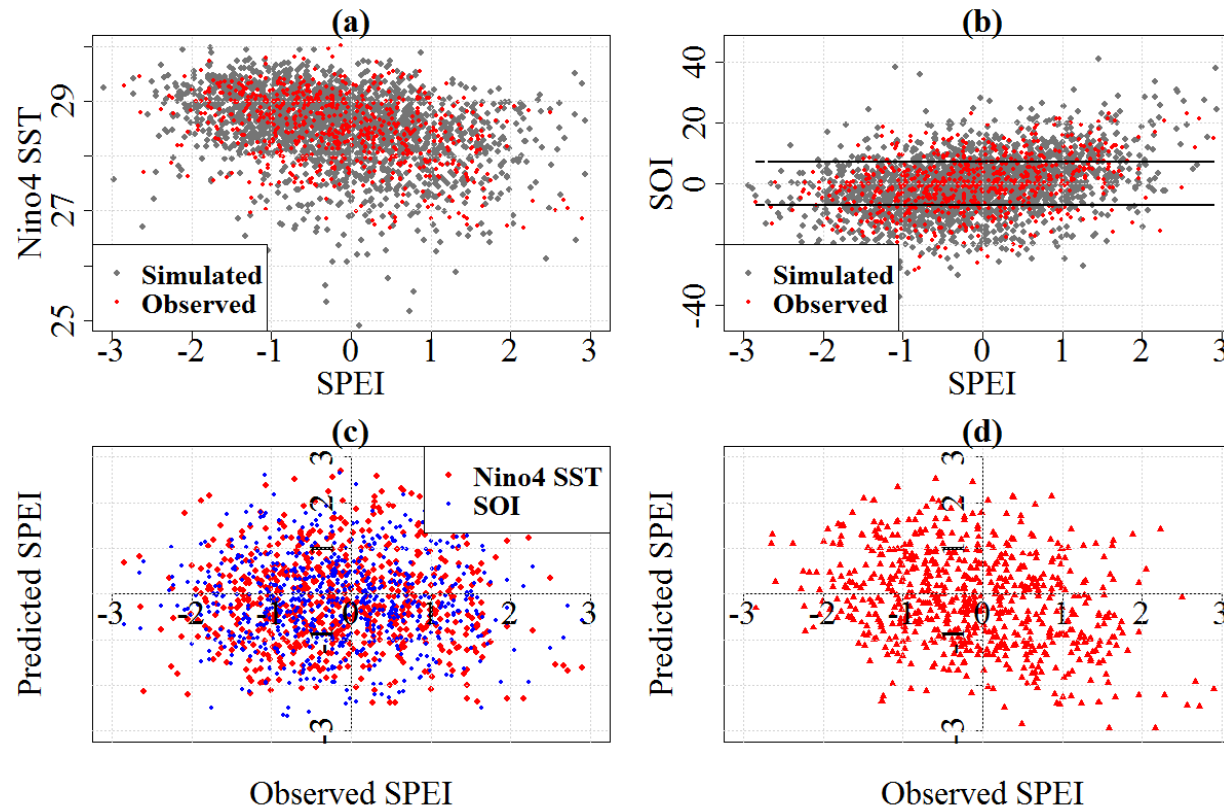
Figure 6.3: Observed vs. 2,000 random simulated SPEI samples (a, b). Scatter plot of observed versus predicted SPEI given information of Niño 4 SST and EMI using bivariate (c) Frank (for Niño 4 SST; *red*) and Gumbel (for SOI; *blue*) copula and using trivariate (d) Frank copula given combined information of Niño SST and SOI.

Table 6.5 provides a comparison of the basic statistics of the data representing the observed and the predicted SPEI. Importantly, these results show relatively small differences between the observed and the predicted SPEI statistics. The absolute difference in the mean value of the trivariate copula-based prediction is slightly larger (≈ 0.0161) compared to the bivariate copula-based predictions (≈ 0.0045 and 0.0008). The root mean squared error (RMSE) computed between the observed and predicted SPEI is also slightly larger (≈ 1.5990) in the trivariate copula-based prediction case compared to approximately 1.3742 and 1.3545 from the bivariate copula model predictions. The prediction errors of SPEI using copula-statistical model are generally small, suggesting that the conditional probability bivariate or trivariate copula-based predictions have good accuracy and are potentially suitable for application in prediction modelling.

Table 6.5: Comparison statistics for observed and predicted SPEI for bivariate and trivariate joint copula models.

Conditional Variable	Minimum	1st Quartile	Median	Mean	3rd Quartile	Maximum	AD$_{mean}$	AD$_{median}$
N/A	-2.8490	-0.8938	-0.2018	-0.1459	0.5683	2.8930	-	-
Niño4	-2.5170	-0.7791	-0.1797	-0.1504	0.4576	2.7430	0.0045	0.0221
SOI	-2.5230	-0.7492	-0.1399	-0.1451	0.4921	2.5130	0.0008	0.0619
[Niño4, SOI]	-2.9470	-0.8326	-0.1543	-0.1620	0.4869	2.4540	0.0161	0.0475

AD: Absolute Difference

The Figures 6.4 and 6.5 show the conditional probability of the SPEI occurrence expressed via the joint probabilistic bivariate and trivariate copula models, respectively. The negative SPEI indicate the drought conditions given in terms of their standard deviations. In Figure 6.4a, conditional on negative SOI values, the probability of obtaining a negative SPEI corresponding to drought conditions is higher in contrast to obtaining a lower probability with positive SOI values. For instance, in order to obtain a SPEI = -2.0 (*i.e.,* when the normalised deficit in water resources are below two standard deviations relative to the comparative base period), the probability is found to be ~0.98 with conditional SOI = -25.0, whereas when the SOI = 25.0, the probability is ~0.57. Similarly, the probability of obtaining negative SPEI conditional on the Niño 4 SST data is higher with a larger Niño 4 SST value, as shown in Figure 6.4b. For instance, in order to obtain SPEI = -1, the probability is found to be ~0.98 (~0.88) with Niño 4 SST = 30°C (27°C). Similarly, Figure 6.5 shows probability distribution of SPEI conditional on Niño 4 SST and SOI simultaneously.
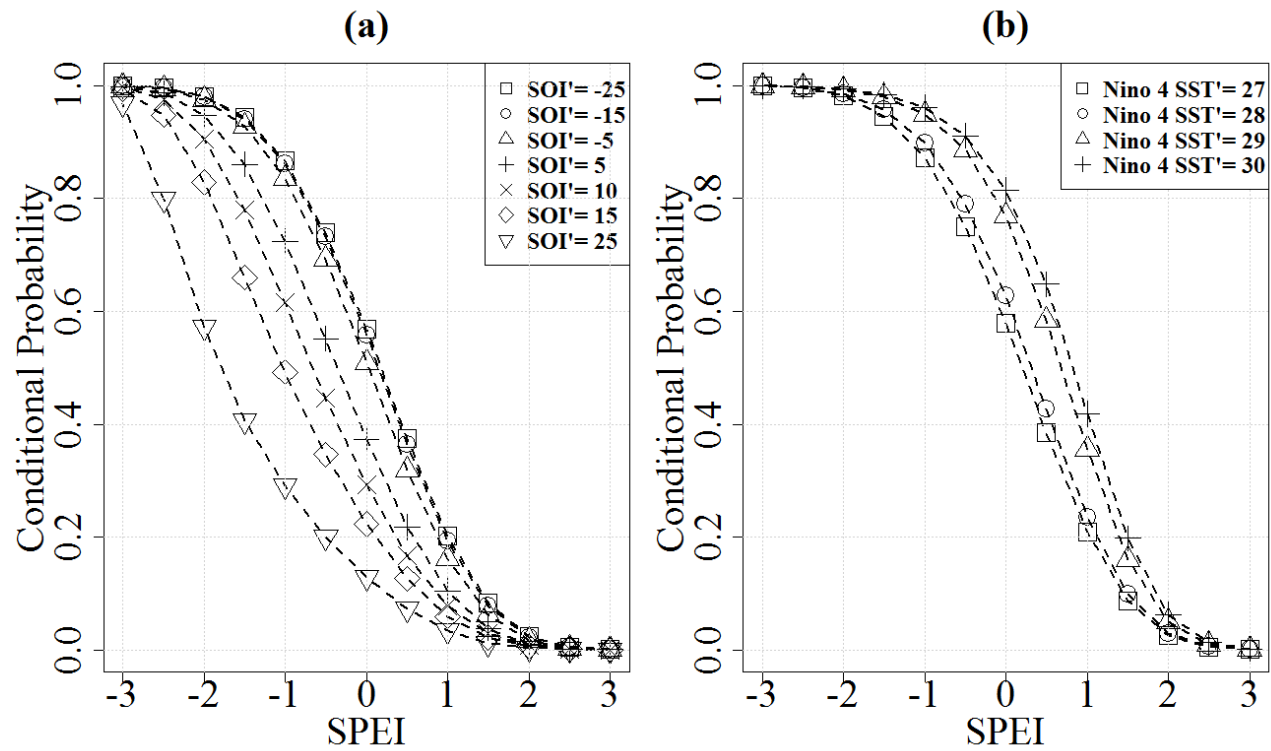
Figure 6.4: Conditional probability distribution of SPEI given SOI and Niño 4 SST values using bivariate Gumbel (a) and Frank (b) copula. The Niño 4 SST' is in degrees Celsius.
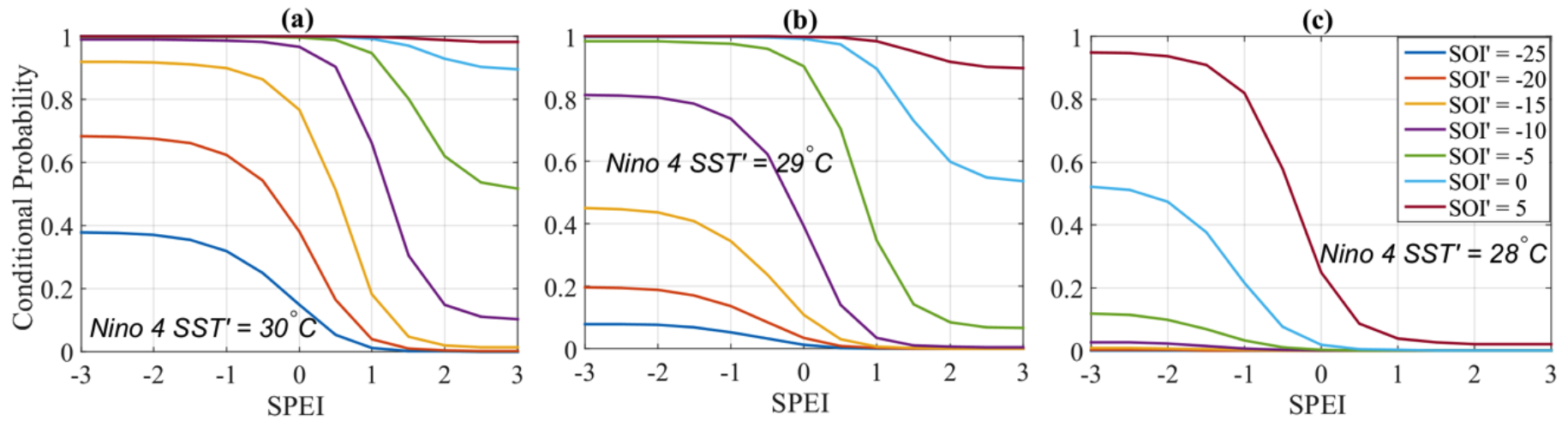
Figure 6.5: Conditional probability distribution of SPEI different Niño 4 SST (˚C) and SOI values using trivariate Frank copula. Legend applies to all panels.

6.3.2 Applications on drought properties and climate mode indices

The drought properties represented as D, S and I are also modelled with climate mode indices using the optimal copulae developed in this study. The selected bivariate copula for D and Niño 4 SST is Clayton while for S and EMI, and I and EMI are Frank. Using copula parameters, random values for D, S and I and their corresponding CI are simulated and predicted, as shown in Fig. 6.6. The comparison statistics between observed and predicted D, S and I are given in Table 6.6. The absolute difference in mean (AD_{mean}) is the smallest for the prediction of drought intensity, followed by the drought duration and drought severity. Since the information of EMI is used to predict both the intensity and the severity, and both use bivariate Frank copula, the smaller AD_{mean} for intensity could be due to the larger Frank copula parameter ($\theta = 2.02$). The larger copula parameter indicates a higher dependence between the bivariate pair of variables. Importantly, the RMSE is also found to be the smallest for prediction of intensity.
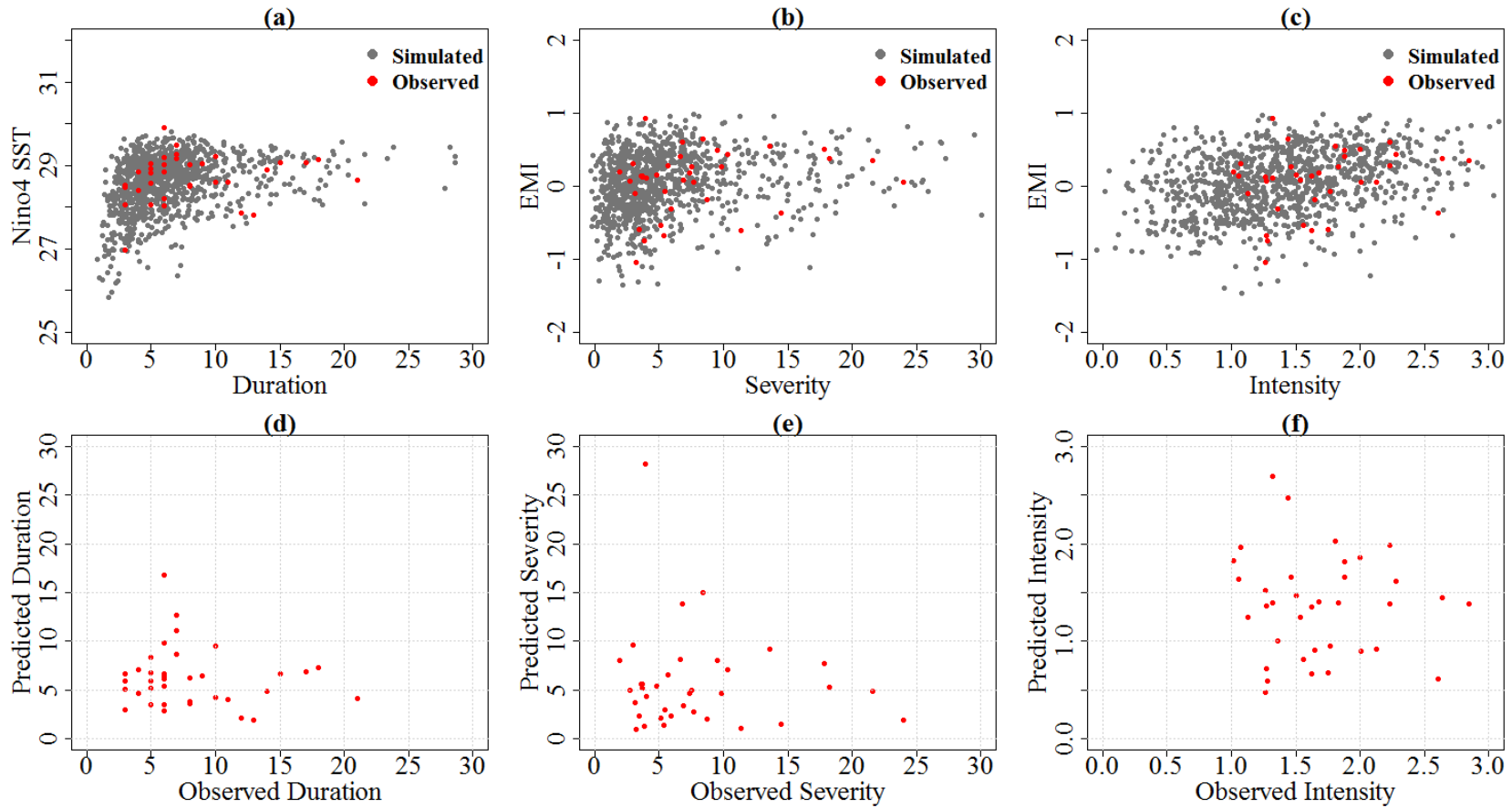
Figure 6.6: Comparison of observed data with 2,000 random samples (a, b, c) simulated from Clayton (a, b) and Frank (c) copula. Scatter plot of observed versus predicted duration (d), severity (e) and intensity (f) given information of Niño 4 SST (d) and EMI (e, f).

Table 6.6: Comparison statistics for observed and predicted duration, and intensity from the bivariate copula models.

	Minimum	1st Quartile	Median	Mean	3rd Quartile	Maximum	AD_{mean}	AD_{median}
Observed	3	5	6	8	10	21	-	-
Predicted	1.8380	4.0570	6.0170	6.1930	6.9100	16.7500	1.8073	0.0167
Observed	1.9450	3.7840	6.2840	7.8760	9.6080	24.0200	-	-
Predicted	0.9066	2.2670	4.8740	5.7090	7.2210	28.1900	2.1670	1.4091
Observed	1.0200	1.3070	1.6230	1.6830	1.9090	2.8490	-	-
Predicted	0.4731	0.9193	1.3880	1.3620	1.6560	2.6970	0.3209	0.2354

AD: Absolute Difference

An estimation of drought return period, which represents how often a drought is likely to occur (and hence, is closely linked to drought-risk on agriculture and water resources), is an important quantity in drought studies. Since every drought is different with the general notion that some events may persist as long drought episodes, an estimate of return period is crucial for designing hydraulic facilities (*e.g.,* dams and irrigation systems). In this case study, the average inter-arrival time (*i.e., EL)* between drought events is found to be approximately 13.53 months. Figure 6.7 shows the isopleths of the bivariate joint return period for the 'AND' (a, c, e) and 'OR' (b, d, f) cases of drought properties. The contours show the return periods (in years) for given drought properties and *CIs*. Notice that the isopleth patterns for the 'AND' and the 'OR' cases are unique because those for the various joint return periods defined by the 'AND' case are bounded by horizontal (*x*) and vertical (*y*) axes, whereas there is no bound for isopleths for the specific return periods defined by the "OR" case.

The return periods using two bivariate ('AND' and 'OR') cases also differ markedly. Take for instance; for *D* versus Niño 4 SST joint pair (Fig. 6.7a, b), for any particular value of *D* and the corresponding Niño 4 SST, the estimated return period T_{OR} is less than the T_{AND} return period. In fact, for the 'AND' case, the isopleths representing a given bivariate *D* and Niño 4 SST, *I* and EMI, and *S* and EMI, the joint pairs are situated over a much larger return period. For example, an estimated duration of 10 months and Niño 4 SST of 29˚C, the 'OR' case yields a return period of ~3 years (Fig. 6.7b), whereas the respective bivariate equivalent return period, *i.e.,* 'AND' case, registers about ~20 years (Fig. 6.7a). Similarly, the bivariate return periods of severity and intensity with EMI for 'AND' and 'OR' cases are shown. The return period values using 'AND' case suggest that for any drought event with specific thresholds of *D*, *S*, *I* and *CIs* to occur simultaneously will have larger return periods as such events are relatively rare compared to when each variable is analysed separately using 'OR' case.
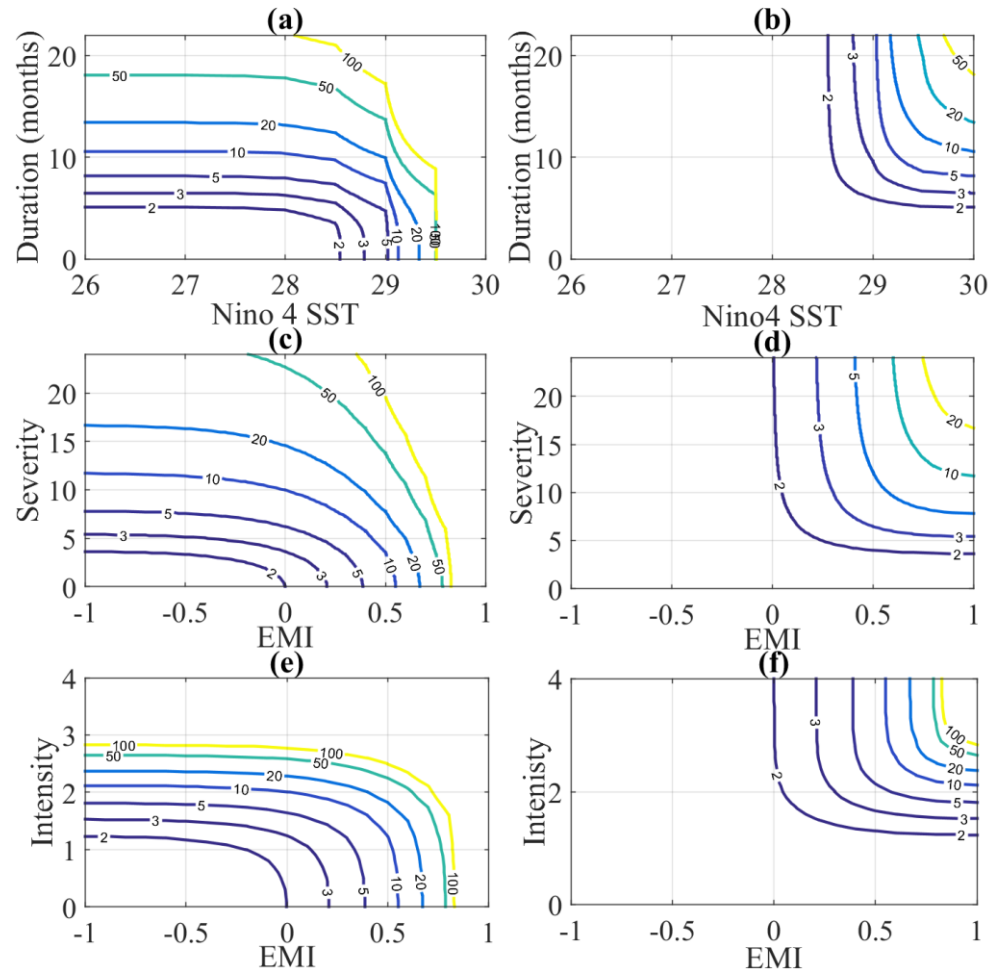
Figure 6.7: Bivariate drought return period for 'AND' and 'OR' case for the duration (a, b) using Gumbel, severity (c, d) using Frank and intensity (e, f) using Clayton copula.

The bivariate conditional return periods of *D*, *S* and *I* have been calculated (Fig. 6.8). The results show an increase in the return period as conditioned variable value increases. For instance, the return periods to obtain a drought event with a duration, *D* = 20 months under Niño 4 SST conditions (27˚C, 28˚C, and 29˚C) are 69.94, 85.33 and 544.82 years, respectively (Fig. 6.8a). Similarly, the return periods for severity, *S* = 10.0 *(and Intensity, I = 2.0)* under EMI conditions (0, 0.2, 0.4 and 0.6) are 17.81 *(17.46)*, 33.90 *(33.01)*, 94.52 *(91.46)* and 493.18 *(475.01)* years, respectively, (Fig. 6.8b, 6.8c). This shows that as the magnitude of ENSO indicators shift towards their extreme values, in the direction of enhancing the drought conditions, the return period of drought properties increase as well, suggesting the rarity of such extreme events. The results thus reveal the importance of jointly modelling the drought properties to encapsulate the true associative behaviour of drought properties with climate mode indices and how they manifest to produce an overall drought-risk in agricultural systems.
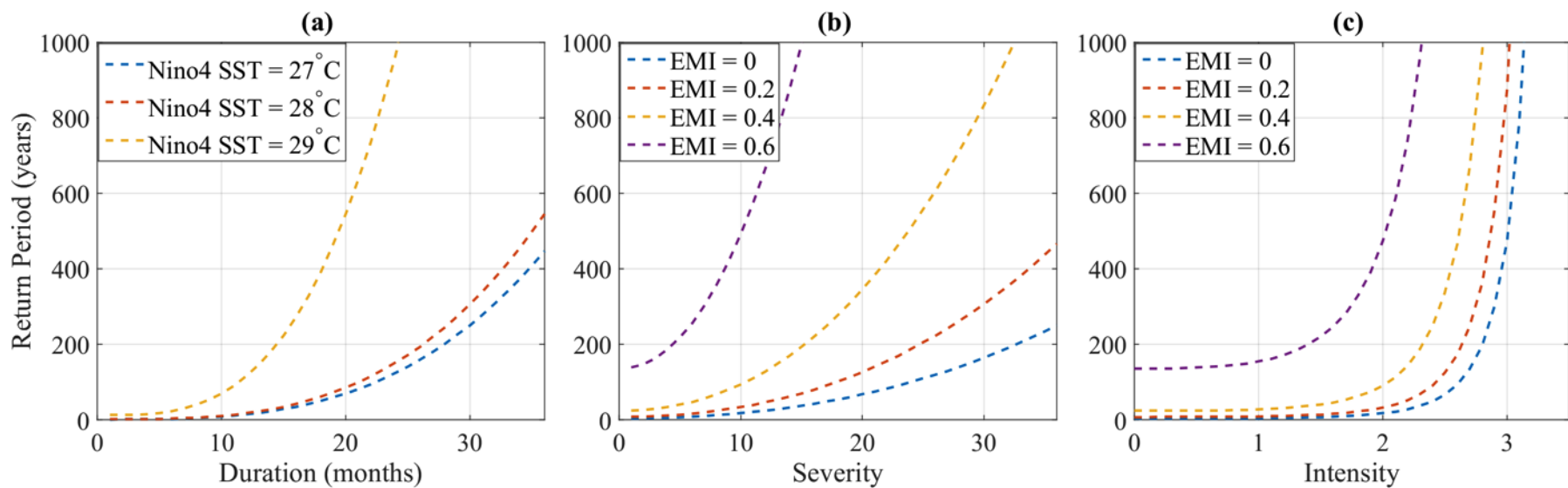
Figure 6.8: Conditional return period of drought (a) duration, (b) severity and (c) intensity.

6.3.3 Applications on drought properties

Many previous studies have shown the interrelation between droughts D, S and I properties. For agriculture and water management, estimates of return period of a given drought event are crucial. As such, using the marginal and joint probabilities, the univariate, bivariate and trivariate return periods are also calculated. Table 6.7 lists the marginal probabilities, univariate, bivariate and trivariate return periods. The physical interpretation of this plot is greatly important for understanding the pertinent drought-risk. Take for instance a $D = 10.22$ months, the univariate return period is 5 years, whereas the joint bivariate return period with S *(or I)* for 'AND' case is 5.87 *(or 17.69)* years and for 'OR' case it is 4.36 *(or 2.91)* years. Similarly, when all three variables are combined, the joint return period using trivariate model for 'AND' *(or 'OR')* case is 31.25 *(or 3.33)* years. The dramatic difference between the bivariate (and trivariate) return period compared with univariate counterpart clearly outlays the significance of considering the joint behaviour of different properties to avoid an underestimation of the overall risk posed by a given drought event. Although univariate return period is somewhat limited in its ability to represent the joint behaviour of more than one drought property, it is nonetheless important for drought-risk assessment when one random variable (*e.g.,* duration) is considered relevant over the others.

The data in Table 6.7 shows that the univariate return period is less than the joint return period T_{AND} and larger than T_{OR}. The trivariate T_{OR} is less than both univariate and bivariate ones. This is because adding one or more variables in the drought prediction model makes the exceedance probabilities $P(X_1 \geq x_1, X_2 \geq x_2, X_3 \geq x_3)$ smaller than two bivariate $P(X_1 \geq x_1, X_2 \geq x_2)$ or a univariate $P(X_1 \geq x_1)$ case. This is evident across the rows where the marginal probabilities appear to be decreasing from the univariate to the trivariate models.

Table 6.7: Univariate and copula-based joint return periods of drought duration, severity and intensity. $F(\bullet)$ is the marginal probability.

	Univariate Model				*Bivariate Model*									*Trivariate Model*		
T	$F(x)$	D_d	S_s	I_i	$F(d,s)$	T_{AND}	T_{OR}	$F(d,i)$	T_{AND}	T_{OR}	$F(s,i)$	T_{AND}	T_{OR}	$F(d,s,i)$	T_{AND}	T_{OR}
5	0.77	10.22	9.96	2.00	0.74	5.87	4.36	0.61	9.25	2.91	0.67	9.52	3.39	0.66	11.97	3.33
10	0.89	14.54	16.27	2.26	0.87	11.91	8.62	0.79	27.69	5.41	0.81	30.95	5.96	0.80	29.49	5.51
20	0.94	17.34	19.40	2.62	0.93	24.00	17.14	0.89	91.77	10.41	0.90	109.42	11.01	0.88	50.83	9.26
50	0.98	20.34	23.50	2.80	0.97	60.24	42.73	0.96	501.06	25.41	0.96	629.47	26.03	0.94	90.13	19.64
100	0.99	21.00	24.02	2.85	0.99	120.65	85.38	0.98	1906.29	50.41	0.98	2444.97	51.04	0.97	150.67	36.48

6.4 Further Discussion

This case study has explored and developed a probabilistic drought prediction model using Archimedean copulae (*i.e.,* Clayton, Gumbel and Frank) which has never been applied for drought-risk modelling in the drought-prone SEQ region. It, therefore, represents an important advancement in terms of potential applications for agriculture, water management and related socio-economic sectors where drought presents a significant risk. The need for drought-risk assessment in a non-stationary climate has been emphasised in many studies, *e.g.,* (Mpelasoka et al. 2008; Verdon-Kidd and Kiem 2010) and in recent studies, copula models have been adopted to illustrate the dependence structure of drought properties under different ENSO conditions, *e.g.,* (Ganguli and Reddy 2014; Wong et al. 2009). The study of Wong et al. (2009) in New South Wales Australia provided a strong evidence of dependence between drought duration, intensity and severity under different ENSO conditions using Elliptical and Archimedean copulae. To further the investigation, three popular in hydrology, Archimedean copulae have been adopted to successfully derive joint distributions of SPEI drought index and duration, severity and intensity properties with ENSO climate mode indices, prior to developing the probabilistic prediction models. The probabilistic prediction is considered as an essential tenet for a number of end-users like water resource managers and farmers to develop management strategies for informed decision-making (Goddard et al. 2001).

It is imperative to mention that this is the first study to investigate series of climate mode indices to produce a conditional probabilistic prediction of the drought index SPEI and drought properties (duration, severity and intensity) in Australia. The SPEI is a relatively new drought index that, in addition to precipitation, uses potential evapotranspiration in determining drought conditions. The incorporation of potential evapotranspiration in the equation allows the index to capture the increased temperature impact on water demand (Vicente-Serrano et al. 2010) and while Australia's drought is often influenced by warming and cooling phases of ENSO, the choice of SPEI justifies the drought-risk assessment in this case study. The application of copula and SPEI in recent investigations have demonstrated the significance of SPEI for drought-risk assessments in China (Chen et al. 2016; Fan et al. 2017) and the

outcomes in this case study have highlighted the suitability of SPEI and copula-based drought modelling for Australian droughts. Furthermore, the forecasting of seasonal rainfall has been considered very important for sustainable agricultural management in Australia, *e.g.,* (Moeller et al. 2008; Nguyen-Huy et al. 2017; Stephens et al. 1994) and in the USA *e.g.,* (Khedun et al. 2014; Mishra et al. 2015). In this case study, a further step has been taken where the importance of drought forecasting is addressed using 3-month timescale SPEI that is important for providing information to agricultural sectors.

This case study has utilised the vine copulae (Brechmann and Schepsmeier 2013) that have remained largely unexplored in the area of drought modelling and predictions in Australia. Unlike previous studies that have investigated joint relationships of drought properties only (*e.g.,* duration with severity, duration with intensity, severity with intensity, or all three as trivariate), this case study has developed the copula-based probabilistic prediction models for SPEI and drought properties (*D*, *S* and *I*) using ENSO indicators (Niño 4 SST, SOI and EMI) as predictors, providing significant novelty via probabilistic prediction of droughts with universal indicators of atmospheric circulation that modulates the supply of water and regulation of solar energy at the ground surface. The results are significant for activities like agriculture because vine copulae allow the modelling of high-dimensional dependency between drought and its climate variables, and application of vines can be extended to both bivariate and trivariate copula-based modelling. Since application of vines in hydrological studies is relatively new, *e.g.,* (Gräler et al. 2013; Khedun et al. 2014; Nguyen-Huy et al. 2017; Vernieuwe et al. 2015), its application to drought modelling in Australia is a novel contribution.

In contrast to previous studies that have produced the simulations for assessing dependence structure for two or more variables simultaneously (Wong et al. 2008), this case study successfully predicted the core variables (SPEI, *D*, *S* and *I*) based on the information available from the climate mode indices (Niño 4 SST, SOI and EMI). For better suitability in hydrology, the vine copula offer benefits of high-dimensional dependency between predictor and predictand have better computational tractability (Joe 1996) and are flexible in deducing multi-dimensional dependence structure using *tree* methods. Given the flexibility, vine copula offers a potential for multivariate

dependence modelling by decomposing multi-dimensional multivariate density into bivariate copulae, and its application in other climatic regions as well.

The initial stages of analysis involved evaluation of correlation of SPEI and its properties with thirteen climate mode indices, the subsequent analysis used only Niño 4 SST, SOI and EMI as these had statistically significant correlation and that are indicators of the ENSO event. For SPEI prediction, ten indices had statistically significant correlations with SPEI, however, only Niño 4 SST and SOI have been selected as they had highest correlations and are independently estimated. That is, the Niño 4 SST is solely based on temperature while SOI is based on pressure. The analysis yielded satisfactory simulation and prediction by utilising the most relevant, yet few climate mode indices. Using the evaluation metrics, the results captured emphatically the joint dependence structure between predictors and predictand and highlights the importance of jointly predicting drought and its properties where the correlation between predictors and predictand can be established. It is possible, however, that further investigation could incorporate other climate mode indices that have been found to influence Australian droughts in earlier studies (Ummenhofer et al. 2009; van Dijk et al. 2013; Verdon-Kidd and Kiem 2009) for drought predictions.

In spite of the significant outcomes, this pilot study has shortcomings that create the opportunity for a follow-up work. While only the SPEI on a 3-month timescale has been used and for only one case study location in the agricultural Murray Darling Basin region, the results may be applicable to the study location considered owing to the regional nature of drought, yet the methodology can be easily adapted to any case. Therefore, the practical application of the methodology adopted in this case study requires site-specific SPEI for the derivation of drought properties and selection of marginal distribution for predictors and predictand to be used in copula models. Also, to be consistent with the Australian BoM definition of drought (and associated drought response) (Mpelasoka et al. 2008), droughts with $D \geq 3$ months duration have been evaluated for modelling. The models have been successful in yielding predictions for drought indicator and its properties conditioned on climatic indices that modulate droughts in Australia. As an alternative, the copula-based probabilistic predictive models can be applied to flash droughts that could be in the form of heat-wave or precipitation deficit over the relatively short period (Mo and Lettenmaier 2016). In spite of the limited scope of this study, a follow-up study could implement vine

copulae to droughts on different timescales and for study locations with varying climatic conditions, short- or long-term droughts, and flash droughts for a wide variety of statistical prediction modelling. This would provide appropriate information to agriculturists and farmers for their specific cropping needs and demand for water/soil moisture for different crops.

6.5 Conclusion

A study of the joint behaviour of drought and its properties with climate mode indices is critical for water resource planning and drought-risk management. Drought is stochastic in nature where the duration, severity and peak intensity property of various episodes can vary from one event to another, yet these properties can be strongly correlated with each other, and therefore, contribute differently to the overall risk of a given event. These properties are also influenced by large-scale oscillations in the atmosphere, such as the ENSO. In this study, vine copulae have been employed as a new contribution to Australian drought-risk study to model the joint behaviour of SPEI and its drought properties (duration, severity, and intensity) with climate mode indices (Niño 4 SST, SOI and EMI). The Niño 4 SST, SOI and EMI are indicators of ENSO, which modulates drought conditions in Australia, where Niño 4 SST $> 26°$C, SOI < -7 and EMI > 0 represent El-Niño, *i.e., the* warm phase of ENSO that enhances the drought conditions.

Archimedean copulae (*i.e.,* Clayton, Gumbel and Frank) have been the most suitable models for modelling the joint behaviour of multivariable. The findings in this case study have demonstrated the joint dependence structure of SPEI and drought properties with climate mode indices while the vine copulae have illustrated the usefulness of the conditional probability-based drought predictions. The comparison between predicted and observed SPEI values have shown similarity, indicating satisfactory model performance. Similarly, the prediction of D, S and I using Clayton, and Frank copulae, conditional on Niño 4 SST and EMI, have yielded small absolute difference in mean values from the observed.

Overall, this case study has demonstrated the feasibility of copula-statistical models in understanding the joint relationships between drought variables and climate mode indices in the present case study region. However, the practical relevance of these copula-statistical models can be further enhanced in a separate study by

considering many other climate mode indices on other timescales (*e.g.,* 1-, 6-, 12-, 24-months, seasonal, annual, decadal, etc) using multivariate copula-statistical models, making them more applicable to an improved assessment of the combined risk of drought event. This limitation has been acknowledged in Section 3.4.

Chapter 7

SPATIO-TEMPORAL DROUGHT-RISK MAPPING APPROACH FOR SOUTHEAST QUEENSLAND, AUSTRALIA

Note:

The results from this chapter have been submitted to and are *Under Review* in the *Natural Hazards* journal. The following is the tentative reference to the article:

Dayal Kavina S., R. C. Deo and A. A. Apan, (2017) "Spatio-temporal drought-risk mapping approach for southeast Queensland, Australia", *Natural Hazards*, (Under Review).

7.1 Introduction

Chapters 4, 5, and 6 used point-based study locations for the temporal assessment of drought-risk. As mentioned earlier on, nature of drought is both temporal and spatial. As the next novel contribution of this study, the current chapter assesses drought-risk geospatially on the seasonal and annual basis.

Drought-risk management involves three primary activities: (1) identification of the risk and the assessment of its significance, (2) development of new methods and utilisation of available resources to minimise or mitigate the drought-risk, and (3) development of new strategies to manage the drought-risk. The difficulty, however, in enforcing any of these perspectives, is the subjectivity in the measurement of regional drought vulnerability that is usually quantified as a relative measure (Downing and Bakker 2000). The challenges with vulnerability mapping and assessment are an

ongoing issue because vulnerability levels are dynamic, and they are moderated due to the changes in land use, population density, technology, farming practices and climate variability. Therefore, mitigating the regional drought impacts could involve some level of subjectivity in the assessment as there are no standard criteria for mapping drought vulnerability, hence to quantify drought-risk. However, to minimise the subjectivity in the vulnerability assessment, the application of fuzzy logic theory in Geospatial Information System (GIS) for natural hazard mapping is instrumental in the design of efficient tools for spatial decision making (Aksoy and Ercanoglu 2012; Al-Abadi et al. 2017; Espada Jr et al. 2012; Jun et al. 2013; Wu et al. 2013).

Developing a comprehensive set of metrics for drought assessment is challenging due to the dynamic nature of environmental and socio-economic factors (Hinkel 2011). In many previous drought vulnerability assessment studies, the indicating variables were mainly aggregated with the deductive approach (*e.g.,* expert judgement) or by normative approach (*e.g.,* equal weighting). Consequently, the delivery of robust results is an issue due to subjective judgements in the former approach and the multi-dimensionality of variables to different stakeholders in the latter approach (Hinkel 2011). Assigning equal weights to factors or through expert judgement based on the experience leaves room for errors. To circumvent the issue of multi-dimensionality in the normative argument of equal weights, the Bayesian joint conditional probability of each indicating variable for the weighted overlay operations is recommended.

Since vulnerability assessment is a relative measure due to its region-specific nature, drought analysts must define the critical levels (Downing and Bakker 2000). There are numerous factors that influence drought vulnerability (Price et al. 2011) and their inclusion may depend on available data. Undeniably, drought vulnerability has a close correlation with man-made infrastructure and socio-economic conditions (Wilhelmi and Wilhite 2002). According to the literature, studies performed outside of Australia has included various climatic and physiographic factors to produce integrated maps of vulnerability, *e.g.,* (Ekrami et al. 2016; Jain et al. 2015; Pandey et al. 2010; Safavi et al. 2014; Thomas et al. 2016; Wilhelmi and Wilhite 2002). Therefore, region-specific integrated physiographic, climatic and social factors are essential for the assessment of drought vulnerability.

Considering the need for a spatially-relevant drought-risk mapping for the drought-prone SEQ region, the purpose of this chapter is to apply the fuzzy logic tool to generate drought hazard, exposure and vulnerability indices using multiple physiographic and climatic factors where the indices are then overlayed to generate a risk map. The aim is to develop a model for assessing drought-risk that is expected to improve rationality and accuracy of results. The drought-risk map could be used as a framework for a timely implementation of mitigation measures and effective monitoring system. The specific objectives of this chapter, after the breakdown of the third major objective outlined in Section 1.3 are to: (1) identify available spatial and temporal physiographic and climatic factors relevant for the region; (2) estimate probable weights of each factor conditional on rainfall departure using Bayesian theorem; (3) standardise factors using fuzzy membership functions and generate vulnerability, exposure and hazard indices maps; and (4) produce integrated drought-risk map using fuzzy overlay operation available in ArcGIS 10.5.

7.2 Theoretical Overviews

7.2.1 Concept of vulnerability, exposure and risk

The risk is a product (or sum) of hazard, vulnerability and/or exposure. According to Downing and Bakker (2000), the risk can be expressed mathematically as:

$$\text{Risk} = \text{Hazard} \times \text{Vulnerability} \times \text{Exposure} \qquad (7.1)$$

$$\text{Risk} = \text{Hazard} + \text{Vulnerability} \qquad (7.2)$$

IPCC (2012) defines *hazard* as "the potential occurrence of a natural or human-induced physical event that may cause loss of life, injury, or other health impacts, as well as damage and loss to property, infrastructure, livelihoods, service provision, and environmental resources". The *risk* is defined as "the likelihood over a specified time period of severe alterations in normal functioning of a community or a society due to hazardous physical events interacting with vulnerable social conditions, leading to widespread adverse human, material, economic, or environmental effects that require immediate emergency response to satisfy critical human needs and that may require external support for recovery" (IPCC 2012). The term *vulnerability* has numerous definitions. Since vulnerability usually bounds by context, a specific definition is difficult to justify. In response to the hazard-centric perception of disasters in the

1970s, the term *vulnerability* was introduced to describe the extent to which people suffer from calamities and socio-economic circumstances to cope with (Schneiderbauer and Ehrlich 2004). Geoscience Australia (2010a) conceptualised vulnerability as the impact a hazard has on the people, infrastructure, and the economy. Lastly, *exposure* is defined in terms of the assets such as "people, property, systems or other elements present in hazard zones that are thereby subject to potential losses" (ISDR 2009).

7.2.2 Fuzzy logic approach

The fuzzy logic is an approach that computes the "degree of truth" instead of absolute terms "true or false" (*i.e.,* 1 or 0) Boolean logic (Zadeh 1968; Zadeh 1975). Fuzzy theory embraces the membership function (or the True and False) to operate over a range of numbers between 0 and 1, reflecting the degree of certainty of the membership (Pradhan 2011). It includes 0 and 1 as the extreme cases of truth but also various states in between, *i.e.,* fuzzy logic permits partial membership mathematically given as:

$$\mu_A(x): X \to [0,1] \qquad (7.3)$$

In Equation (7.3), $\mu_A(x)$ refers to the grade of membership for element x in a fuzzy set A, and the X is the universal set defined in a specific problem.

To build a fuzzy logic-based model, a careful selection must be made for the appropriate membership function. In the context of the present study, the fuzzy membership functions transform the input raster onto a 0 to 1 scale based on a specified fuzzification algorithm. A value of 1 indicates full membership in a fuzzy set, while membership decreasing to a value of 0 indicate it is not a member of the fuzzy set. In this investigation, three membership algorithms, LINEAR, LARGE and SMALL are used.

In the LARGE fuzzy membership, the larger inputs have membership values closer to 1 and the function is defined by a user-specified midpoint value that is assigned a membership value of 0.5. The mathematical expression of the LARGE fuzzy membership function is given as (Tsoukalas and Uhrig 1996):

$$\mu(x) = \frac{1}{1 + \left(\dfrac{x}{f2}\right)^{-f1}} \tag{7.4}$$

In Equation (7.4), $f1$ is the spread and $f2$ is the midpoint. The fuzzy LARGE function is useful when large input values have a higher membership where the input values can be either an integer or floating-point positive values.

The fuzzy SMALL defines membership function with smaller input values having a membership value closer to 1. The mathematical expression for the fuzzy SMALL function is given as:

$$\mu(x) = \frac{1}{1 + \left(\dfrac{x}{f2}\right)^{f1}} \tag{7.5}$$

The fuzzy SMALL function is useful when small input values have a higher membership. Figure 7.1 shows the geometric representation of fuzzy SMALL and fuzzy LARGE memberships.

The fuzzy LINEAR membership function applies a linear function between the user-specified minimum and maximum values. Anything below the minimum is assigned a value of 0 (definitely not a member) and anything above the maximum is assigned a value of 1 (definitely a member).
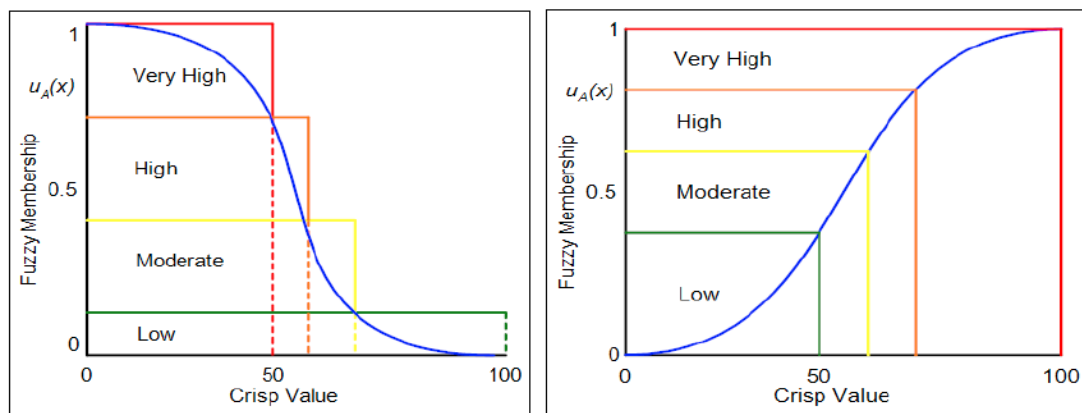
Figure 7.1: Geometric representation of SMALL (left) and LARGE (large) fuzzy membership functions.

After the input variable standardisation, the fuzzy overlay operation is performed. There are five different fuzzy overlay types: AND, OR, PRODUCT, SUM and GAMMA in ArcGIS 10.5, where the user can choose the overlay type to suit the purpose of their study. This study has used GAMMA overlay that uses the algebraic product of the "increasive" fuzzy SUM and "decreasive" fuzzy PRODUCT effects, both raised to the power of gamma. The fuzzy GAMMA overlay operation is chosen to avoid bias on which risk equation (Eq. 7.1 & 7.2) to be used in the assessment (Espada Jr et al. 2012; Espada Jr et al. 2013) where the mathematical expression of fuzzy GAMMA is given as (Tangestani 2003):

$$\mu_{gamma} = \left(\mu_{sum}\right)^{\gamma} \times \left(\mu_{product}\right)^{1-\gamma} \tag{7.6}$$

where μ_{gamma} is the calculated fuzzy membership function, γ is a parameter chosen between 0 and 1; μ_{sum} is the fuzzy algebraic SUM and $\mu_{product}$ is the fuzzy algebraic PRODUCT that is mathematically expressed as:

$$\mu_{sum} = 1 - \prod_{i=1}^{n}\left(1 - \mu_i\right) \text{ and } \mu_{product} = 1 - \prod_{i=1}^{n}\left(\mu_i\right) \tag{7.7}$$

where μ_i is the fuzzy membership for the ith map, and i = 1, 2, …, n maps to be combined. In the fuzzy GAMMA operation, $\gamma = 0$ is equivalent to the fuzzy algebraic PRODUCT and $\gamma = 1$ is equivalent to fuzzy algebraic SUM. The judicious choice of the gamma value depends on the user in order to ensure a flexible compromise between the "decreasive" and "increasive" tendencies of fuzzy PRODUCT and fuzzy SUM, respectively. This study uses the default gamma value of 0.9, consistent with Espada Jr et al. (2013) that also used fuzzy GAMMA overlay for developing flood-risk maps for Brisbane city area.

7.3 Materials and Method

To produce an integrated drought-risk map for the SEQ study region, various layers representing spatial maps of different factors are prepared using ArcGIS software. Spatial maps representing vulnerability, exposure and hazard per unit area are prepared on a grid system of 100 x 100 m. Spatial information on the above maps is categorised

in sub-classes in respect of their degree of significance in vulnerability to drought to obtain the probable weight of a factor conditional on the hazard.

7.3.1 Identification and significance of factors

Drought is driven by precipitation deficiency in space and time while the severity of drought depends on numerous factors. Drought-risk to agriculture can be viewed as a product of exposure to the climatic hazard and vulnerability to cropping practices to drought conditions (Wilhelmi and Wilhite 2002). To assess regions with high risk for droughts from the integrated drought-risk map, drought vulnerability, exposure and hazard factors need to be identified. While there are various, yet no certain fixed factors, previous investigations elsewhere have shown a number of static and semi-static physiographic and dynamic climatic factors that are closely associated with drought conditions. The most common yet immediate association with droughts are the slope, soil type, elevation, plant available water capacity (PAWC), soil depth, land use, and population density. The rainfall deficiency is considered as the drought hazard.

Rainfall: The best and most common single measure of water availability in Australia is the rainfall (ABS 2012). The rainfall deficiency is the primary factor responsible for the occurrence of drought as it is the cause of subsequent soil moisture shortage for crops (Jain et al. 2015). In this investigation, the rainfall departure (RD) from normal (*i.e.,* normal/base period from 1971 to 2000) is considered as the hazard index. The formula for calculating RD is given as:

$$RD\left(\%\right) = \frac{x_i - \bar{x}_i}{\bar{x}_i} \times 100 \tag{7.8}$$

where x_i =rainfall for the given month, season or year and $\bar{x}_i$ = average rainfall for the month, season or year over the base period 1971-2010 (Deo et al. 2009).

The year 2007 was one of the driest years, and the Spring season (September-October-November; SON) was the driest season in 2007 during the Millennium Drought. In SON 2007 season, ~12.70% of the study region had RD ≤ -75%, ~12.41% of the study region had -75% < RD < -50%, ~13.08% of the study region had -50% < RD < -25%, and ~11.12% of the study region had -25% < RD < 0%. In other words, a total of ~49.31% of the study region has been under rainfall deficient state in the spring

season of the year 2007. The numerical weighting of RD subclasses was based according to Jain et al. (2015). Similarly, rainfall departure for autumn (March-April-May; MAM) and summer (December-January-February; DJF) seasons of 2007, and annual, *i.e.,* 2007, 2009 and 2013 drought years have been estimated and Table 7.1 enumerates the extreme values in the study region.

Figure 7.2 shows an example of annual (1960-2013) and seasonal (2000-2013) percent rainfall departure for a point location in the study region, *i.e.,* for Brisbane (153.03°E, 27.47°S). The seasonal rainfall departure has been mostly negatives as well during this Millennium drought period.

Table 7.1: The maximum and minimum values of rainfall departure from the base period during the drought years in the present study region.

Rainfall Departure	Drought season (2007)			Drought year		
	DJF	MAM	SON	2007	2009	2013
Maximum	225.26%	466.34%	378.56%	19.50%	27.74%	41.08%
Minimum	-73.18%	-100.00%	-100.00%	-41.71%	-49.47%	-62.51%

(*DJF=December-January-February; MAM=March-April-May; SON=September-October-November; JJA=June-July-August.*
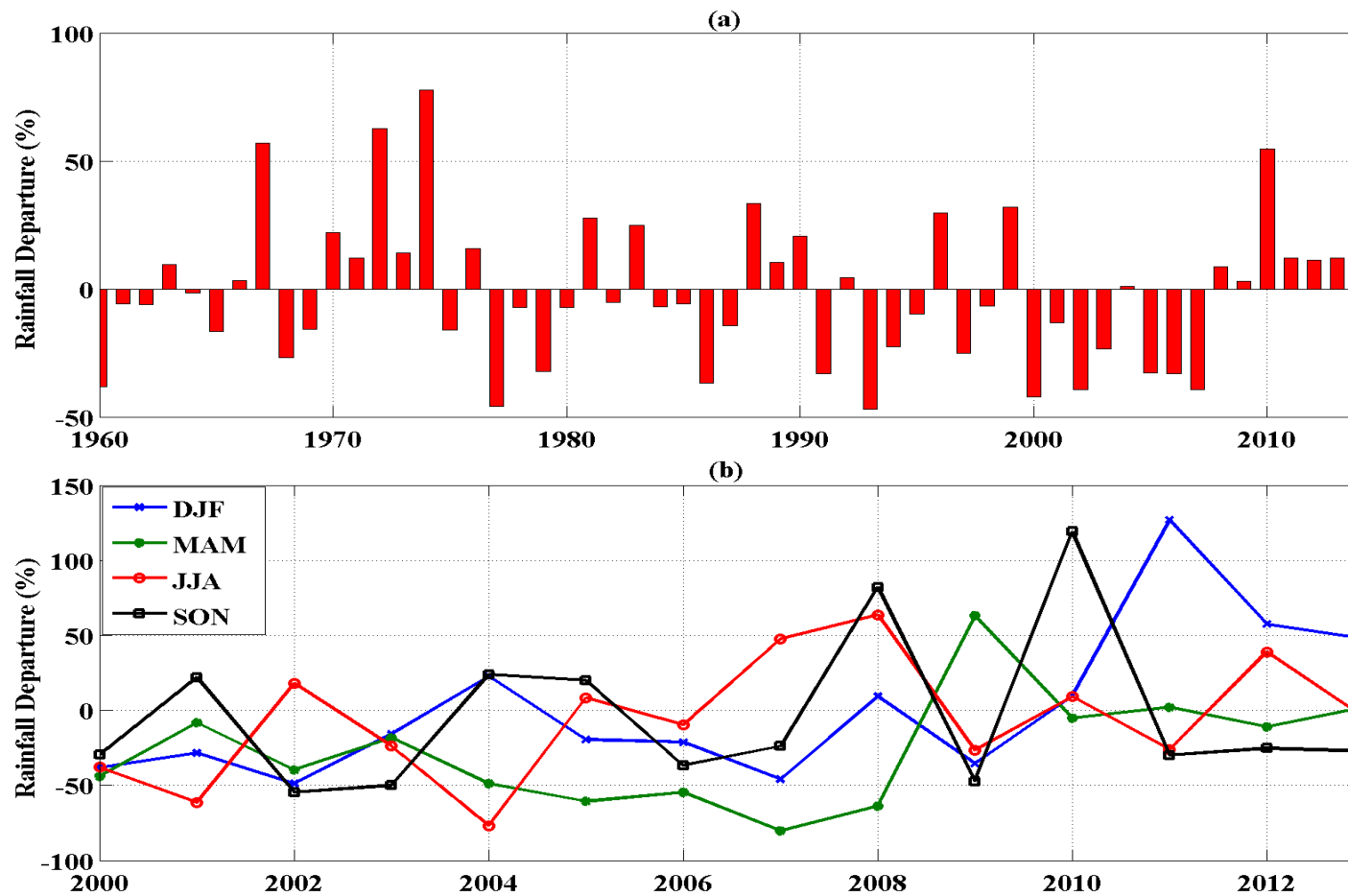
Figure 7.2: Climatological conditions for the study region (Brisbane, 153.03°E, 27.47°S).
(a) Annual rainfall departure (expressed as a percentage) over 1960–2013.
(b) Seasonal rainfall departure (expressed as a percentage) over Millennium drought.

171

Soil: In seasonally dry and semi-arid tropics and subtropics, the low and erratic rainfall puts a major constraint on rain-fed agriculture. In these areas, soil moisture is crucially important for fullest expression of the production potential of plants over time. It is important, however, to note that irregular and an insufficient amount of rainfall is not the only cause of lack of moisture in the soil. For instance, the water-holding capacity of the soil depends on the soil porosity, which in turn depends on the soil texture. The soil texture is important because it influences the amount of water soil can hold, the rate of water movement through the soil and how workable the soil is for growing plants (FAO 2005). In the SEQ region, soil texture varies from clay, loam, silt, and sand. The clay soil generally holds more water while the sandy soil is well aerated but does not hold much water, *i.e.,* it has high water infiltration rate. Therefore, sandy soils are most vulnerable to drought due to its least moisture holding capacity.

This study utilized the sandy soil type data for the year 2014, sourced from the Terrestrial Ecosystem Research Network (TERN) (TERN 2009). Sand data are estimated in percentages by taking 20μm - 2mm mass fraction of the <2mm soil material determined using the pipette method. The sand digital maps are available at 6-defined depth intervals: 0-5cm, 5-15cm, 15-30cm, 30-60cm, 60-100cm and 100-200cm. In this study, the values for all depth levels have been averaged to obtain a single layer map of the sand. Figure 7.3 shows the spatial distribution of the sand percentages. Much of the low sand percentage is found at the higher elevation area.

Soil depth: Soil depth refers to the thickness of the soil materials that provide structural support, nutrients and water for plants (Scherer et al. 2013). The greater the depth of the soil, the higher the capacity of the soil to store and supply moisture to plants for growth. Therefore, greater soil depths are considered less vulnerable to droughts. Shallow depths mean less water storage by the soil, hence it is more vulnerable to droughts. The soil depth data has been obtained from TERN for the year 2014. The depth of soil on a geospatial map is shown in Figure 7.3.

Slope: The slope that measures the inclination of the land surface from the horizontal is another important drought vulnerability factor. The water runoff is considerably higher on steeper terrain compared to the near ground surface. Therefore, the terrain areas with lesser slopes are relatively less vulnerable to droughts compared to the hilly plains (Jain et al. 2015). The slope data (in percentages) has been obtained from TERN

for the year 2000. The spatial distribution of the slope percentage is shown in Figure 7.3.

Plant Available Water Capacity (PAWC): The PAWC refers to the difference in water content between field capacity and permanent wilting point of plants. The study of Stone and Potgieter (2008), following the work of Wilhelmi et al. (2002), provided a compelling argument on the importance of PAWC for the Australian droughts. In their study, Stone and Potgieter (2008) developed initial indications of PAWC based on the knowledge of local specialists, agronomists, and rural extension officers working "in the field". It was found that many parts of the eastern Australia had relatively low levels of PAWC (*e.g.,* 75-100mm) that, potentially, increased the vulnerability to drought-risk. To be consistent with the scales used in their study, similar effective index-scale of PAWC has been applied in this study, as shown in Table 7.2. The PAWC data has been obtained from the National Agricultural Monitoring system (NAMS; http://www.nams.gov.au). The PAWC spatial distribution is shown in Figure 7.3.

Elevation: Water availability also greatly depends on the elevation of the plain. The digital elevation model (DEM) describes landforms and ground surface topography is crucial for addressing issues relating to the impacts of climate change, disaster management, water security and environmental management. The 3-second DEM data for the year 2000 has been obtained from Queensland Spatial Catalogue – QSpatial. The elevation concurs well with the percent slope where higher elevation has higher slopes and vice versa. For instance, the elevation less than 500m has a slope less than 5%. In Figure 7.3, the high elevations are where the Great Diving Range is, while the area close to the coast is mostly low-elevated zone.

Land use: The drought vulnerability can be regarded in a dynamic sense as a result of land use and management, including government farm practices and societal factors (Nelson et al. 2005). Land use is one of the most important factors influencing vulnerability to drought. In this study, it is considered as an exposure factor because of its dynamic nature. The land use data has been obtained from the Queensland Land use Mapping Program (QLUMP) for the year 2016, available at QSpatial data portal. Land use in the study region is dominated by pasture/grassland (about 63.8%) followed by agriculture (20.3%), production forestry (7.4%), nature conservation (4.3%), urban

173

use (3.1%) and water body (1.1%), as shown in Figure 7.3. Among the six listed land use types, it is implicit that agriculture (urban use) becomes the first (second) sufferer due to water deficiency and drought compared to other land uses because of their dependency on water for survival. Therefore, agriculture subclass is given the highest numerical weight value because it is considered as relatively more vulnerable to drought. In contrast, the nature conservation encompasses rare socio-economic activities and is therefore assigned less weight as it is considered less sensitive to water shortages. The water bodies such as lakes, dams and reservoir are assigned a negative value of -100 for masking as these areas are considered non-vulnerable to drought.

Population: The water demand is also affected by the population density. In the areas where population density is high, the water usage and demand is also high. Therefore, areas with larger population density are considered relatively more vulnerable to drought than areas with smaller population density. In this study, population density is categorized as an exposure factor because as the population grows, the demand for water mounts and pressure on finite water resources intensifies. The continuous growth of population density will impact water availability in any given area, hence the exposure to drought is likely to subsequently increase. The population density data has been obtained from the Australian Bureau of Statistics (ABS; (ABS 2012)) for the year 2011. Much of the study area has less than 1,000 people to none per square grid, therefore the exposure to drought is less in these areas, as shown in Figure 7.3. Conversely, the population density is relatively high in the southeast study region that covers the populous Brisbane city and Gold Coast. This indicates that high population density and high population growth rates in the SEQ region have high chances to face water scarcity or water stress situations.

7.3.2 Study area

In contrast to the point-based study locations in Chapters 4-6, the study area in this chapter is the entire highlighted SEQ region.

7.3.3 Proposed weighting scheme

To produce vulnerability, exposure and hazard indices map, a differential weighting scheme based on relative importance of the factors is proposed. The weight assignment is based on the assumption of a relative degree of influence of a factor on overall

vulnerability to droughts. In the proposed scheme, the rainfall deficiency in terms of rainfall departure is considered most influential factor and is therefore assigned highest weights ranging from 0 to 25 (Table 7.2). The weight value of 25 represents very extreme dryness that poses the highest risk to droughts. Comparatively, other factors are considered moderately influential to drought vulnerability and are thus given weight assignment between 0 and 10, where a value of 10 corresponds to the factor subclass being highly vulnerable to drought. For instance, the water demand and availability tend to vary considerably with land use types and since agriculture and urban use are the primary focus of this study, they are assigned higher weights. Similarly, elevation, soil depth, sand soil type, plant available water capacity and slope are divided into subclasses and assigned weights based on their relative importance to drought vulnerability. The differential weights are then used to determine the joint conditional probability based on Bayes theorem discussed next. It is important to note that the weight assignment to the factor subclasses has been carried out only to estimate the joint conditional probability that shows the relevance of each factor conditional on the hazard.

Table 7.2: Numerical weights assigned to the sub-classes of drought vulnerability, drought exposure and drought hazard factors.

Factors	Assumption	Classification of drought vulnerability factors	Weights assigned
Land use	The classified land use after numerical weight assignment is **directly related** to the degree of vulnerability. The subclass with higher numerical weight is more vulnerable to drought, and vice versa. - fuzzy LARGE	Waterbody Nature conservation Production Forestry Pasture/grassland Urban use Agriculture	-100 (*masking*) 2 4 6 8 10
Soil texture - Sand	Sand: **directly related** to the degree of vulnerability. The higher the percentage of sand means a higher degree of vulnerability. - fuzzy LARGE	<50 % >50%	5 10
Slope (%)	**Directly related** to the degree of vulnerability. The higher the percentage of slope means a higher degree of vulnerability. - fuzzy LARGE	$0 - 2$ $2 - 5$ $5 - 8$ $8 - 12$ > 12	2 4 6 8 10
Population density (per km^2)	**Directly related** to the degree of vulnerability. The higher the number of people living in a square kilometre grid, the higher the degree of vulnerability. - fuzzy LINEAR	$0 - 1000$ $1000 - 2000$ $2000 - 3000$ $3000 - 4000$ ≥ 4000	2 4 6 8 10
Soil depth (m)	**Inversely related** to the degree of vulnerability. The greater the depth of soil, the less the degree of vulnerability. - fuzzy SMALL	≥ 1 < 1 to ≥ 0.8 < 0.8 to ≥ 0.6 < 0.6	1 3 6 9

Plant Available Water Capacity (*PAWC*; mm)	**Inversely related** to the degree of vulnerability. The less amount of PAWC, the higher the degree of vulnerability. - fuzzy SMALL	≥ 175 150 – 175 100 – 150 75 – 100 ≤ 75	-100 (masking) 2 4 8 10
Elevation (m)	**Directly related** to the degree of vulnerability. The higher the elevation, the higher the degree of vulnerability. - fuzzy LARGE	> 500 250 – 500 0 – 250 ≤ 0	10 6 3 -100 *(masking)*
Rainfall Departure (%)	**Inversely related** to the degree of vulnerability. The smaller the rainfall departure index, the higher the degree of vulnerability. - fuzzy LINEAR › fuzzy SMALL	> -10 (near normal + surplus) -10 to -15 (dry spell) -15 to -25 (mild drought) -25 to -35 (moderate drought) -35 to -50 (severe drought) < -50 (extreme drought)	0 5 10 15 20 25

7.3.4 Bayesian joint conditional probability

Normative argument is often used for assigning equal weights to the indicating variables. In the normative argument, the indicating variables are aggregated such that each dimension is given equal importance in characterising the state of development. However, vulnerability assessment is not a simple, straightforward exercise because multiple stakeholders value the dimensions differently (Hinkel 2011). In the spatial dimension context, the development of risk maps from the indicating variables varies spatially. To address the multi-dimensionality issue in the normative argument of equal weights, the Bayesian probability is used in this study. The Bayesian joint conditional probable weights are calculated as:

$$P(DR_i \mid V_i) = \frac{P_{\max}(DR_i \cap V_i)}{\sum nP_{\max}(DR_i \cap V_i)} \text{ and } P(DR_i \mid E_i) = \frac{P_{\max}(DR_i \cap E_i)}{\sum nP_{\max}(DR_i \cap E_i)} \quad (7.9)$$

where:

DR is the drought-risk represented by drought hazard as a priori event

V and E are vulnerability and exposure indicating variables, respectively

i is the level of perceived drought-risk (vulnerability/exposure sub-classes)

P_{max} is the maximum probability of an indicating variable

n is the number of indicating variables

The weight values are used in aggregating the vulnerability and exposure indicating variables. Table 7.3 lists the probable importance of each factor to the rainfall departure hazard index. It is important to note that no matter what month, season or year is considered for the analysis, these probability values do not change and it has been confirmed by the computational analysis of all the seasons and years considered in this investigation.

178

Table 7.3: Probable weights applied for the vulnerability and exposure factors conditional on rainfall departures based on the Bayes theorem.

Exposure Factors	P_{max}	Bayes Conditional Probability
Land Use	0.3590	**0.3941**
Population	0.5519	**0.6059**
Total P_{max}	*0.9109*	*1.0000*
Vulnerability Factors		
DEM	0.3124	**0.1634**
PAWC	0.2525	**0.1321**
Sand	0.5158	**0.2698**
Slope	0.3392	**0.1775**
Soil Depth	0.4916	**0.2572**
Total P_{max}	*1.9115*	*1.0000*

Subsequently, the fuzzy-standardised vulnerability and exposure factors (fw_j) are first multiplied by 100 to obtain integer values, then weighted overlay operation is performed where weights are the percent conditional probability values (P_j). The output is then divided by a factor of 100 to obtain the vulnerability and exposure index maps (V_i or E_i) on 0 to 1 scale, as per the Eq. (7.10).

$$V_i \ or \ E_i = \left(\sum_{j=1}^{n} P_j \times \left(100 \times fw_j \right) \right) / 100 \qquad (7.10)$$

7.3.5 Framework for derivation of drought-risk map

A diagram of the input-process-output model that presents the flowchart of the study is shown in Figure 7.4. Under the input component, drought hazard (rainfall departure), vulnerability (soil type, soil depth, elevation, PAWC, and slope), and exposure (population and land use) are assessed with corresponding details and assumptions, enumerated in Table 7.2. All inputs are continuous data except for land use that needed to be reclassified and assigned weights based on their significance and influence on droughts. Under process component, the inputs are standardised from original values into 0 to 1 scale, analysed and processed using applicable GIS operations with emphasis on fuzzy logic operations in ArcGIS 10.5. The standardised vulnerability and exposure factors are then evaluated using Eq. 10. The procedure, in turn, produced

initial outputs representing drought-risk component indices maps (*i.e.,* hazard, vulnerability and exposure indices). The analytical and processing operations using fuzzy GAMMA overlay led to the generation of the drought-risk map as the ultimate output. Figure 7.3 shows the original values of the vulnerability and exposure factors in the left column while the right column shows the corresponding standardised factors based on respective fuzzy operations.

Digital Elevation Model (m)
High : 1360.24
Low : -14.7411

Digital Elevation Model
High : 0.949738
Low : 0.000319898

Plant Available Water Capacity (mm)
High : 199
Low : 8

Plant Available Water Capacity
High : 0.999997
Low : 0.0366619

Sand (%)
High : 104.658
Low : 31.8941

Sand
High : 0.894325
Low : 0.0217595

180
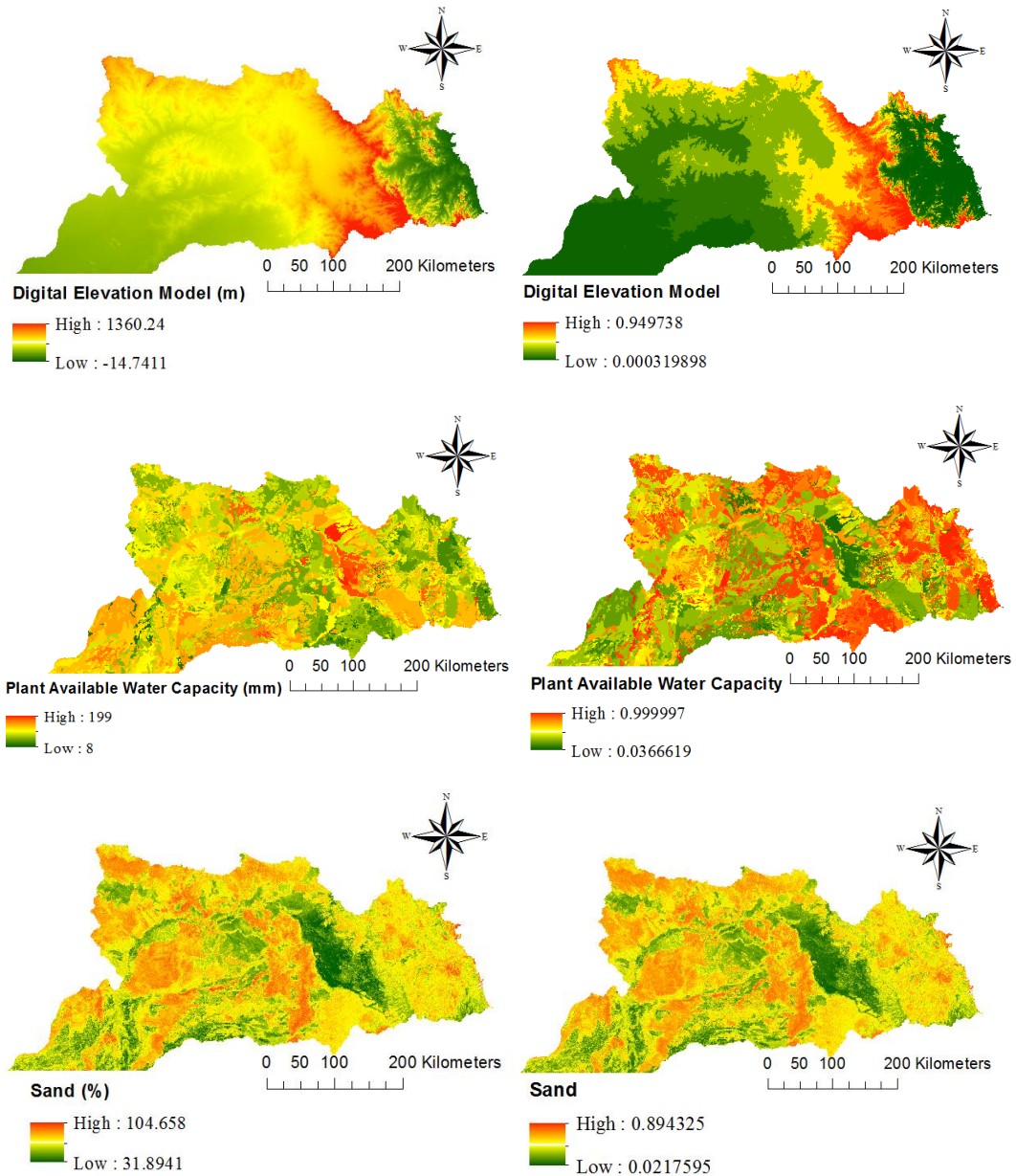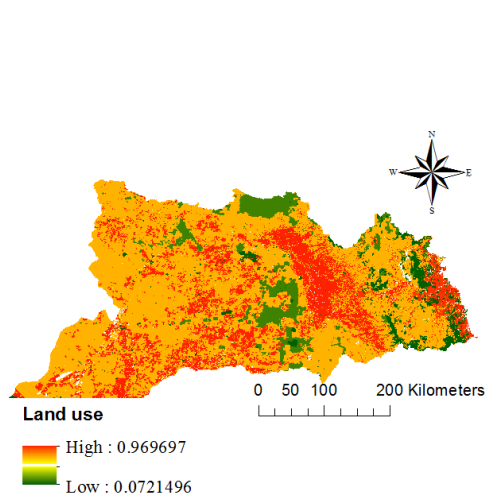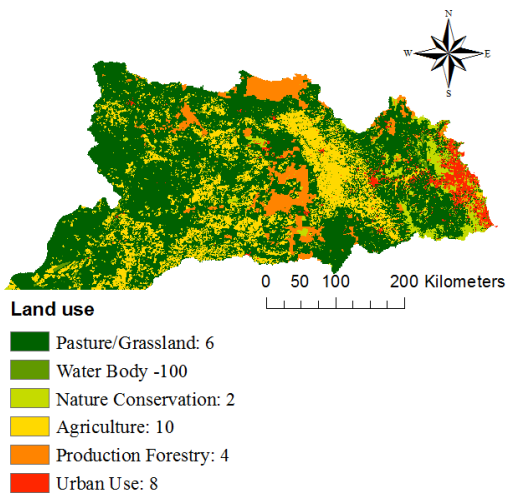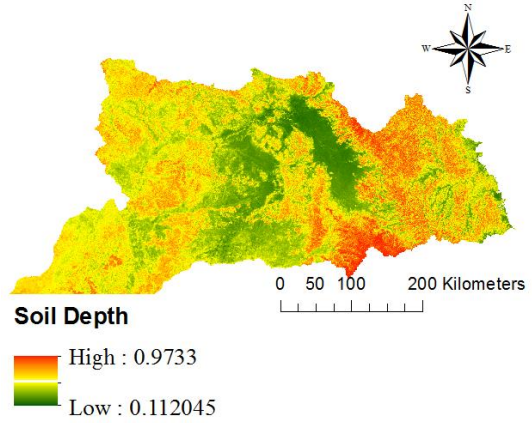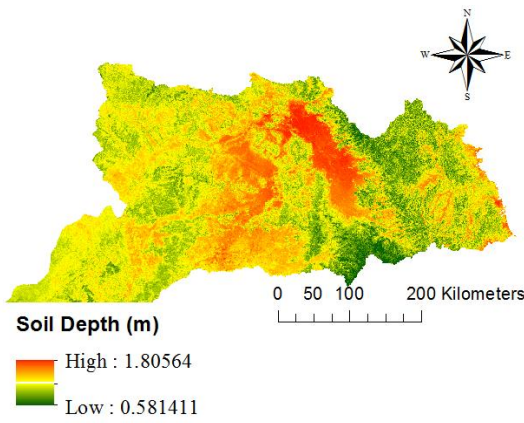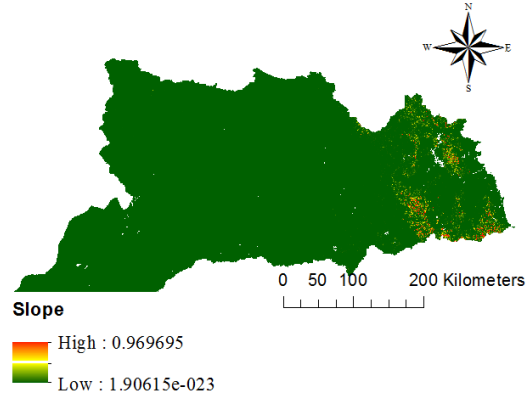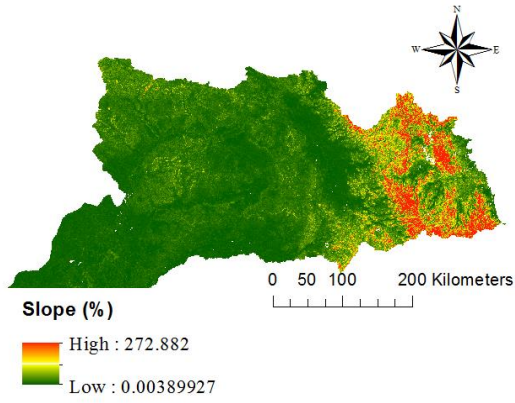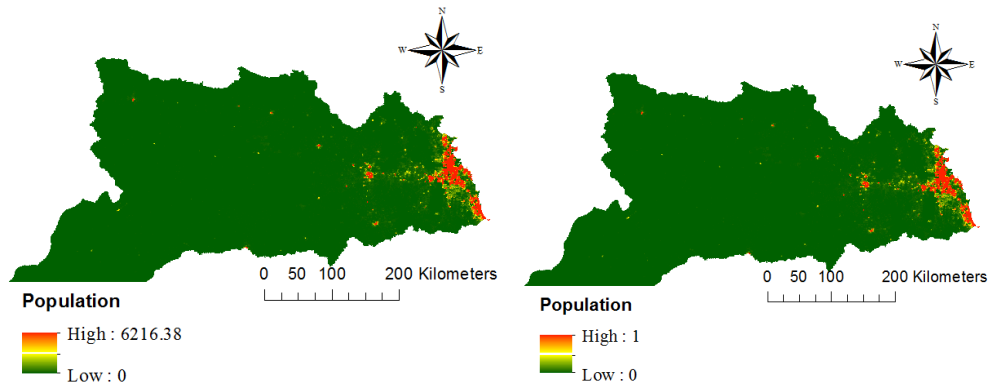
Figure 7.3: Original drought vulnerability factors in absolute units (left) and corresponding standardised factors (right) using the fuzzy membership functions bounded by [0, 1].
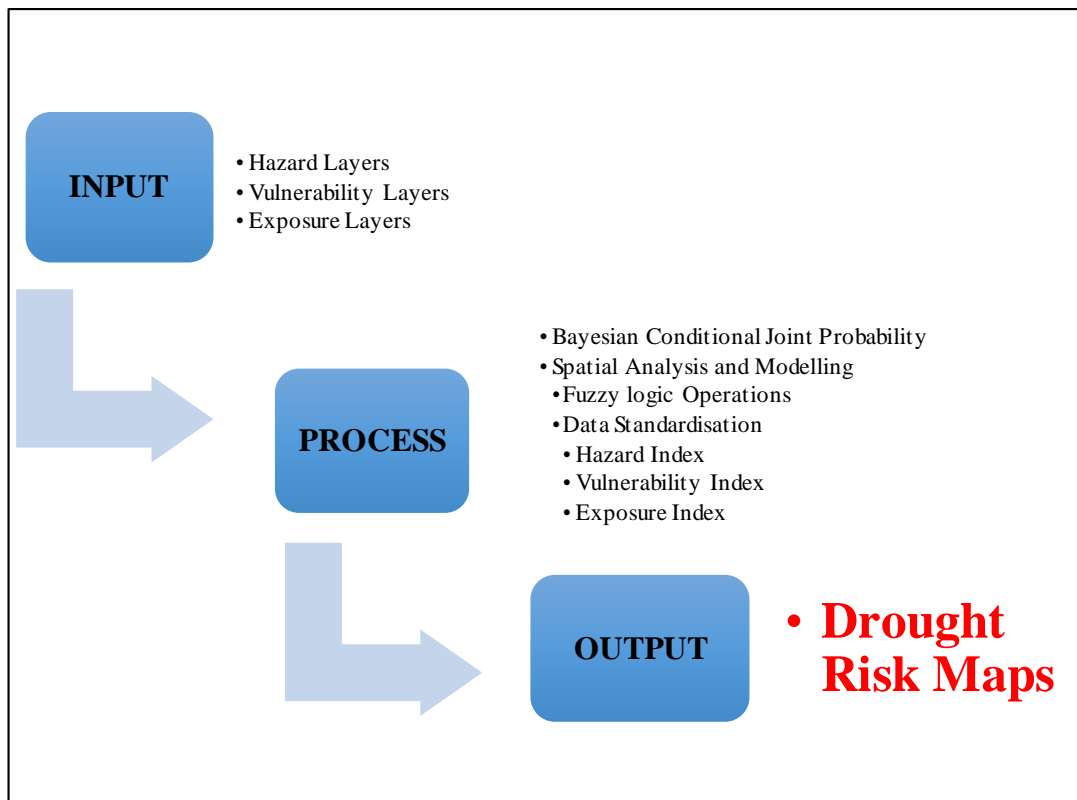
Figure 7.4: Conceptual flowchart of a 3-layer Input-Process-Output schematic model for drought risk mapping adopted in the present study.

The *hazard index* consisted of the rainfall departure (%). Relative to the base period (1971 - 2000), the seasonal and annual rainfall departure are used as the sole hazard indices. To obtain the hazard index, the fuzzy LINEAR followed by fuzzy SMALL membership function is applied to the rainfall departure. The fuzzy SMALL transformation function is used when the smaller input values are more likely to be a

member of the set, as in this study the negative rainfall departure percentages corresponded to the drought condition, hence the hazard in consideration. The midpoint of the rainfall departure identified the crossover point (assigned a membership of 0.5) with values greater than the midpoint having a lower possibility of being a member of the fuzzy set and vice versa. Accordingly, the values closer to 1 in the standardised rainfall departure corresponded to the high drought-risk member. Seasonal and annual drought hazard indices are prepared and the results for seasonal (2007) and annual (2007, 2009 and 2013) are presented. These years are recent drought years in the SEQ region. The 2007 and 2009 are part of the catastrophic Millennium Drought while the 2013 drought occurred after the wet La Niña season (2010-2011). Figure 7.5 shows the hazard indices maps for drought years 2009 and 2011. The red colours correspond to high-risk areas, *i.e.,* rainfall departure below normal.
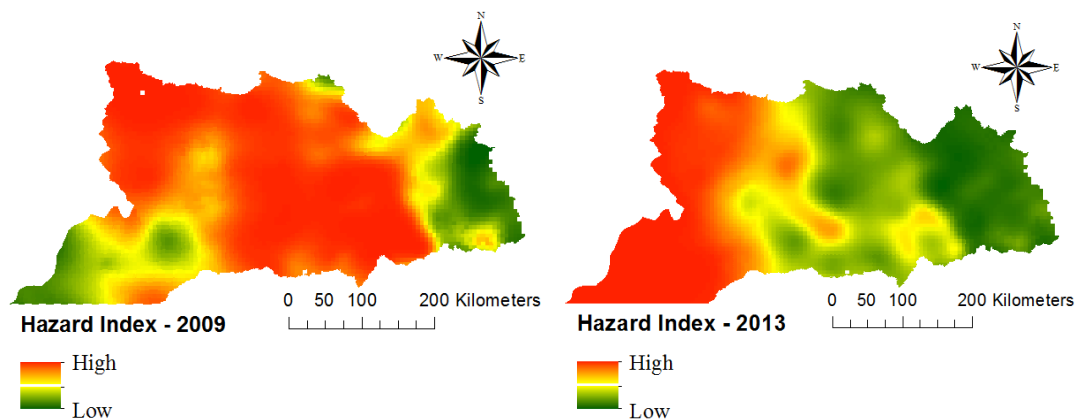
Figure 7.5: Drought hazard index for two selected study years (*i.e.,* 2009 & 2013) defined by the standardised rainfall departure.

The *vulnerability index* consisted of an integrated layer of soil depth, sand, PAWC, elevation, and slope. Guided by the assumptions in Table 7.2, the fuzzy LARGE or fuzzy SMALL membership functions are applied to the indicators. With fuzzy SMALL membership function, the smaller original pixel values are assigned with higher fuzzy membership values (closer to 1) in the function to indicate higher vulnerability. Conversely, the fuzzy LARGE membership function has been applied whereby the larger original pixel values are assigned with higher fuzzy membership values (closer to 1) in the function to indicate higher vulnerability. Equation (7.10) has been applied following the standardisation process. The resulting map is the vulnerability index, as shown in Figure 7.6.

183

The *exposure index* consisted of integrated layer of land use and population. The fuzzy LARGE and fuzzy LINEAR membership functions are applied to the land use and population, respectively. The fuzzy LINEAR membership function is more appropriate to standardise population density since the availability and demand for water resources vary with change in population density over time, hence there is a direct proportionality between water demand and population density. The resulting exposure index is shown in Figure 7.6.
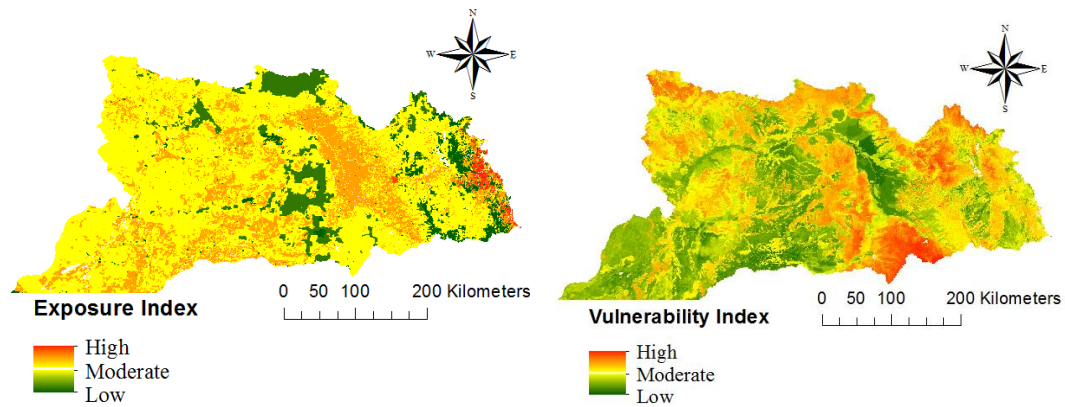
Figure 7.6: The drought exposure (a) and vulnerability (b) indices.

Usually, the analyst has the choice of whether to defuzzify the output of the fuzzy system to generate the crisp output or leave the output without modification, which is also appropriate. In this study, the final output has been defuzzified into five discrete intervals according to the perceived level of drought risk: none, low, moderate, high and very high. Defuzzification is a process in the fuzzy synthetic evaluation that calculates the crisp value (*i.e.,* grade interval) of a fuzzy set (Sadiq et al. 2004). The grade intervals for this study have been obtained through geometric interval classification of the raster data fuzzy set. As a compromise method between equal interval and quantile (ESRI 2017), geometric intervals have been used to delineate classes based on natural groupings of fuzzy membership values. This option tries to find a balance between highlighting the changes in the middle and the extreme values.

Drought-risk assessment methods are generally designed to characterise and understand the system's degree of risk to drought (*e.g.,* low, moderate, high and very high). In GIS, this is known as descriptive modelling that refers to the characterisation

of direct interactions of system components to gain insight and understand the system processes (Berry 1996).

This study attempts to contribute a new knowledge by developing spatial analytical technique in generating descriptive drought-risk maps. Hence, it is suggested that this type of approach can provide useful strategic information for decision makers involved in drought-risk monitoring.

7.3.6 Validation of the drought-risk index

In order to validate the drought-risk output maps, the ideal measure would be a field study that can literally verify the areas subjected to a certain level of risk. Since a field study was beyond the scope of this study, this study has undertaken the spatial correlation approach using the band collection (Erdey-Heydorn 2008; GERGELY et al. 2016), a spatial analyst tool, that provides statistics for the multivariate analysis of a set of raster bands. The correlation between two layers is a measure of dependency between the layers, in which the correlation matrix presents the cell values from one raster layer as they relate to the cell values of another layer. It is the ratio of the covariance between the two layers *(i, j)* divided by the product of their standard deviations, given as:

$$Corr_{i,j} = \frac{Cov_{i,j}}{\sigma_i \sigma_j} \qquad (7.11)$$

Seasonal and annual drought-risk maps are correlated with rainfall departures to estimate the dependency between them. Since rainfall departure is a core hazard variable in generating the drought-risk maps, and to avoid such bias, the upper (0 – 0.2m) and lower (0.2 – 1.5m) layers of soil moisture have been used alternatively. Validation of drought-risk maps with soil moisture is appropriate since moisture content is an important indicator of the agricultural droughts and its memory contributes to spatial and temporal variation of the regional drought (Mpelasoka et al. 2008). Subsequently, seasonal drought-risk maps have been correlated with the 3-month running mean of soil moisture leading up to the following season.

185

7.4 Results and Discussion

The resulting seasonal and annual maps of drought-risk are obtained by the application of fuzzy GAMMA overlay operation in ArcGIS. Figures 7.7 and 7.8 show the seasonal and annual drought-risk maps, respectively, while Table 7.4 enumerates the percentage area of the five risk classes: no risk, low risk, moderate risk, high risk and very high risk. The maps show that the majority of the study area is at moderate to the very high risk of drought. The very high-risk regions in the SON 2007 seasonal drought-risk maps carry much higher percentages compared to the annual drought-risk maps. This could be due to the JJA season rainfall offsetting the total accumulated rainfall in other seasons of the year 2007. In the JJA season, the rainfall departure index is in the positives (*i.e.,* minimum of 34.69% and a maximum of 1508.78% in the study region). This is why the 2007 annual drought-risk map (Fig. 7.7d) has a smaller percentage of high and very high-risk regions compared to individual DJF, MAM and SON seasons.

It is apparent that the regions' drought-risk levels coincide well with the corresponding hazard indices where regions with high hazard index are also critically vulnerable to drought. This is possibly due to hazard index values being assigned an entire probability value of 1 in the GAMMA overlay operation while the vulnerability and exposure factors have been multiplied by their probability values conditional on the hazard index. Overall, the results indicate that regions receiving much less rainfall relative to the base period consequently have greater drought-related negative impacts. Considering the temporally and spatially varying factors, the simple yet effective methodology developed in this study will help to identify regions vulnerable to droughts and can be greatly useful in better decision-making processes for drought mitigation and management. The descriptive vulnerability and drought-risk map are also intended for farmers who can make judicious decisions as to which crop to plant based on the given water availability.

(a)

Drought Risk Map - DJF 2007

- None
- Low
- Moderate
- High
- Very High

(b)

Drought Risk Map - MAM 2007

- None
- Low
- Moderate
- High
- Very High

(c)

Drought Risk Map - SON 2007

- None
- Low
- Moderate
- High
- Very High

(d)

Drought Risk Map - 2007

- None
- Low
- Moderate
- High
- Very High
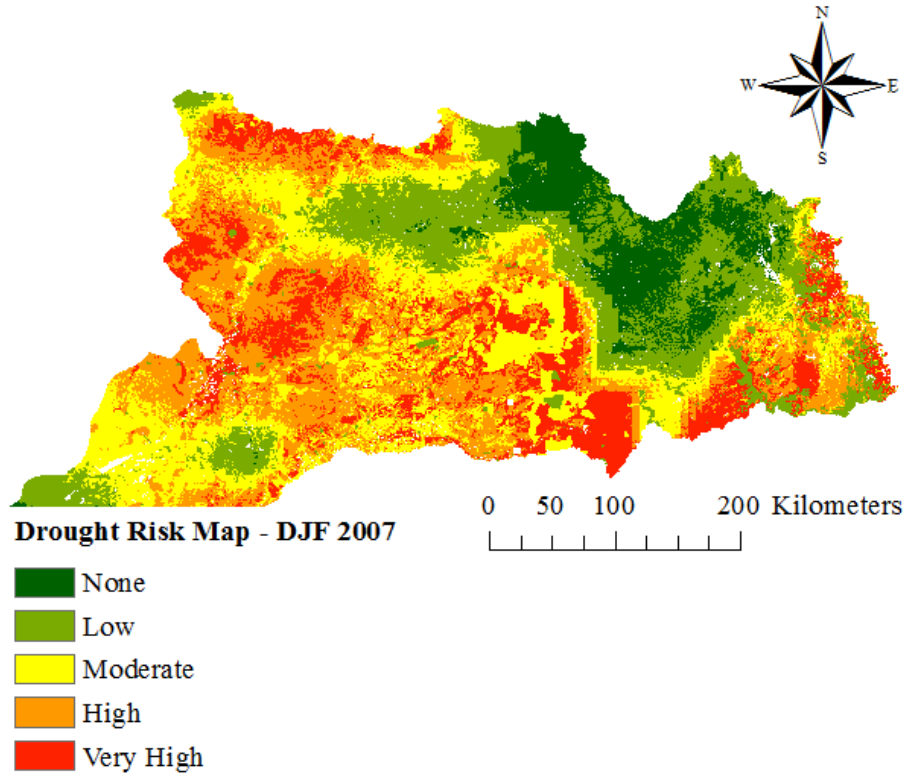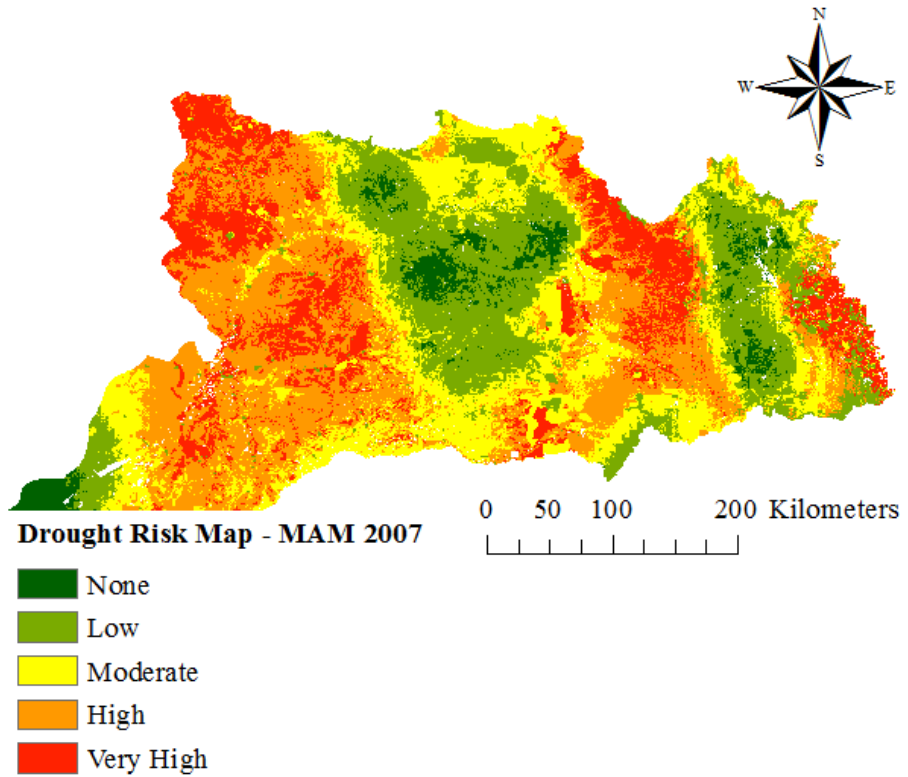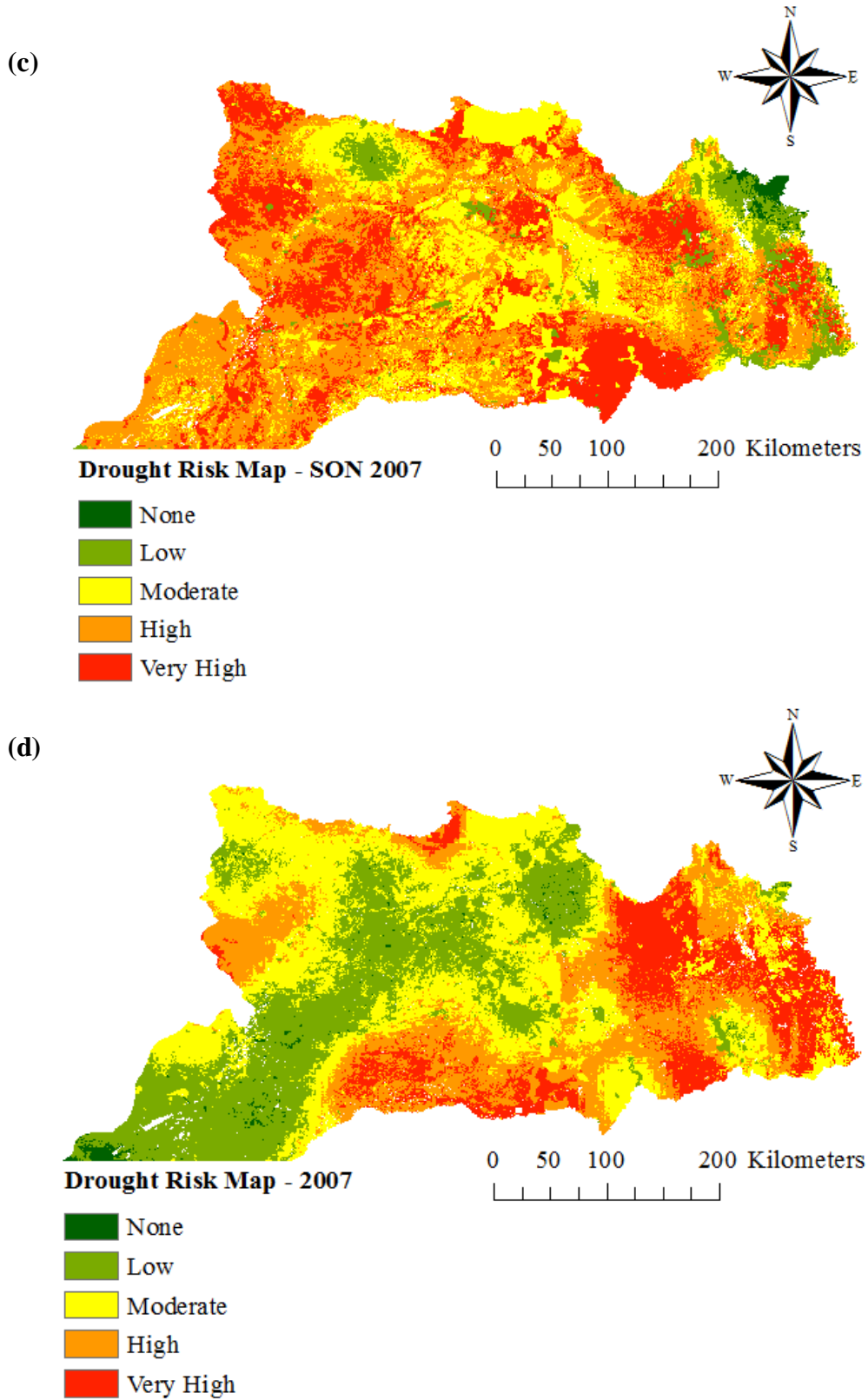
Figure 7.7: Spatial drought risk map and its classification thresholds for the serious drought year (2007) generated from the fuzzy Gamma overlay function.

(a) December-January-February (DJF) summer period

(b) March-April-May (MAM) autumn period

188

(c) September-October-November (SON) spring period

(d) Annual map. *Note: drought year was selected according to Figure 1.*

(a)

(b)
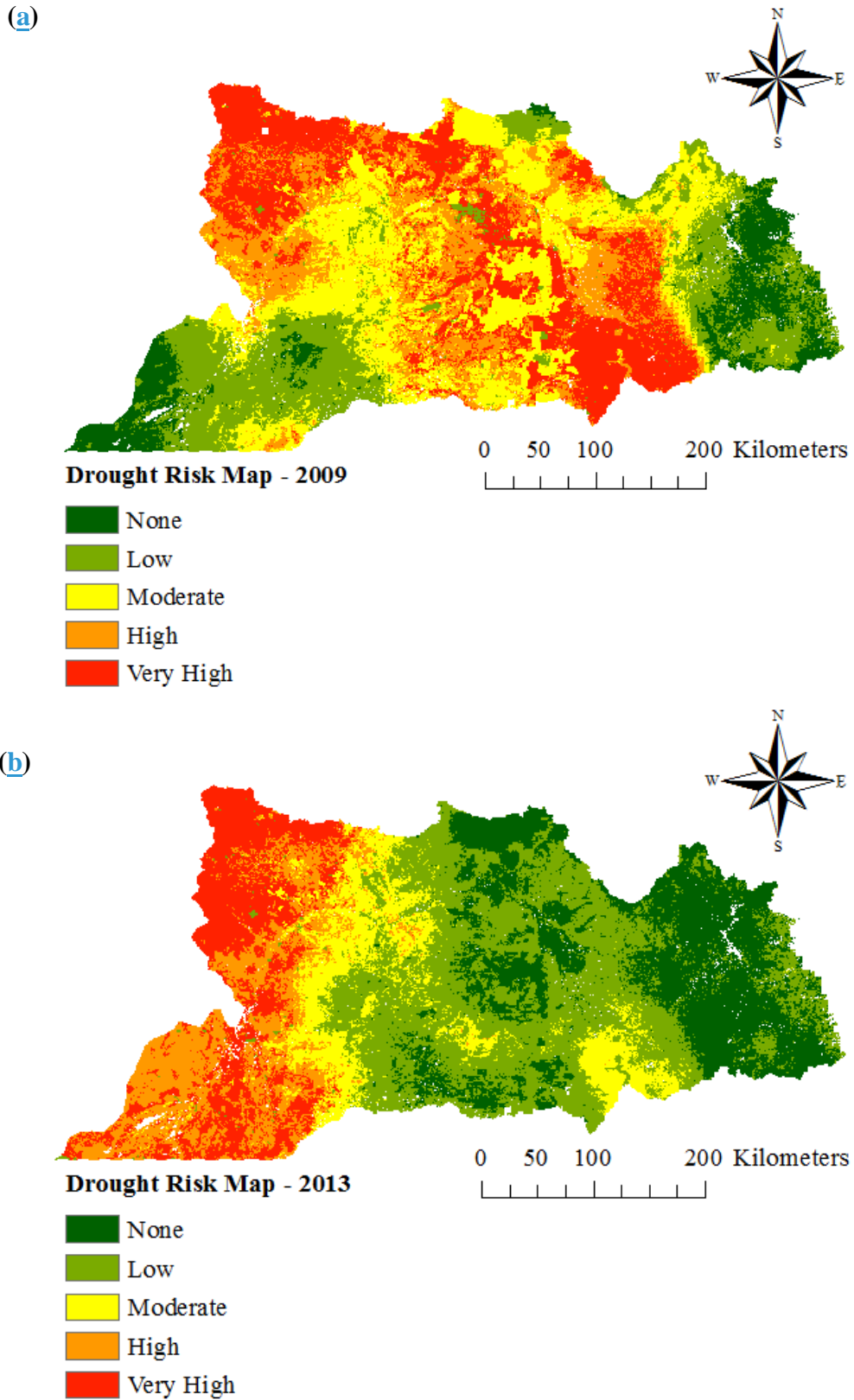
Figure 7.8: Spatial drought risk map and its classification thresholds for moderate drought year (2009) and non-drought year (2013) generated from the fuzzy Gamma overlay function.

Table 7.4: Percent area falling under various vulnerability classes.

Vulnerability Class	Discrete Interval	Area (%)	Discrete Interval	Area (%)	Discrete Interval	Area (%)
Seasonal	**DJF 2007**		**MAM 2007**		**SON 2007**	
None	0.14 - 0.51	0.10	0.14 - 0.49	0.04	0.12 - 0.50	0.01
Low	0.51 - 0.69	0.22	0.49 - 0.68	0.23	0.50 - 0.69	0.07
Moderate	0.69 - 0.78	0.26	0.68 - 0.77	0.24	0.69 - 0.78	0.26
High	0.78 - 0.82	0.27	0.77 - 0.83	0.32	0.78 - 0.83	0.41
Very High	0.82 - 0.91	0.15	0.83 - 0.93	0.17	0.83 - 0.92	0.25
Annual	**2007**		**2009**		**2013**	
None	0.11 - 0.35	0.01	0.13 - 0.50	0.10	0.11 - 0.50	0.24
Low	0.35 - 0.54	0.28	0.50 - 0.68	0.21	0.50 - 0.68	0.34
Moderate	0.54 - 0.68	0.34	0.68 - 0.77	0.26	0.68 - 0.76	0.13
High	0.68 - 0.79	0.23	0.77 - 0.81	0.20	0.76 - 0.80	0.14
Very High	0.79 - 0.93	0.14	0.81 - 0.90	0.24	0.80 - 0.89	0.15

For verification of the drought-risk maps, Table 7.5 shows the correlation matrix of drought-risk with rainfall departure and soil moisture. There is a high correlation of drought-risk with rainfall departure due to the latter being used as a hazard index in producing the former. To avoid the bias, the upper (0 – 0.2m depth) and lower (0.2 – 1.5m depth) layer soil moisture are also correlated with drought-risk index. The upper layer soil moisture is well correlated with both seasonal and annual droughts while the lower layer soil moisture tends to show a higher correlation in JJA and SON seasons of 2007, as well as for 2009 and 2013 annual drought periods. For the case of seasonal droughts (Table 7.5a), the correlation remains high for 3-month running mean soil moisture values leading up to the next season. Therefore, despite the field study verification of the drought-risk maps not feasible in this study, the correlations with soil moisture reveal the effectiveness of the drought-risk output maps, which therefore validates the drought-risk index to be adopted for drought management purposes.

Table 7.5: Validation of drought-risk index in terms of the correlation matrix of seasonal (a) and annual (b) drought-risk index with rainfall departure (RD) and the upper and lower layer soil moisture (SM).

(a)

Soil Moisture	DJF 2007		MAM 2007		JJA 2007		SON 2007	
	Correlation Matrix		*Correlation Matrix*		*Correlation Matrix*		*Correlation Matrix*	
		Drought Risk		**Drought Risk**		**Drought Risk**		**Drought Risk**
	Drought Risk	**1.0000**	**Drought Risk**	**1.0000**	**Drought Risk**	**1.0000**	**Drought Risk**	**1.0000**
	RD (%)	-0.8555	RD (%)	-0.8623	RD (%)	-0.8665	RD (%)	-0.5543
Upper SM	DJF	-0.3808	MAM	-0.4486	JJA	-0.6800	SON	-0.2748
Lower SM	DJF	0.0450	MAM	0.1348	JJA	-0.2266	SON	-0.2987
Upper SM	JFM	-0.1064	AMJ	-0.3312	JAS	-0.5499	OND	-0.0092
Lower SM	JFM	0.0402	AMJ	0.0901	JAS	-0.2880	OND	-0.2211
Upper SM	FMA	-0.0937	MJJ	-0.3546	ASO	-0.4437	NDJ	-0.1957
Lower SM	FMA	0.0486	MJJ	0.0071	ASO	-0.2910	NDJ	-0.1903
Upper SM	MAM	-0.0538	JJA	-0.3515	SON	-0.2394	DJF	-0.3530
Lower SM	MAM	0.0576	JJA	-0.0627	SON	-0.2559	DJF	-0.1915

(b)

2007	Layer Statistics				Correlation Matrix
Layer	MIN	MAX	MEAN	STD	Drought Risk
Drought Risk	0.1108	0.9273	0.6265	0.1328	**1.0000**
RD (%)	-41.71	19.5005	-11.9427	10.9399	**-0.8738**
Upper layer SM	0.1346	0.4339	0.2177	0.0338	**0.1039**
Lower layer SM	0.0250	0.6432	0.1762	0.0847	**0.0991**

2009	Layer Statistics				Correlation Matrix
Layer	MIN	MAX	MEAN	STD	Drought Risk
Drought Risk	0.1254	0.9031	0.7121	0.1310	**1.0000**
RD (%)	-49.47	27.7423	-21.3567	13.6609	**-0.8865**
Upper layer SM	0.1059	0.5883	0.1976	0.0565	**-0.5520**
Lower layer SM	0.0341	0.9024	0.3090	0.1534	**-0.4452**

2013	Layer Statistics				Correlation Matrix
Layer	MIN	MAX	MEAN	STD	Drought Risk
Drought Risk	0.1146	0.8870	0.6282	0.1511	**1.0000**
RD (%)	-62.51	41.0766	-12.4865	23.3613	**-0.8949**
Upper layer SM	0.0864	0.5684	0.2092	0.0675	**-0.7302**
Lower layer SM	0.1137	0.8815	0.3773	0.1429	**-0.5785**

Assessment of drought-risk and vulnerability in this study has largely reinforced the initial concept of Wilhite (2000), and several other studies on vulnerability assessment elsewhere (*e.g.,* (Jain et al. 2015; Pandey et al. 2010; Thomas et al. 2016; Wilhelmi and Wilhite 2002)). It, however, does extend the only study performed in Australia (Stone and Potgieter 2008). This study has shown that drought-risk must be viewed as a product (and sum) of exposure to the climatic hazard and the underlying vulnerability of economic, demographic and agricultural practices including physiographic features. Droughts occur in virtually all climatic regimes, *i.e.,* in both high and low-precipitation areas where aridity is considered a normal feature (Wilhite 2009). This makes droughts to be considered as a relative phenomenon and therefore, the risk of drought must be addressed as a relative measure (Downing and Bakker 2000). In consequence, it is difficult to reach standard criteria for drought-risk assessment. The overlay of several factors based on regional conditions, therefore, has established a relative criterion that makes the drought-risk assessment feasible. A further refinement on the sub-classification of factors may also be required given the nature of the regional climate. This study has attempted to present a methodology that can be used to assess drought vulnerability and risk in any given area.

The selection of vulnerability, exposure and hazard factors can be arbitrarily executed (Araya-Muñoz et al. 2017; Hinkel 2011; Luers et al. 2003). In this study, the drought associated physiographic and climatic factors had been selected based on the current knowledge of the drought hazard as well as on the availability of reliable and most recent data. It had been assumed that this would explain the regions with high risk of drought, however, the results could change as knowledge on the subject expands and more data become available. There are, however, several other factors that could be considered in the drought-risk analysis. For instance, Thomas et al. (2016) used soil moisture availability, Ekrami et al. (2016) used evaporation, and Jain et al. (2015) used soil moisture deficit index for their study regions. These factors had been a limitation to the entire study region and their inclusion could be possible if the analysis had been carried out for the basins where these datasets are readily available. Future analyses could also incorporate social factors such as diversity of local economies, people's sources of income, percent of farms acquiring insurance, and so on. Data acquisition of the biophysical and socio-economic factors has been beyond the scope of this study and this limitation has been acknowledged in Section 3.4. The

spatial resolution of the indicators is also very important for mapping high-resolution details. The hazard indicator, *i.e.,* rainfall departure, initially had been at a coarser 5km $\times$ 5km spatial resolution compared to other factors used in the analysis. The resolution of the hazard index used in this study is considered as a limitation because after reducing the cell size to 100m $\times$ 100m, the several neighbouring pixels consequently had similar rainfall value.

Application of fuzzy logic tool to develop the drought-risk index is a novel contribution to this study. Although the fuzzy logic theory has been in existence for a long time, its application on geospatial analysis has just made a breakthrough in the recent years. Fuzzy logic is an alternative logical foundation coming from artificial intelligence technology with several useful implications for spatial data handling, where it accommodates the imprecision in information, human cognition, perception and thought (Karabegovic et al. 2006). Accordingly, fuzzy logic is more suitable for dealing with real-world problems, because most human reasoning is imprecise. The major advantage of this fuzzy logic theory is that it avoids the bias through subjective judgements and allows the natural description, in linguistic terms, of problems that should be solved rather than in terms of relationships between precise numerical values. With this advantage, the fuzzy logic theory is a widely applied technique to deal with the complex systems in a simple way. Therefore, fuzzy logic appears to be instrumental in the design of efficient tools for spatial decision making and its application for drought-risk assessment in this study has shown it to be excellent for designing efficient tools to support the spatial decision-making processes.

In spite of the significant merits and foresight provided by the spatio-temporal drought-risk mapping approach, the scope of this study has been limited to the computational analysis only. To further validate the drought-risk output maps, the actual field study is thus required that creates an opportunity for future and more extensive independent work. It is hoped that this study will seed better insights into the assessment of relative vulnerability and exposure to droughts in the SEQ region and is likely to assist decision-makers in better planning, management and mitigation strategies. The fuzzy logic method has provided a good estimate of the agricultural drought-risk due to its high correspondence with soil moisture on the spatial and temporal domain, and therefore could be useful for the demarcation of areas vulnerable to drought to facilitate the proactive planning for coping with future drought events.

7.5 Conclusions

A descriptive drought-risk assessment index has been accomplished by a new methodology that incorporates vulnerability, exposure and hazard factors via integration with the fuzzy logic analytical tool in ArcGIS. The fuzzy logic approach has been advantageous as it aimed to minimise the subjectivity in the drought-risk assessment. By choosing fuzzy GAMMA overlay, the different fuzzy overlay operations available in the ArcGIS has allowed great flexibility in quantifying drought-risk expressed in truth values that range in degrees between 0 and 1. Given the significance of the approach and its ability for spatio-temporal risk assessment, the results are likely to advance the application of ArcGIS for disaster-risk reduction and in solving complex drought issues through adaptation strategies.

In terms of the application, this study has found the hazard index to be the determining factor of the level of risk associated with droughts. Where there has been a deficiency in rainfall, the drought-risk in that area has been high as well.

The methodology developed in this study can be applied to support the existing drought (or any disaster) risk reduction plans and policies prepared by any authorities, organisations, enterprises, or sectors involved in coordinating their development plans, resource allocation, and the implementation of their respective program of activities. Given that this study has presented an advanced methodology for drought-risk assessment, the coverage for the entire nature and extent for drought-risk has been limited as there could be many more hydro-meteorological, physiographic, environmental and social factors incorporated in the analysis, provided the availability and reliability of the data. Therefore, some recommended future work may include the following: inclusion of other factors in analysing drought hazard (*e.g.,* meteorological, hydrological and agricultural drought indices); review of the technical characteristics of climate change and how it could affect drought-risk assessment process; and identification and field validation of the vulnerability, exposure, hazard and drought-risk indices, including the quantity and quality of the data to be used as inputs in the model. Such studies can employ the current approach to yield useful pathways for water resource management in a drought-prone region.

Chapter 8

CONCLUSION

8.1 Introduction

This study aimed to develop and evaluate the drought-risk framework using statistical and geospatial modelling and analysis tools. To achieve this goal, three specific objectives, as detailed in Section 1.3, were addressed in Chapters 4 through 7. The current chapter presents the summary of the findings and offers recommendations for future research work.

8.2 Summary of Findings

The study has provided novel knowledge, innovative framework and fresh insights on drought-related disaster-risk in urban and agricultural sectors. This has yielded new information in relation to the assessment of drought through the integration of statistical (copula models) and spatial analytical (fuzzy logic in ArcGIS) tools.

The study from *Chapter 3* served as the "gateway" for modelling of drought-risk. It scoped the statistical and spatial analytical tools that allowed the derivation of drought properties (severity, intensity and duration) for every drought event recorded since 1915 to 2016, formulation of joint distribution functions, and transformation and standardisation of drought-risk indicating variables. The primary outputs were the characterisation of drought events using SPEI, development of the conditional probabilistic model, and generation of 100m×100m gridded drought-risk maps using indicating variables representing a hazard, vulnerability, and exposure to droughts.

Using the analyses in *Chapters 4 & 5*, the suitability of SPEI for characterising Australian drought events for four point-based locations (namely R1, R2, R3 and R4) in the SEQ region was detailed. The following were the major findings:

- The SPEI precisely identified the major and minor, well-documented droughts compared to SPI, RDDI and RAI, and was well in phase with the upper layer soil moisture (*WRel1*);

- Comparison of SPEI with upper layer soil moisture validated the ability of SPEI to capture the agricultural consequences of persisting droughts. Here, very low values of SPEI corresponded with very low values of soil moisture, demonstrating the agricultural effect of underlying dryness;

- Drought *D-S-I* properties exhibited a strong association between each other, where the majority of events with longer duration also attained a higher severity and intensity. However, droughts with high intensity did not necessarily have high severity or long duration as such events can be short-lived but very acute in terms of paucity of water resources;

- SPEI on longer timescales consistently detected and ranked the severity of various drought events that lasted for generally long periods, such as the Millennium and WWII Droughts.

In *Chapter 6*, the copula-statistical models were applied to assess drought-risk in terms of conditional return periods based on the multivariate joint distributions. Three sets of analysis were carried out: (i) SPEI vs. climate mode indices; (ii) drought *D-S-I* properties vs. climate mode indices; and (iii) *D* vs. *S*, *D* vs. *I* and *S* vs. *I*. The probabilistic prediction models were developed to predict SPEI and *D-S-I* using the information from climate mode indices (Niño 4 SST, SOI and EMI) given the appropriate copulae. The following were major findings:

- For bivariate joint distributions, a mix of Gumbel, Clayton and Frank copula were found to be most appropriate to the paired datasets. For trivariate, only the Frank copula was found to reveal greater dependence between three variables in consideration, *i.e.,* [Niño 4 SST, SOI | SPEI] and [*S*, *D* | *I*];

- Predicted values of SPEI conditional on separate Niño 4 SST and SOI and coupled [Niño 4 SST, SOI] combination generated marginal errors

when compared with observed values, suggesting copula-based joint distributions to be potentially suitable for drought predictions;

- The probability of the certain value of SPEI to occur, conditional on certain thresholds of Niño 4 SST and SOI, was well achieved by the bivariate and trivariate-based copula models. Thus, the probability of obtaining a negative value of SPEI (corresponding to droughts) was high with substantial (*negative*) value of Niño 4 SST (*SOI*);

- Prediction models generated very small errors in visualising D, S and I properties using the information from Niño 4 SST and EMI;

- Analyses also found that as the magnitude of ENSO indicators shift towards their extreme values, in the direction of enhancing drought conditions, the return period of drought properties increase as well, suggesting the rarity of such extreme events;

- The study also ascertained the trivariate return period, 'T_{OR}', to be less than both univariate and bivariate ones. This was attributable to the additional variables in the drought prediction model making the trivariate exceedance probabilities smaller than two bivariate or a univariate case.

In *Chapter 7*, drought-risk on seasonal (DJF, MAM and SON for the year 2007) and annual (2007, 2009 and 2013) timescales using various vulnerability and exposure factors was assessed on spatial maps. The percent rainfall departure was considered as the drought hazard index, land use and population factors produced the exposure index, while soil depth, sand soil type, plant available water capacity, elevation and slope factors generated the vulnerability index. The individual factors were initially categorised into subclasses in order to obtain the probable influence of each factor to the drought-risk. The following were major findings:

- Based on Bayes theorem, among exposure factors, the population was found to have higher probability conditional on drought-risk with 0.61, while land use had 0.39. Among vulnerability factors, the sand type had the highest probability (0.27) while plant available water capacity had the lowest (0.13).

200

The values suggested that population density and type of soil (*i.e.*, sand) would pose greater risk to drought impacts;

- Level of drought-risk was heavily reliant on the drought hazard index, *i.e.*, the percent rainfall departure. In other words, regions with highly deficient rainfall had the highest level of risk to droughts;

- The validation against soil moisture, which was an independent variable in the study, showed high correlation accompanying the risk magnitudes. Hence, the significant findings revealed this methodology to be potentially suitable for drought-risk assessments.

This research thus proved the hypothesis that "*statistically and spatially explicit drought-risk models can provide sets of information that are useful in planning and developing strategies from the potential effects of extreme drought events to agriculture and availability of water resources*".

In the aspect of technical and analytical contribution, usefulness, and innovation, the findings from this study were equal to or exceeded all other studies reported in the literature due to the following reasons:

- The reference evapotranspiration component in the revised statistical-based drought index, *i.e.*, SPEI, well represented the Australian droughts in the analyses for identification of onset/termination points, and derivation of drought severity, intensity and duration based on the run-sum approach;

- The evaluation of SPEI against one of the most important identifiers of agricultural droughts, *i.e.*, the soil moisture content verified the linkage between the two and rendered the importance of SPEI for drought monitoring and quantifying purposes;

- The application of vine copula method for multivariate joint distribution, (particularly the Clayton, Gumbel and Frank for bivariate and Frank copula for trivariate-based probabilistic drought prediction model that has never been applied for drought-risk modelling in the drought-prone SEQ region), rendered an important advancement in terms of potential applications for agriculture,

water management and related socio-economic sectors where droughts constitute significant risk;

- Through the novel, easy-to-implement, statistical and geospatial-based framework, this study revolutionised the old compartmentalised methods of assessing drought-risk;

- Finally, the evaluation of series of climate mode indices to produce conditional probabilistic prediction of drought index (SPEI) and properties (*D-S-I*) in Australia was the first major contribution of this study;

- The nexus between the hazard, vulnerability and exposure factors for descriptive modelling technique with Bayesian-based conditional probability and GIS-enabled fuzzy logic application to drought-risk assessment was the second major contribution to the body of knowledge.

A number of advantages can be generated from the above studies. First, the feasibility of integrating copula and GIS-based fuzzy logic analyses in setting up a comprehensive drought-risk management system. This is expected to significantly help in reducing the amount of damage caused by future droughts. Furthermore, for a highly competitive environment, especially financial resource and support for farmers, the analyses of drought-risk denote great promise for finding the optimum strategies. Second, the framework developed in this study can be applied to any study locations. The methodology developed is not limited to the current study region because it is primarily data-dependent; hence, the methodology can be used anywhere where data is available.

8.3 Recommendations for Future Works

The following analyses were found limited in this study, hence recommended for future works:

- The unavailability of gridded reference evapotranspiration (ET_o) data for computation of Supply-Demand Balance in generating SPEI. For Chapters 4-6, a clustering technique could have been possible if gridded ET_o data were

202

available to assess drought-risk in a broader study region. To circumvent this issue, potential evapotranspiration can be estimated from FAO Penman-Monteith method using climatological records of wind speed, humidity, sunshine and temperature if such data are available;

- Generation of copula-based multivariate joint distribution using a profusion other climate mode indices that tend to influence Australian rainfall. This study exclusively used ENSO indicators, however, there are several other large-scale drivers that influence Australian rainfall;

- Use of even higher resolution gridded rainfall data. In this study a 5km× 5km rainfall data from AWAP was utilised, however, an increase in data resolution may help in obtaining much more detailed information on drought-risk levels, especially on the spatially-explicit maps;

- Integration of socio-economic and climate change factors in the spatial representation of drought-risk on a catchment scale;

- Analysis of climate adaptation capacity in addition to the risk and vulnerability assessment of droughts;

- The most appropriate way to validate spatial drought-risk maps requires field study, which was beyond the scope of this investigation. Hence, there is an opportunity to conduct an investigation as such in the future.

REFERENCES

Aas, K., Czado, C., Frigessi, A., and Bakken, H. (2009). "Pair-copula constructions of multiple dependence." *Insurance: Mathematics and economics*, 44(2), 182-198.

ABS (2004). "Yearbook Australia 2004 - mpact of the drought on Australian production in 2002-03."Canberra, Australia: Australian Bureau of Statistics.

ABS (2012). "Year Book Australia, 2012." Australian Bureau of Statistics Canberra.

Acosta-Michlik, L., Eierdanz, F., Alcamo, J., Kromker, D., Galli, F., Klein, R. J., Kumar, K. K., Campe, S., Carius, A., and Tanzler, D. (2006). "An empirical application of the security diagram to assess the vulnerability of india to climatic stress." *Die Erde*, 137(3), 199.

Adger, W. N. (2006). "Vulnerability." *Global environmental change*, 16(3), 268-281.

Adger, W. N., Huq, S., Brown, K., Conway, D., Hulme, M., and Adger, N. (2002). "Adaptation to climate change: Setting the Agenda for Development Policy and Research." *Progress in Development Studies*, 3(3), 179-195.

Aksoy, B., and Ercanoglu, M. (2012). "Landslide identification and classification by object-based image analysis and fuzzy logic: An example from the Azdavay region (Kastamonu, Turkey)." *Computers & Geosciences*, 38(1), 87-98.

Al-Abadi, A. M., Shahid, S., Ghalib, H. B., and Handhal, A. M. (2017). "A GIS-Based Integrated Fuzzy Logic and Analytic Hierarchy Process Model for Assessing Water-Harvesting Zones in Northeastern Maysan Governorate, Iraq." *Arabian Journal for Science and Engineering*, 42(6), 2487-2499.

Allen, R. G., Pereira, L. S., Raes, D., and Smith, M. (1998). "Crop evapotranspiration-Guidelines for computing crop water requirements-FAO Irrigation and drainage paper 56." *FAO, Rome*, 300(9), D05109.

Alley, W. M. (1984). "The Palmer drought severity index: limitations and assumptions."*Journal of climate and applied meteorology*, 23(7), 1100-1109.

Alston, M. (2012). "Rural male suicide in Australia." *Social Science & Medicine*, 74(4), 515-522.

Araya-Muñoz, D., Metzger, M. J., Stuart, N., Wilson, A. M. W., and Carvajal, D. (2017). "A spatial fuzzy logic approach to urban multi-hazard impact assessment in Concepción, Chile." *Science of The Total Environment*, 576, 508-519.

Australia, G. (2010a). "Risk Impact Analysis." <http://www.ga.gov.au/scientific-topics/hazards >. (08 August, 2017).

Babaei, H., Araghinejad, S., and Hoorfar, A. (2013). "Developing a new method for spatial assessment of drought vulnerability (case study: Zayandeh-Rood river basin in Iran)." *Water and Environment Journal*, 27(1), 50-57.

Bacanli, U. G., Firat, M., and Dikbas, F. (2009). "Adaptive neuro-fuzzy inference system for drought forecasting." *Stochastic Environmental Research and Risk Assessment*, 23(8), 1143-1154.

Baethgen, W. E. (1997). "Vulnerability of the agricultural sector of Latin America to climate change." *Climate Research*, 1-7.

Banik, P., Mandal, A., and Rahman, M. S. (2002). "Markov chain analysis of weekly rainfall data in determining drought-proneness." *Discrete Dynamics in Nature and Society*, 7(4), 231-239.

Barbeta, A., Ogaya, R., and Peñuelas, J. (2013). "Dampening effects of long-term experimental drought on growth and mortality rates of a Holm oak forest." *Global change biology*, 19(10), 3133-3144.

Barua, S., Ng, A., and Perera, B. (2010). "Comparative evaluation of drought indexes: Case study on the Yarra River catchment in Australia." *Journal of Water Resources Planning and Management*, 137(2), 215-226.

Bedford, T., and Cooke, R. M. (2002). "Vines: A new graphical model for dependent random variables." *Annals of Statistics*, 1031-1068.

Berry, J. K. (1996). *Spatial reasoning for effective GIS*, John Wiley & Sons.

Birkmann, J. (2006). "Measuring vulnerability to promote disaster-resilient societies: Conceptual frameworks and definitions." *Measuring vulnerability to natural hazards: Towards disaster resilient societies*, 1, 9-54.

Birkmann, J., and Wisner, B. (2006). *Measuring the unmeasurable: the challenge of vulnerability*, UNU-EHS.

Bogardi, I., Matyasovszky, I., Bardossy, A., and Duckstein, L. (1994). "A hydroclimatological model of areal drought." *Journal of Hydrology*, 153(1), 245-264.

Bojórquez-Tapia, L. A., Juárez, L., and Cruz-Bello, G. (2002). "Integrating fuzzy logic, optimization, and GIS for ecological impact assessments." *Environmental management*, 30(3), 418-433.

BoM (2015). "Drought." *Australian Meteorology: Cmate Glossary*, <http://www.bom.gov.au/climate/glossary/drought.shtml>.

Bonaccorso, B., Cancelliere, A., and Rossi, G. (2003). "An analytical formulation of return period of drought severity." *Stochastic Environmental Research and Risk Assessment*, 17(3), 157-174.

Brechmann, E. C., and Schepsmeier, U. (2013). "Modeling dependence with C-and D-vine copulas: The R-package CDVine." *Journal of Statistical Software*, 52(3), 1-27.

Bui, D. T., Pradhan, B., Lofman, O., Revhaug, I., and Dick, O. B. (2012). "Spatial prediction of landslide hazards in Hoa Binh province (Vietnam): a comparative assessment of the efficacy of evidential belief functions and fuzzy logic models." *Catena*, 96, 28-40.

Burke, E. J., Brown, S. J., and Christidis, N. (2006). "Modeling the recent evolution of global drought and projections for the twenty-first century with the Hadley Centre climate model." *Journal of Hydrometeorology*, 7(5), 1113-1125.

Burton, I., Huq, S., Lim, B., Pilifosova, O., and Schipper, E. L. (2002). "From impacts assessment to adaptation priorities: the shaping of adaptation policy." *Climate policy*, 2(2-3), 145-159.

Byun, H.-R., and Wilhite, D. A. (1999). "Objective quantification of drought severity and duration." *Journal of Climate*, 12(9), 2747-2756.

Cancelliere, A., Di Mauro, G., Bonaccorso, B., and Rossi, G. (2007). "Drought forecasting using the standardized precipitation index." *Water resources management*, 21(5), 801-819.

Cancelliere, A., and Salas, J. D. (2004). "Drought length properties for periodic-stochastic hydrologic data." *Water Resources Research*, 40(2).

Cancelliere, A., and Salas, J. D. (2010). "Drought probabilities and return period for annual streamflows series." *Journal of hydrology*, 391(1), 77-89.

Carroll, N., Frijters, P., and Shields, M. A. (2009). "Quantifying the costs of drought: new evidence from life satisfaction data." *Journal of Population Economics*, 22(2), 445-461.

Cavin, L., Mountford, E. P., Peterken, G. F., and Jump, A. S. (2013). "Extreme drought alters competitive dominance within and between tree species in a mixed forest stand." *Functional Ecology*, 27(6), 1424-1435.

Chang, T.-P., Liu, F.-J., Ko, H.-H., and Huang, M.-C. (2017). "Oscillation characteristic study of wind speed, global solar radiation and air temperature using wavelet analysis." *Applied Energy*, 190, 650-657.

Chen, X., Koenker, R., and Xiao, Z. (2009). "Copula-based nonlinear quantile autoregression." *The Econometrics Journal*, 12(s1), S50-S67.

Chen, Y. D., Zhang, Q., Xiao, M., Singh, V. P., and Zhang, S. (2016). "Probabilistic forecasting of seasonal droughts in the Pearl River basin, China." *Stochastic environmental research and risk assessment*, 30(7), 2031-2040.

Chiew, F. H., Piechota, T. C., Dracup, J. A., and McMahon, T. A. (1998). "El Nino/Southern Oscillation and Australian rainfall, streamflow and drought: Links and potential for forecasting." *Journal of Hydrology*, 204(1), 138-149.

Commonwealth of Australia (2017). "White Paper: White Paper At a Glance." *Agricultural Competitiveness White Paper*, <http://agwhitepaper.agriculture.gov.au/white-paper/white-paper-at-a-glance >. (August 21, 2017).

Council, C. (2015). "Thirsty Country: Climate Change and Drought in Australia."

CPC (2014). "Climate Prediction Center - Oceans and Atmospheric Data." National Oceanic and Atmospheric Administation (NOAA), College Road, Maryland.

CSIRO (2008a). "Water Availability in the Murray-Darling Basin." *CSIRO Water for a Healthy Country, Canberra*, 68.

CSIRO (2008b). "Water Availability in the Murray. A Report to the Australian Government from the CSIRO Murray-Darling Basin Sustainable Yields Project." CSIRO, Canberra, 217.

Cutter, S. L. (1996). "Vulnerability to environmental hazards." *Progress in human geography*, 20(4), 529-539.

Cutter, S. L., Boruff, B. J., and Shirley, W. L. (2003). "Social vulnerability to environmental hazards." *Social science quarterly*, 84(2), 242-261.

Dai, A. (2011). "Characteristics and trends in various forms of the Palmer Drought Severity Index during 1900–2008." *Journal of Geophysical Research: Atmospheres*, 116(D12).

Das, P. K., Dutta, D., Sharma, J., and Dadhwal, V. (2016). "Trends and behaviour of meteorological drought (1901–2008) over Indian region using standardized precipitation–evapotranspiration index." *Int. J. Climatol.*, 36(2), 909-916.

Davidson, B. R. (1969). "Australia wet or dry? The physical and economic limits to the expansion of irrigation." *Australia wet or dry? The physical and economic limits to the expansion of irrigation.*

Dayal, K., Deo, R., and Apan, A. "Application of hybrid artificial neural network algorithm for the prediction of Standardized Precipitation Index." *Proc., IEEE Region 10 International Conference: Technologies for Smart Nation*, IEEE, 2962-2966.

Dayal, K., Deo, R., and Apan, A. (2018). "Investigating drought duration-severity-intensity characteristics using the Standardised Precipitation-Evapotranspiration Index: case studies in drought-prone southeast Queensland." *Journal of Hydrologic Engineering*, 23(1).

Dayal, K., Deo, R., and Apan, A. A. (2017). "Drought modelling based on artificial intelligence and neural network algorithms: a case study in Queensland, Australia." *Climate Change Adaptation in Pacific Countries*, Springer International Publishing, 177-198.

De Michele, C., and Salvadori, G. (2003). "A generalized Pareto intensity-duration model of storm rainfall exploiting 2-copulas." *Journal of Geophysical Research: Atmospheres*, 108(D2).

De Michele, C., Salvadori, G., Canossi, M., Petaccia, A., and Rosso, R. (2005). "Bivariate statistical approach to check adequacy of dam spillway." *Journal of Hydrologic Engineering*, 10(1), 50-57.

Deo, R., and Şahin, M. (2015). "Application of the Artificial Neural Network model for prediction of monthly Standardized Precipitation and Evapotranspiration Index using hydrometeorological parameters and climate indices in eastern Australia." *Atmospheric Research*, 161, 65-81.

Deo, R. C., Byun, H.-R., Adamowski, J., and Begum, K. (2015). "Application of effective drought index for quantification of meteorological drought events: a case study in Australia." *Theoretical and Applied Climatology*, DOI 10.1007/s00704-015-1706-5(http://link.springer.com/article/10.1007%2Fs00704-015-1706-5).

Deo, R. C., Kisi, O., and Singh, V. P. (2017). "Drought forecasting in eastern Australia using multivariate adaptive regression spline, least square support vector machine and M5Tree model." *Atmospheric Research*, 184, 149-175.

Deo, R. C., and Şahin, M. (2015). "Application of the extreme learning machine algorithm for the prediction of monthly Effective Drought Index in eastern Australia." *Atmospheric Research*, 153, 512-525.

Deo, R. C., and Şahin, M. (2016). "An extreme learning machine model for the simulation of monthly mean streamflow water level in eastern Queensland." *Environmental monitoring and assessment*, 188(2), 90.

Deo, R. C., Syktus, J., McAlpine, C., Lawrence, P., McGowan, H., and Phinn, S. R. (2009). "Impact of historical land cover change on daily indices of climate extremes including droughts in eastern Australia." *Geophysical Research Letters*, 36(8).

Dogan, S., Berktay, A., and Singh, V. P. (2012). "Comparison of multi-monthly rainfall-based drought severity indices, with application to semi-arid Konya closed basin, Turkey." *Journal of Hydrology*, 470-471, 255-268.

Dougill, A., Fraser, E., and Reed, M. (2010). "Anticipating vulnerability to climate change in dryland pastoral systems: using dynamic systems models for the Kalahari." *Ecology and Society*, 15(2).

Downing, T. E., and Bakker, K. (2000). "Drought discourse and vulnerability." *Drought: A global assessment*, 2, 213-230.

Downing, T. E., Butterfield, R., Cohen, S., Huq, S., Moss, R., Rahman, A., Sokona, Y., and Stephen, L. (2001). "Vulnerability indices: climate change impacts and adaptation." *UNEP Policy Series, UNEP, Nairobi*.

Dracup, J. A., Lee, K. S., and Paulson, E. G. (1980). "On the definition of droughts." *Water Resources Research*, 16(2), 297-302.

Dragicevic, S., and Marceau, D. J. (2000). "An application of fuzzy logic reasoning for GIS temporal modeling of dynamic processes." *Fuzzy sets and Systems*, 113(1), 69-80.

Dubrovsky, M., Svoboda, M. D., Trnka, M., Hayes, M. J., Wilhite, D. A., Zalud, Z., and Hlavinka, P. (2009). "Application of relative drought indices in assessing climate-change impacts on drought conditions in Czechia." *Theoretical and Applied Climatology*, 96(1-2), 155-171.

Eakin, H., and Conley, J. (2002). "Climate variability and the vulnerability of ranching in southeastern Arizona: a pilot study." *Climate Research*, 21(3), 271-281.

Ekrami, M., Marj, A. F., Barkhordari, J., and Dashtakian, K. (2016). "Drought vulnerability mapping using AHP method in arid and semiarid areas: a case study for Taft Township, Yazd Province, Iran." *Environmental Earth Sciences*, 75(12), 1-13.

Erdey-Heydorn, M. D. (2008). "An ArcGIS seabed characterization toolbox developed for investigating benthic habitats." *Marine Geodesy*, 31(4), 318-358.

Espada Jr, R., Apan, A., and McDougall, K. "Spatial modelling of adaptation strategies for urban built infrastructures exposed to flood hazards." *Proc., Proceedings of the Queensland Surveying and Spatial Conference (QSSC 2012)*, Surveying and Spatial Sciences Institute Queensland.

Espada Jr, R., Apan, A., and McDougall, K. "Using spatial modelling to develop flood risk and climate adaptation capacity metrics for assessing urban community and critical electricity infrastructure vulnerability." *Proc., Proceedings of the 20th International Congress on Modelling and Simulation (MODSIM 2013)*, Modelling and Simulation Society of Australia and New Zealand Inc., 2304-2310.

Espada Jr, R., Apan, A., and McDougall, K. "Using spatial modelling to develop flood risk and climate adaptation capacity metrics for

vulnerability assessments of urban community and critical water supply infrastructure." *Proc., Proceedings of the 49th International Society of City and Regional Planners Congress (ISOCARP 2013)*, International Society of City and Regional Planners (ISOCARP), 1-12.

ESRI (2017). "ArcGIS Resources." <http://resources.arcgis.com/en/help/>. (August 24, 2017).

Fan, L., Wang, H., Wang, C., Lai, W., and Zhao, Y. (2017). "Exploration of Use of Copulas in Analysing the Relationship between Precipitation and Meteorological Drought in Beijing, China." *Advances in Meteorology*, 2017.

FAO (2005). "Drought-resistant soils: Discussion papers." *Land and Water Division*, Food and Agriculture Organization of the United Nations.

Favre, A. C., El Adlouni, S., Perreault, L., Thiémonge, N., and Bobée, B. (2004). "Multivariate hydrological frequency analysis using copulas." *Water resources research*, 40(1).

Felch, R. E. (1978). "Drought: Characteristics and assessment." *North American Droughts*, 15, 25-42.

Fernández, B., and Salas, J. D. (1999). "Return period and risk of hydrologic events. I: mathematical formulation." *Journal of Hydrologic Engineering*, 4(4), 297-307.

Fisher, N., and Switzer, P. (1985). "Chi-plots for assessing dependence." *Biometrika*, 72(2), 253-265.

Fraser, E. D., Dougill, A., Hubacek, K., Quinn, C., Sendzimir, J., and Termansen, M. (2011). "Assessing vulnerability to climate change in dryland livelihood systems: conceptual challenges and interdisciplinary solutions." *Ecology and Society*, 16(3).

Fuchs, B., Svoboda, M., Nothwehr, J., Poulsen, C., Sorensen, W., and Guttman, N. (2012). "A new national drought risk Atlas for the US from the National Drought Mitigation Center."

Gabriel, K., and Neumann, J. (1962). "A Markov chain model for daily rainfall occurrence at Tel Aviv." *Quarterly Journal of the Royal Meteorological Society*, 88(375), 90-95.

Gallant, A. J., Reeder, M. J., Risbey, J. S., and Hennessy, K. J. (2013). "The characteristics of seasonal-scale droughts in Australia, 1911–2009." *International Journal of Climatology*, 33(7), 1658-1672.

Ganguli, P., and Reddy, M. J. (2012). "Risk assessment of droughts in Gujarat using bivariate copulas." *Water resources management*, 26(11), 3301-3327.

Ganguli, P., and Reddy, M. J. (2013). "Analysis of ENSO-based climate variability in modulating drought risks over western Rajasthan in India." *Journal of earth system science*, 122(1), 253-269.

Ganguli, P., and Reddy, M. J. (2014). "Evaluation of trends and multivariate frequency analysis of droughts in three meteorological subdivisions of western India." *International Journal of Climatology*, 34(3), 911-928.

Gbetibouo, G. A., and Ringler, C. (2009). *Mapping South African farming sector vulnerability to climate change and variability: A subnational assessment*, International Food Policy Research Institute (IFPRI)

and Center for Environmental Economics and Policy in Africa (CEEPA).

Gemitzi, A., Tsihrintzis, V. A., Voudrias, E., Petalas, C., and Stravodimos, G. (2007). "Combining geographic information system, multicriteria evaluation techniques and fuzzy logic in siting MSW landfills." *Environmental Geology*, 51(5), 797-811.

Genest, C., and Boies, J.-C. (2003). "Detecting dependence with Kendall plots." *The American Statistician*, 57(4), 275-284.

Genest, C., and Favre, A.-C. (2007). "Everything you always wanted to know about copula modeling but were afraid to ask." *Journal of hydrologic engineering*, 12(4), 347-368.

GERGELY, T., OPRITA, G., and PASCAL, G. (2016). "STATISTICAL ANALYSIS OF A DIGITAL ELEVATION MODEL USING ARCGIS." *Journal of Young Scientist*, 4.

Gibbs, W. J., and Maher, J. V. (1967). "Rainfall deciles as drought indicators." *Bureau of Meteorology*, 48.

Giovinazzi, S., and Lagomarsino, S. "A macroseismic method for the vulnerability assessment of buildings." *Proc., 13th world conference on earthquake engineering, Vancouver, BC, Canada*, 1-6.

Goddard, L., Mason, S. J., Zebiak, S. E., Ropelewski, C. F., Basher, R., and Cane, M. A. (2001). "Current approaches to seasonal to interannual climate predictions." *International Journal of Climatology*, 21(9), 1111-1152.

Gogu, R., and Dassargues, A. (2000). "Current trends and future challenges in groundwater vulnerability assessment using overlay and index methods." *Environmental geology*, 39(6), 549-559.

Golnaraghi, M., Etienne, C., Guha-Sapir, D., and Below, R. (2014). *Atlas of Mortality and Economic Losses from Weather, Climate, and Water Extremes (1970-2012)*, World Meteorological Organization.

González, J., and Valdés, J. B. (2006). "New drought frequency index: Definition and comparative performance analysis." *Water Resources Research*, 42(11), W11421.

Gorsevski, P. V., and Jankowski, P. (2010). "An optimized solution of multi-criteria evaluation analysis of landslide susceptibility using fuzzy sets and Kalman filter." *Computers & Geosciences*, 36(8), 1005-1020.

Gräler, B., van den Berg, M., Vandenberghe, S., Petroselli, A., Grimaldi, S., De Baets, B., and Verhoest, N. (2013). "Multivariate return periods in hydrology: a critical and practical review focusing on synthetic design hydrograph estimation." *Hydrology and Earth System Sciences*, 17(4), 1281-1296.

Grimaldi, S., and Serinaldi, F. (2006). "Design hyetograph analysis with 3-copula function." *Hydrological Sciences Journal*, 51(2), 223-238.

Grinsted, A., Moore, J. C., and Jevrejeva, S. (2004). "Application of the cross wavelet transform and wavelet coherence to geophysical time series." *Nonlinear processes in geophysics*, 11(5/6), 561-566.

Guttman, N. B., Wallis, J. R., and Hosking, J. (1992). "Spatial comparability of the Palmer drought severity index." *JAWRA Journal of the American Water Resources Association*, 28(6), 1111-1119.

Haan, C. T. (2002). *Statistical methods in hydrology*, The Iowa State University Press.

Haines, A., Kovats, R. S., Campbell-Lendrum, D., and Corvalán, C. (2006). "Climate change and human health: impacts, vulnerability and public health." *Public health*, 120(7), 585-596.

Hanson, R. L. (1988). "Evapotranspiration and droughts." *Paulson, RW, Chase, EB, Roberts, RS, and Moody, DW, Compilers, National Water Summary*, 99-104.

Hargreaves, G. H. (1994). "Defining and using reference evapotranspiration." *Journal of Irrigation and Drainage Engineering*, 120(6), 1132-1139.

Hayes, M. J., Wilhelmi, O. V., and Knutson, C. L. (2004). "Reducing drought risk: bridging theory and practice." *Natural Hazards Review*, 5(2), 106-113.

Heim Jr, R. R. (2002). "A review of twentieth-century drought indices used in the United States." *Bulletin of the American Meteorological Society*, 83(8), 1149-1165.

Helfer, F., Lemckert, C., and Zhang, H. (2012). "Impacts of climate change on temperature and evaporation from a large reservoir in Australia." *J. Hydrol.*, 475, 365-378.

Hendon, H. H., Thompson, D. W., and Wheeler, M. C. (2007). "Australian rainfall and surface temperature variations associated with the Southern Hemisphere annular mode." *Journal of Climate*, 20(11), 2452-2467.

Hertzler, G., Kingwell, R., Crean, J., and Carter, C. (2006). "Managing and Sharing the Risks of Drought in Australia." *26th Conference of the International Association of Agricultural Economists, "Contributions of Agricultural Economics to Critical Policy Issues*Gold Coast, Queensland Australia, 12-18 August.

Hewitt, K. (2014). *Regions of risk: A geographical introduction to disasters*, Routledge.

Hinkel, J. (2011). ""Indicators of vulnerability and adaptive capacity": Towards a clarification of the science–policy interface." *Global Environmental Change*, 21(1), 198-208.

Hobbins, M., Wood, A., Streubel, D., and Werner, K. (2012). "What drives the variability of evaporative demand across the conterminous United States?" *Journal of Hydrometeorology*, 13(4), 1195-1214.

Hobbins, M. T. (2016). "The variability of ASCE standardized reference evapotranspiration: A rigorous, CONUS-wide decomposition and attribution." *American Society of Agricultural and Biological Engineers*, 59(2), 561-576.

Hobbins, M. T., Dai, A., Roderick, M. L., and Farquhar, G. D. (2008). "Revisiting the parameterization of potential evaporation as a driver of long-term water balance trends." *Geophysical Research Letters*, 35(12), L12403.

Hufschmidt, G. (2011). "A comparative analysis of several vulnerability concepts." *Natural hazards*, 58(2), 621-643.

IPCC (2012). "Glossary of terms." *Managing the Risks of Extreme Events and Disasters to Advance Climate Change Adaptation*, 555-564.

ISDR, U. (2009). "UNISDR terminology on disaster risk reduction." *Geneva, Switzerland, May*.

Jain, V. K., Pandey, R., and Jain, M. K. (2015). "Spatio-temporal assessment of vulnerability to drought." *Natural Hazards*, 76(1), 443-469.

Jain, V. K., Pandey, R. P., Jain, M. K., and Byun, H.-R. (2015). "Comparison of drought indices for appraisal of drought characteristics in the Ken River Basin." *Weather and Climate Extremes*, 8, 1-11.

Janga Reddy, M., and Ganguli, P. (2012). "Application of copulas for derivation of drought severity–duration–frequency curves." *Hydrological Processes*, 26(11), 1672-1685.

Jarraud, M. (2008). "Guide to meteorological instruments and methods of observation (WMO-No. 8)." *World Meteorological Organisation: Geneva, Switzerland*.

Joe, H. (1996). "Families of m-variate distributions with given margins and m (m-1)/2 bivariate dependence parameters." *Lecture Notes-Monograph Series*, 120-141.

Joe, H. (1997). *Multivariate models and multivariate dependence concepts*, CRC Press.

Jones, D. A., Wang, W., and Fawcett, R. (2009). "High-quality spatial climate data-sets for Australia." *Australian Meteorological and Oceanographic Journal*, 58(4), 233.

Jones, R. N. (2001). "An environmental risk assessment/management framework for climate change impact assessments." *Natural hazards*, 23(2-3), 197-230.

Jun, K.-S., Chung, E.-S., Kim, Y.-G., and Kim, Y. (2013). "A fuzzy multi-criteria approach to flood risk vulnerability in South Korea by considering climate change impacts." *Expert Systems with Applications*, 40(4), 1003-1013.

Kang, J.-E., and Lee, M.-J. (2012). "Assessment of flood vulnerability to climate change using fuzzy model and GIS in Seoul." *Journal of the Korean Association of Geographic Information Studies*, 15(3), 119-136.

Kao, S.-C., and Govindaraju, R. S. (2010). "A copula-based joint deficit index for droughts." *Journal of Hydrology*, 380(1), 121-134.

Kao, S. C., and Govindaraju, R. S. (2007). "A bivariate frequency analysis of extreme rainfall with implications for design." *Journal of Geophysical Research: Atmospheres*, 112(D13).

Karabegovic, A., Avdagic, Z., and Ponjavic, M. (2006). *Applications of fuzzy logic in geographic information systems for multiple criteria decision making*, na.

Karl, T. R. (1983). "Some spatial characteristics of drought duration in the United States." *Journal of Climate and Applied Meteorology*, 22(8), 1356-1366.

Kendall, M., and Stuart, A. (1977). "The advanced theory of statistics. Vol. 1: Distribution theory." *London: Griffin, 1977, 4th ed.*, 1.

Keyantash, J., and Dracup, J. A. (2002). "The quantification of drought: an evaluation of drought indices." *Bulletin of the American Meteorological Society*, 83(8), 1167-1180.

Khedun, C. P., Mishra, A. K., Singh, V. P., and Giardino, J. R. (2014). "A copula-based precipitation forecasting model: Investigating the interdecadal modulation of ENSO's impacts on monthly precipitation." *Water Resources Research*, 50(1), 580-600.

Khoshnodifar, Z., Sookhtanlo, M., and Gholami, H. (2012). "Identification and measurement of indicators of drought vulnerability among wheat farmers in Mashhad County, Iran." *Annals of Biological Research*, 3(9), 4593-4600.

Kiem, A., and Verdon-Kidd, D. (2010). "Towards understanding hydroclimatic change in Victoria, Australia-preliminary insights into the" Big Dry"." *Hydrology and Earth System Sciences*, 14(3), 433.

Kiem, A. S. (2013). "Drought and water policy in Australia: Challenges for the future illustrated by the issues associated with water trading and climate change adaptation in the Murray–Darling Basin." *Global environmental change*, 23(6), 1615-1626.

Kiem, A. S., and Franks, S. W. (2004). "Multi-decadal variability of drought risk, eastern Australia." *Hydrological Processes*, 18(11), 2039-2050.

Kim, T.-W., and Valdés, J. B. (2003). "Nonlinear model for drought forecasting based on a conjunction of wavelet transforms and neural networks." *Journal of Hydrologic Engineering*, 8(6), 319-328.

Kim, T.-W., Valdés, J. B., and Yoo, C. (2003). "Nonparametric approach for estimating return periods of droughts in arid regions." *Journal of Hydrologic Engineering*, 8(5), 237-246.

Kogan, F. N. (2000). "Contribution of remote sensing to drought early warning." *Early warning systems for drought preparedness and drought management*, 75-87.

Kuhn, G., Khan, S., Ganguly, A. R., and Branstetter, M. L. (2007). "Geospatial–temporal dependence among weekly precipitation extremes with applications to observations and climate model simulations in South America." *Advances in Water Resources*, 30(12), 2401-2423.

Kumar, V., and Panu, U. (1997). "PREDICTIVE ASSESSMENT OF SEVERITY OF AGRICULTURAL DROUGHTS BASED ON AGRO-CLIMATIC FACTORS." *Jawra Journal of the American Water Resources Association*, 33(6), 1255-1264.

Le Houérou, H. N. (1996). "Climate change, drought and desertification." *Journal of Arid Environments*, 34(2), 133-185.

Leblanc, M., Tweed, S., Van Dijk, A., and Timbal, B. (2012). "A review of historic and future hydrological changes in the Murray-Darling Basin." *Global and planetary change*, 80, 226-246.

Lee, S. (2007). "Application and verification of fuzzy algebraic operators to landslide susceptibility mapping." *Environmental Geology*, 52(4), 615-623.

Lee, T., Modarres, R., and Ouarda, T. B. (2013). "Data-based analysis of bivariate copula tail dependence for drought duration and severity." *Hydrological Processes*, 27(10), 1454-1463.

Leilah, A., and Al-Khateeb, S. (2005). "Statistical analysis of wheat yield under drought conditions." *Journal of Arid environments*, 61(3), 483-496.

Li, L., Shi, Z.-H., Yin, W., Zhu, D., Ng, S. L., Cai, C.-F., and Lei, A.-L. (2009). "A fuzzy analytic hierarchy process (FAHP) approach to eco-environmental vulnerability assessment for the Danjiangkou reservoir area, China." *Ecological Modelling*, 220(23), 3439-3447.

Li, W., Hou, M., Chen, H., and Chen, X. (2012). "Study on drought trend in south China based on standardized precipitation evapotranspiration index." *J Nat Disasters*, 21, 84-90.

Liu, W., and Juárez, R. N. (2001). "ENSO drought onset prediction in northeast Brazil using NDVI." *International Journal of Remote Sensing*, 22(17), 3483-3501.

Liu, Z., Zhou, P., Chen, X., and Guan, Y. (2015). "A multivariate conditional model for streamflow prediction and spatial precipitation refinement." *Journal of Geophysical Research: Atmospheres*, 120(19).

Lloyd-Hughes, B., and Saunders, M. A. (2002). "A drought climatology for Europe." *International Journal of Climatology*, 22(13), 1571-1592.

Lohani, V., Loganathan, G., and Mostaghimi, S. (1998). "Long-term analysis and short-term forecasting of dry spells by Palmer Drought Severity Index." *Hydrology Research*, 29(1), 21-40.

Lohani, V. K., and Loganathan, G. (1997). "An early warning system for drought management using the Palmer drought index." *JAWRA Journal of the American Water Resources Association*, 33(6), 1375-1386.

Lorenzo-Lacruz, J., Vicente-Serrano, S. M., López-Moreno, J. I., Beguería, S., García-Ruiz, J. M., and Cuadrat, J. M. (2010). "The impact of droughts and water management on various hydrological systems in the headwaters of the Tagus River (central Spain)." *Journal of Hydrology*, 386(1), 13-26.

Luers, A. L., Lobell, D. B., Sklar, L. S., Addams, C. L., and Matson, P. A. (2003). "A method for quantifying vulnerability, applied to the agricultural system of the Yaqui Valley, Mexico." *Global Environmental Change*, 13(4), 255-267.

Malczewski, J. (2006). "Ordered weighted averaging with fuzzy quantifiers: GIS-based multicriteria evaluation for land-use suitability analysis." *International journal of applied earth observation and geoinformation*, 8(4), 270-277.

Martin-Benito, D., Beeckman, H., and Canellas, I. (2013). "Influence of drought on tree rings and tracheid features of Pinus nigra and Pinus sylvestris in a mesic Mediterranean forest." *European Journal of Forest Research*, 132(1), 33-45.

McAlpine, C., Syktus, J., Deo, R. C., Lawrence, P., McGowan, H., Watterson, I., and Phinn, S. (2007). "Modeling the impact of historical land cover change on Australia's regional climate." *Geophysical Research Letters*, 34(22).

McAlpine, C., Syktus, J., Ryan, J., Deo, R. C., McKeon, G., McGowan, H., and Phinn, S. (2009). "A continent under stress: interactions, feedbacks and risks associated with impact of modified land cover on Australia's climate." *Global Change Biology*, 15(9), 2206-2223.

McBride, J. L., and Nicholls, N. (1983). "Seasonal relationships between Australian rainfall and the Southern Oscillation." *Monthly Weather Review*, 111(10), 1998-2004.

McKee, T. B., Doesken, N. J., and Kleist, J. "The relationship of drought frequency and duration to time scales." *Proc., Proceedings of the 8th Conference on Applied Climatology*, American Meteorological Society Boston, MA, 179-183.

Meneghini, B., Simmonds, I., and Smith, I. N. (2007). "Association between Australian rainfall and the southern annular mode." *International Journal of Climatology*, 27(1), 109-121.

Mishra, A., Desai, V., and Singh, V. (2007). "Drought forecasting using a hybrid stochastic and neural network model." *Journal of Hydrologic Engineering*, 12(6), 626-638.

Mishra, A. K., Ines, A. V., Das, N. N., Khedun, C. P., Singh, V. P., Sivakumar, B., and Hansen, J. W. (2015). "Anatomy of a local-scale drought: Application of assimilated remote sensing products, crop model, and statistical methods to an agricultural drought study." *Journal of Hydrology*, 526, 15-29.

Mishra, A. K., and Singh, V. P. (2010). "A review of drought concepts." *Journal of Hydrology*, 391(1-2), 202-216.

Mishra, A. K., and Singh, V. P. (2011). "Drought modeling – A review." *Journal of Hydrology*, 403(1-2), 157-175.

Mo, K. C., and Lettenmaier, D. P. (2016). "Precipitation deficit flash droughts over the United States." *Journal of Hydrometeorology*, 17(4), 1169-1184.

Moeller, C., Smith, I., Asseng, S., Ludwig, F., and Telcik, N. (2008). "The potential value of seasonal forecasts of rainfall categories—case studies from the wheatbelt in Western Australia's Mediterranean region." *agricultural and forest meteorology*, 148(4), 606-618.

Mohammadi, K., Niknam, R., and Majd, V. J. (2009). "Aquifer vulnerability assessment using GIS and fuzzy system: a case study in Tehran–Karaj aquifer, Iran." *Environmental geology*, 58(2), 437-446.

Morid, S., Smakhtin, V., and Bagherzadeh, K. (2007). "Drought forecasting using artificial neural networks and time series of drought indices." *International Journal of Climatology*, 27(15), 2103-2111.

Morid, S., Smakhtin, V., and Moghaddasi, M. (2006). "Comparison of seven meteorological indices for drought monitoring in Iran." *International Journal of Climatology*, 26(7), 971-985.

Mpelasoka, F., Hennessy, K., Jones, R., and Bates, B. (2008). "Comparison of suitable drought indices for climate change impacts assessment over Australia towards resource management." *International Journal of Climatology*, 28(10), 1283-1292.

Nam, W.-H., Hayes, M. J., Svoboda, M. D., Tadesse, T., and Wilhite, D. A. (2015). "Drought hazard assessment in the context of climate change for South Korea." *Agricultural Water Management*, 160, 106-117.

Narasimhan, B., and Srinivasan, R. (2005). "Development and evaluation of Soil Moisture Deficit Index (SMDI) and Evapotranspiration Deficit

Index (ETDI) for agricultural drought monitoring." *Agricultural and Forest Meteorology*, 133(1), 69-88.

Naumann, G., Barbosa, P., Garrote, L., Iglesias, A., and Vogt, J. (2014). "Exploring drought vulnerability in Africa: an indicator based analysis to be used in early warning systems." *Hydrology and Earth System Sciences*, 18(5), 1591-1604.

Nelsen, R. B. (1999). "Introduction." *An Introduction to Copulas*, Springer, 1-4.

Nelson, R., Kokic, P., Elliston, L., and King, J.-A. (2005). "Structural adjustment: a vulnerability index for Australian broadacre agriculture." *Australian Commodities: Forecasts and Issues*, 12(1), 171.

Neshat, A., Pradhan, B., and Dadras, M. (2014). "Groundwater vulnerability assessment using an improved DRASTIC method in GIS." *Resources, Conservation and Recycling*, 86, 74-86.

Nguyen-Huy, T., Deo, R. C., An-Vo, D.-A., Mushtaq, S., and Khan, S. (2017). "Copula-statistical precipitation forecasting model in Australia's agro-ecological zones." *Agricultural Water Management*, 191, 153-172.

Nicholls, N. (2004). "The changing nature of Australian droughts." *Climatic Change*, 63(3), 323-336.

Ochola, W., and Kerkides, P. (2003). "A Markov chain simulation model for predicting critical wet and dry spells in Kenya: analysing rainfall events in the Kano Plains." *Irrigation and drainage*, 52(4), 327-342.

Özger, M., Mishra, A. K., and Singh, V. P. (2012). "Long lead time drought forecasting using a wavelet and fuzzy logic combination model: a case study in Texas." *Journal of Hydrometeorology*, 13(1), 284-297.

Palmer, W. C. (1965). *Meteorological drought*, US Department of Commerce, Weather Bureau Washington, DC, USA.

Palmer, W. C. (1968). "Keeping track of crop moisture conditions, nationwide: The new crop moisture index."

Pandey, R. P., Dash, B. B., Mishra, S. K., and Singh, R. (2008). "Study of indices for drought characterization in KBK districts in Orissa (India)." *Hydrological Processes*, 22(12), 1895-1907.

Pandey, R. P., Pandey, A., Galkate, R. V., Byun, H.-R., and Mal, B. C. (2010). "Integrating Hydro-Meteorological and Physiographic Factors for Assessment of Vulnerability to Drought." *Water Resources Management*, 24(15), 4199-4217.

Parry, M., Canziani, O., Palutikof, J., van der Linden, P. J., and Hanson, C. E. (2007). *Climate change 2007: impacts, adaptation and vulnerability*, Cambridge University Press Cambridge.

Pathak, D. R., and Hiratsuka, A. (2011). "An integrated GIS based fuzzy pattern recognition model to compute groundwater vulnerability index for decision making." *Journal of Hydro-environment Research*, 5(1), 63-77.

Paulo, A., Ferreira, E., Coelho, C., and Pereira, L. (2005). "Drought class transition analysis through Markov and Loglinear models, an approach to early warning." *Agricultural water management*, 77(1), 59-81.

Paulo, A., Rosa, R., and Pereira, L. (2012). "Climate trends and behaviour of drought indices based on precipitation and evapotranspiration in Portugal." *Natural Hazards and Earth System Sciences*, 12, 1481-1491.

Pearce, K., Holper, P., Hopkins, M., Bouma, W., Whetton, P., Hennessy, K., and Power, S. (2007). "Climate Change in Australia: technical report 2007."

Potop, V. (2011). "Evolution of drought severity and its impact on corn in the Republic of Moldova." *Theoretical and applied climatology*, 105(3-4), 469-483.

Poulin, A., Huard, D., Favre, A.-C., and Pugin, S. (2007). "Importance of tail dependence in bivariate frequency analysis." *Journal of Hydrologic Engineering*, 12(4), 394-403.

Pradhan, B. (2011). "GIScience Tools for Climate Change Related Natural Hazards and Modelling." *Geoinformatics for Climate Change Studies*, The Energy and Resources Institute New Delhi, India.

Pradhan, B. (2011). "Use of GIS-based fuzzy logic relations and its cross application to produce landslide susceptibility maps in three test areas in Malaysia." *Environmental Earth Sciences*, 63(2), 329-349.

Prasad, R., Deo, R. C., Li, Y., and Maraseni, T. (2017). "Input selection and performance optimization of ANN-based streamflow forecasts in a drought-prone Murray Darling Basin using IIS and MODWT algorithm." *Atmospheric Research*.

Price, K., Jackson, C. R., Parker, A. J., Reitan, T., Dowd, J., and Cyterski, M. (2011). "Effects of watershed land use and geomorphology on stream low flows during severe drought conditions in the southern Blue Ridge Mountains, Georgia and North Carolina, United States." *Water Resources Research*, 47(2).

Priestley, C., and Taylor, R. (1972). "On the assessment of surface heat flux and evaporation using large-scale parameters." *Monthly weather review*, 100(2), 81-92.

Rashed, T., and Weeks, J. (2003). "Assessing vulnerability to earthquake hazards through spatial multicriteria analysis of urban areas." *International Journal of Geographical Information Science*, 17(6), 547-576.

Rauf, U. F. A., and Zeephongsekul, P. (2014). "Analysis of Rainfall Severity and Duration in Victoria, Australia using Non-parametric Copulas and Marginal Distributions." *Water. Resour. Manag.*, 28(13), 4835-4856.

Raupach, M., Briggs, P., Haverd, V., King, E., Paget, M., and Trudinger, C. (2009). "Australian water availability project (AWAP): CSIRO marine and atmospheric research component: final report for phase 3." *Centre for Australian weather and climate research (bureau of meteorology and CSIRO). Melbourne, Australia*.

Raupach, M., Briggs, P., Haverd, V., King, E., Paget, M., and Trudinger, C. (2012). "Australian Water Availability Project. CSIRO Marine and Atmospheric Research."Canberra, Australia.

Reddy, J. M., and Ganguli, P. (2012). "Application of copulas for derivation of drought severity–duration–frequency curves." *Hydrological Processes*, 26(11), 1672-1685.

Reddy, M. J., and Ganguli, P. (2013). "Spatio-temporal analysis and derivation of copula-based intensity–area–frequency curves for droughts in western Rajasthan (India)." *Stochastic environmental research and risk assessment*, 27(8), 1975-1989.

Redmond, K. (2002). "The depiction of drought—A commentary." *Bulletin of American Meteorological Society*, 83, 1143-1147.

Renard, B., and Lang, M. (2007). "Use of a Gaussian copula for multivariate extreme value analysis: some case studies in hydrology." *Advances in Water Resources*, 30(4), 897-912.

Rezaei, F., Safavi, H. R., and Ahmadi, A. (2013). "Groundwater vulnerability assessment using fuzzy logic: a case study in the Zayandehrood aquifers, Iran." *Environmental management*, 51(1), 267-277.

Riebsame, W. E., Changnon Jr, S. A., and Karl, T. R. (1991). *Drought and natural resources management in the United States. Impacts and implications of the 1987-89 drought*, Westview Press Inc.

Roderick, M. L., Rotstayn, L. D., Farquhar, G. D., and Hobbins, M. T. (2007). "On the attribution of changing pan evaporation." *Geophysical research letters*, 34(17), L17403.

Roderick, M. L., Rotstayn, L. D., Farquhar, G. D., and Hobbins, M. T. (2007). "On the attribution of changing pan evaporation." *Geophysical research letters*, 34(17).

Sadiq, R., Husain, T., Veitch, B., and Bose, N. (2004). "Risk-based decision-making for drilling waste discharges using a fuzzy synthetic evaluation technique." *Ocean Engineering*, 31(16), 1929-1953.

Sadri, S., and Burn, D. H. (2012). "Copula-based pooled frequency analysis of droughts in the Canadian Prairies." *Journal of Hydrologic Engineering*, 19(2), 277-289.

Safavi, H. R., Esfahani, M. K., and Zamani, A. R. (2014). "Integrated index for assessment of vulnerability to drought, case study: Zayandehrood River Basin, Iran." *Water resources management*, 28(6), 1671-1688.

Salas, J. D., Fu, C., Cancelliere, A., Dustin, D., Bode, D., Pineda, A., and Vincent, E. (2005). "Characterizing the severity and risk of drought in the Poudre River, Colorado." *Journal of Water Resources Planning and Management*.

Salvadori, G., and De Michele, C. (2004). "Frequency analysis via copulas: Theoretical aspects and applications to hydrological events." *Water Resources Research*, 40(12).

Scherer, T. F., Seelig, B. D., and Franzen, D. W. (2013). *Soil, water and plant characteristics important to irrigation*, NDSU Extension Service, North Dakota State University.

Schirmacher, D., and Schirmacher, E. (2008). "Multivariate dependence modeling using pair-copulas." Technical report.

Schneiderbauer, S., and Ehrlich, D. (2004). *Risk, hazard and people's vulnerability to natural hazards: A review of definitions, concepts and data*, Office for Official Publication of the European Communities.

Sen, Z. (1990). "Critical drought analysis by second-order Markov chain." *Journal of Hydrology(Amsterdam)*, 120(1), 183-202.

218

Seqwater (2015). "Water for life Your say on South East Queensland's water future 2015 – 2045." Queensland Bulk Water Supply Authority, Ipswich QLD 4305, 28.

Serinaldi, F., Bonaccorso, B., Cancelliere, A., and Grimaldi, S. (2009). "Probabilistic characterization of drought properties through copulas." *Physics and Chemistry of the Earth, Parts A/B/C*, 34(10), 596-605.

Shafer, B., and Dezman, L. "Development of a Surface Water Supply Index (SWSI) to assess the severity of drought conditions in snowpack runoff areas." *Proc., Proceedings of the Western Snow Conference*, 164-175.

Sharma, L., Patel, N., Ghose, M., and Debnath, P. (2013). "Synergistic application of fuzzy logic and geo-informatics for landslide vulnerability zonation—a case study in Sikkim Himalayas, India." *Applied Geomatics*, 5(4), 271-284.

Sheffield, J., Wood, E. F., and Roderick, M. L. (2012). "Little change in global drought over the past 60 years." *Nature*, 491(7424), 435-438.

Shiau, J.-T., and Modarres, R. (2009). "Copula-based drought severity-duration-frequency analysis in Iran." *Meteorological Applications*, 16(4), 481-489.

Shiau, J.-T., and Shen, H. W. (2001). "Recurrence analysis of hydrologic droughts of differing severity." *Journal of Water Resources Planning and Management*.

Shiau, J. (2006). "Fitting drought duration and severity with two-dimensional copulas." *Water resources management*, 20(5), 795-815.

Shiau, J. T., Feng, S., and Nadarajah, S. (2007). "Assessment of hydrological droughts for the Yellow River, China, using copulas." *Hydrological Processes*, 21(16), 2157-2163.

Shiau, J. T., Wang, H. Y., and Tsai, C. T. (2006). "Bivariate Frequency Analysis of Floods Using COPULAS1." *JAWRA Journal of the American Water Resources Association*, 42(6), 1549-1564.

SILO (2017). "(Scientific Information for Land Owners). "Patched point dataset". Queensland Government."Australia.

Sklar, A. (1959). "Fonctions de répartition à n dimensions et leurs marges. Publications de l'Institut de Statistique de l'Université de Paris."

Song, S., and Singh, V. P. (2010). "Frequency analysis of droughts using the Plackett copula and parameter estimation by genetic algorithm." *Stochastic Environmental Research and Risk Assessment*, 24(5), 783-805.

Song, S., and Singh, V. P. (2010). "Meta-elliptical copulas for drought frequency analysis of periodic hydrologic data." *Stochastic Environmental Research and Risk Assessment*, 24(3), 425-444.

Statistics, A. B. o. (2013). "Population Projections, Australia, 2012 (base) to 2101." *3222.0*Australia.

Steinemann, A. (2003). "Drought indicators and triggers: a stochastic approach to evaluation." *JAWRA Journal of the American Water Resources Association*, 39(5), 1217-1233.

Stephens, D., Walker, G., and Lyons, T. (1994). "Forecasting Australian wheat yields with a weighted rainfall index." *Agricultural and Forest Meteorology*, 71(3-4), 247-263.

Stone, R. C., and Potgieter, A. (2008). "Drought risk and vulnerability in rainfed agriculture: Example of a case study from Australia., Drought management: scientific and technological innovations." *Options Mediterraneennes*(80), 29-40.

Szalai, S., Szinell, C., and Zoboki, J. (2000). "Drought monitoring in Hungary." *Early warning systems for drought preparedness and drought management*, 182-199.

Tallaksen, L. M., Madsen, H., and Clausen, B. (1997). "On the definition and modelling of streamflow drought duration and deficit volume." *Hydrological Sciences Journal*, 42(1), 15-33.

Tánago, I. G., Urquijo, J., Blauhut, V., Villarroya, F., and De Stefano, L. (2016). "Learning from experience: a systematic review of assessments of vulnerability to drought." *Natural Hazards*, 80(2), 951-973.

Tangestani, M. H. (2003). "Landslide susceptibility mapping using the fuzzy gamma operation in a GIS, Kakan catchment area, Iran." *Map India*, 86-88.

Taylor, K. E. (2001). "Summarizing multiple aspects of model performance in a single diagram." *Journal of Geophysical Research: Atmospheres*, 106(D7), 7183-7192.

Taylor, W. A. (2000). "Change-point analysis: a powerful new tool for detecting changes."

TERN (2009). "Soil and Landscape Grid of Australia." Terrestrial Ecosystem Research Network (TERN).

Thomas, T., Jaiswal, R., Galkate, R., Nayak, P., and Ghosh, N. (2016). "Drought indicators-based integrated assessment of drought vulnerability: a case study of Bundelkhand droughts in central India." *Natural Hazards*, 81(3), 1627-1652.

Thornthwaite, C. W. (1948). "An approach toward a rational classification of climate." *Geographical review*, 55-94.

Timbal, B., and Fawcett, R. (2013). "A Historical Perspective on Southeastern Australian Rainfall since 1865 Using the Instrumental Record." *Journal of Climate*, 26(4), 1112-1129.

Toromani, E., Sanxhaku, M., and Pasho, E. (2011). "Growth responses to climate and drought in silver fir (Abies alba) along an altitudinal gradient in southern Kosovo." *Canadian journal of forest research*, 41(9), 1795-1807.

Torrence, C., and Compo, G. P. (1998). "A practical guide to wavelet analysis." *Bulletin of the American Meteorological society*, 79(1), 61-78.

TRA (2010). "Impact of the Drought on Tourism in the Murray River Region: Summary of Results." *Tourism Research Australia (TRA), Department of Resources, Energy and Tourism.* Canberra, ACT, Australia, 3.

Trenberth, K. E., Dai, A., van der Schrier, G., Jones, P. D., Barichivich, J., Briffa, K. R., and Sheffield, J. (2014). "Global warming and changes in drought." *Nature Climate Change*, 4(1), 17-22.

Tsoukalas, L. H., and Uhrig, R. E. (1996). *Fuzzy and neural approaches in engineering*, John Wiley & Sons, Inc.

Turner, B. L., Kasperson, R. E., Matson, P. A., McCarthy, J. J., Corell, R. W., Christensen, L., Eckley, N., Kasperson, J. X., Luers, A., and Martello, M. L. (2003). "A framework for vulnerability analysis in sustainability science." *Proceedings of the national academy of sciences*, 100(14), 8074-8079.

Ummenhofer, C. C., England, M. H., McIntosh, P. C., Meyers, G. A., Pook, M. J., Risbey, J. S., Gupta, A. S., and Taschetto, A. S. (2009). "What causes southeast Australia's worst droughts?" *Geophysical Research Letters*, 36(4), L04706.

van Dijk, A. I. J. M., Beck, H. E., Crosbie, R. S., de Jeu, R. A. M., Liu, Y. Y., Podger, G. M., Timbal, B., and Viney, N. R. (2013). "The Millennium Drought in southeast Australia (2001-2009): Natural and human causes and implications for water resources, ecosystems, economy, and society." *Water Resources Research*, 49(2), 1040-1057.

Van Loon, A. F. (2015). "Hydrological drought explained." *Wiley Interdisciplinary Reviews: Water*, 2(4), 359-392.

Van Rooy, M. (1965). "A rainfall anomaly index independent of time and space." *Notos*, 14, 43-48.

Verdon-Kidd, D. C., and Kiem, A. S. (2010). "Quantifying Drought Risk in a Nonstationary Climate." *Journal of Hydrometeorology*, 11(4), 1019-1031.

Verdon-Kidd, D. C., and Kiem, A. S. (2009). "Nature and causes of protracted droughts in southeast Australia: Comparison between the Federation, WWII, and Big Dry droughts." *Geophysical Research Letters*, 36(22).

Verdon, D. C., Wyatt, A. M., Kiem, A. S., and Franks, S. W. (2004). "Multidecadal variability of rainfall and streamflow: Eastern Australia." *Water Resources Research*, 40(10).

Vernieuwe, H., Vandenberghe, S., De Baets, B., and Verhoest, N. (2015). "A continuous rainfall model based on vine copulas." *Hydrology and Earth System Sciences*, 19(6), 2685-2699.

Vicente-Serrano, S. M. (2007). "Evaluating the impact of drought using remote sensing in a Mediterranean, semi-arid region." *Natural Hazards*, 40(1), 173-208.

Vicente-Serrano, S. M., Beguería, S., and López-Moreno, J. I. (2010). "A multiscalar drought index sensitive to global warming: the standardized precipitation evapotranspiration index." *J. Climatol.*, 23(7), 1696-1718.

Vicente-Serrano, S. M., Beguería, S., López-Moreno, J. I., Angulo, M., and El Kenawy, A. (2010). "A new global 0.5 gridded dataset (1901-2006) of a multiscalar drought index: comparison with current drought index datasets based on the Palmer Drought Severity Index." *Journal of Hydrometeorology*, 11(4), 1033-1043.

Vicente-Serrano, S. M., Beguería, S., Lorenzo-Lacruz, J., Camarero, J. J., López-Moreno, J. I., Azorin-Molina, C., Revuelto, J., Morán-Tejeda, E., and Sanchez-Lorenzo, A. (2012). "Performance of drought indices for ecological, agricultural, and hydrological applications." *Earth Interactions*, 16(10), 1-27.

Vicente-Serrano, S. M., Gouveia, C., Camarero, J. J., Beguería, S., Trigo, R., López-Moreno, J. I., Azorín-Molina, C., Pasho, E., Lorenzo-Lacruz, J., and Revuelto, J. (2013). "Response of vegetation to drought time-scales across global land biomes." *Proceedings of the National Academy of Sciences*, 110(1), 52-57.

Vicente-Serrano, S. M., and López-Moreno, J. I. (2005). "Hydrological response to different time scales of climatological drought: an evaluation of the Standardized Precipitation Index in a mountainous Mediterranean basin." *Hydrology and Earth System Sciences Discussions*, 9(5), 523-533.

Vicente-Serrano, S. M., López-Moreno, J. I., Gimeno, L., Nieto, R., Morán-Tejeda, E., Lorenzo-Lacruz, J., Beguería, S., and Azorin-Molina, C. (2011). "A multiscalar global evaluation of the impact of ENSO on droughts." *Journal of Geophysical Research: Atmospheres (1984–2012)*, 116(D20).

Villa, F., and McLEOD, H. (2002). "Environmental vulnerability indicators for environmental planning and decision-making: guidelines and applications." *Environmental management*, 29(3), 335-348.

Vogel, C., and O'Brien, K. (2004). "Vulnerability and global environmental change: rhetoric and reality."

Vogel, R. M., Lall, U., Cai, X., Rajagopalan, B., Weiskel, P. K., Hooper, R. P., and Matalas, N. C. (2015). "Hydrology: The interdisciplinary science of water." *Water Resources Research*, 51(6), 4409-4430.

Wang, X., Gebremichael, M., and Yan, J. (2010). "Weighted likelihood copula modeling of extreme rainfall events in Connecticut." *Journal of Hydrology*, 390(1), 108-115.

Weghorst, K. "The reclamation drought index: Guidelines and practical applications." *Proc., North American Water and Environment Congress & Destructive Water*, ASCE, 637-642.

Wells, N., Goddard, S., and Hayes, M. J. (2004). "A self-calibrating Palmer drought severity index." *Journal of Climate*, 17(12), 2335-2351.

Werick, W., Willeke, G., Guttman, N., Hosking, J., and Wallis, J. (1994). "National drought atlas developed." *Eos, Transactions American Geophysical Union*, 75(8), 89-90.

Wilhelmi, O. V., Hubbard, K. G., and Wilhite, D. A. (2002). "Spatial representation of agroclimatology in a study of agricultural drought." *International Journal of Climatology*, 22(11), 1399-1414.

Wilhelmi, O. V., and Wilhite, D. A. (2002). "Assessing vulnerability to agricultural drought: a Nebraska case study." *Natural Hazards*, 25(1), 37-58.

Wilhite, D. A. (2000). "Drought as a natural hazard: concepts and definitions."

Wilhite, D. A. (2009). "Drought monitoring as a component of drought preparedness planning." *Coping with Drought Risk in Agriculture and Water Supply Systems*, 3-19.

Wilhite, D. A., and Glantz, M. H. (1985). "Understanding: the drought phenomenon: the role of definitions." *Water international*, 10(3), 111-120.

Wilhite, D. A., Sivakumar, M. V., and Pulwarty, R. (2014). "Managing drought risk in a changing climate: The role of national drought policy." *Weather and Climate Extremes*, 3, 4-13.

Wittwer, G., Adams, P. D., Horridge, M., and Madden, J. R. (2002). "Drought, regions and the Australian economy between 2001-02 and 2004-05." *Australian Bulletin of Labour*, 28(4), 231.

WMO, and GWP (2016). "Handbook of Drought Indicators and Indices " *Integrated Drought Management Programme (IDMP), Integrated Drought Management Tools and Guidelines Series 2.* Geneva.

Wong, G. (2013). "A comparison between the Gumbel-Hougaard and distorted Frank copulas for drought frequency analysis." *International Journal of Hydrology Science and Technology*, 3(1), 77-91.

Wong, G., Lambert, M., Leonard, M., and Metcalfe, A. (2009). "Drought analysis using trivariate copulas conditional on climatic states." *Journal of Hydrologic Engineering*, 15(2), 129-141.

Wong, G., Lambert, M. F., and Metcalfe, A. V. (2008). "Trivariate copulas for characterisation of droughts." *Anziam Journal*, 49, 306-323.

Wu, D., Yan, D.-H., Yang, G.-Y., Wang, X.-G., Xiao, W.-H., and Zhang, H.-T. (2013). "Assessment on agricultural drought vulnerability in the Yellow River basin based on a fuzzy clustering iterative model." *Natural hazards*, 67(2), 919-936.

Wu, H., Qian, H., Chen, J., and Huo, C. (2017). "Assessment of Agricultural Drought Vulnerability in the Guanzhong Plain, China." *Water Resources Management*, 31(5), 1557-1574.

Yamaguchi, Y., and Shinoda, M. (2002). "Soil moisture modeling based on multiyear observations in the Sahel." *Journal of applied meteorology*, 41(11), 1140-1146.

Yevjevich, V. M. (1967). "An objective approach to definitions and investigations of continental hydrologic droughts." *Hydrology papers (Colorado State University); no. 23*.

Yu, M., Li, Q., Hayes, M. J., Svoboda, M. D., and Heim, R. R. (2014). "Are droughts becoming more frequent or severe in China based on the Standardized Precipitation Evapotranspiration Index: 1951–2010?" *International Journal of Climatology*, 34(3), 545-558.

Yuan, X.-C., Tang, B.-J., Wei, Y.-M., Liang, X.-J., Yu, H., and Jin, J.-L. (2015). "China's regional drought risk under climate change: a two-stage process assessment approach." *Natural Hazards*, 76(1), 667-684.

Zadeh, L. A. (1965). "Fuzzy sets." *Information and control*, 8(3), 338-353.

Zadeh, L. A. (1968). "Fuzzy algorithms." *Information and control*, 12(2), 94-102.

Zadeh, L. A. (1975). "The concept of a linguistic variable and its application to approximate reasoning—I." *Information sciences*, 8(3), 199-249.

Zajaczkowski, J., Wong, K., and Carter, J. (2013). "Improved historical solar radiation gridded data for Australia." *Environmental modelling & software*, 49, 64-77.

Zarafshani, K., Sharafi, L., Azadi, H., Hosseininia, G., De Maeyer, P., and Witlox, F. (2012). "Drought vulnerability assessment: the case of

wheat farmers in western Iran." *Global and Planetary Change*, 98, 122-130.

Zargar, A., Sadiq, R., Naser, B., and Khan, F. I. (2011). "A review of drought indices." *Environmental Reviews*, 19(NA), 333-349.

Zhang, L., and Singh, V. (2006). "Bivariate flood frequency analysis using the copula method." *Journal of hydrologic engineering*, 11(2), 150-164.

Zhang, L., and Singh, V. P. (2007). "Gumbel–Hougaard copula for trivariate rainfall frequency analysis." *Journal of Hydrologic Engineering*, 12(4), 409-419.

Zhang, X., Alexander, L., Hegerl, G. C., Jones, P., Tank, A. K., Peterson, T. C., Trewin, B., and Zwiers, F. W. (2011). "Indices for monitoring changes in extremes based on daily temperature and precipitation data." *Wiley Interdisciplinary Reviews: Climate Change*, 2(6), 851-870.

APPENDICES

Appendix A

Chapter 4
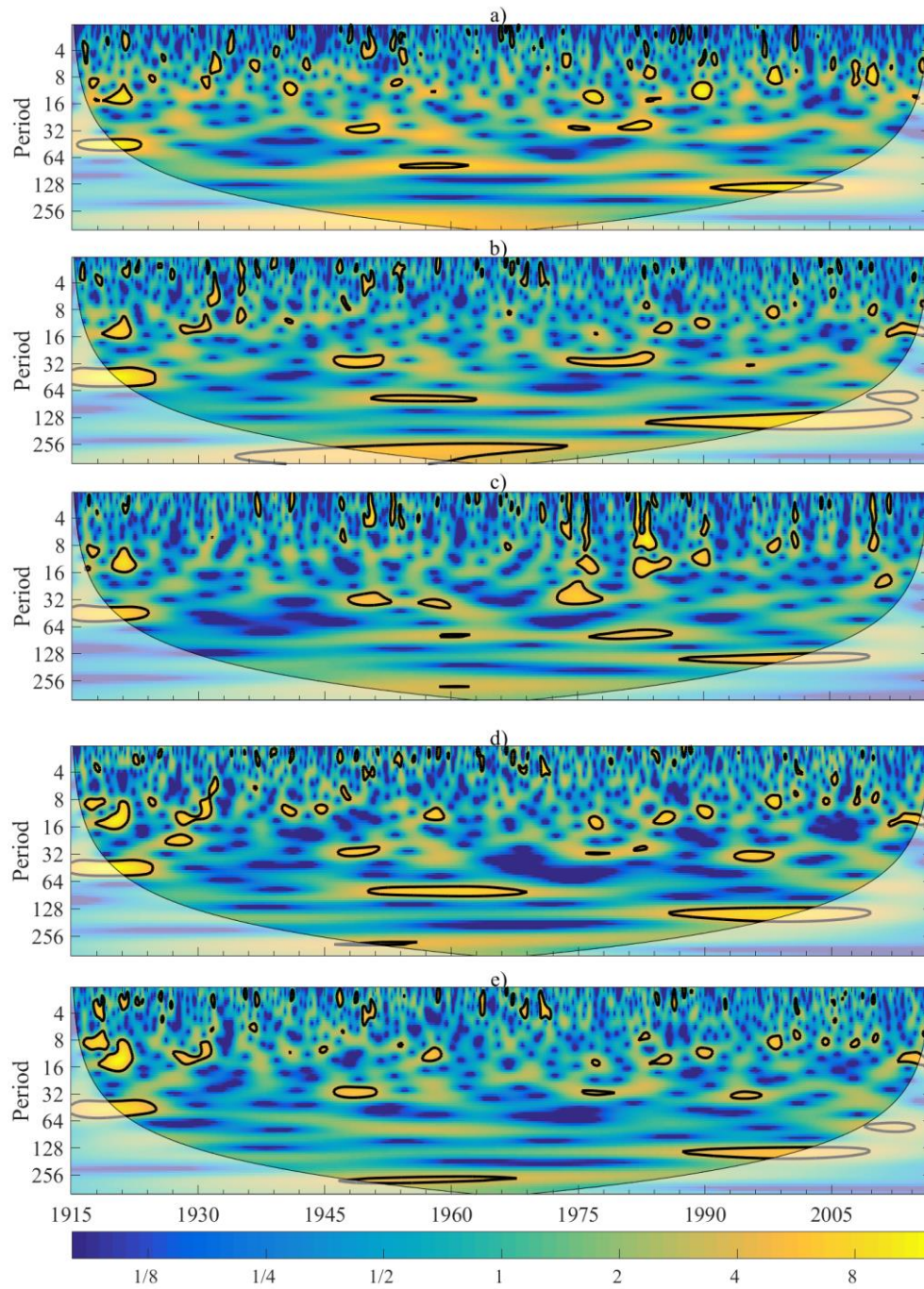
Figure A4.1: The Continuous Wavelet Transform (CWT) for (a) WRel1, (b) SPEI, (c) SPI, (d) RDDI and (e) RAI for the location R2.
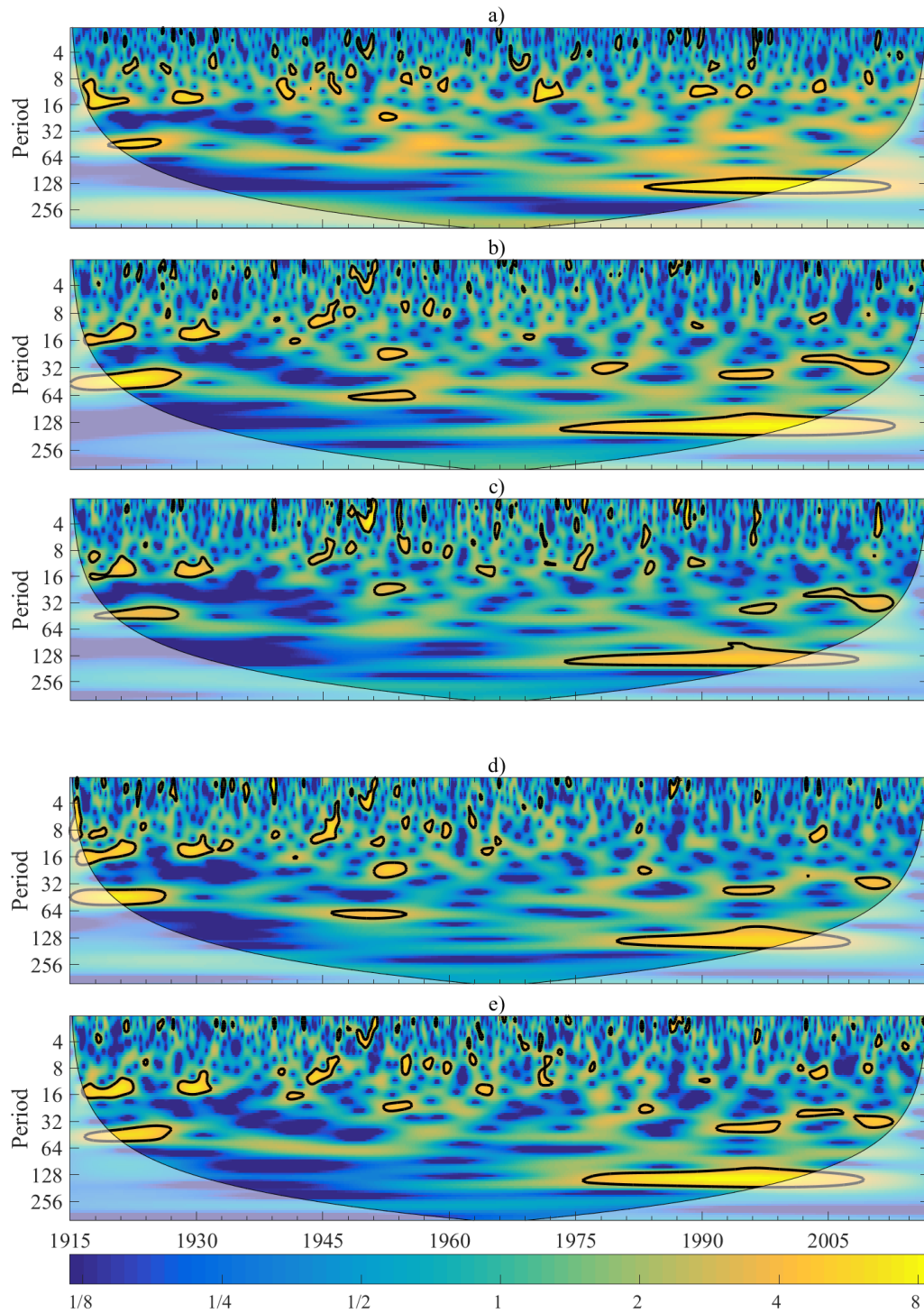
Figure A4.2: The Continuous Wavelet Transform (CWT) for (a) WRel1, (b) SPEI, (c) SPI, (d) RDDI and (e) RAI for the location R3.
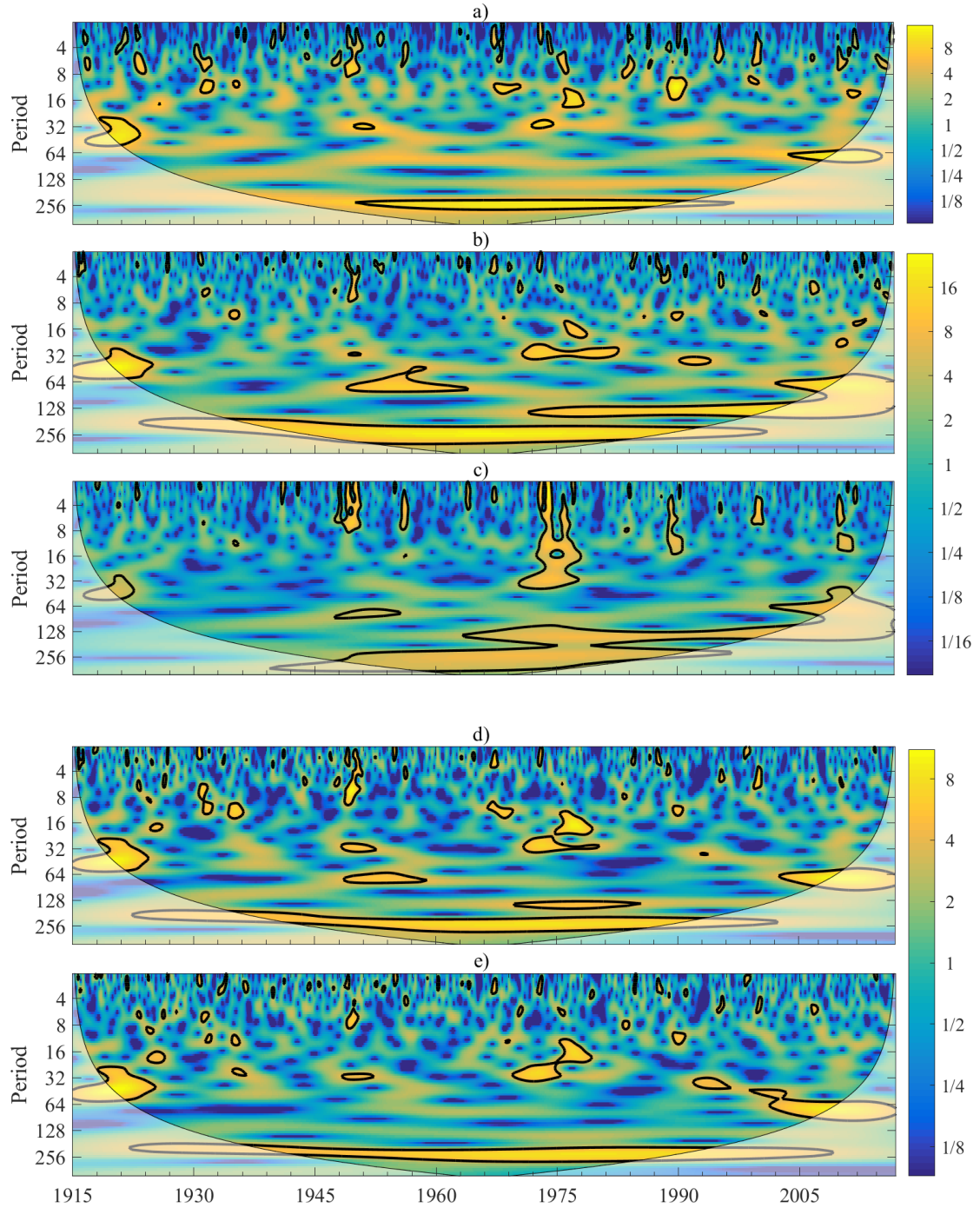
Figure A4.3: The Continuous Wavelet Transform (CWT) for (a) WRel1, (b) SPEI, (c) SPI, (d) RDDI and (e) RAI for the location R4.

No Significant Changes for SPEI

Confidence Level for Candidate Changes = 50%, Confidence Level for Inclusion in Table = 90%, Confidence Interval = 95%,
Bootstraps = 1000, Without Replacement, MSE Estimates

Estimated Average = -0.074752308
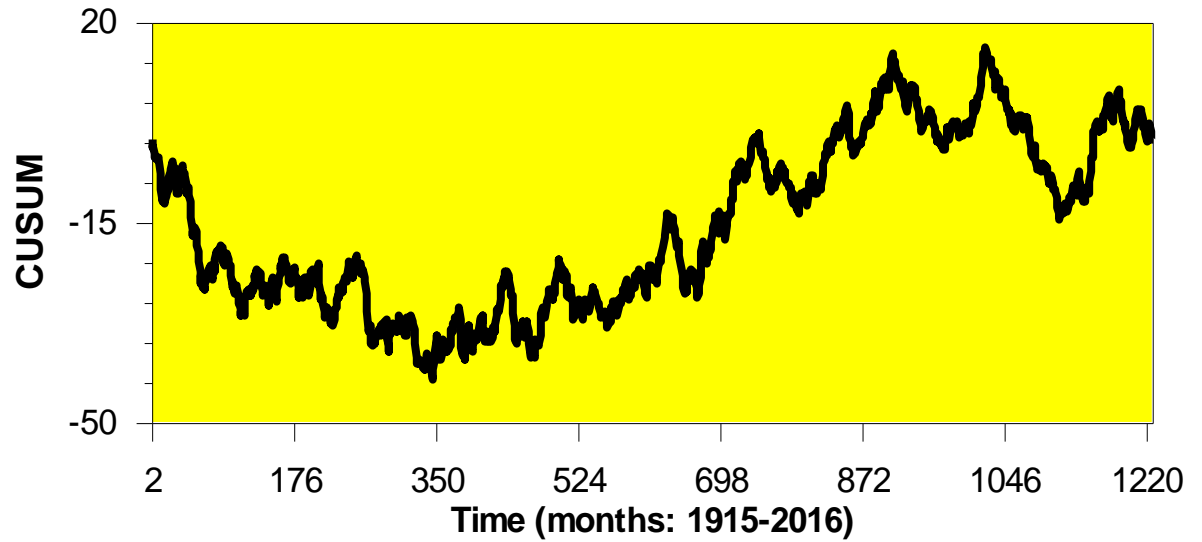
Figure A4.4: CUSUM chart of SPEI data for location R2 with significant changes shown in the background.

Chapter 5

Table A5.1: Number of drought events for different timescales

SPEI Timescale	R1	R2	R3	R4
1	82	83	85	91
3	92	85	82	85
6	66	60	56	61
9	43	50	51	39
12	40	40	40	36
24	24	27	27	33

Table A5.2: Kendall's tau of SPEI vs. RAI and SPEI vs. *WRel1* for different timescales

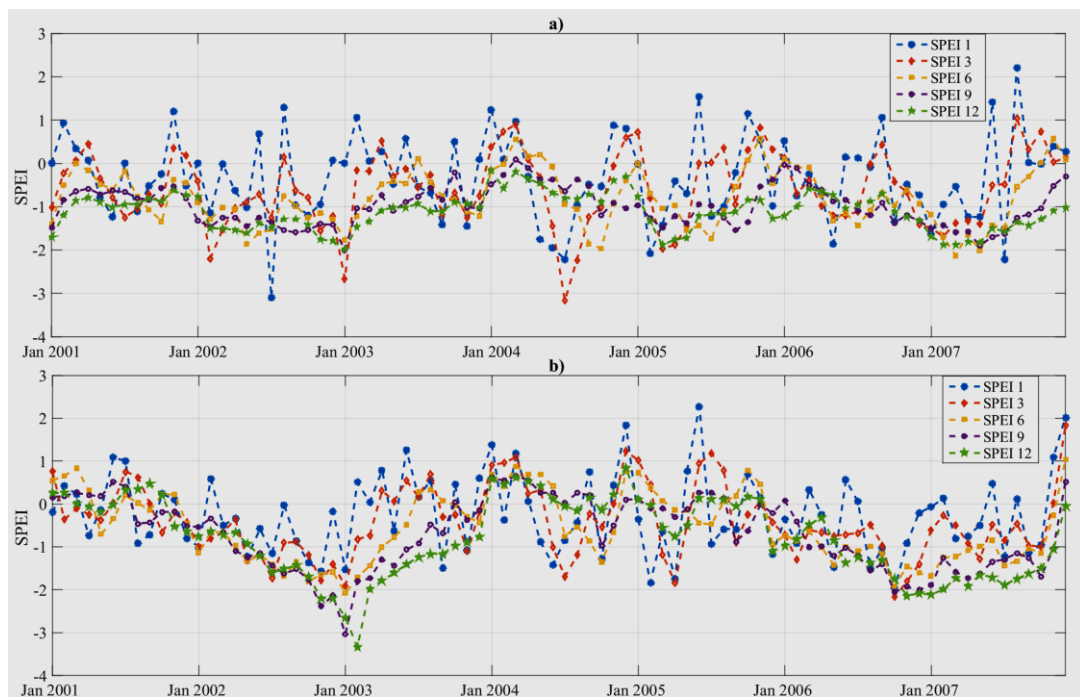| Timescale (months)	R1		R2		R3		R4	
	RAI	WRel1	RAI	WRel1	RAI	WRel1	RAI	WRel1
1	0.769	0.505	0.743	0.598	0.799	0.528	0.609	0.578
3	0.818	0.546	0.792	0.726	0.847	0.604	0.682	0.689
6	0.841	0.594	0.826	0.765	0.844	0.638	0.717	0.701
9	0.883	0.662	0.845	0.753	0.850	0.678	0.766	0.717
12	0.914	0.613	0.857	0.752	0.851	0.709	0.806	0.744
24	0.913	0.724	0.869	0.761	0.850	0.707	0.813	0.763

Figure A5.1: Monthly SPEI for a segment of Millennium Drought for different time scales.
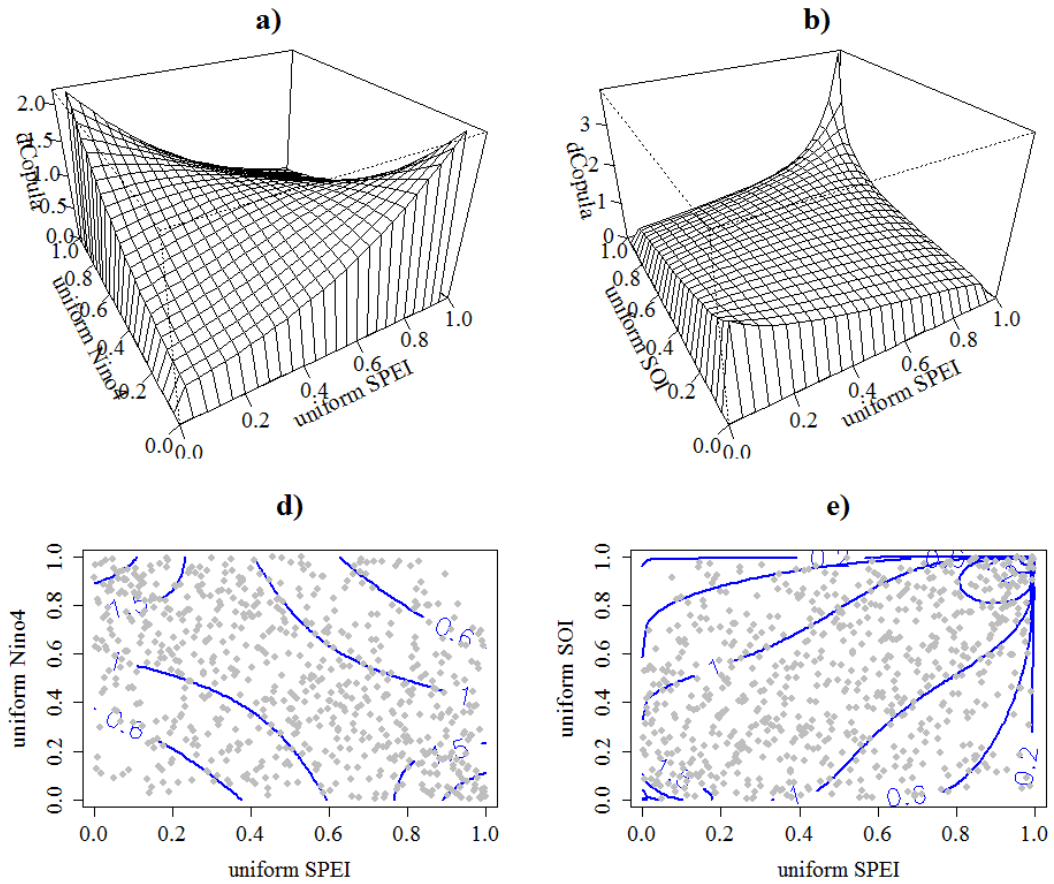
Chapter 6

Figure A6.1: Density plots of SPEI vs Niño 4 SST and SPEI vs SOI using Frank and Gumbel copula, respectively.
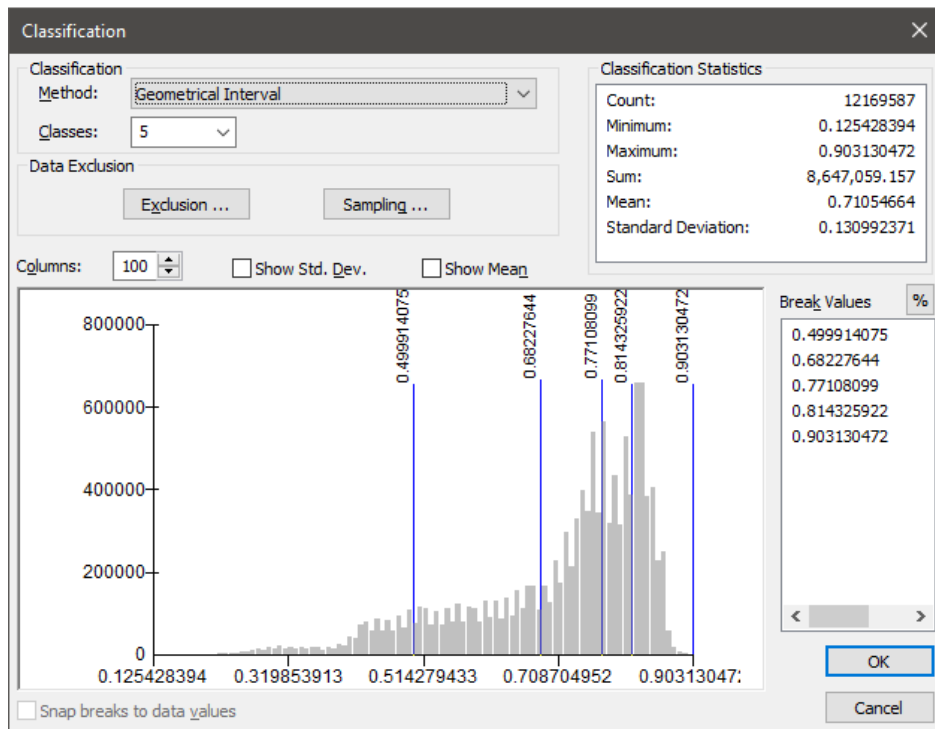
Chapter 7

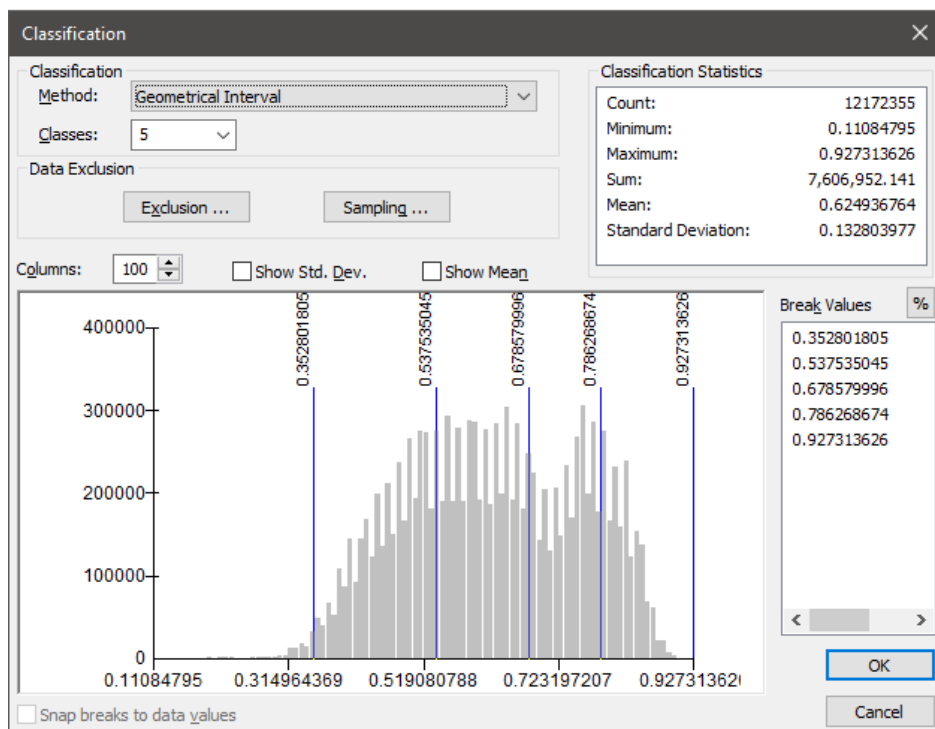**Figure A7.1**: Geometric interval of drought-risk classification for 2007.

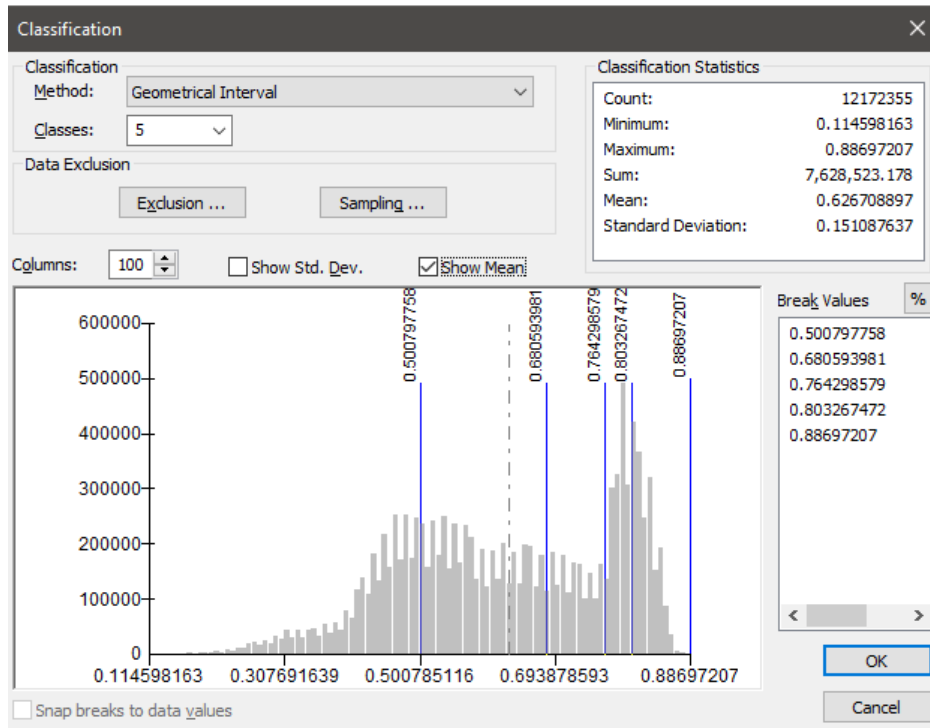**Figure A7.2**: Geometric interval of drought-risk classification for 2009.

Figure A7.3: Geometric interval of drought-risk classification for 2013.